

2011

Understanding the selective detection of Homocysteine and studies toward the synthesis of vinigrol

Dong Wang

Louisiana State University and Agricultural and Mechanical College, dwang5@tigers.lsu.edu

Follow this and additional works at: https://digitalcommons.lsu.edu/gradschool_dissertations



Part of the [Chemistry Commons](#)

Recommended Citation

Wang, Dong, "Understanding the selective detection of Homocysteine and studies toward the synthesis of vinigrol" (2011). *LSU Doctoral Dissertations*. 3424.

https://digitalcommons.lsu.edu/gradschool_dissertations/3424

This Dissertation is brought to you for free and open access by the Graduate School at LSU Digital Commons. It has been accepted for inclusion in LSU Doctoral Dissertations by an authorized graduate school editor of LSU Digital Commons. For more information, please contact gradetd@lsu.edu.

**UNDERSTANDING THE SELECTIVE DETECTION OF HOMOCYSTEINE
AND STUDIES TOWARD
THE SYNTHESIS OF VINIGROL**

A Dissertation

Submitted to the Graduate Faculty of the
Louisiana State University and
Agricultural and Mechanical College
in partial fulfillment of the
requirements for the degree of
Doctor of Philosophy

in

The Department of Chemistry

by
Dong Wang
B.E., Beijing Institute of Technology, 2003
M.E., Beijing Institute of Technology, 2006
May, 2011

DEDICATION

To my parents,
Jigang Wang and Guicao Yang
And my sister
Xiao Wang

ACKNOWLEDGMENTS

First of all, I wish to express my sincerest gratitude to my advisor, Professor William E. Crowe. He is such a great person: he is a great teacher, I benefited a lot from his synthetic organic chemistry class; he provided me with abundant guidance and support, and always believed in me and encouraged me to do my best; he is always there to help me with my research and my career plans. I would like to say that he is the most kind, generous, optimistic and knowledgeable person I ever met and I was so lucky to have him as my advisor.

My special thanks go to my committee: Professors William E. Crowe, Evgueni E. Nesterov, Carol M. Taylor, M. Graca H. Vicente, and Henrique Cheng for the time and patience they have spent reading and editing the manuscript of this dissertation. I thank Professor Evgueni E. Nesterov for teaching me computational chemistry, which used to be a completely new area for me. I thank Professor Evgueni E. Nesterov, Carol M. Taylor, and M. Graca H. Vicente for writing the recommendation letters for me. Meanwhile, I want to thank my former research advisor-Professor Changjin Zhu, for providing me invaluable research opportunities in his group, for his kind help and support during my master study in China.

My thanks go to my collaborative research group: Professor Robert M. Strongin and his postdoctoral fellow Martha Sibrian-Vazquez. I also want to thank Dr. Dale Treleven and Dr. Thomas Weldeghiorghis for the help in NMR and Dr. Frank Fronczek for the X-ray structures.

I would like to thank all the current and former members of Dr. Crowe's group. Especially, thanks to Dr. Lawrence for his help and support, and for always being "the friend in need". I also like to thank my friend Douglas Wong from Dr. Taylor's group for his true friendship.

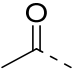
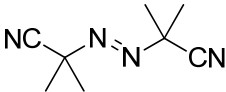
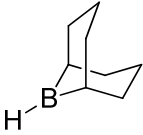
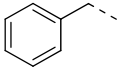

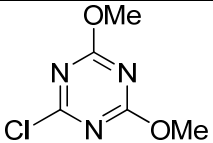
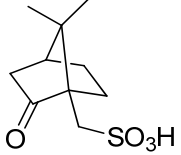
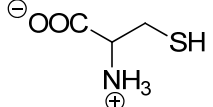
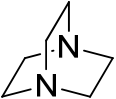
I would also like to acknowledge my family, especially my parents for their unconditional love and support.

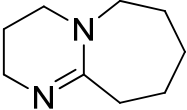
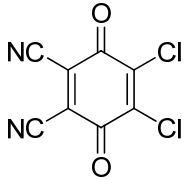
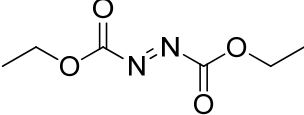
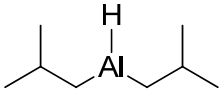
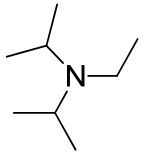
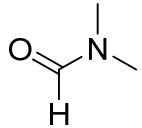
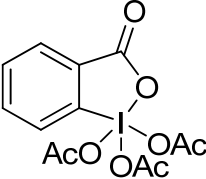
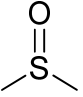
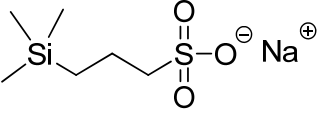
TABLE OF CONTENTS

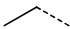
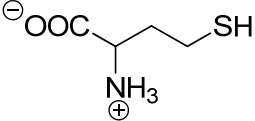
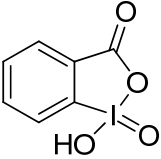
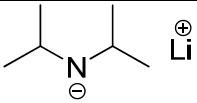
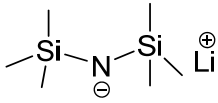
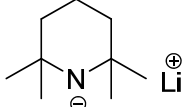
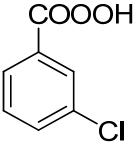
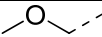
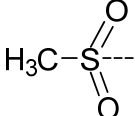
DEDICATION	ii
ACKNOWLEDGMENTS	iii
LIST OF ABBREVIATIONS	vi
ABSTRACT	xi
CHAPTER 1 UNDERSTANDING THE SELECTIVE DETECTION OF HOMOCYSTEINE	1
1.1 Background and Significance.....	1
1.2 Current State-of-the-Art in Selective Detection Methods of Hcy	1
1.3 Proposed Thermodynamic Model	4
1.4 Preparation of the Viologens.....	5
1.5 Effect of pH on the Reduction Potentials of α -Carbon Radicals.....	6
1.6 Conclusion.....	11
1.7 Experimental	11
1.7.1 General Experimental.....	11
1.7.2 Preparative Procedures	12
1.7.3 Control Experiments.....	14
1.7.4 Spectral Data.....	16
1.8 References	16
CHAPTER 2 STUDIES ON THE SYNTHESIS OF BICYCLO[3.3.1]NONANES	29
2.1 Introduction	29
2.2 First Generation on Approach to Bicyclo[3.3.1]nonanes.....	30
2.3 Revised Approach to Bicyclo[3.3.1]nonanes	32
2.3.1 One-Carbon Bridge Stereocontrol in Forming Bicyclo[3.3.1]nonanes.....	32
2.3.2 Epimerization of the One-Carbon Bridge Stereocenter.....	39
2.4 Computational Mechanism Studies on the Robinson Annulations	44
2.5 Conclusion.....	51
2.6 Experimental	52
2.6.1 General Considerations.....	52
2.6.2 First Generation on Approach to Bicyclo[3.3.1]nonanes	53
2.6.3 General Procedure for the Robinson Annulations.....	56
2.6.4 Preparation of Compounds 2.28a and 2.28b	61
2.6.5 General Procedure for Thermodynamic Control Reaction.....	62
2.6.6 General Computational Consideration	63
2.6.7 Spectral Data.....	63
2.7 References	63

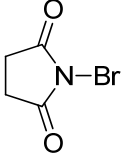
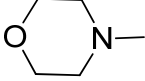
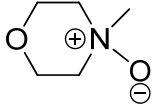
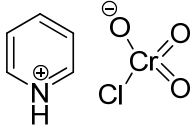
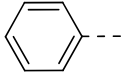
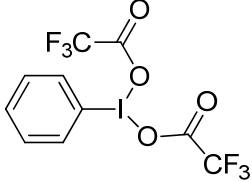


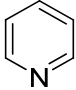
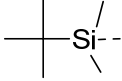
CHAPTER 3 AN APPROACH TO THE SYNTHESIS OF VINIGROL VIA TWO-CARBON RING EXPANSION STRATEGY	105
3.1 Background and Significance.....	105
3.2 Previous Synthetic Approaches to Vinigrol	107
3.2.1 Paquette's Attempt Based on a <i>cis</i> -Decalin Framework	107
3.2.2 Hanna's Approach toward Vinigrol	107
3.2.3 Corey's Attempt toward Vinigrol.....	109
3.2.4 Barriault's Approach toward Vinigrol.....	110
3.2.5 Fallis's Approach toward Vinigrol.....	111
3.2.6 Njardarson's Approach toward Vinigrol	112
3.2.7 Baran's Total Synthesis of Vinigrol.....	113
3.3 Retrosynthetic Analysis.....	116
3.4 Gram Scale Synthesis of the Tricyclic Precursor of Vinigrol.....	117
3.4.1 First Generation Approach to the Tricyclic Precursor.....	117
3.4.2 Revised Approach to the Tricyclic Precursor.....	119
3.5 A Potential Synthesis of the Tricyclic Precursor	124
3.5.1 De Mayo Photoannulations	124
3.5.2 A Potential Synthesis of the Precursor by Thermal [2+2].....	127
3.6 Efforts toward the Skeleton of Vinigrol Based on Thermal [2+2] Reactions.....	128
3.6.1 Initial Attempt for the Cycloaddition Reaction	128
3.6.2 Revised Cycloaddition Reaction with Neutral Olefins.....	130
3.7 Efforts toward the Skeleton of Vinigrol Based on Electrocyclic Reactions	132
3.7.1 Efforts to Prepare the Bicyclic Enone	133
3.7.2 An Alternative Route to Prepare the Bicyclic Enone.....	139
3.7.3 Efforts to Prepare the Tricyclic Enone	141
3.7.4 Efforts to Prepare the Conjugated Diene.....	142
3.8 Future Plan	144
3.9 Conclusion.....	146
3.10 Experimental Section	147
3.10.1 General Considerations.....	147
3.10.2 Preparative Procedures	148
3.10.3 Spectral Data.....	171
3.11 References	171
APPENDIX: LETTERS OF PERMISSION.....	232
A.1 Copyright Permission from RSC.....	232
A.2 Copyright Permission from ACS	234
VITA	235

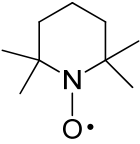
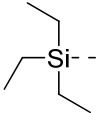
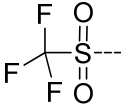

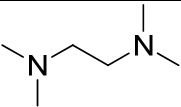
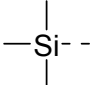
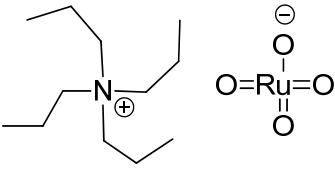
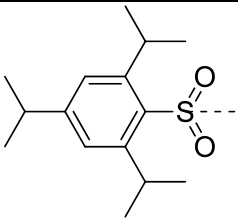
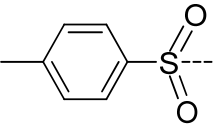
LIST OF ABBREVIATIONS

Abbreviation	Chemical Name	Chemical Structure
Ac	acetyl	
AIBN	2,2'-azo bisisobutyronitrile	
aq	aqueous	N/A
9-BBN	9-borabicyclo[3.3.1]nonane	
B3LYP	Becke three-parameter Lee-Yang-Parr correlation functional	N/A
Bn	benzyl	
<i>t</i> -Bu	<i>tert</i> -butyl	
CDMT	2-chloro-4,6-dimethoxy[1,3,5]triazine	
CSA	camphorsulfonic acid	
Cys	cysteine	
DABCO	1,4-diazabicyclo[2.2.2]octane	

DBU	1,8-diazabicyclo[5.4.0]undec-7-ene	
DCM	dichloromethane	CH_2Cl_2
DDQ	2,3-dichloro-5,6-dicyano-1,4-benzoquinone	
DEAD	diethyl azodicarboxylate	
DFT	density functional theory	N/A
DIBAL	diisobutylaluminum hydride	
DIEA	diisopropylethylamine	
DMF	<i>N,N</i> -dimethylformamide	
DMP	Dess-Martin periodinane	
DMSO	dimethylsulfoxide	
DSS	3-(trimethylsilyl)-1-propanesulfonic acid sodium salt	

ee	enantiomeric excess	N/A
eq.	equivalent	N/A
Et	ethyl	
Hcy	homocysteine	
IBX	o-iodoxybenzoic acid	
LAH	lithium aluminum hydride	LiAlH ₄
LDA	lithium diisopropylamide	
LG	leaving group	N/A
LHMDS	lithium bis(trimethylsilyl)amide	
LiTMP	lithium 2,2,6,6-tetramethylpiperidide	
<i>m</i> -CPBA	<i>meta</i> chloroperbenzoic acid	
Me	methyl	---CH ₃
MOM	methoxymethyl	
Ms	methanesulfonyl	

NBS	<i>N</i> -bromosuccinimide	
NMM	<i>N</i> -methylmorpholine	
NMO	<i>N</i> -methylmorpholine oxide	
PCC	pyridinium chlorochromate	
PG	protective group	N/A
Ph	phenyl	
PIFA	phenyliodonium bis(trifluoroacetate)	
PMB	<i>p</i> -methoxybenzyl	
Pr	propyl	
Py	pyridine	
SM	starting material	N/A
TBAF	tetra- <i>n</i> -butylammonium fluoride	$\text{Bu}_4\text{N}^{\oplus} \text{F}^{\ominus}$
TBS	<i>t</i> -butyldimethylsilyl	

TEMPO	2,2,6,6-tetramethyl-1-piperidinyloxy free radical	
TES	triethylsilyl	
Tf	trifluoromethanesulfonyl	
THF	tetrahydrofuran	
TMEDA	<i>N,N,N',N'</i> -tetramethylethylenediamine	
TMS	trimethylsilyl	
TPAP	tetra- <i>n</i> -propylammonium perruthenate	
Tris	2,4,6-triisopropylbenzenesulfonyl	
TS	transition state (or transition structure)	N/A
Ts	<i>p</i> -toluenesulfonyl	

ABSTRACT

The first part of the work is dedicated to the selective detection of Homocysteine (Hcy). In order to better understand this colorimetric detection method, a thermodynamic model for the pH dependence of the effective reduction potential of Hcy derived α -carbon radicals has been proposed. And using viologen indicators of varying reduction potentials, we demonstrate that colorimetric changes occur at experimental pH values consistent with the model.

The one-carbon bridge stereochemistry of bicyclo[3.3.1]nonane framework is critical to make the third ring of the tricyclic precursor of vinigrol. We studied this stereochemistry carefully and found that the major diastereomer formed from Robinson annulations places the one-carbon bridge substituent *anti* to the β -keto ester/amide unit introduced in the reaction and stereoselectivity appears to be kinetically controlled. The origin of this diastereoselection has been identified by density functional theory calculations.

Efforts toward the total synthesis of vinigrol have been described. The tricyclic precursor of vinigrol has been efficiently synthesized in gram scale utilizing the Robinson annulation, base catalyzed epimerization and intramolecular alkylation as the pivotal steps. The thermal [2+2] reaction with dichloroketene remains in vain although several different approaches have been explored. Finally, an alternative route using the tricyclic enone as the electrocyclic reaction precursor has been investigated. This enone can be obtained from the tricyclic precursor via either a selenation- or a bromination-elimination sequence. Further transformation involving olefination, electrocyclic reaction and oxidative cleavage to generate the bridging eight-membered ring, would complete the synthesis of the vinigrol core.

CHAPTER 1 UNDERSTANDING THE SELECTIVE DETECTION OF HOMOCYSTEINE*

1.1 Background and Significance

Homocysteine (Hcy) is an accepted independent risk factor for several major pathologies including cardiovascular disease, birth defects, osteoporosis, Alzheimer's disease, and renal failure.^[1] Elevated levels of both Hcy and cysteine (Cys) have been associated with neurotoxicity. In the case of Cys, this has been demonstrated *in vivo* in animals with immature blood-brain barriers and in cultured neurons *in vitro*.^[2] Additionally, Cys induced hypoglycemic brain damage has been studied as an alternative mechanism to excitotoxicity.^[3]

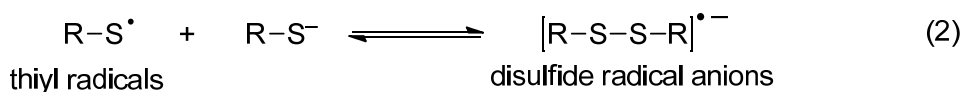
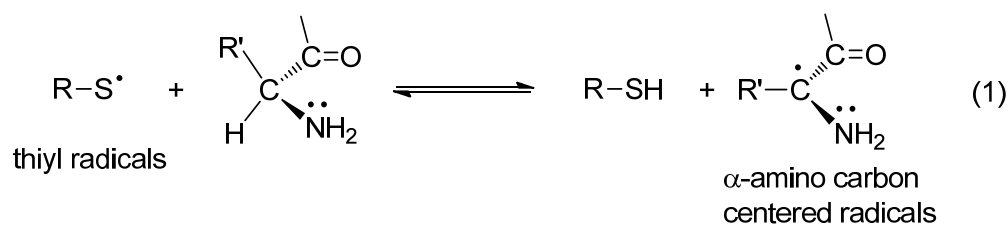
The role of Hcy in disease is unclear. After many years of study and impressive progress, it is still not yet known if Hcy causes disease, is a consequence of it, or is simply a biomarker.^[4] There is an ongoing effort in the biomedical community involving the study of hyperhomocysteinemia.^[4]

Because Hcy is associated with a wide range of diseases,^[5] there has been great interest in the development of selective detection methods for it. Interference from structurally related biological thiols such as Cys and GSH, typically present in much higher concentration, hinders selective detection methods. Unlike Hcy, the relatively more common biological thiols, such as GSH, are typically associated with beneficial antioxidant activity. It is thus also important to understand the differences between the fundamental chemistry of Hcy and other biothiols.

1.2 Current State-of-the-Art in Selective Detection Methods of Hcy

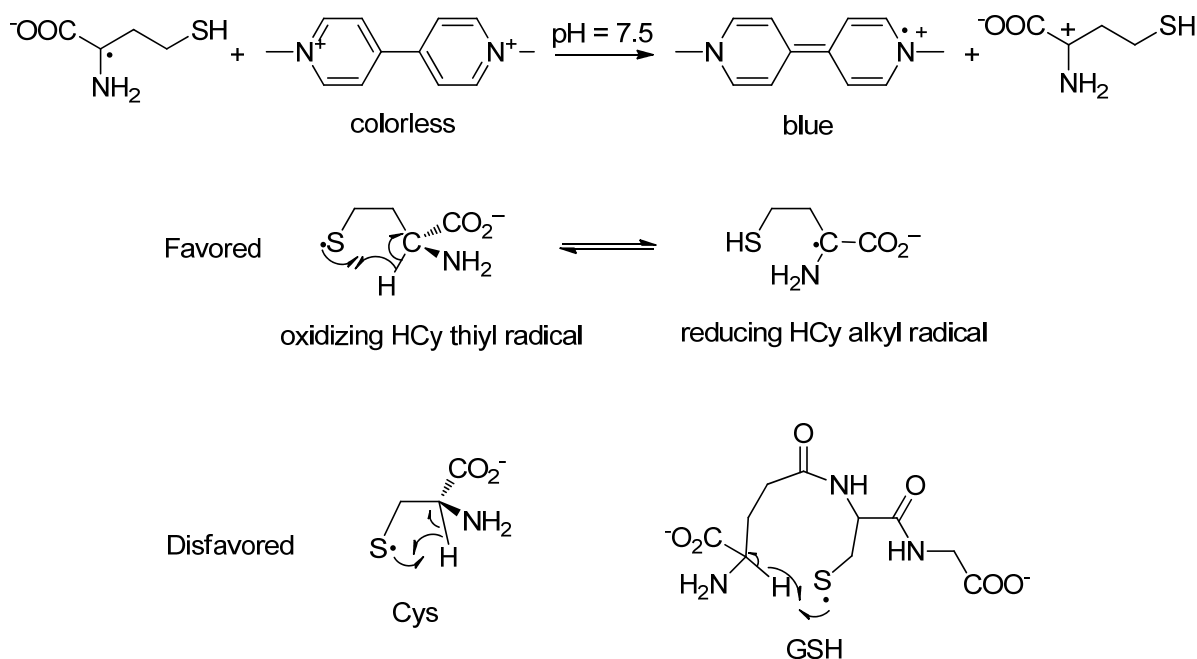
Thiyl radicals, which can be produced from biological thiols,^[6] have attracted a lot of attention due to their important biological redox processes. The two major and interesting species can be formed by thiyl radicals are α -amino carbon centered radicals and disulfide radical anions (Scheme 1.1).

* Portions of this chapter are printed by permission of Chemical Communications.



Scheme 1.1 Interconversion between Thiyl Radicals, Carbon Radicals and Disulfide Radical Anions

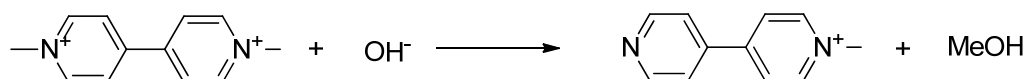
The formation of carbon radicals is not favored unless thiyl radicals could abstract hydrogen atoms from suitably activated C-H groups, for example, from alcohols and ethers,^[7] or from the α carbon of amino acids.^[8]



Scheme 1.2 Proton Abstraction Leading to Formation of the α -Aminoalkyl Radical

Oxidizing thiyl radicals formed from biological thiols interconvert with reducing, α -amino carbon centered radicals under physiological, aerobic conditions (Scheme 1.1). The rate constant for the thiyl radical interconverting with the carbon radical derived from Hcy has been detected at pH 10.5 by Zhao et al.^[9]

Strongin *et al.* recently reported a colorimetric detection method based on the selective reduction of colorless methyl viologen (MV^{2+}) to its blue radical cation ($MV^{+\bullet}$) by Hcy at neutral pH (Scheme 1.2).^[10] The selectivity of this detection method for Hcy was proposed to arise from an intramolecular hydrogen atom abstraction converting the oxidizing Hcy thiyl radical to the reducing Hcy α -amino carbon-centered radical through a kinetically favorable, five-membered ring transition state (Scheme 1.2). In contrast, in the cases of Cys and GSH, H-atom abstraction to afford a reducing carbon-centered radical would proceed via less-favored four- and nine-membered ring transition-state geometries, respectively (Scheme 1.2).



Scheme 1.3 Dealkylation of Alkyl Viologens under Basic Conditions

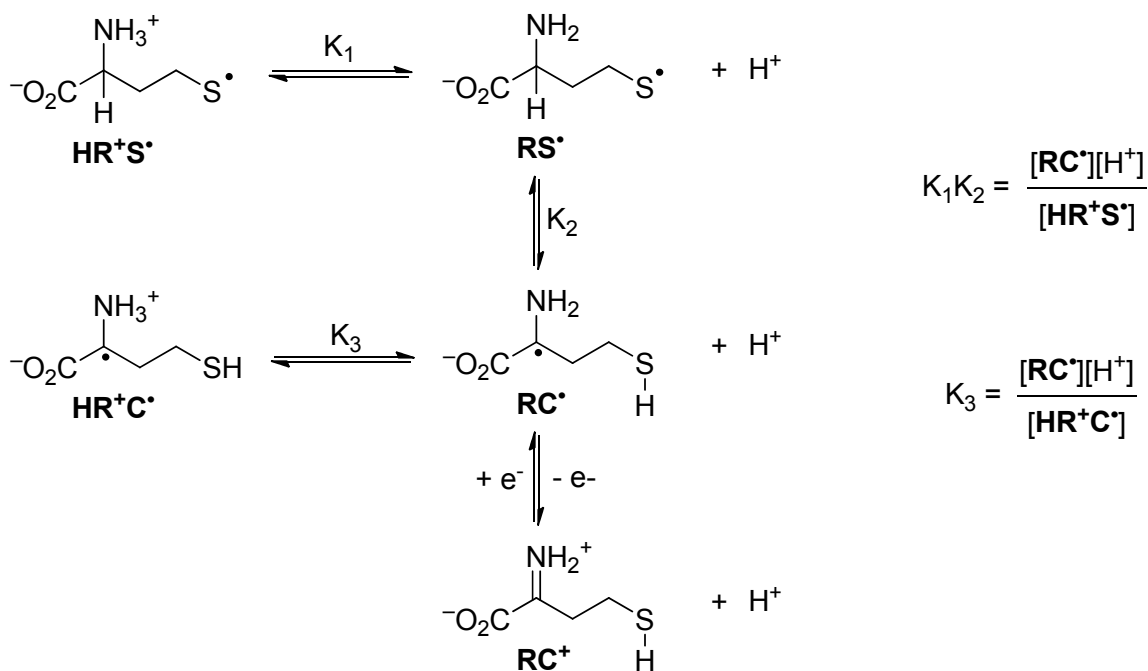
Earlier work by Zhao had shown that at pH 10.5 colorimetric detection of GSH, Cys and Hcy was observed with no discernable selectivity.^[9] Interconversion of thiyl radicals with reducing disulfide radical anions (Scheme 1.1, eqn (2)) becomes more prominent with increasing pH, and it is possible that at pH 10.5 nonselective MV^{2+} reduction results from the equally facile formation of disulfide radical anions from all three biological thiols. Another possibility is the well-known dealkylation process of methyl viologen itself (Scheme 1.3).^[11] Because the methanol resulting from the dealkylation can be a reducing agent, solutions of methyl viologen under basic conditions can spontaneously be reduced and will then turn blue as the radical cation is formed.

Conducting the viologen-mediated colorimetric assay at neutral pH has the advantage of minimizing interference from nonselective MV^{2+} reduction by disulfide radical anions. However, captodative stabilization of α -amino carbon-centered radicals requires lone pair donation from nitrogen, and at neutral pH only a small fraction of the amino groups are not protonated. This

begs the question whether the reducing species producing the colorimetric response in the MV²⁺ assay could really be α -carbon radicals. To address this question we proposed a thermodynamic model for the pH dependence of the effective reduction potential of Hcy derived α -carbon radicals and, using viologen indicators of varying reduction potentials, tested whether colorimetric changes occur at experimental pH values consistent with this model.

1.3 Proposed Thermodynamic Model

The ability of the carbon radicals to reduce a given substrate (*e.g.*, methyl viologen) has pH-dependence which is determined by Scheme 1.4.



Scheme 1.4 The Equilibrium Between Thiol Radicals and Carbon Radicals

The mid-point potential $E_m(\text{RC}^+/\text{RC}^\bullet)$ at a given pH determines whether the α -carbon radical will be able to reduce a particular substrate. The following relationship between $E_m(\text{RC}^+/\text{RC}^\bullet)$ and $[\text{H}^+]$ was derived from the Nernst equation:^[12]

$$E_m(\text{RC}^+/\text{RC}^\bullet) = E^\circ(\text{RC}^+/\text{RC}^\bullet) + \frac{RT \ln 10}{F} \log \left\{ 1 + \frac{[\text{H}^+]}{K_{\text{obs}}} \right\} \quad (3)$$

Where $E^{\circ}(\text{RC}^+/\text{RC}^{\bullet})$ is the standard potential, which is also the minimum value possible for $E_m(\text{RC}^+/\text{RC}^{\bullet})$, and the pseudo-equilibrium constant, K_{obs} , is given by:

$$K_{\text{obs}} = \frac{K_1 K_2 K_3}{K_1 K_2 + K_3}$$

When $[\text{H}^+] \gg K_{\text{obs}}$ (low pH), E_m varies linearly with pH:

$$E_m(\text{RC}^+/\text{RC}^{\bullet}) \approx E^{\circ}(\text{RC}^+/\text{RC}^{\bullet}) + \frac{RT \ln 10}{F} \left\{ \log[\text{H}^+] - \log K_{\text{obs}} \right\} \quad (4)$$

At 298K, $RT \ln 10 / F = 59.2$ mV. Since $\text{pH} = -\log[\text{H}^+]$ and we can define $\text{p}K_{\text{obs}} = -\log K_{\text{obs}}$, the above equation can be re-written as:

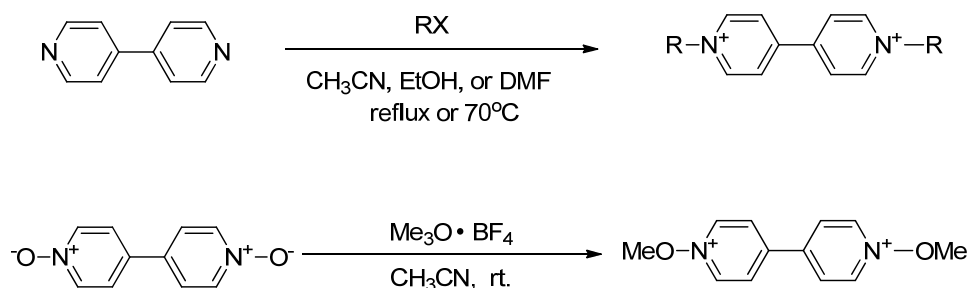
$$E_m(\text{RC}^+/\text{RC}^{\bullet}) = E^{\circ}(\text{RC}^+/\text{RC}^{\bullet}) + 59.2 [\text{p}K_{\text{obs}} - \text{pH}] \quad (5)$$

When $[\text{H}^+] \ll K_{\text{obs}}$ (high pH), the pH-dependant part of the function goes to zero and E_m becomes constant, which is also the minimum value of E_m :

$$E_m(\text{RC}^+/\text{RC}^{\bullet}) = E^{\circ}(\text{RC}^+/\text{RC}^{\bullet}) \quad (6)$$

To test this model, the effect of pH on the aminothiols-mediated reduction of a series of viologen indicators was determined. This was accomplished by gently refluxing a buffered, aqueous solution of the aminothiol (Hcy or Cys, 17 mM) and viologen (4.0 mM). In order to study the reduction potential of α -carbon radicals derived from Hcy in the whole pH range, a number of viologens with different reduction potentials were chosen.

1.4 Preparation of the Viologens



Scheme 1.5 Preparation of Viologens

While viologens in entries 1, 4, 5, 7 and 8 in Table 1.1 are commercially available, the other ones were prepared by nucleophilic alkylation of 4,4'-bipyridine as described in the literature (Scheme 1.5).^[13] Dimethoxy viologen was prepared by alkylation of N-Oxide according to a known process (Scheme 1.5).^[14]

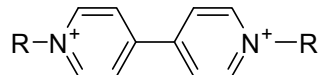
1.5 Effect of pH on the Reduction Potentials of α -Carbon Radicals

Typically, color formation was observed (*e.g.*, colorless to blue for MV²⁺) above a certain pH. As the pH was increased, faster onset of color formation and deeper color change were observed as well as longer persistence of color after the sample was removed from heating. For most viologens (entries 3-8, Table 1.1) there was a pH range where color formation is observed for Hcy but not Cys (selective Hcy detection). Hcy should have a stronger reduction potential because of the particularly favorable formation of α -carbon radicals.

As solution pH decreases, we predict that $E_m(\text{RC}^+/\text{RC}^\bullet)$ should increase until $E_m(\text{RC}^+/\text{RC}^\bullet) > E^0(\text{viologen})$ at which point no color formation could be observed. Upon lowering the pH we observed slower onset of color formation and less intense color change as well as shorter persistence of color after the sample is removed from heating. For six of the eight viologens examined we were able to obtain a pH endpoint (minimum pH where color formation was observable) below which no color formation occurred. As predicted, lower pH endpoints were observed for viologens possessing higher (*i.e.*, less negative) reduction potentials (E^0 values). No pH endpoint was observed (color formation for all pH values ≥ 0) for the two most easily reduced viologens. These pH endpoint results are summarized in Table 1.1.

We propose that $E_m(\text{RC}^+/\text{RC}^\bullet) \approx E^0(\text{viologens})$ for the pH endpoints obtained in entries 4-8 of this table. As can be seen from Table 1.1, entry 3 through entry 8 viologens can be used to detect Hcy and Cys selectively during lower pH. For example, benzylic viologen (entry 5) can be used to detect Hcy selectively between pH 3.6 and pH 4.8 since there is no color change for Cys.

Table 1.1 The Minimum pH that α -Carbon Radicals Can Reduce Viologens



Entry	R (viologen)	E^0 /mV	pH endpoint ^a of Hcy	pH(calc) ^b of Hcy	pH endpoint of Cys
1	2,4-dinitrophenyl	N.D.	none	< 0	≤ 0
2	-CH ₂ CN	-150	N.D.	0	≤ 0
3	-CH ₂ CO ₂ Et	-267	3.8	1.9	5.8
4	Ph-	-288	2.5	2.3	3.8
5	PhCH ₂ -	-370	3.6	3.7	4.8
6	CH ₂ =CHCH ₂ -	-408	4.2	4.3	4.7
7	CH ₃ (CH ₂) ₅ CH ₂ -	-415	4.3	4.4	5.8-7.0, 7.8
8	CH ₃ -	-446	5.0	4.9	6.0-7.0, 8.2

^a Data from entries 4-8 show a linear correlation between E^0 and pH endpoint. The best linear fit of this data gives the empirical equation: $E^0 = -132.57 - 64.498 \text{ pH}$ ($R^2 = 0.9872$). See Figure 1.1.

^b pH(calc) are calculated from $(-153.3 - E^0)/59.2$ which represents the best fit of the data from entries 4-8 to the theoretical equation $E^0(\text{viologen}) = E^0(\text{Hcy}) + 59.2(\text{p}K_{\text{obs}} - \text{pH})$. We calculate an average value: $[E^0(\text{Hcy}) + 59.2\text{p}K_{\text{obs}}]_{\text{avg}} = [E^0(\text{viologen}) + 59.2\text{pH}]_{\text{avg}} = -153.3 \text{ mV}$.

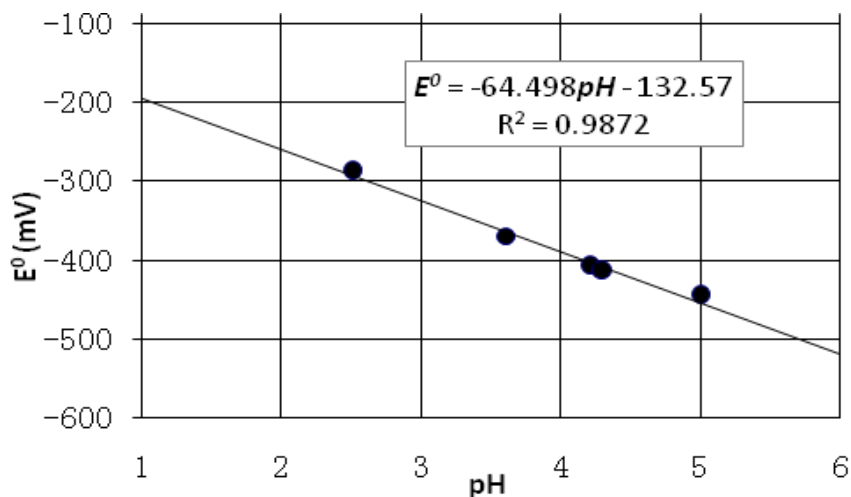


Figure 1.1 Reduction Potential vs. pH Plot

We also prepared dimethoxy viologen (Scheme 1.5, $E^0 = -651$ mV, pH (calc) = 8.4) and found that no color formation occurred in the pH range 8-11. A tempting interpretation of this data is that the reduction potential of dimethoxy viologen is more negative than $E^0(\text{RC}^+/\text{RC}^\bullet)$, and therefore there is no pH at which the mid-point potential $E_m(\text{RC}^+/\text{RC}^\bullet)$ is negative enough for dimethoxy viologen reduction to occur. This interpretation is represented graphically in Figure 1.2.

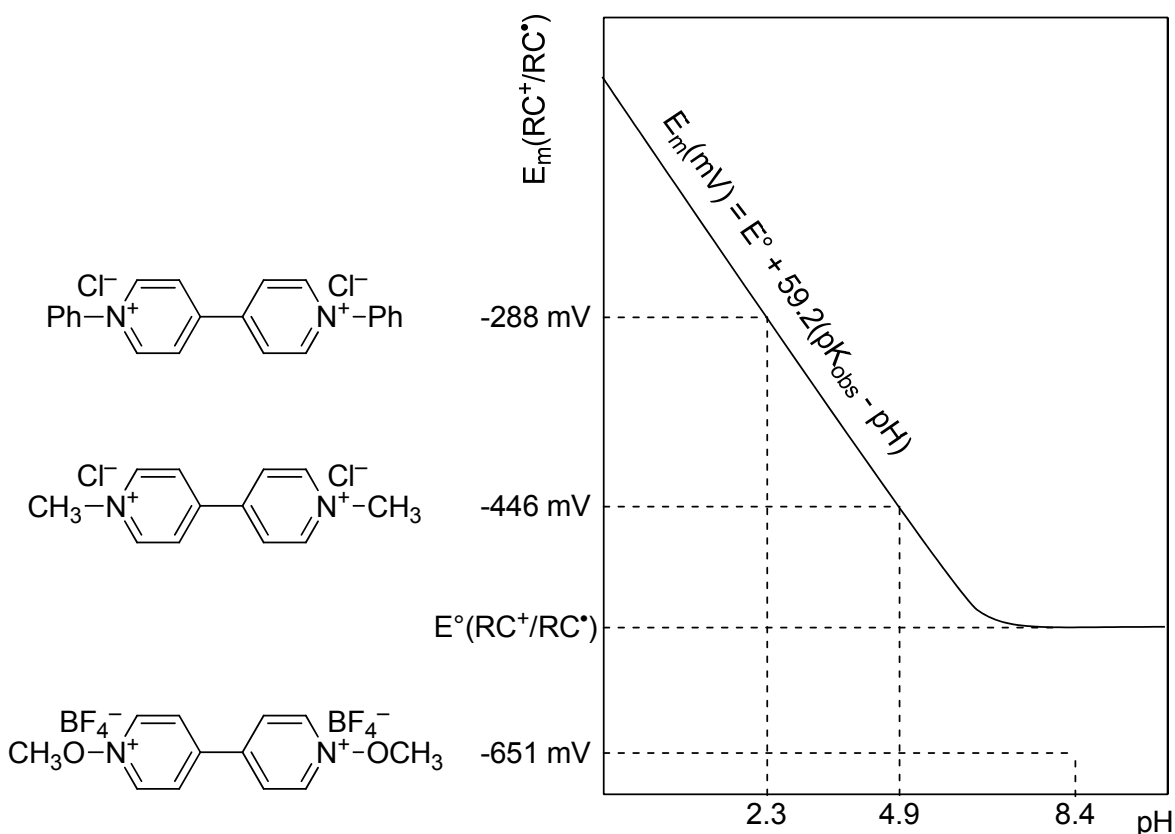
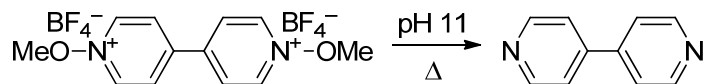


Figure 1.2 Reduction Potential vs. Whole pH Range

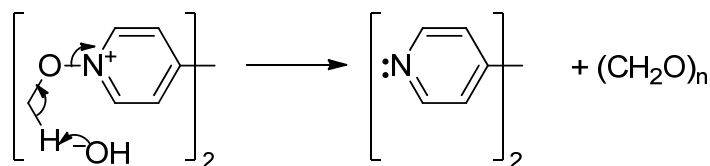
This interpretation would allow us to bracket the standard potential of the homocysteine-derived α -carbon radical as: $-651 \text{ mV} < E^0(\text{RC}^+/\text{RC}^\bullet) < -446 \text{ mV}$. While the upper value of this bracketing is certainly valid (-446 mV for MV^{2+} falls on the linear part of the $E_m(\text{RC}^+/\text{RC}^\bullet)$ vs. pH curve), the lower value is uncertain. At pH 11 there should be color formation associated with formation of the disulfide radical anion ($[\text{HcyS-SHcy}]^{\bullet-}$, $E^0 \approx -1700$ mV for $[\text{CysS-SCys}]^\bullet$).

Lack of color formation at pH 11 probably suggests that dimethoxy viologen is not stable at this pH. Indeed, gently refluxing a solution of dimethoxy viologen at pH 11 leads to complete conversion of the viologen to a mixture of decomposition products from which 4,4'-bipyridine can be isolated in 80-85% yield (Scheme 1.7).

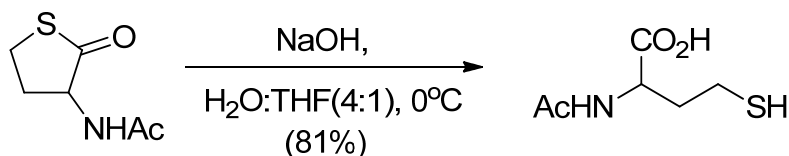


Scheme 1.7 Decomposition of Dimethoxy Viologen under Basic Conditions

Net demethoxylation of dimethoxy viologen might occur by a β -elimination pathway where a pyridine leaving group is ejected and the methoxyl group is oxidized to formaldehyde (Scheme 1.8).^[15] An interesting possibility to explore is the preparation of a stable analog of dimethoxy viologen lacking this β -elimination decomposition pathway.



Scheme 1.8 Mechanism for the Decomposition of Dimethoxy Viologen



Scheme 1.9 Preparation of *N*-acetyl homocysteine

We prepared *N*-acetyl homocysteine according to a known procedure (Scheme 1.9).^[16] Since the amide group cannot be protonated under experimental conditions, the reduction potential of *N*-acetyl Hcy derived α -carbon radicals is expected to be pH independent. However, we are surprisingly to find out that no color change could be observed with methyl viologen at neutral or slightly acidic conditions, indicating that the reducing α -carbon radicals were never formed probably due to the weaker captodative effect of *N*-acetyl Hcy derived α -carbon radicals.

1.6 Conclusion

In order to better understand the colorimetric detection method of Hcy using viologens, a thermodynamic model for the pH dependence of the effective reduction potential of Hcy derived α -carbon radicals has been proposed. And using viologen indicators of varying reduction potentials, we demonstrate that colorimetric changes occur at experimental pH values consistent with the model.

We found that viologen reduction mediated by α -amino carbon-centered radicals can occur under acidic conditions. The reduction potential of α -carbon radicals was found to be pH dependent, and it shows a linear correlation between the reduction potential and pH for Hcy. The pH profiles of Cys and Hcy have been established for six viologens. Most of the viologens can be used to selectively detect Hcy and Cys under acidic conditions. The determination of standard reduction potentials of α -carbon radicals is currently underway in our lab.

1.7 Experimental

1.7.1 General Experimental

The preparation experiments were performed under a nitrogen atmosphere in oven- and/or flame-dried glassware using a Vacuum Atmospheres dry box or by using standard Schlenk techniques. Solvents used as reaction media were distilled immediately before use: acetonitrile were distilled from Na/benzophenone ketyl. Ethyl bromoacetate was purchased from Alfa Aesar. NMR solvent (D_2O , $CDCl_3$) was purchased from Cambridge Isotope Laboratories, Inc. All of the other reagents were purchased from Sigma-Aldrich and used without any further purification.

1H spectra was recorded on a Bruker AV-400 (400 MHz 1H) or a Bruker AC-250 (250 MHz 1H) spectrometer in deuterated solvents using the solvent residual protons as an internal reference (H_2O : 4.68 ppm, $CDCl_3$: 7.26 ppm) for 1H NMR or using DSS as an internal reference for ^{13}C NMR ($CDCl_3$: 77.0 ppm, t for ^{13}C NMR). Chemical shifts (δ) are given in parts per

million down from tetramethylsilane (TMS). Data for ^1H NMR spectra are reported as follows: chemical shift (δ ppm), multiplicity (s = singlet, d = doublet, t = triplet, q = quartet, quin = quintet, dd = doublet of doublets, dt = doublet of triplets, ddd = doublet of doublet of doublets, ddt = doublet of doublet of triplets, m = multiplet), coupling constant (Hz), and integration.

The buffer solution that we use in the experiment is shown in Table 1.2.

Table 1.2 Buffer Components

pH range	Buffer Component (1+2)	Concentration 1	Concentration 2
1.0--2.2	HCl + KCl	x ml 0.2 M, dilute to 100 ml	0.05 M
2.3--6.9	Citric Acid + Na ₂ HPO ₄	x ml 0.1 M	(100-x) ml 0.2 M
7.0--9.0	Tris + HCl	0.05 M	x ml 0.1 M, dilute to 100 ml
10.0--11.0	NaHCO ₃ + NaOH	0.025 M	x ml 0.1 M, dilute to 100 ml
12.0--13.0	NaOH + KCl	x ml 0.2 M, dilute to 100 ml	0.05 M

1.7.2 Preparative Procedures

General procedure for the preparation of viologens:^[13a] A mixture of alkyl bromide (10 equiv) and 4,4'-bipyridine (1 equiv) were heated to reflux in anhydrous acetonitrile under nitrogen for 4 to 20 hours. After the reaction mixture was cooled down to room temperature, the precipitate was filtered off and purified by recrystallization from ethanol.

1,1'-Bis(cyanomethyl)-4,4'-bipyridinium dibromide (entry 2):^[13b] Under Ar atmosphere 4,4'-bipyridine (0.781g, 0.05 mol) and 2-bromo acetonitrile (1.799g, 0.015 mol) were dissolved in anhydrous DMF (50 mL). The mixture was heated at 60 °C for 16 hours, and then cooled to room temperature. 200 mL of acetone were added and the reaction mixture allowed to stand overnight at room temperature. The yellow precipitate was filtered, washed with acetone, and dried under vacuum. The product (1.46g, 74%) was obtained as a yellow powder. ¹H NMR (400 MHz, D₂O): δ 9.26 (d, J = 7.0 Hz, 4H), 8.64 (d, J = 7.0 Hz, 4H), 5.98 (s, 4H, diminished integration due to partial deuterium exchange). ¹³C NMR (100 MHz, D₂O): δ 151.7, 146.3, 127.9, 112.8, 48.2.

1,1'-Bis(2-ethoxy-2-oxoethyl)-4,4'-bipyridinium dibromide (entry 3): Following the general procedure, ethyl bromoacetate (3.55 mL, 0.032 mol) and 4,4'-bipyridine (0.50 g, 0.0032 mol) were refluxed in anhydrous acetonitrile (60 mL) for 20 hours. The product (1.24 g, 80%) was obtained as cubic yellow crystals. ¹H NMR (400 MHz, D₂O): δ 9.07 (d, J = 6.4 Hz, 4H), 8.59 (d, J = 6.4 Hz, 4H), 5.63 (s, 4H, diminished integration due to partial deuterium exchange), 4.29 (q, J = 7.1 Hz, 4H), 1.24 (t, J = 7.1 Hz, 6H). ¹³C NMR (100 MHz, D₂O): δ 166.8, 151.2, 147.1, 127.1, 64.3, 61.2, 13.3.

1,1'-Diallyl-4,4'-bipyridinium dibromide (entry 6): Following the general procedure, allyl bromide (1.77 mL, 0.02 mol) and 4,4'-bipyridine (0.32 g, 0.002 mol) were refluxed in anhydrous acetonitrile (40 mL) for 4 hours. The product (0.53 g, 65%) was obtained as deep yellow needles. ¹H NMR (400 MHz, D₂O): δ 9.05 (d, J = 6.8 Hz, 4H), 8.50 (d, J = 6.8 Hz, 4H), 6.10-6.18 (m, 2H), 5.54 (dd, J₁ = 10 Hz, J₂ = 17 Hz, 4H), 5.29 (d, J = 6.4 Hz, 4H). ¹³C NMR (100 MHz, D₂O): δ 150.4, 145.6, 129.6, 127.1, 123.8, 63.7.

4,4'-dipyridyl 1,1'-dioxide: Following the literature procedure,^[14] 4,4'-bipyridine (5 g, 0.032 mol) in glacial acetic acid (25 mL) was heated to 70°C. After complete dissolution of the

bipyridine, a 30% solution of H₂O₂ in H₂O (3.64 g, 0.032 mol) was added dropwise, and the mixture was stirred at 70 °C for 6 hours. After dropwise addition of a second equivalent of H₂O₂, the mixture was stirred at 70 °C for another 24 hours. The solvent was then removed, and the remainder was neutralized with saturated aqueous NaHCO₃. Recrystallization from water afforded the product as the hemihydrate as yellow needles (5 g, 76%). ¹H NMR (400 MHz, D₂O): δ 8.32 (d, J = 6.9 Hz, 4H), 7.86 (d, J = 6.9 Hz, 4H). ¹³C NMR (100 MHz, D₂O): δ 139.5, 137.9, 124.7.

1,1'-Dimethoxy-4,4'-bipyridinium bis[tetrafluoroborate]: Following the literature procedure,^[14] trimethyloxonium tetrafluoroborate (847 mg, 5.70 mmol) and 4,4'-dipyridyl 1,1'-dioxide (511 mg, 2.49 mmol) were stirred in 10 mL of acetonitrile for 4 hours. Recrystallization from acetonitrile afforded the product (620 mg 65%) as colorless prisms. ¹H NMR(400 MHz, D₂O): δ 9.38 (d, J = 7.0 Hz, 4H), 8.59 (d, J = 7.0 Hz, 4H), 4.50 (s, 6H). ¹³C NMR (100 MHz, D₂O): δ 149.2, 141.4, 128.4, 69.8.

N-acetyl Hcy: Following the known procedure,^[16] N-acetyl Hcythiolactone (1.0 g, 6.3 mmol) was dissolved in an aqueous NaOH solution (6.4 ml, 3.0 M) and THF (1.6 ml), and the resulting mixture was stirred at 0°C for half an hour. After which the mixture was acidified by 3 N HCl to pH 0. Then the mixture was extracted with ethyl acetate (3×20 ml), and the combined organic extracts were washed with brine, dried (MgSO₄), filtered and concentrated to give the product (0.9 g, 81%) as white powders.

1.7.3 Control Experiments

- **Entry 3 Hydrolysis**

1. 1,1'-Bis(2-ethoxy-2-oxoethyl)-4,4'-bipyridinium dibromide (9.8 mg, 0.02 mmol) was dissolved in 5 mL of sulfuric acid (pH = 3.0, solvent: D₂O), and the resulting mixture was gently

refluxed for one hour. An aliquot of the resulting mixture was examined by ^1H NMR. The spectrum showed that less than 5% hydrolysis product was formed.

2. The viologen substrate (9.8 mg, 0.02 mmol) was dissolved in 5 mL of hydrochloric acid (pH = 2.3, solvent: D_2O), and the resulting mixture was gently refluxed for one hour. An aliquot of the resulting mixture was examined by ^1H NMR. A similar spectrum was obtained.

3. The viologen substrate (9.8 mg, 0.02 mmol) and Hcy (11.5 mg, 0.085 mmol) were dissolved in 5 ml of citric acid and Na_2HPO_4 buffer (pH = 3.8, solvent: D_2O), and the resulting mixture was gently refluxed for one hour. An aliquot of the resulting mixture was examined by ^1H NMR. A similar spectrum was obtained except for the extra Hcy and citric acid peaks.

- **Dimethoxy Viologen Control Experiment**

1. The substrate dimethoxy viologen (7.8 mg, 0.02 mmol) was dissolved in 5 ml of sodium hydroxide solution (pH = 11.0, solvent: D_2O), and the resulting mixture was gently refluxed for one hour. An aliquot of the resulting mixture was examined by ^1H NMR. The spectrum indicated complete conversion of the viologen substrate to unidentified decomposition products. 4,4'-dipyridyl 1,1'-dioxide was not present in the mixture.

2. The substrate dimethoxy viologen (7.8 mg, 0.02 mmol) and Hcy (11.5 mg, 0.085 mmol) were dissolved in 5 ml of sodium hydroxide solution (pH = 11.0, solvent: D_2O), and the resulting mixture was gently refluxed for one hour. An aliquot of the resulting mixture was examined by ^1H NMR. A similar spectrum was obtained except for the extra Hcy peaks.

3. The substrate dimethoxy viologen (40 mg, 0.10 mmol) was dissolved in 5 ml of the buffer solution (pH = 11.0, components: $\text{NaOH} + \text{NaHCO}_3$), and the resulting mixture was gently refluxed for one hour. After cooled down to room temperature, the mixture was extracted with chloroform (3×5 ml). The combined organic solvent was dried (MgSO_4), filtered and concentrated to give 4,4'-bipyridine (13.0 mg, 82%) as the major product.

4. The substrate dimethoxy viologen (16 mg, 0.04 mmol) and Hcy (23 mg, 0.17 mmol) were dissolved in 10 ml of the buffer solution (pH = 11.0, component: NaOH + NaHCO₃), and the resulting mixture was gently refluxed for one hour. After cooled down to room temperature, the mixture was extracted with chloroform (3 × 10 ml). The combined organic solvent was dried (MgSO₄), filtered and concentrated to give 4,4'-bipyridine (5.4 mg, 85%) as the major product. ¹H NMR(400 MHz, CDCl₃): δ 8.47 (d, J = 6.1 Hz, 4H), 7.57 (d, J = 6.1 Hz, 4H). ¹³C NMR (100 MHz, CDCl₃): δ 150.7, 145.5, 121.4.

5. The substrate dimethoxy viologen (16 mg, 0.04 mmol) was dissolved in 10 ml of sodium hydroxide solution (pH = 12.0), and the resulting mixture was gently refluxed for one hour. After cooled down to room temperature, the mixture was extracted with chloroform (3 × 10 ml). The combined organic solvent was dried (MgSO₄), filtered and concentrated to give 4,4'-bipyridine (5.2mg, 82%) as the major product. ¹H NMR(400 MHz, CDCl₃): δ 8.47 (d, J = 6.1 Hz, 4H), 7.57 (d, J = 6.1 Hz, 4H). ¹³C NMR (100 MHz, CDCl₃): δ 150.7, 145.5, 121.4.

1.7.4 Spectral Data

Spectral data are shown from the next page.

1.8 References

- [1] A. V. Glushchenko and D. W. Jacobsen, *Antioxid. Redox Signaling* **2007**, *9*, 1883-1898.
- [2] R. Janaky, V. Varga, A. Hermann, P. Saransaari and S. S. Oja, *Neurochem. Res.* **2000**, *25*, 1397-1405.
- [3] V. Gazit, R. Ben-Abraham, R. Coleman, A. Weizman and Y. Katz, *Amino Acids* **2004**, *26*, 163-168.
- [4] S. R. Lentz and W. G. Haynes, *Cleve. Clin. J. Med.* **2004**, *71*, 729-734.
- [5] a) A. De Bree, W. M. M. Verschuren, D. Kromhout, L. A. J. Kluijtmans and H. J. Blom, *Pharmacol. Rev.* **2002**, *54*, 599-618; b) O. Nekrassova, N. S. Lawrence and R. G. Compton, *Talanta* **2003**, *60*, 1085-1095; c) H. Refsum, A. D. Smith, P. M. Ueland, E. Nexo, R. Clarke, J. McPartlin, C. Johnston, F. Engbaek, J. Schneede, C. McPartlin and J. M. Scott, *Clin. Chem.* **2004**, *50*, 3-32.

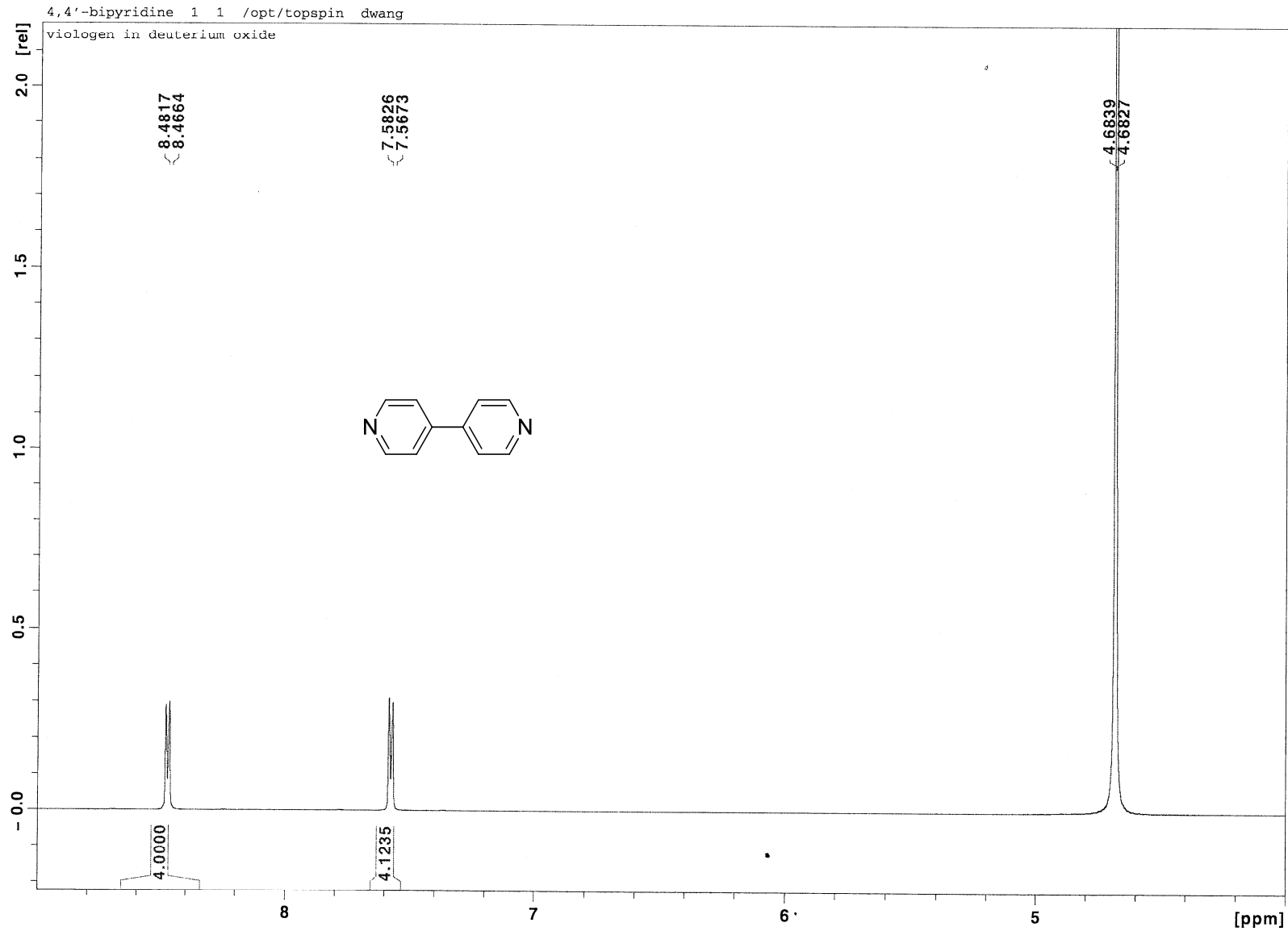


Figure 1.3 ^1H NMR (400 MHz, D_2O) of Viologen

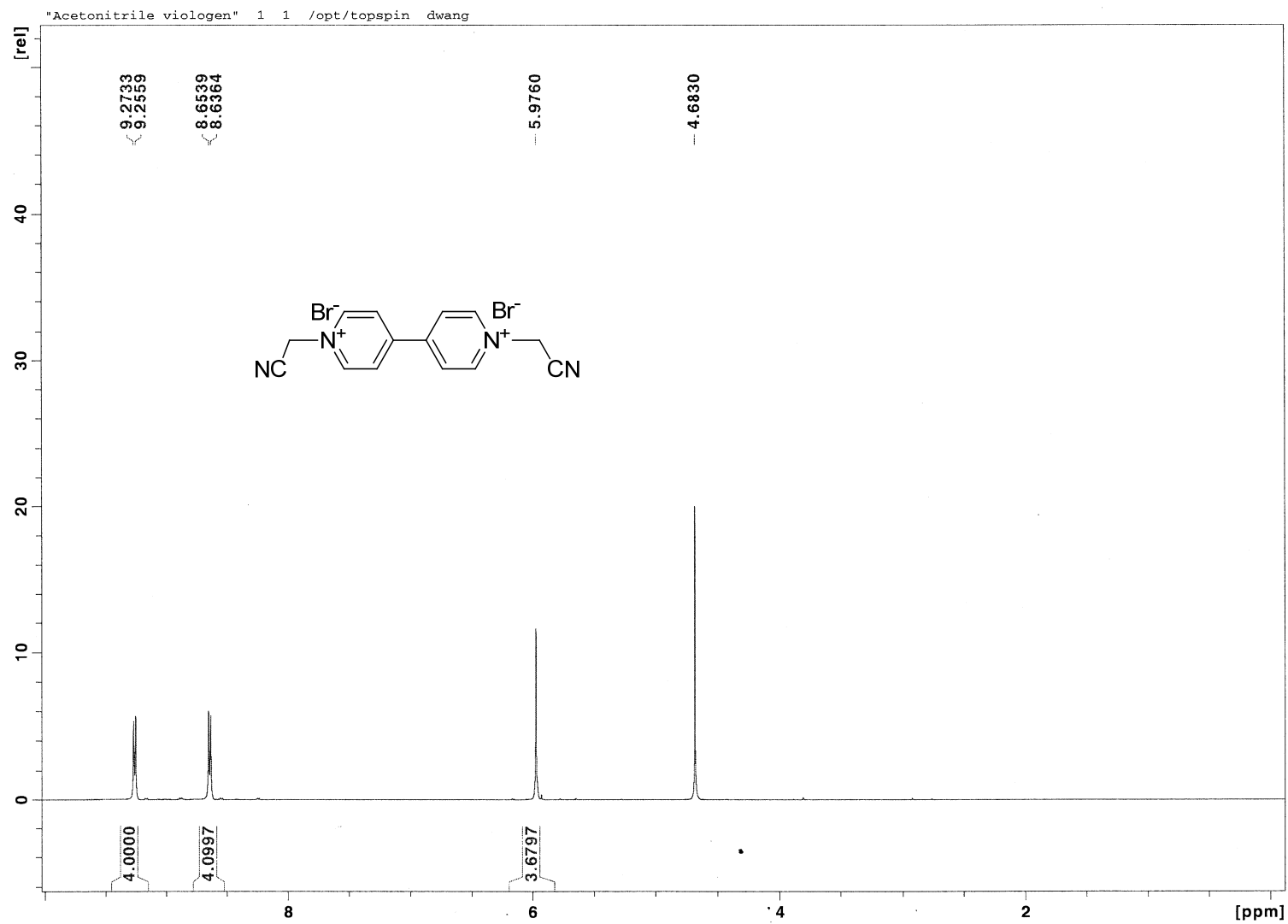


Figure 1.4 ^1H NMR (400 MHz, D_2O) of Cyanomethyl Viologen

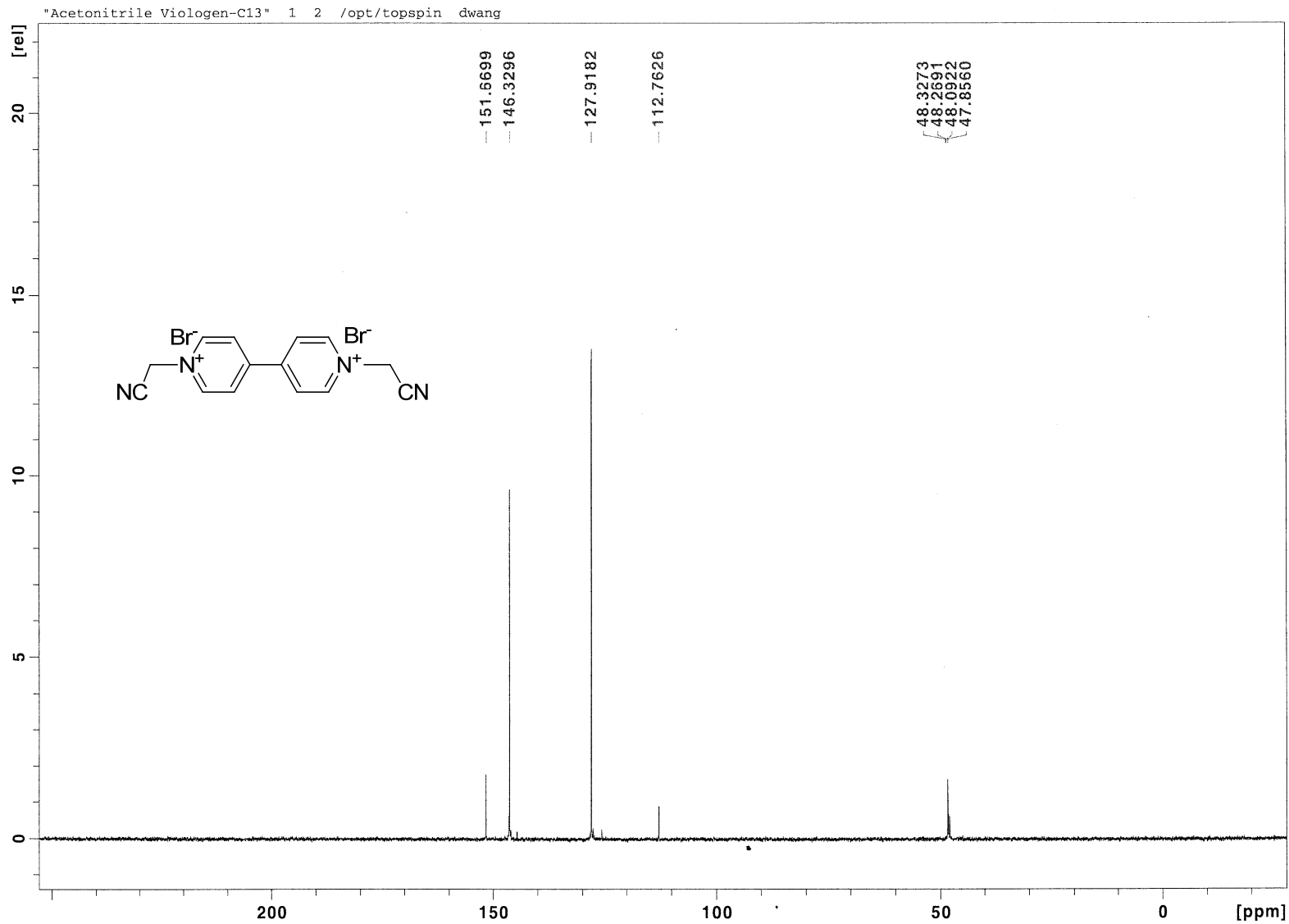


Figure 1.5 ^{13}C NMR (100 MHz, D_2O) of Cyanomethyl Viologen

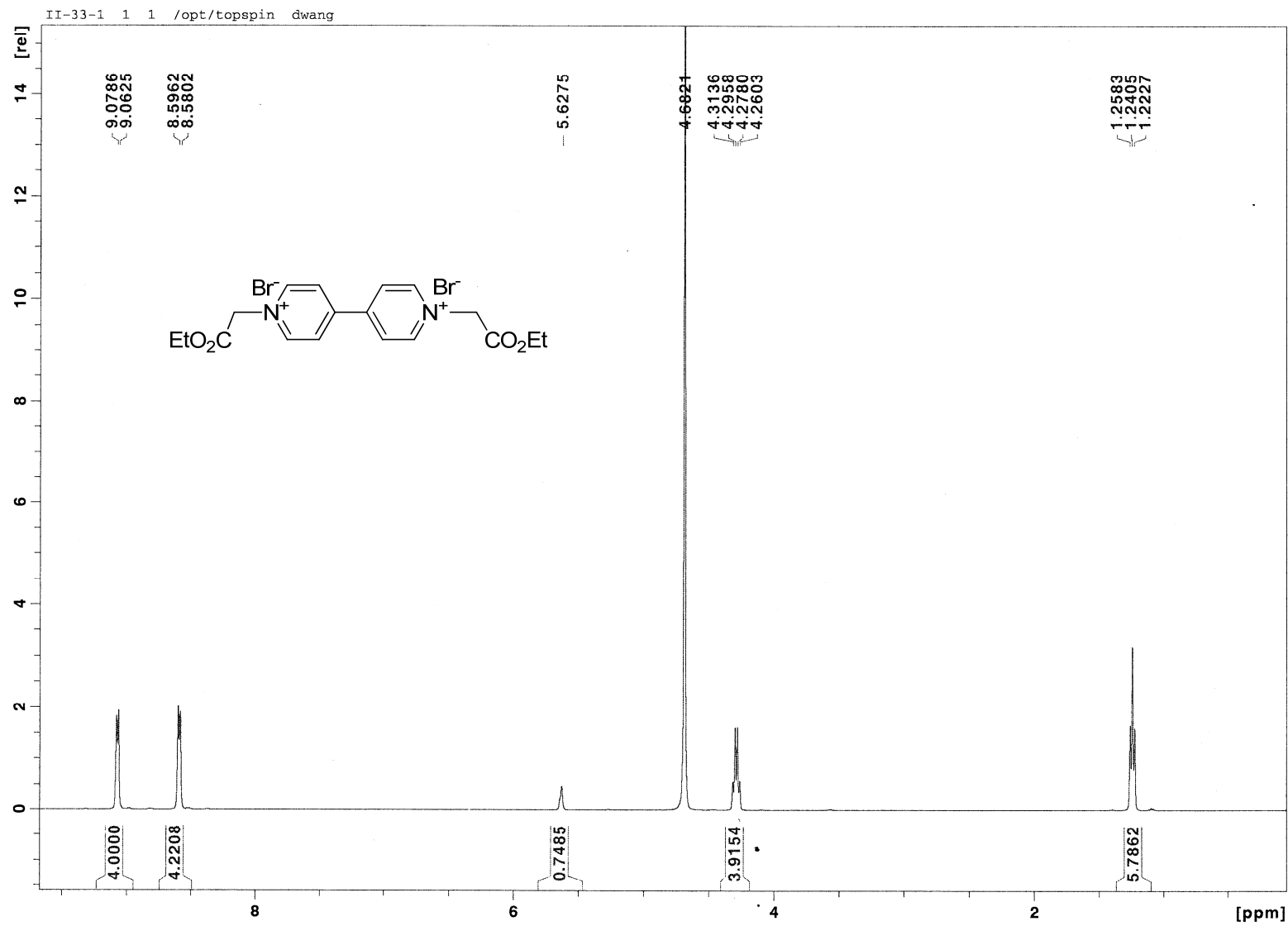


Figure 1.6 ^1H NMR (400 MHz, D_2O) of Diester Viologen

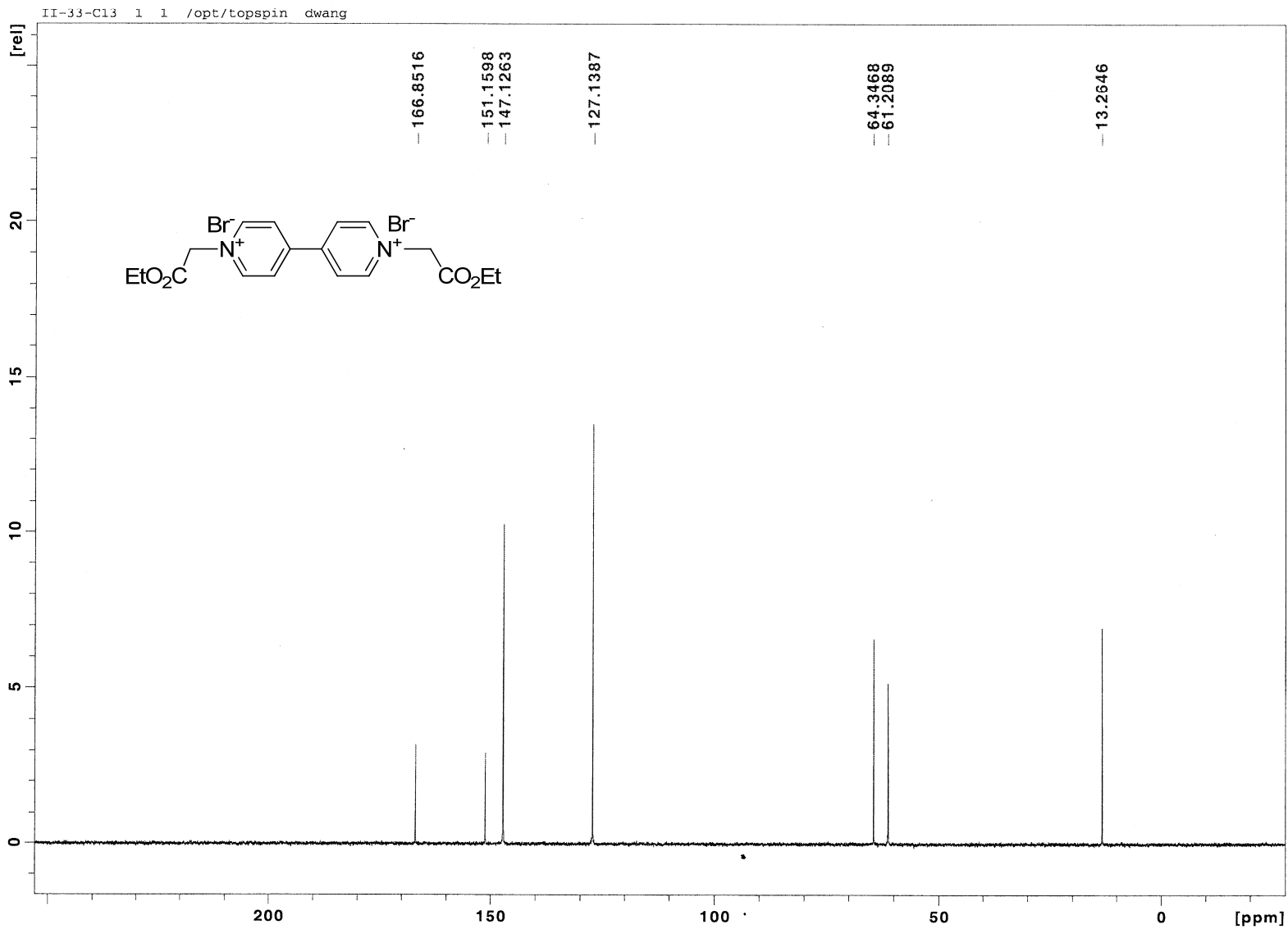


Figure 1.7 ^{13}C NMR (100 MHz, D_2O) of Diester Viologen

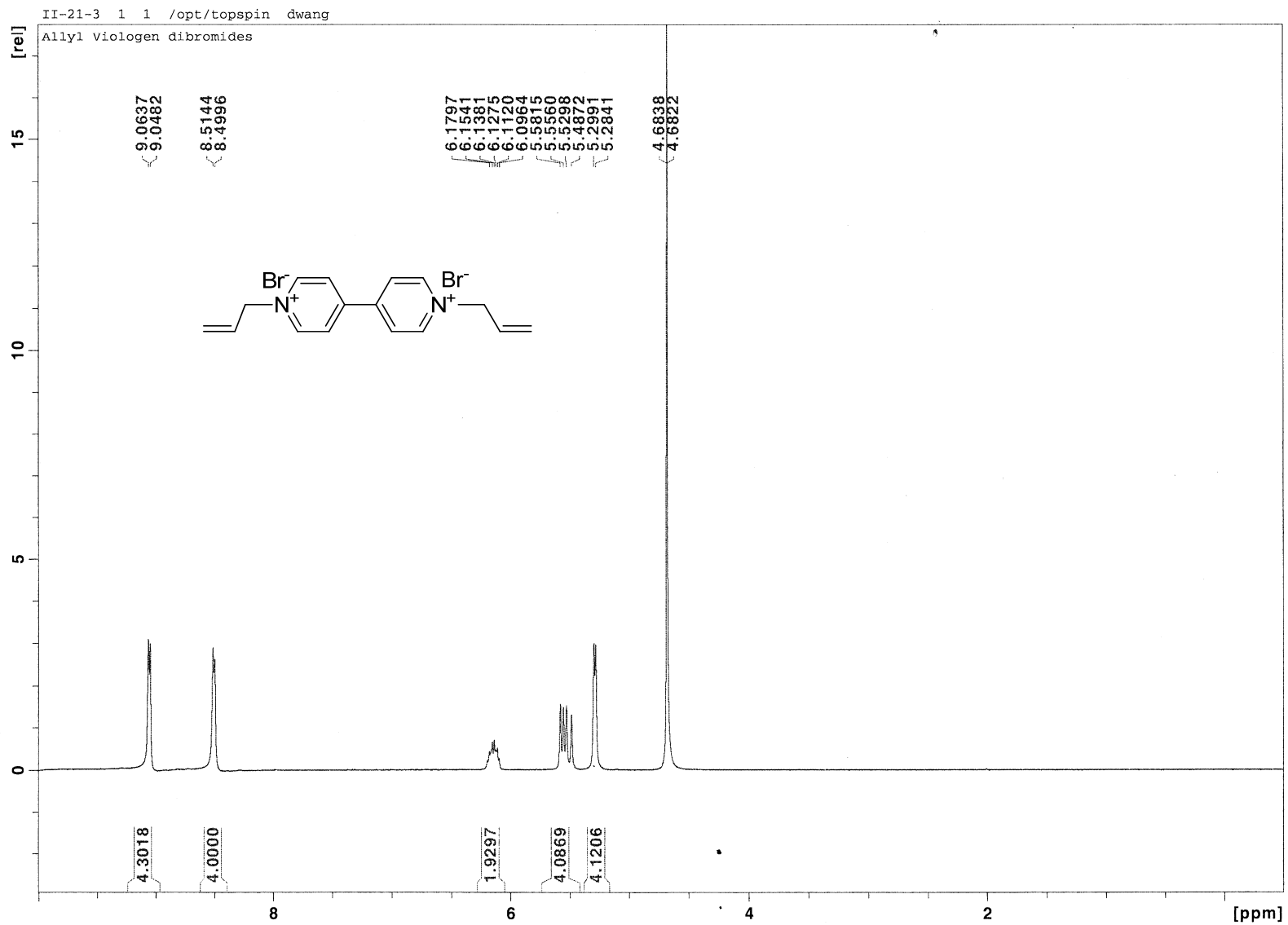


Figure 1.8 ^1H NMR (400 MHz, D_2O) of Allyl Viologen

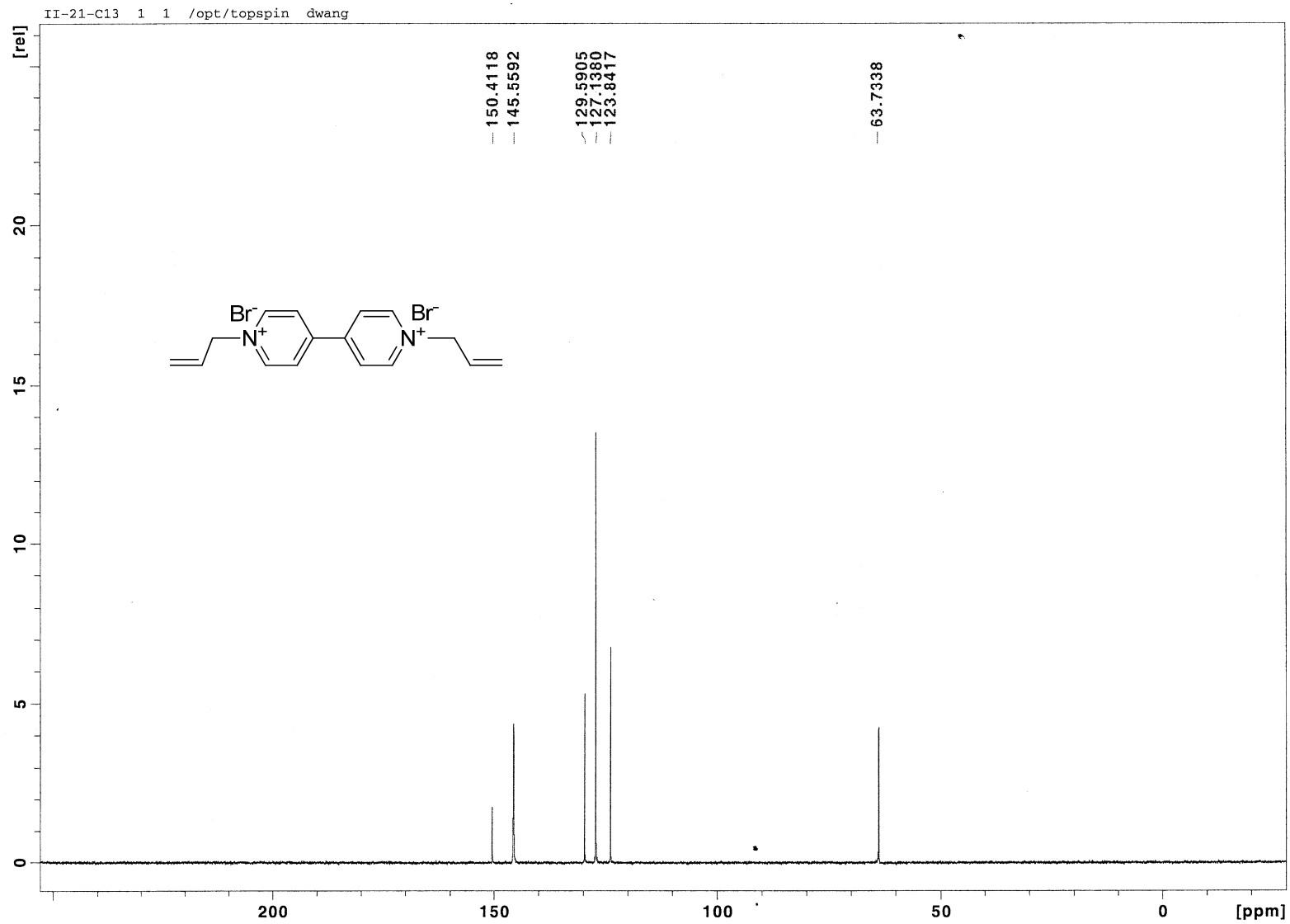


Figure 1.9 ^{13}C NMR (100 MHz, D_2O) of Allyl Viologen

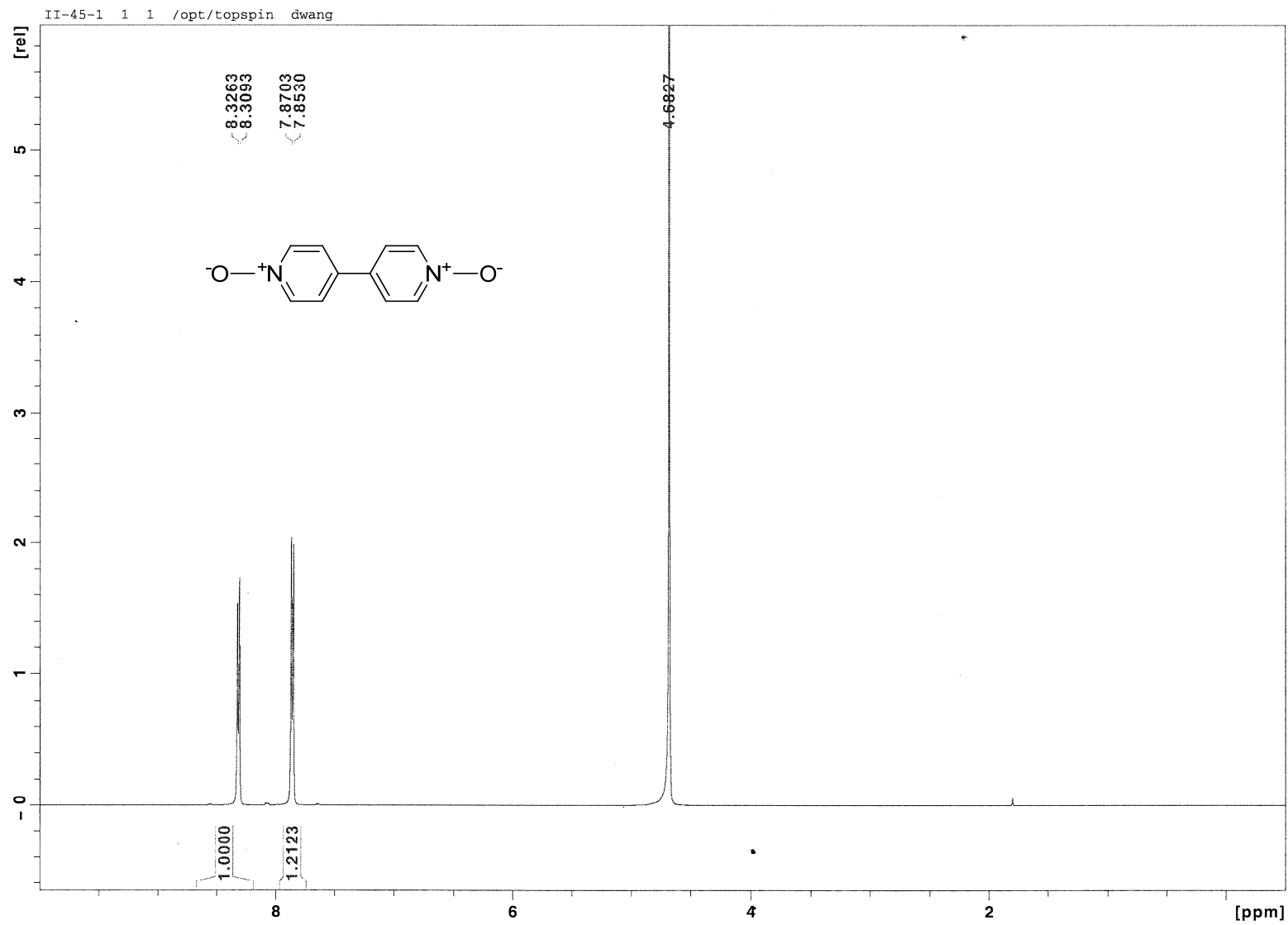


Figure 1.10 ^1H NMR (400 MHz, D_2O) of Dioxide Viologen

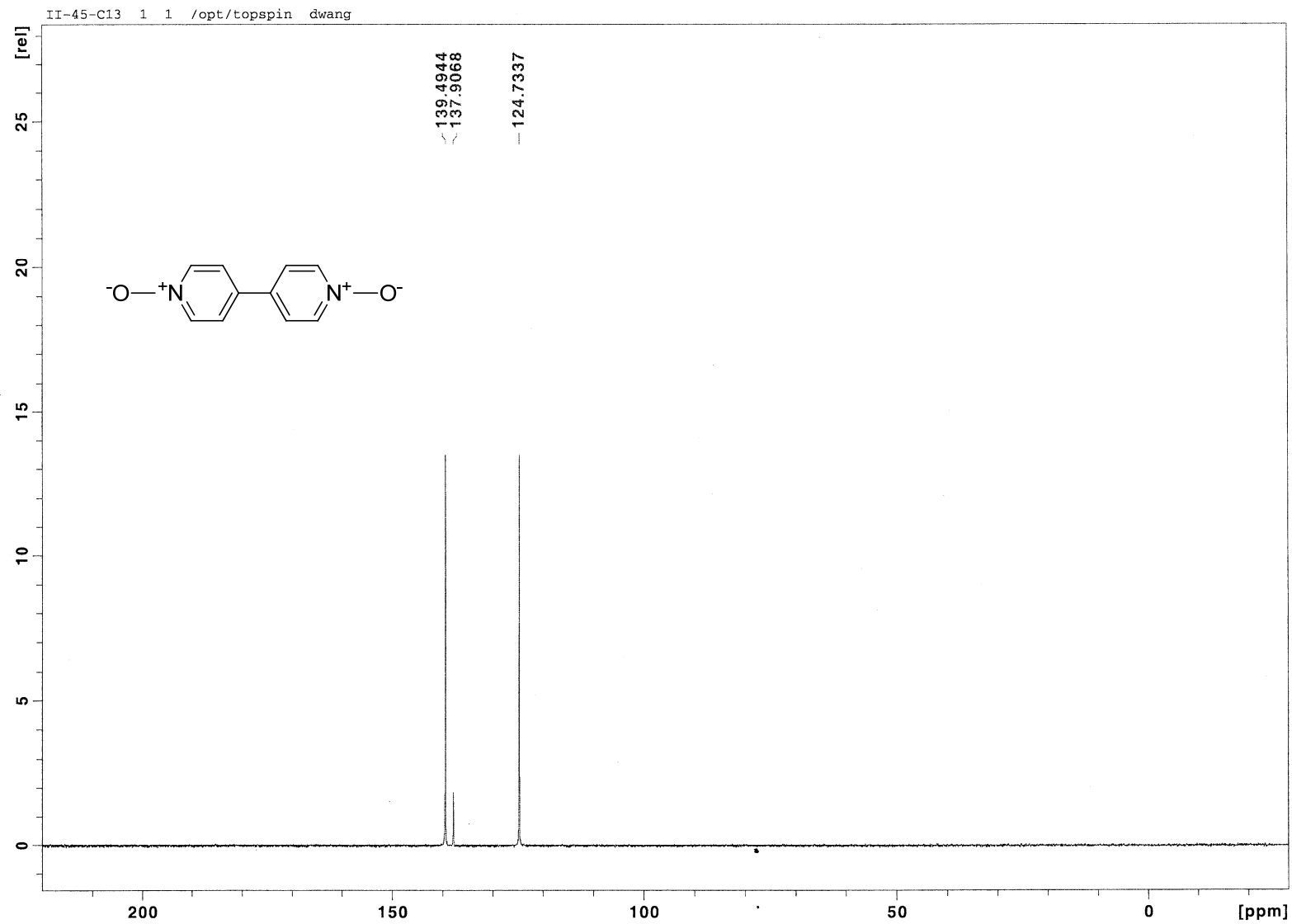


Figure 1.11 ^{13}C NMR (100 MHz, D_2O) of Dioxide Viologen

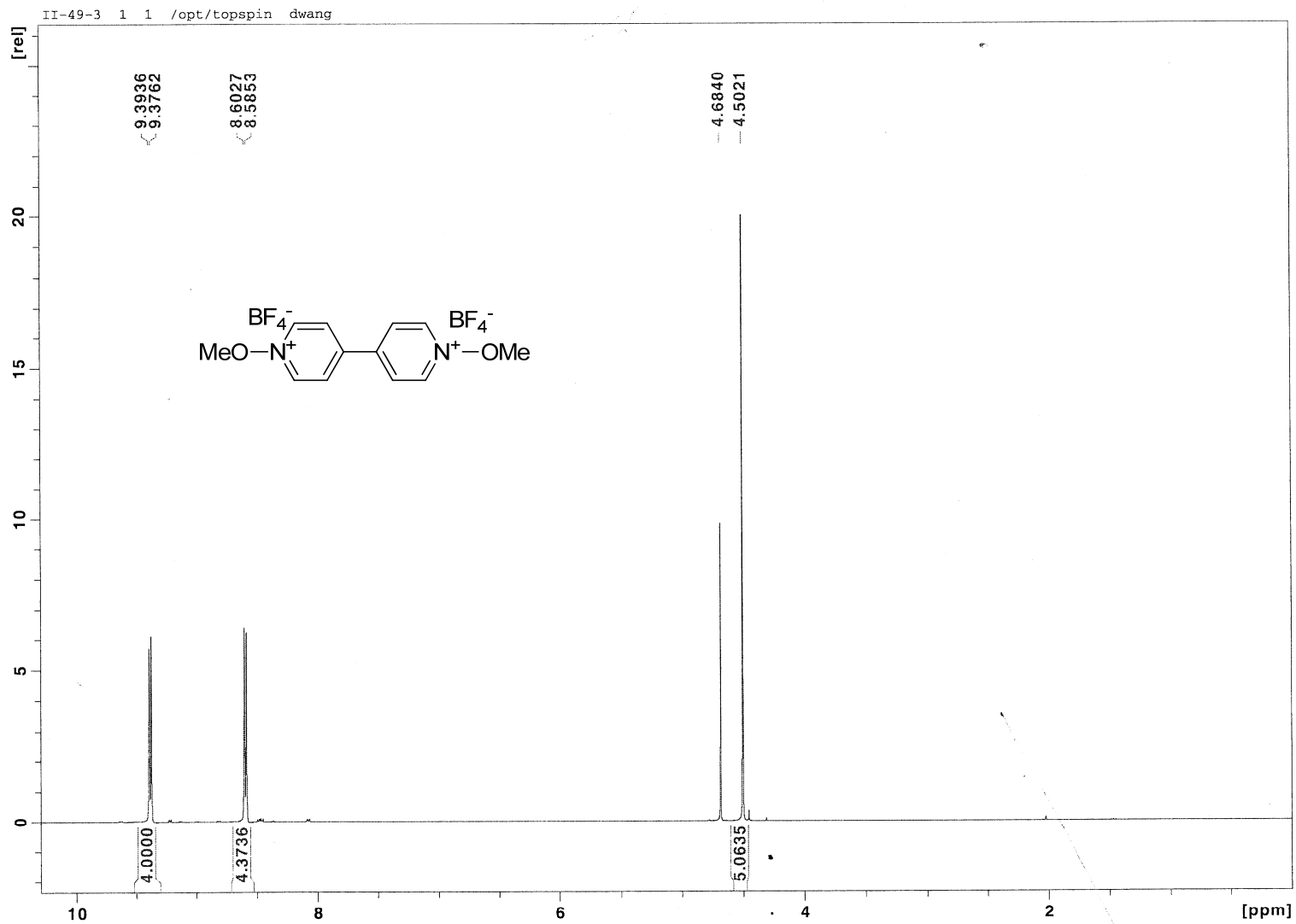


Figure 1.12 ^1H NMR (400 MHz, D_2O) of Dimethoxy Viologen

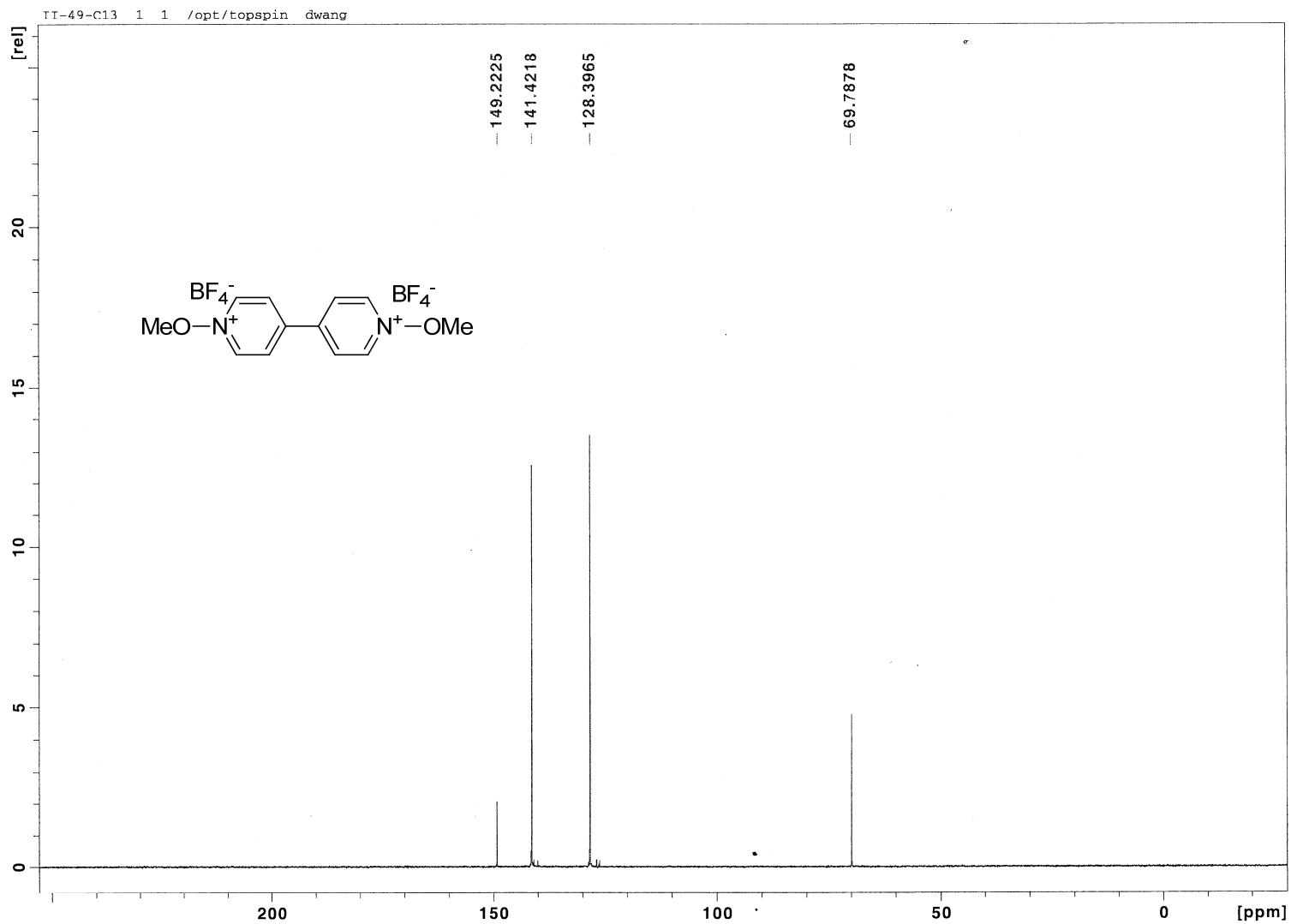


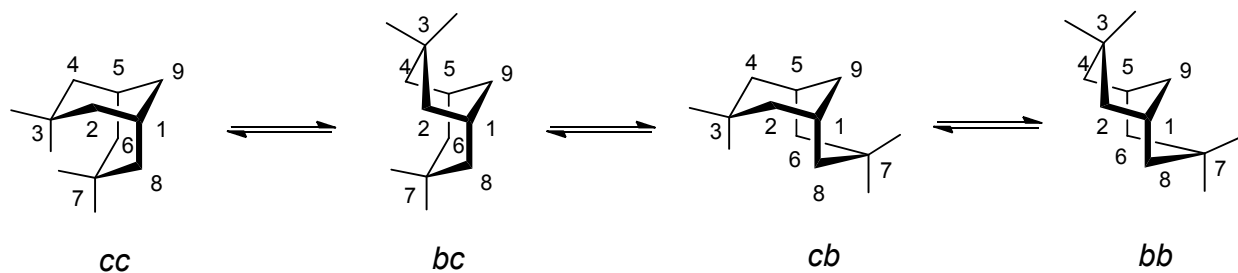
Figure 1.13 ^{13}C NMR (100 MHz, D_2O) of Dimethoxy Viologen

- [6] Z. Abedinzadeh, *Can. J. Physiol. Pharmacol.* **2001**, 79, 166-170.
- [7] a) C. Schoneich, K. D. Asmus, U. Dillinger and F. von Bruchhausen, *Biochem. Biophys. Res. Commun.* **1989**, 161, 113-120; b) C. Schoneich, U. Dillinger, F. von Bruchhausen and K. D. Asmus, *Arch. Biochem. Biophys.* **1992**, 292, 456-467.
- [8] L. Grierson, K. Hildenbrand and E. Bothe, *Int. J. Radiat. Biol.* **1992**, 62, 265-277.
- [9] a) R. Zhao, J. Lind, G. Merenyi and T. E. Eriksen, *J. Am. Chem. Soc.* **1994**, 116, 12010-12015; b) R. Zhao, J. Lind, G. Merenyi and T. E. Eriksen, *J. Chem. Soc., Perkin Trans. 2* **1997**, 569-574.
- [10] a) W. H. Wang, J. O. Escobedo, C. M. Lawrence and R. M. Strongin, *J. Am. Chem. Soc.* **2004**, 126, 3400-3401; b) W. H. Wang, O. Rusin, X. Y. Xu, K. K. Kim, J. O. Escobedo, S. O. Fakayode, K. A. Fletcher, M. Lowry, C. M. Schowalter, C. M. Lawrence, F. R. Fronczek, I. M. Warner and R. M. Strongin, *J. Am. Chem. Soc.* **2005**, 127, 15949-15958.
- [11] C. L. Bird and A. T. Kuhn, *Chem. Soc. Rev.* **1981**, 10, 49-82.
- [12] P. Wardman, *J. Phys. Chem. Ref. Data.* **1989**, 18, 1637-1755.
- [13] a) J. Bruinink, C. G. A. Kregting and J. J. Ponjee, *J. Electrochem. Soc.* **1977**, 124, 1854-1858; b) M. Kijima, A. Sakawaki and T. Sato, *Bull. Chem. Soc. Jpn.* **1994**, 67, 2323-2325.
- [14] E. D. Lorance, W. H. Kramer and I. R. Gould, *J. Am. Chem. Soc.* **2002**, 124, 15225-15238.
- [15] W. Feely, W. L. Lehn and V. Boekelheide, *J. Org. Chem.* **1957**, 22, 1135-1135.
- [16] M. E. Houston, Jr. and J. F. Honek, *J. Chem. Soc., Chem. Commun.* **1989**, 761-762.

CHAPTER 2 STUDIES ON THE SYNTHESIS OF BICYCLO[3.3.1]NONANES*

2.1 Introduction

The framework of bicyclo[3.3.1]nonanes are quite common in nature as a constituent of many naturally and biologically active products or their metabolites.^[1] Biosynthetic pathway of many sesquiterpenoids and other naturally occurring materials involve formation and transformation of this framework.^[2]



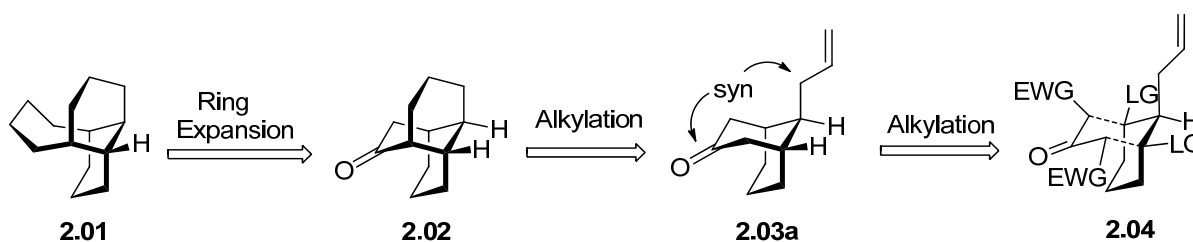
Scheme 2.1 Conformations of Bicyclo[3.3.1]nonanes

Moreover, the bicyclo[3.3.1]nonane system shows interesting conformational features (Scheme 2.1).^[3] Three groups of conformations must be envisaged: (1) the rigid double-chair (*cc*), in which a severe interaction between H_{3a} and H_{7a} occurs, (2) the rigid chair-boats (*cb*, *bc*), and (3) the flexible double-boat conformations (*bb*). It is obvious that substituents at the 3- and 7-positions have a strong influence on the conformational preferences. The unsubstituted, the 3e- or 7e-, and the 3e,7e-substituted compounds occur predominantly in a strongly flattened *cc* conformation. A 3a- or 7a-substituent forces the wing concerned into the boat conformation. When both the 3a- and 7a-positions are substituted, the conformational preference depends on the steric requirements of these substituents. With bulky substituents, the *bb* conformation predominates, whereas with small substituents the *cb* and the *bc* conformations may also be populated.

* Portions of this chapter are printed by permission of Organic Letters.

Due to this important structural feature, the chemistry of bicyclo[3.3.1]nonanes has received much attention from synthetic and theoretical points of view. Indeed, a lot of efficient and highly stereoselective synthetic methods to access this framework have been established.^[4] The synthetic methods typically include annulation of cyclohexanone derivatives, annulation of cyclooctane derivatives, tandem Michael addition and related reactions, ring cleavage of adamantane derivatives, *et al.* However, introduction of a stereocenter at the one-carbon bridge has rarely been reported and remains an unsolved problem. Herein, our research will be focused on this problem.

2.2 First Generation on Approach to Bicyclo[3.3.1]nonanes

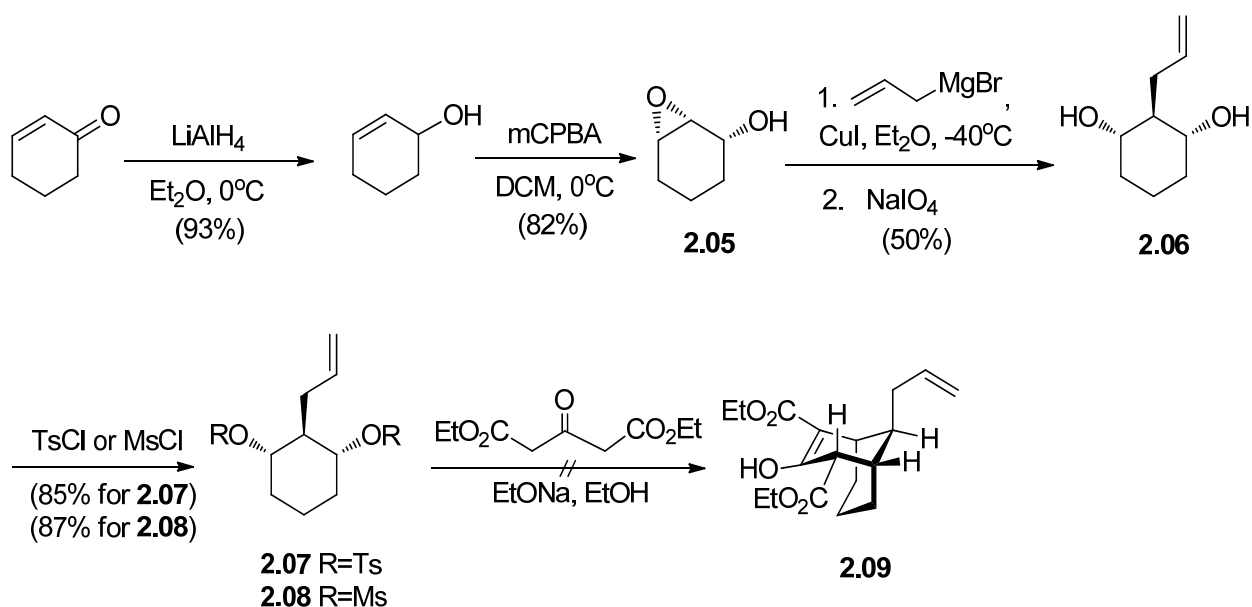


Scheme 2.2 Retrosynthetic Analysis of the Tricyclic Core of Vinigrol

Interest in ring system **2.01**, present in the natural product vinigrol^[5] prompted us to investigate the two-carbon ring expansion of a tricyclic precursor **2.02** which we envisioned could be prepared from an appropriately substituted bicyclo[3.3.1]nonane **2.03a** via an intramolecular alkylation (Scheme 2.2). According to Baldwin, such a 6-exo-tet cyclization should prove favorable.^[6] Since the stereochemistry at the one-carbon bridge of the bicyclo[3.3.1]nonane is critical for the intramolecular alkylation, we explored this stereoselectivity carefully.

The bicyclic **2.03a** in turn could be prepared by an intermolecular alkylation between **2.04** and activated form of acetone. If the reaction occurs via a S_N2 pathway, we will be able to construct **2.03a** with the desired stereoselectivity.

As the first step in the synthesis (Scheme 2.3), the allyl alcohol was prepared by reduction of the commercially available 2-cyclohexenone with LAH in Et₂O. Subsequent hydroxy directed epoxidation^[7] afforded the *cis*-epoxide alcohol **2.05**. Next, considering the possible regioselectivity issue associated with allyl metal opening of the epoxide **2.05**, the reaction was carefully studied with various conditions. Although this regioselectivity problem was encountered by the previous literature,^[8] no general method to solve the problem has yet been reported.

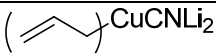
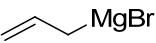
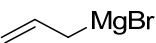
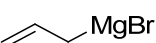
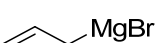


Scheme 2.3 Initial Efforts toward the Synthesis of Bicyclo[3.3.1]nonane

As can be seen in Table 2.1, when compound **2.05** was treated with allyl cuprates or higher order cuprates, the 1,2-diol was formed as the major product. In comparison, allyl magnesium bromide with copper iodide as the catalyst gave the 1,3-diol **2.06** as the major product (Table 2.1, entry 2). THF seems to be harmful to the regioselectivity (1,2-diol is the major product for entry 1 and entry 4). Although the selectivity is poor, the yield is acceptable and the two regioisomers can be easily separated by treating the mixture with sodium periodate. Double tosylation of the diol **2.06** gave **2.07**.

Efforts towards the synthesis of the bicyclic **2.09** from sulfonate ester **2.07** were unsuccessful. Both tosylate **2.07** and mesylate **2.08** did not react at all. The reluctance of **2.07** or **2.08** to undergo alkylation may be due to the steric hindrance of the electrophilic carbon, which is a secondary carbon next to a tertiary carbon. We tried to facilitate the reaction by replacing tosylate with triflate, a better leaving group. Unfortunately, the triflate was readily decomposed in the preparation.

Table 2.1 Allyl-Metal Opening of the Epoxide

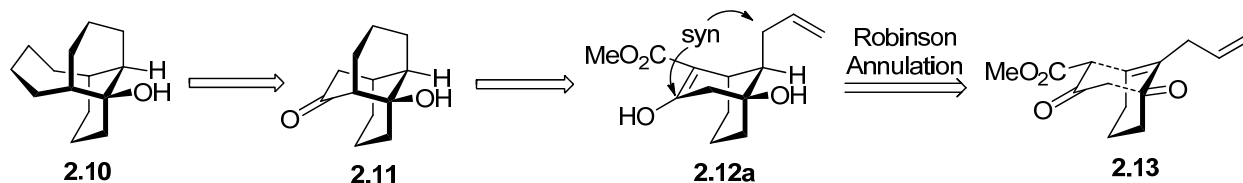
Entry	Allyl Metal	Additive	Solvent	Temp.	Ratio ^a (1,3/1,2-diol)	Yield ^b
1		None	THF	-40°C	1:2	86%
2		CuI	Et ₂ O	-40°C	5:4	90%
3		CuI	Et ₂ O : THF= 6:1	-40°C	4:5	90%
4		CuI	THF	-40°C	5:6	91%
5		None	Et ₂ O	25 °C	1:1	90%

^a Ratio is based on the crude products NMR

^b This is the total yield of the two diols

2.3 Revised Approach to Bicyclo[3.3.1]nonanes

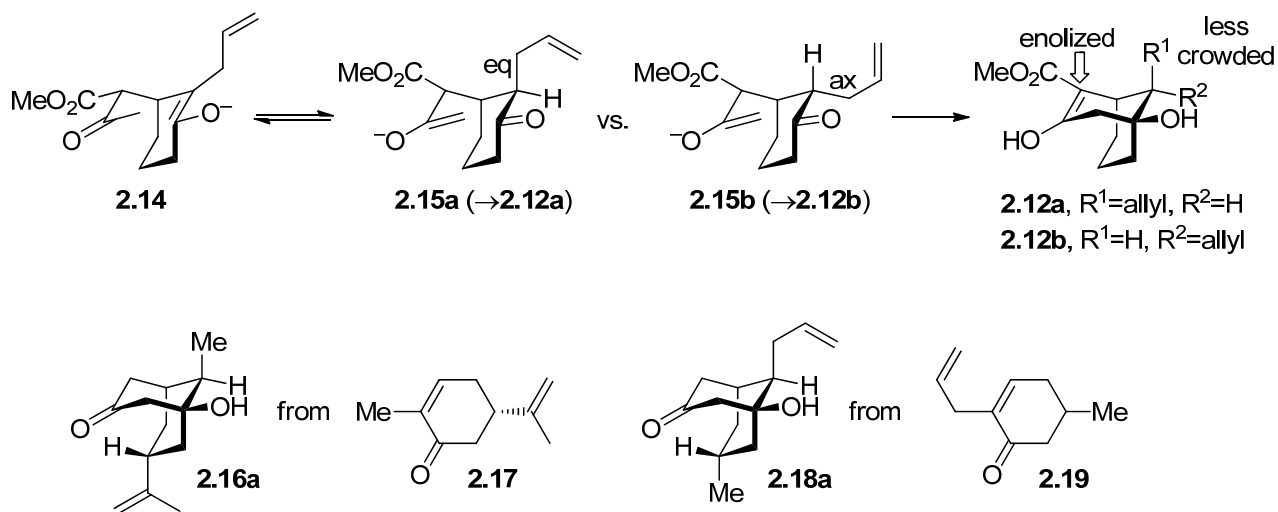
2.3.1 One-Carbon Bridge Stereocontrol in Forming Bicyclo[3.3.1]nonanes



Scheme 2.4 Retrosynthetic Analysis of the Tricyclic Core of Vinigrol

Different from the first generation, we envisioned that the bicyclo[3.3.1]nonanol **2.12a**, whose hydroxyl group does present in the natural product vinigrol, could be generated by a

Robinson annulation reaction (Scheme 2.4). Thus we explored the Robinson annulation depicted schematically in structure **2.13** as a route to **2.12a** paying special attention to the stereochemistry of the allyl group attached to the one-carbon bridge.

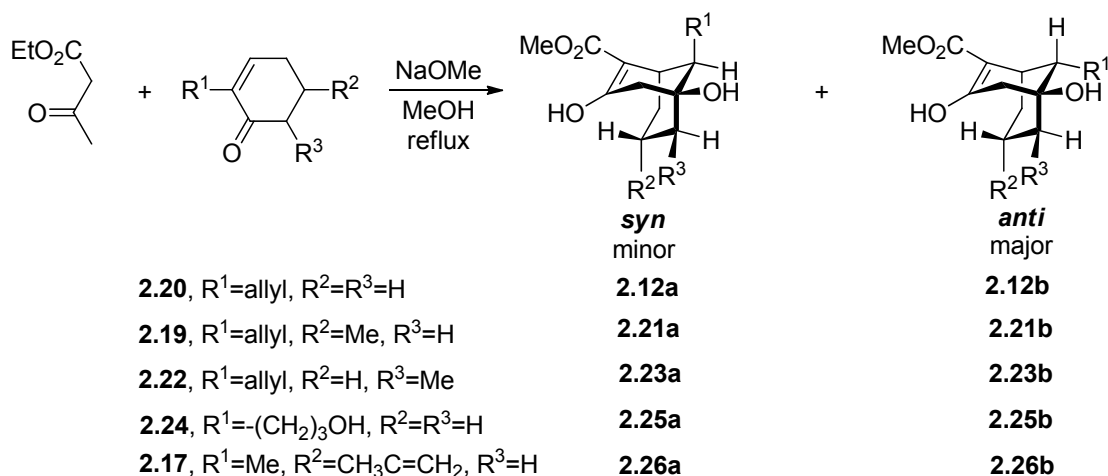


Scheme 2.5 Stereochemistry Governed by the Competing Aldol Reactions

Stereochemistry at the one-carbon bridge will be governed by the competition of aldol ring closure reactions of diastereomeric intermediates **2.15a** and **2.15b** formed from Michael adduct **2.14** (Scheme 2.5). There are several lines of reasoning that might lead one to expect that the aldol ring closure of **2.15a**, leading to the desired stereochemistry present in **2.12a**, might be the favored pathway. First, the reactive conformer of **2.15a** (equatorial allyl) should be more stable than that of **2.15b** (axial allyl). Second, Robinson annulation product **2.12a** (derived from **2.15a**) is more stable than its epimer **2.12b** (derived from **2.15b**) due to the enolization of the keto ester which removes a 1,3-diaxial interaction involving the allyl group. Indeed, two similar Robinson annulations previously reported provide precedent for the major product possessing the desired stereochemistry **2.12a**. Theobald reported that **2.16a** is the major product formed by annulation of (*S*)-carvone (**2.17**) with ethyl acetoacetate, followed by saponification and decarboxylation.^[9] Kraus reported that **2.18a** was the major product (>20:1 diastereoselectivity)

formed from the analogous annulation/decarboxylation sequence utilizing 2-allyl-5-methyl-2-cyclohexenone (**2.19**).^[10]

Table 2.2 Stereochemical Outcome of Robinson Annulations Leading to Bicyclo[3.3.1]nonanes



Entry	Starting material	Ratio (a/b) ^a	Total yield (%)
1	2.20 ^b	1:4.3	54
2	2.19 ^c	1:3.5	42
3	2.22 ^d	1:4.9	31
4	2.24 ^e	1:5	43
5	2.17 ^f	1:4	56

^a The ratio is based upon the ¹H NMR of the crude product.

^b The compound is prepared according to literature.^[11]

^c The compound is prepared according to literature.^[12]

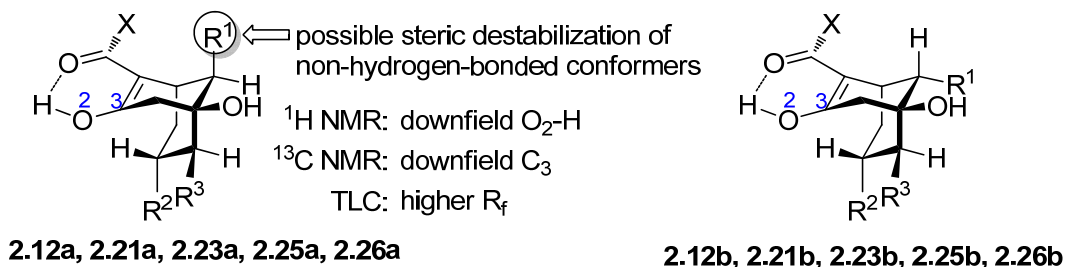
^d The compound is prepared by methylation of compound **2.20**.^[13]

^e The compound is prepared by hydroboration-oxidation of compound **2.20** using Cy₂BH·THF according to a known procedure.^[14]

^f (S)-carvone is commercially available.

To our surprise the Robinson annulation reaction of ethyl acetoacetate with 2-allyl-2-cyclohexenone (**2.20**) gave **2.12b** (*anti*), rather than **2.12a** (*syn*), as the major product (Table 2.2, entry 1). Repeating the Robinson annulation originally reported by Kraus, we were also surprised to find that **2.21b** (*anti*) was the major diastereomer obtained in the reaction of ethyl acetoacetate

with 2-allyl-5-methyl-2-cyclohexenone, **2.19** (entry 2). In order to directly compare our selectivity to the Kraus result, the **2.21b/2.21a** mixture was decarboxylated to produce a **2.18b/2.18a** mixture with the same diastereomer ratio and **2.18b** (*anti*) rather than **2.18a** (*syn*) as the major product. Compound **2.23b** (*anti*) was the major diastereomer obtained in the reaction of ethyl acetoacetate with 2-allyl-6-methyl-2-cyclohexenone, **2.22** (entry 3). Neither the substituent on cyclohexane ring (entries 1-3) nor the substituent at the one carbon bridge (entries 4-5) significantly influences stereoselectivity. In the reaction of ethyl acetoacetate with **2.24** (3-hydroxypropyl is the substituent at the one-carbon bridge) and (S)-carvone (**2.17**), the *anti* diastereomers **2.25b** and **2.26b** are the major products formed. The configuration of the one carbon bridge center has been unambiguously assigned according to the X-ray crystal analysis of compounds **2.21b**, **2.23b**, and **2.26b** (Figure 2.1, 2.2 and 2.3).



Scheme 2.6 Comparative Features of the Two Diastereomers Formed from the Robinson Annulation

It is worth mentioning that, for a mixture of diastereomers formed in a Robinson annulation reaction, we can quickly assign the configuration of the one-carbon bridge stereocenter on the basis of the relative positions of NMR signals for the enolic protons and carbons ($\text{O}_2\text{-H}$ and C_3 ; see Scheme 2.6). In each case that we've examined, both the $\text{O}_2\text{-H}$ and C_3 chemical shifts of the minor diastereomer (*syn*, **a** series) are downfield to those of the major diastereomer (*anti*, **b** series). Another trend that we have observed is that the minor diastereomers are consistently less polar (higher R_f on TLC, shorter retention time in column chromatography) than the major diast-

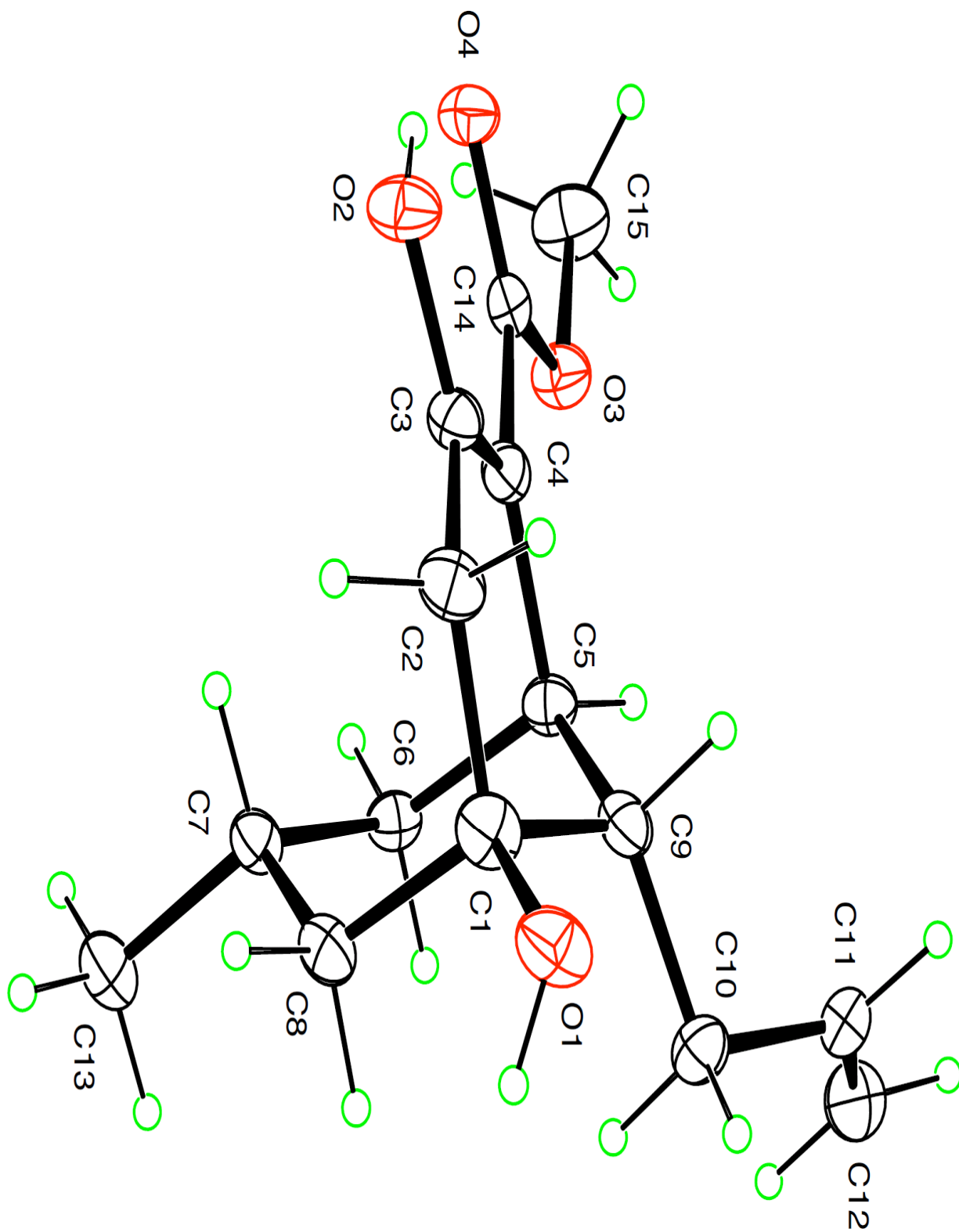


Figure 2.1 ORTEP Plot of Bicyclo[3.3.1]nonane 2.21b

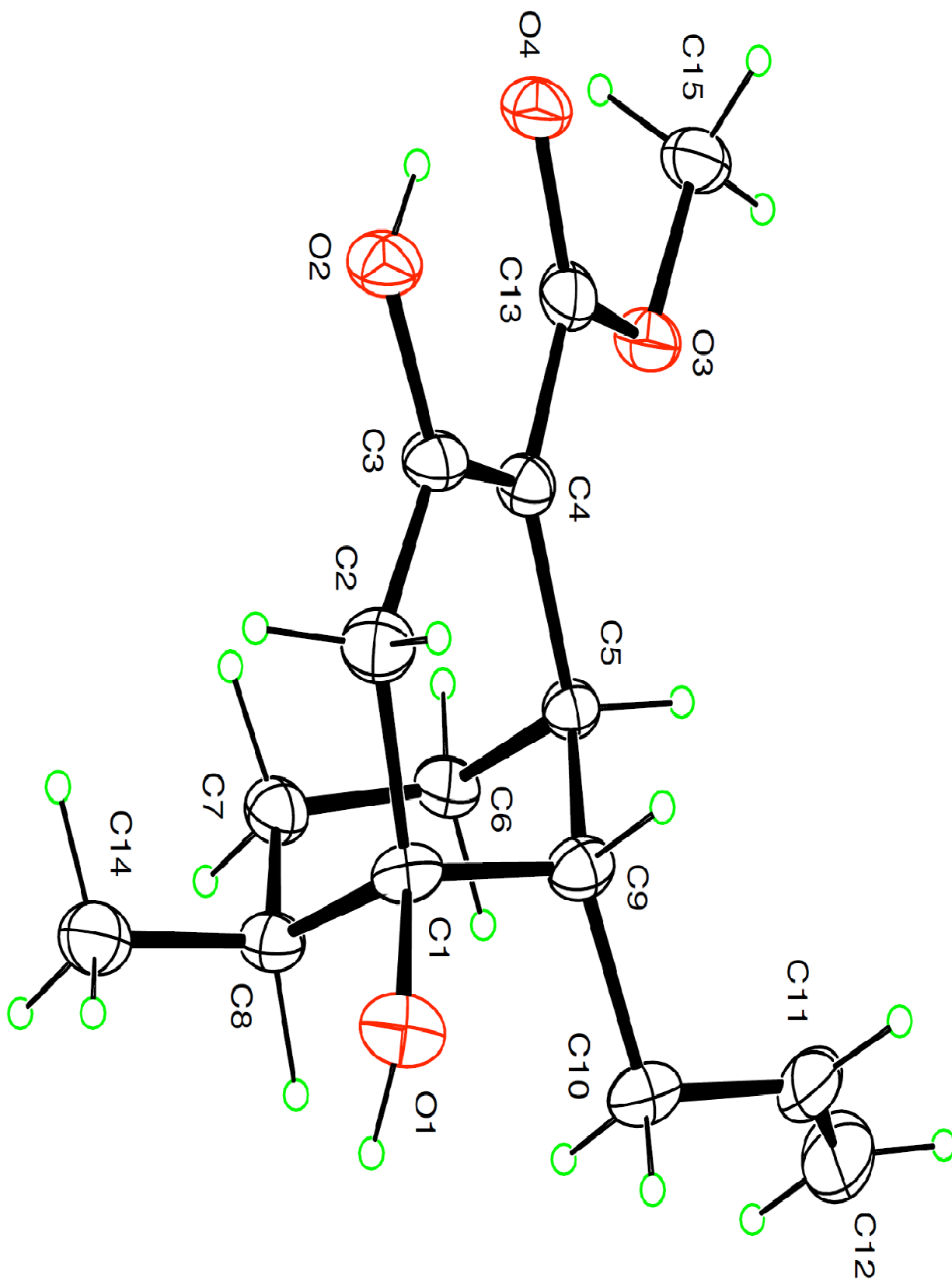


Figure 2.2 ORTEP Plot of Bicyclo[3.3.1]nonane 2.23b

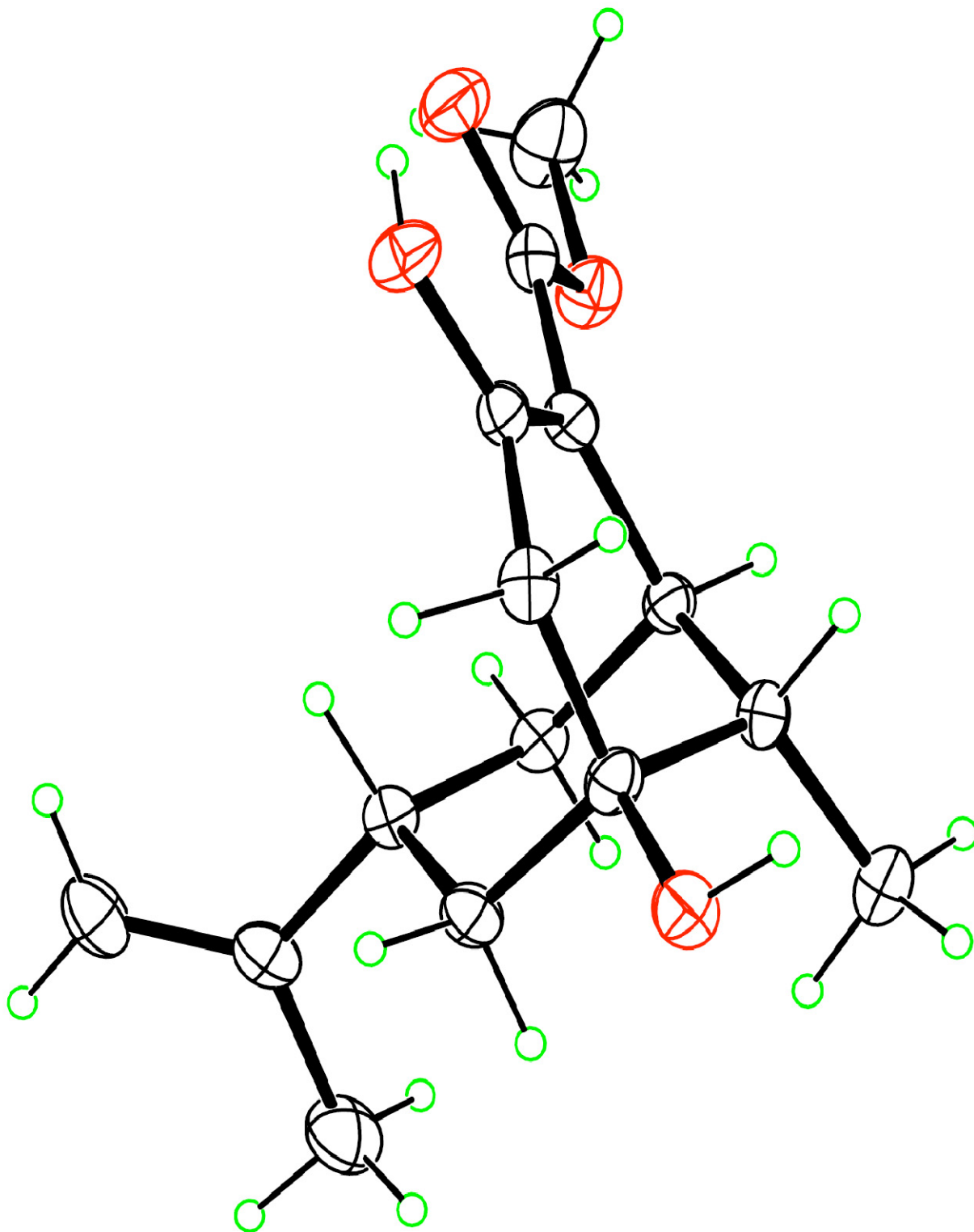


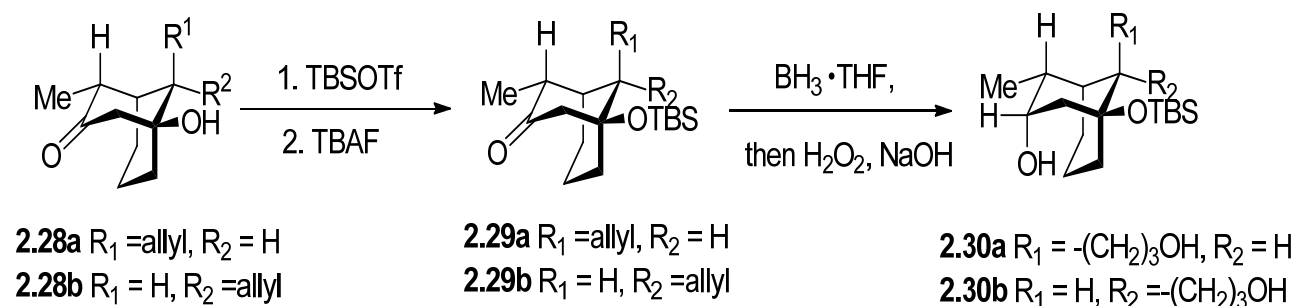
Figure 2.3 ORTEP Plot of Bicyclo[3.3.1]nonane 2.26b

ereomers. Collectively, this data is consistent with conformational equilibrium where the relative stability of hydrogen-bonded conformers is greater for the minor diastereomers. The one-carbon bridge substituent could influence such an equilibrium by sterically destabilizing non-hydrogen bonded conformers.

The unanticipated stereoselectivity appears to be kinetically controlled since major *anti* products (**2.12b**, **2.21b**, **2.23b**, **2.25b**, and **2.26b**) are higher in energy than diastereomeric minor *syn* products (**2.12a**, **2.21a**, **2.23a**, **2.25a**, and **2.26a**). Stereoselectivity also correlates with the expected rate of the aldol ring closure where the major products result from reactions which place the substituent α to the reacting ketone *anti* to the approaching enolate (e.g., **2.15b**→**2.12b** in Scheme 2.5).

2.3.2 Epimerization of the One-Carbon Bridge Stereocenter

While exploring the reaction chemistry of Robinson annulation products we discovered an interesting epimerization reaction which might provide an alternative stereocontrol motif which can influence the stereochemistry of the substituent at the one carbon bridge. It turns out that the decarboxylation reaction of **2.27** is slow and base sensitive (see Table 2.3).^[15] Treatment of a 1:4.3 mixture of **2.27a** and **2.27b** with refluxing methanolic KOH (3 equiv, 24 hr) produced a 1:1 mixture of decarboxylation products **2.28a** and **2.28b** (Table 2.3, entry 3). In contrast, if **2.27** was treated with slightly excess base, no epimerization was observed (Table 2.3, entries 1-2).

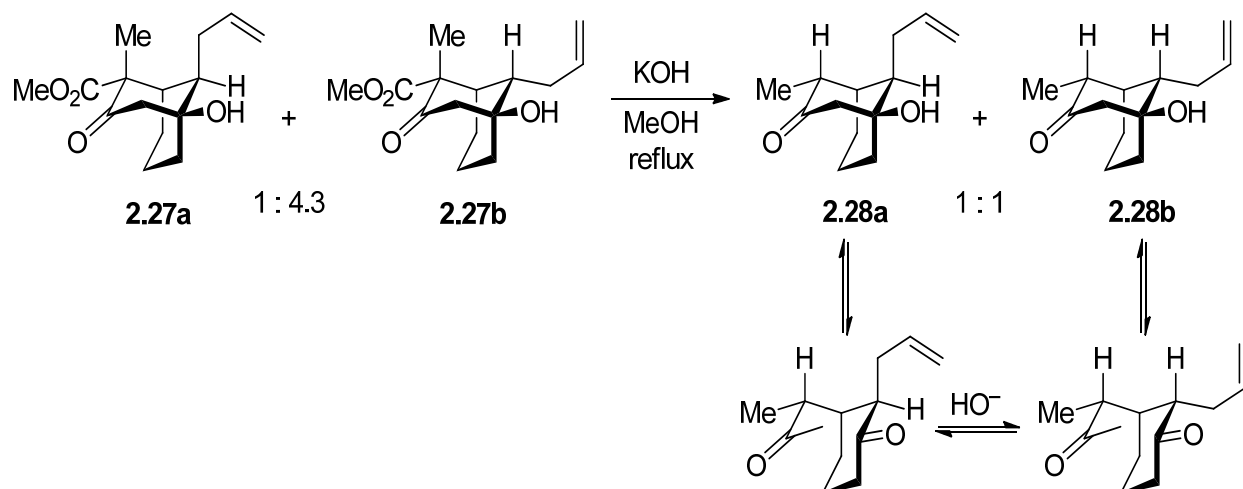


Scheme 2.7 Preparation of the Crystalline Diols 2.30 Derivatived from Ketone 2.28

Subjection of diastereomerically pure **2.28a** or **2.28b** to the same reaction conditions leads to the same 1:1 mixture (Table 2.3, entries 4-5) suggesting that the final product ratio represents thermodynamic control. We propose that this isomerization takes place via a retro-aldol reaction followed by base catalyzed epimerization of the ring opened diketones.

The epimerized products **2.28a** and **2.28b** has been confirmed by single crystal X-ray analysis of its corresponding derivatives **2.30a** and **2.30b** (see Scheme 2.7 for the reactions, and see Figure 2.4 and Figure 2.5 for the crystal structures).

Table 2.3 Stereochemical Outcome of Base-Catalyzed Epimerization of the One-Carbon Bridge Stereocenter



Entry	Substrate (ratio)	Reaction Condition	Product (ratio) ^a	Total Yield
1	2.27 (1 : 4.3)	1.1 eq. KOH(aq), MeOH, 12hs	2.28 (1 : 4.3)	60%
2	2.27 (1 : 4.3)	1.5 eq. KOH(aq), MeOH, 24hs	2.28 (1 : 4.3)	96%
3	2.27 (1 : 4.3)	3 eq. KOH(aq), MeOH, 24hs	2.28 (1 : 1)	90%
4	2.28a (pure)	3 eq. KOH(aq), MeOH, 24hs	2.28 (1 : 1)	91%
5	2.28b (pure)	3 eq. KOH(aq), MeOH, 24hs	2.28 (1 : 1)	90%
6	2.27 (1:4.3)	6 eq. KOH(aq), MeOH, 24hs	2.28 (1 : 1)	70%

^a The ratio is based upon the ¹H NMR of the crude products

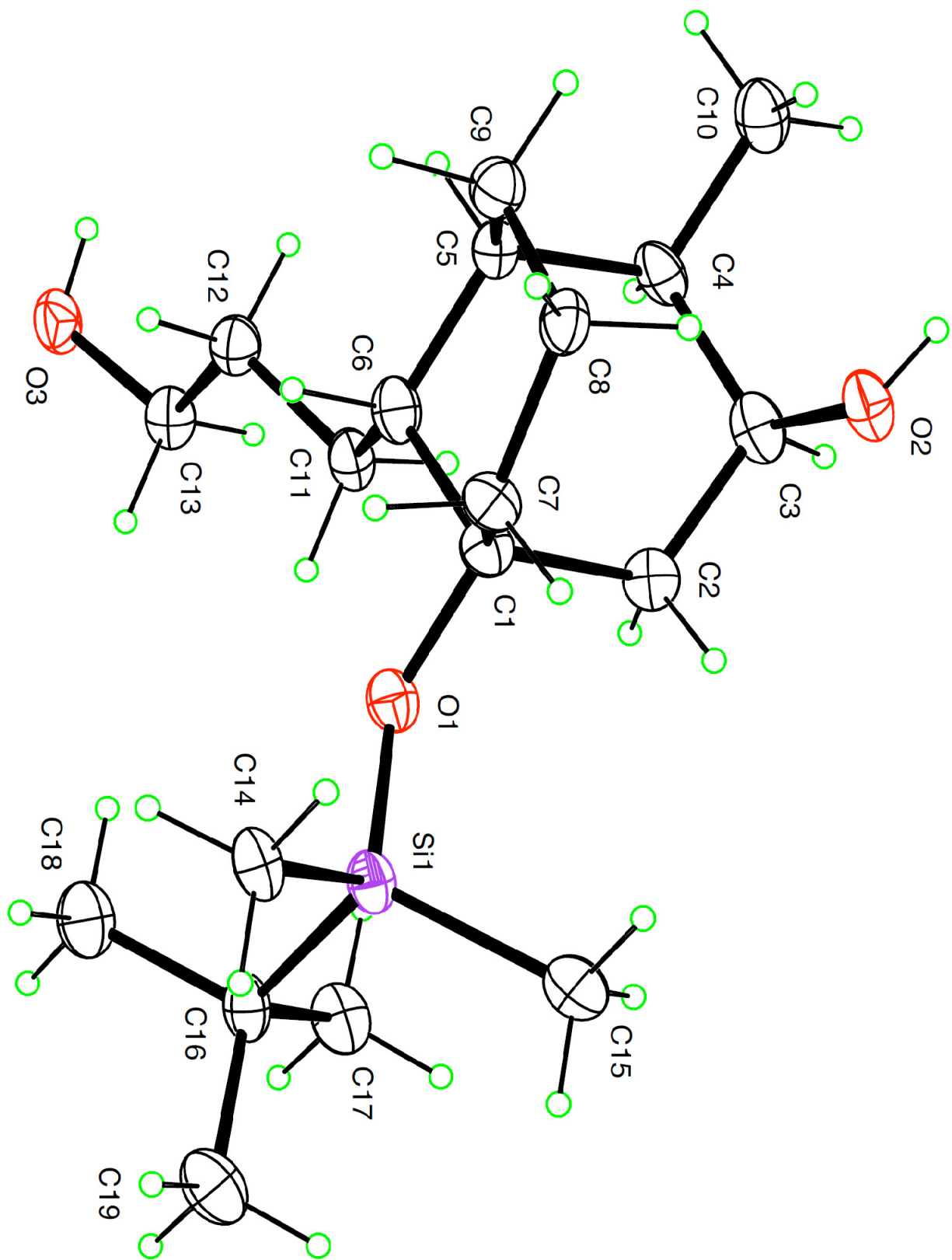


Figure 2.4 ORTEP Plot of Bicyclo[3.3.1]nonane 2.30a

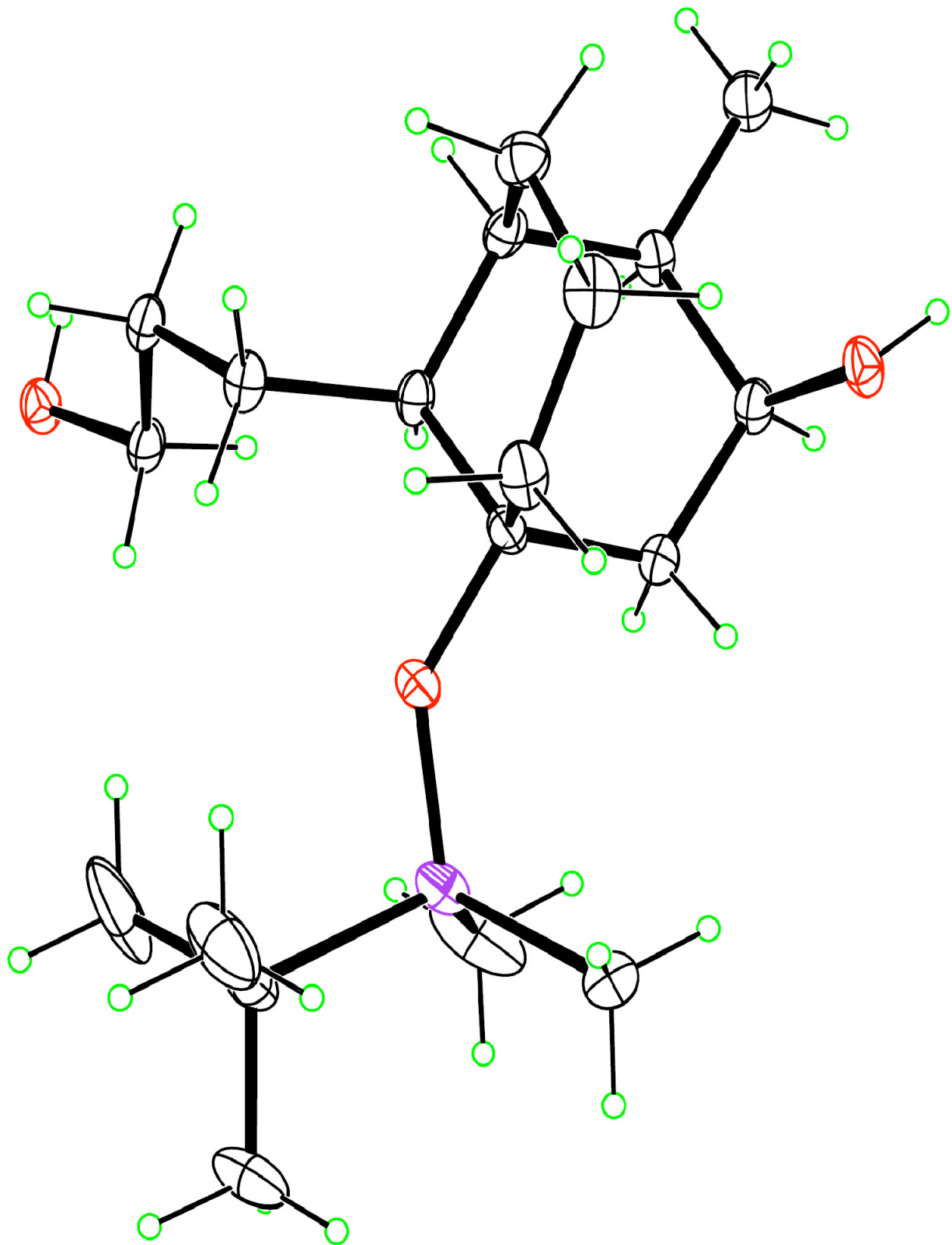


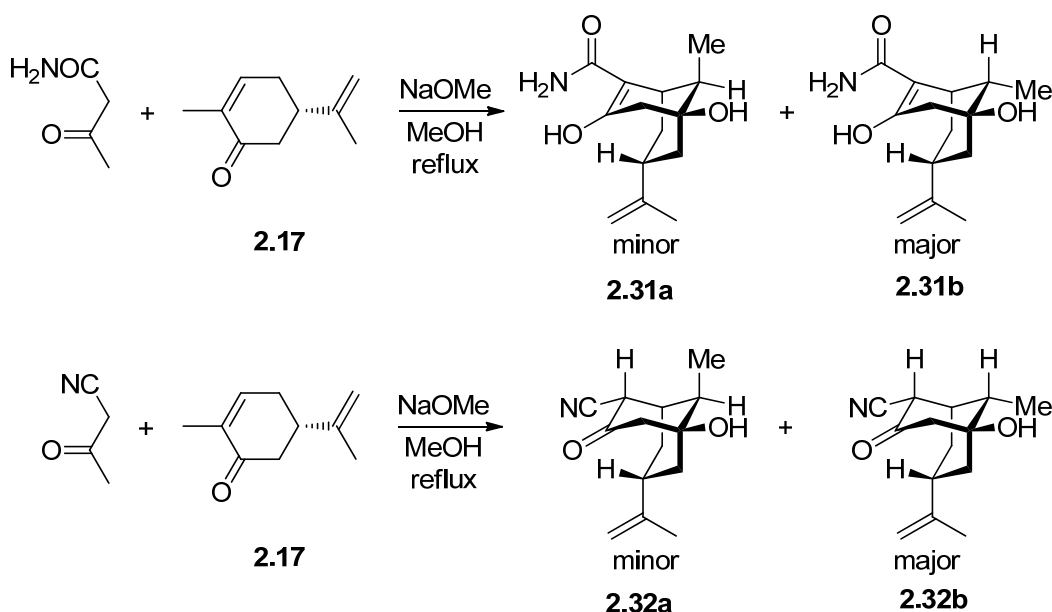
Figure 2.5 ORTEP Plot of Bicyclo[3.3.1]nonane 2.30b

Table 2.4 Base-catalyzed Epimerization of Bicyclo[3.3.1]nonane Products 2.12 Aimed at Preventing Decarboxylation

Substrate (ratio)	Reaction Condition	Product (ratio) ^a	Total Yield
2.12 (1:4.3)	MeONa (6 eq.), MeOH, 84hs reflux	2.12 (1:3)	40%
2.12 (1:4.3)	^t BuOK (6 eq.), ^t BuOH, 84hs reflux	2.12 (1:1)	38%

^aThe ratio is based upon the ¹H NMR of the crude products

Table 2.5 Robinson Annulation Reactions Aimed at Producing Bicyclo[3.3.1]nonane Products Resistant to Base-mediated Decarboxylation



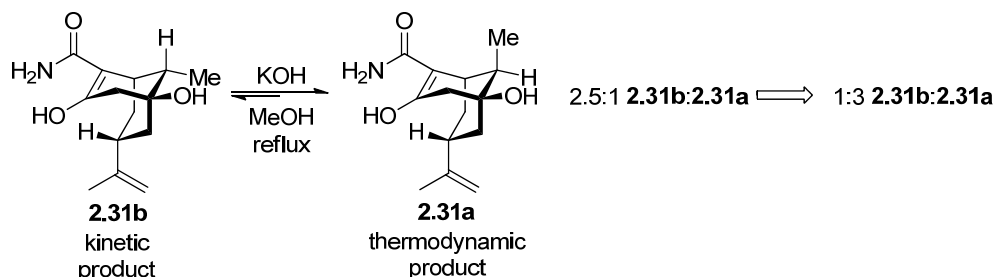
Product	Ratio (b/a) ^a	Total yield (%)
2.31	2.5:1	80
2.32	2.7:1	74

^aThe ratio is based upon the ¹H NMR of the crude products

A similar base-catalyzed epimerization conducted on a mixture of **2.12b** and **2.12a** might change the 4.3:1 **2.12b/2.12a** kinetic ratio to a thermodynamic ratio favoring the more stable isomer **2.12a**. Unfortunately, the base-mediated decarboxylation reaction which takes place under these conditions prevents such an epimerization from being realized. In order to prevent

this decarboxylation from being occurred, compound **2.12** was treated with excess MeONa in refluxing MeOH without the presence of water. Disappointingly, little epimerization was observed with a low recovery of **2.12** (Table 2.4). In comparison, when ^tBuOK in ^tBuOH was used, the epimerization realized but with a low yield (Table 2.4), which limits the use of epimerization as a practical stereochemical control element.

We reasoned that there may be other base stable electron-withdrawing groups still capable of promoting the enolization that stabilizes the desired diastereomer of the Robinson annulation reaction. Thus, we looked at the Robinson annulation of carvone with acetone derivative possessing an α carbon substituted with either a carboxamide or cyano group. We obtained kinetic product ratios similar to those obtained using β -keto-esters (Table 2.5).



Scheme 2.8 Stereoselectivity Reversal via Base-catalyzed Epimerization

Base-catalyzed epimerization (6 equiv KOH, refluxing MeOH, 24 hrs) converted the 2.5:1 **2.31b**:**2.31a** mixture obtained from the Robinson annulation to a 3:1 **2.31a**:**2.31b** mixture (Scheme 2.8). Base-catalyzed epimerization of pure **2.31b** produced the same 3:1 mixture where **2.31a** was the major component. Since the keto form predominated for cyano-substituted Robinson annulation products **2.32a** and **2.32b**, an epimerization reaction favoring **2.32a** was not considered a promising prospect.

2.4 Computational Mechanism Studies on the Robinson Annulations

Although the basic reaction sequence of the Robinson annulation has been well established,^[16] the mechanistic details of the reaction that forms bicyclo[3.3.1]nonanes remain an

unsolved problem. Additionally, the subtle differences in reaction pathways leading to the two diastereomeric products and in favor of the *anti* products are unclear. Therefore, we did a combined experimental and computational study that examines the origins of the diastereoselection in the base catalyzed Robinson annulations leading to the framework of bicyclo[3.3.1]nonanes.

Table 2.6 Effects of Basis Sets for Compound 2.21b

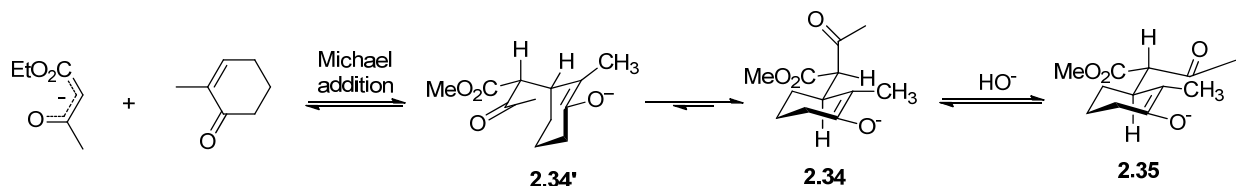
Bond length (Å)/angle (°)	O1- C1	C1- C2	C2- C3	C3- C4	C7- C13	C10- C11	O2-H-- -O4	C1-O1- H	C2-C1- C9
Crystal	1.433	1.536	1.488	1.356	1.537	1.498	1.620	107.1	108.1
6-31g(d)	1.436	1.548	1.504	1.370	1.534	1.507	1.690	107.5	108.0
6-311g(d)	1.472	1.546	1.499	1.368	1.538	1.509	1.726	109.8	108.4
6-311++G(d,p)	1.439	1.546	1.502	1.366	1.532	1.505	1.694	108.7	108.0

To be sure that the DFT method^[17] (B3LYP) is appropriate for this series of compounds, we started by calculating the ground state of compound **2.21b**, whose crystal structure has been obtained previously. Indeed, the optimized structure of compound **2.21b** has a very similar geometry, including bond lengths, bond angles and hydrogen bonding, to the crystal structure we have obtained (see Figure 2.1 for the atom number). These results are summarized in Table 2.6. Additional calculations with basis sets containing diffuse functions at the B3LYP/6-311+G(d) and B3LYP/6-311++G(d,p) levels were also performed for compound **2.21b** (shown in Table 2.6). These additional calculations gave similar relative energies and parameters as those obtained by the B3LYP/6-31G(d) method, suggesting that B3LYP/6-31G(d) is appropriate for studying the bicyclo[3.3.1]nonanes.

To better understand whether the reaction is kinetically controlled, we utilized DFT calculations (B3LYP/6-31G+d) to examine the energies and structures of the two diastereomeric products **2.33a** and **2.33b** (see Table 2.7 for the structure of **2.33a** and **2.33b**). The result of the calculations indicates that the *syn* product **2.33a** is indeed the thermodynamically favored product, lying approximately 1 kcalmol⁻¹ lower in energy than the *anti* product **2.33b**. Furthermore, their corresponding anion species that are formed in the reaction conditions have similar energy differences (**2.47** vs. **2.46**, Figure 2.6).

The solvation energies for **2.46** and **2.47** in methanol were also calculated by single point calculations on the optimized structures with the polarized continuum model (PCM). The energy difference for them is similar to the difference in gas phase, so we stopped calculating solvation energies for other species.

In the first step of the reaction, the Michael addition intermediate **2.34'** will be formed, leaving the β -keto ester branch at the axial position of the half-chair conformation of the cyclohexene ring (Scheme 2.9). After the ring conformational exchange, the Michael addition product will adopt its lowest conformation, leaving the β -keto ester branch at the equatorial position of the cyclohexene moiety yielding **2.34** and **2.35**, which undergo fast epimerization with each other under basic conditions.



Scheme 2.9 Species Formed in the Reaction Mixture

Figure 2.6 shows the computed energy surface for the base catalyzed Robinson annulations to form bicyclo[3.3.1]nonanes. The optimized structures of the transition states involved in this reaction are also given in Figure 2.6. Two possible pathways leading to the two

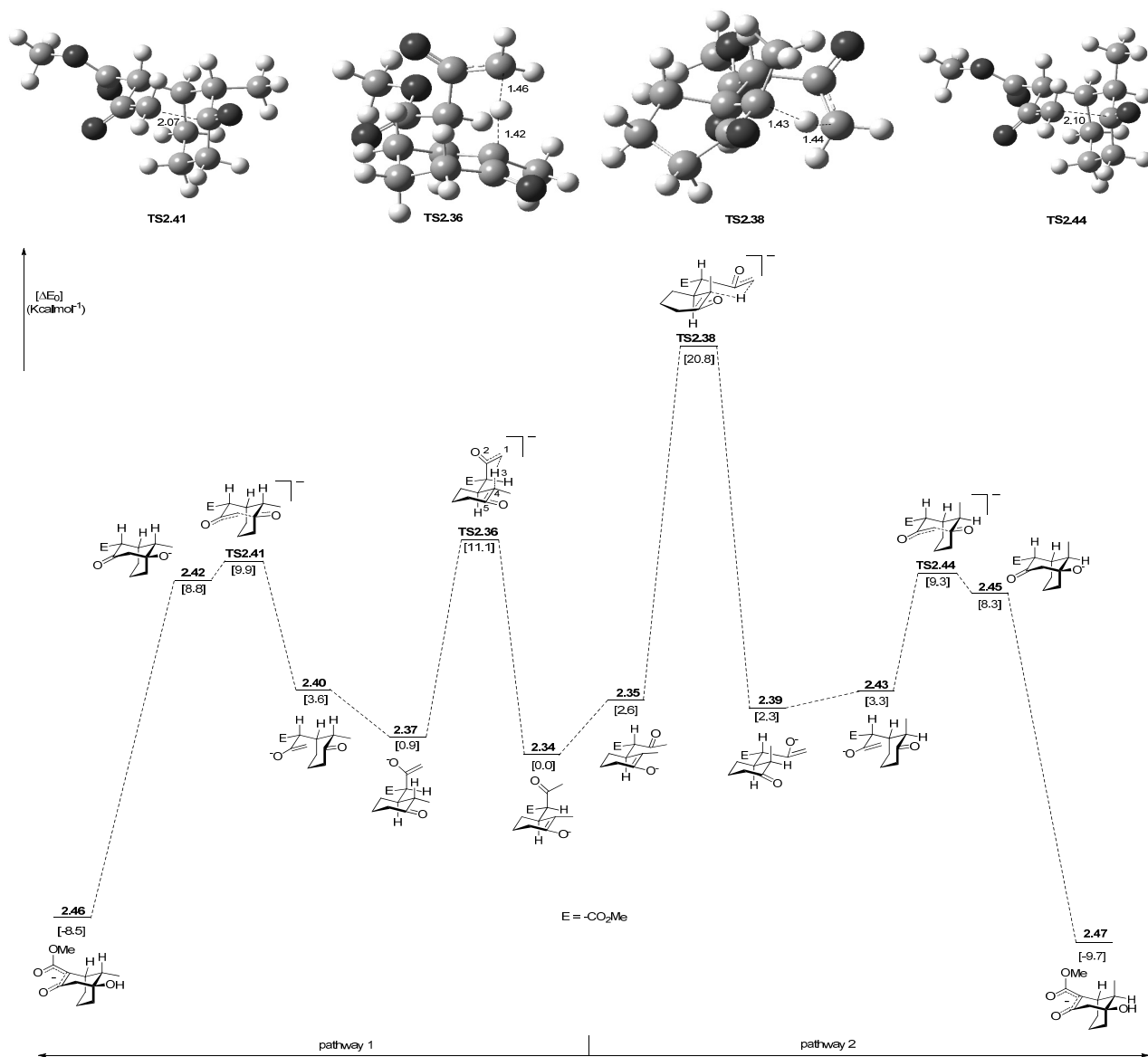


Figure 2.6 Reaction Energy Profile of Robinson Annulations

diastereomeric products have been found (Figure 2.6). Pathway 1 started from the enolate **2.34**, and then an intramolecular proton transfer process took place to form the aldol precursor **2.37**. A favorable six-membered ring transition state **TS2.36** adopting chair conformation was located during this transformation. Pathway 2 started from the enolate **2.35**, and a similar proton transfer from the methyl ketone moiety to the cyclohexyl enolate was located yielding the aldol precursor **2.39**. Pathway 1 is more favorable because the transferred proton in the transition state **TS2.36** is delivered axially to the cyclohexyl enolate moiety, and it is involved in a favorable chair conformation. In contrast, **TS2.38** of pathway 2 is less favorable because equatorial delivery of the proton from the methyl ketone to the cyclohexene ring results in poor orbital overlap. In order to maintain good orbital overlap, the cyclohexene ring of the transition state has to adopt a twisted boat conformation (Figure 2.6). Indeed, the activation energy of this step of pathway 2 is $20.8 \text{ kcalmol}^{-1}$, which is 9.7 kcalmol^{-1} higher than that of pathway 1.

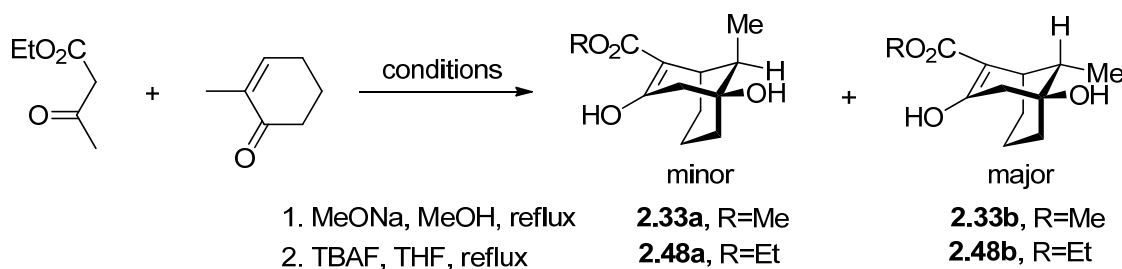
The intrinsic reaction coordinate (IRC)^[18] calculation demonstrates that both **TS2.36** and **TS2.38** directly connect the corresponding starting material and products without involving the formation of any other intermediate. In **TS2.36**, the C1-C2 π bond is forming, C4-C5 π bond is breaking, and H3 is transferring from the C1 atom of the methyl ketone to the C4 atom of the cyclohexene ring. A similar phenomenon is observed in **TS2.38**.

Following the proton transfer step, the intramolecular aldol reaction will take place in both pathways to form **2.42** and **2.45**. Because the reactive conformations of the aldol substrates leave the β -keto ester branch at the axial position, neither **2.37** nor **2.39** could be the appropriate substrate. Instead, their corresponding conformational isomers **2.40** and **2.43** will be the reactive species. The activation barrier of aldol ring closure of pathway 1 is only 9.9 kcalmol^{-1} , which is 1.2 kcalmol^{-1} lower than that of the intramolecular proton transfer step. In comparison, the activation energy of aldol ring closure of pathway 2 is 9.3 kcalmol^{-1} , which is $11.5 \text{ kcalmol}^{-1}$

lower than that of the intramolecular proton transfer step. In addition, we previously expected the aldol ring closure step would correlate with the stereoselectivity. However, activation energies of the aldol ring closures of both pathways are very close, with only 0.6 kcalmol⁻¹ difference.

Obviously, the intramolecular proton transfer step is the rate determining step in both pathways. Moreover, the activation energy of pathway 1 is 9.7 kcalmol⁻¹ lower than that of pathway 2, suggesting that the product of pathway 1 will be favored, which is consistent with the observed experimental results.

Table 2.7 Solvent Effects on the Stereochemical Outcome of Robinson Annulations



Conditions	Product	Ratio (a/b) ^a	Total yield
1	2.33	1:3.9	56%
2	2.48	1:3.3	30%

^aThe ratio is based on the ¹H NMR of the crude products

It is worth mentioning that the intramolecular proton transfer step of both pathway 1 and 2 could be a solvent-assisted intermolecular proton transfer process. This is especially possible in our experimental conditions, using methanol as the solvent. If this is the case, the rate determining step of the reaction could be the aldol ring closure. However, we ruled out this possibility by successfully conducting the reaction in an aprotic solvent---THF. The experimental result is summarized in Table 2.7. As can be seen in the table, the product ratio remains almost unchanged in both conditions, though the yield in THF is slightly lower. Therefore, the solvent has little effect on the stereoselectivity of the reaction. If solvent-assisted proton transfer process

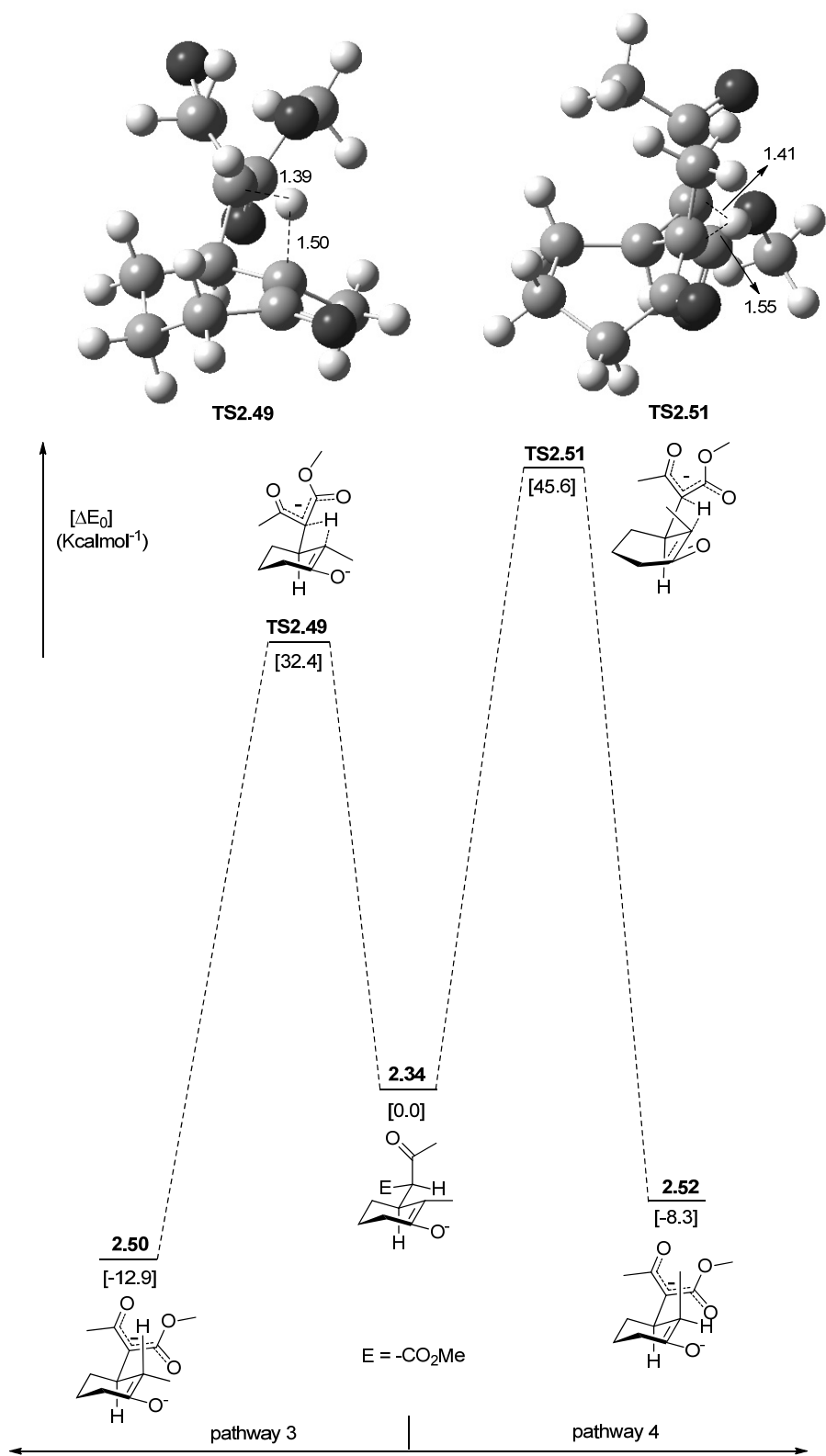


Figure 2.7 Potential Energy Profile of the Intramolecular Proton Transfer Step

did occur in the reaction, it did not bring the activation barrier lower than the aldol ring closure process, which would lead to an approximately 1:1 ratio of the two products because the activation energy of the aldol reaction step of both pathways is very close.

Another possible intramolecular proton transfer process after the formation of the Michael adduct **2.34** needs to be considered because the most acidic proton within the molecule is the β -keto ester proton, and not the methyl ketone proton. Figure 2.7 shows the computed energy surface for this intramolecular proton transfer process. The optimized structures of the transition states involved in this transformation are also given in the figure. Pathway 3 starts from the enolate **2.34**, and leads to the β -keto ester stabilized anion **2.50** via the transition state **TS2.49**, which has a *cis*-fused 6,4-membered ring conformation. The activation energy for this process is 32.4 kcalmol⁻¹. Pathway 4 leads to the β -keto ester stabilized anion **2.52** through the **TS2.51**, which has a *trans*-fused 6,4-membered ring conformation. The preference for pathway 3 over pathway 4 is evident, with a 13.2 kcalmol⁻¹ difference in the activation barrier. However, both pathway 3 and pathway 4 are unlikely because the activation barriers are too high in comparison with the corresponding intramolecular proton transfer step of pathway 1 ($\Delta E_0 = 11.1$ kcalmol⁻¹) and pathway 2 ($\Delta E_0 = 20.8$ kcalmol⁻¹). This is presumably associated with the highly strained, four-membered ring transition state, though the transferred protons are much more acidic.

2.5 Conclusion

In summary, the one-carbon bridge stereochemistry of bicyclo[3.3.1]nonane systems formed by Robinson annulations has been established, and factors influencing stereoselectivity have been examined. For base-catalyzed reactions conducted under previously reported reaction conditions, we found that the major diastereomer formed places the one-carbon bridge substituent *anti* to the β -keto ester/amide unit introduced in the reaction, and stereoselectivity appears to be kinetically controlled. Thermodynamically controlled stereoselectivity can be

realized under more forcing conditions in the presence of a large excess of base through an interesting epimerization reaction. In the case of one β -keto amide system that we have investigated, it appears that it may be possible to use base catalyzed epimerization as a means to reverse the kinetic selectivity obtained in these Robinson annulation reactions, thus obtaining the *syn* diastereomer as the major product.

The mechanism of the base catalyzed Robinson annulations leading to bicyclo[3.3.1]nonanes has been studied with the aid of density functional theory calculations. This mechanism study shows that the intramolecular proton transfer step is the rate determining step, and that the pathway leading to the *anti* products is preferred, which is in agreement with the experimental results. Furthermore, the intramolecular proton transfer process from the most acidic proton of the β -keto ester group with a much higher activation barrier has been excluded. In addition, solvent-assisted proton transfer process has little effect on stereoselectivity based on the experimental results. This mechanism study could be a useful guide for future experimental design to reverse the selectivity of the reaction.

2.6 Experimental

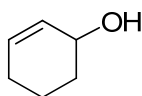
2.6.1 General Considerations

The preparation experiments were performed under a nitrogen atmosphere in oven- and/or flame-dried glassware using a Vacuum Atmospheres dry box or by using standard Schlenk techniques. Solvents used as reaction media were distilled immediately before use: acetonitrile, THF and ether were distilled from Na/benzophenone ketyl. NMR solvent (CDCl_3) was purchased from Cambridge Isotope Laboratories, Inc. All of the other reagents were purchased from Sigma-Aldrich and used without any further purification.

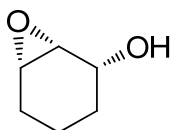
^1H spectra was recorded on a Bruker AV-400 (400 MHz ^1H) or a Bruker AC-250 (250 MHz ^1H) spectrometer in deuterated solvents using the solvent residual protons or carbons as an

internal reference (CDCl₃: 7.26 ppm ¹H for ¹H NMR, CDCl₃: 77.0 ppm, t for ¹³C NMR). Chemical shifts (δ) are given in parts per million down from tetramethylsilane (TMS). Data for ¹H NMR spectra are reported as follows: chemical shift (δ ppm), multiplicity (s = singlet, d = doublet, t = triplet, q = quartet, quin = quintet, dd = doublet of doublets, dt = doublet of triplets, ddd = doublet of doublet of doublets, ddt = doublet of doublet of triplets, m = multiplet), coupling constant (Hz), and integration. HRMS data were obtained using ESI ionization.

2.6.2 First Generation on Approach to Bicyclo[3.3.1]nonanes



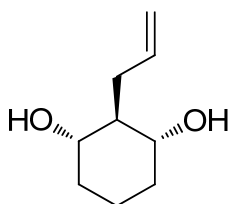
A solution of 2-cyclohexenone (1 g, 0.01 mol) in 5 ml of anhydrous ether was added dropwise to a cold (0°C) stirred suspension of LiAlH₄ (10 ml LiAlH₄ in Et₂O solution, 1.0M) in 20 ml of anhydrous ether. After the addition was complete, the reaction mixture was stirred for 10 min, then slowly quenched with 4 ml of saturated Na₂SO₄ solution. Anhydrous MgSO₄ was added and the mixture was stirred for an additional 30 min, filtered and the solvent was evaporated in vacuo to afford the crude product, which was then purified by column with DCM as eluent furnished the allyl alcohol (0.93 g, 93%) as a pale yellow oil. ¹H NMR (400 MHz, CDCl₃): δ 5.82-5.85 (m, 1H), 5.74-5.77 (m, 1H), 4.20 (s, 1H), 1.88-2.01 (m, 2H), 1.70-1.77 (m, 1H), 1.50-1.60 (m, 2H), 1.26 (s, 1H). ¹³C NMR (100 MHz, CDCl₃): δ 130.10, 130.04, 65.31, 31.88, 24.98, 19.04.



2.05

To a stirred solution of cyclohex-2-enol (0.2 g, 2.0 mmol) in 8 ml of CH₂Cl₂ at 0°C was added *m*-CPBA (0.46 g, 77% max., 2.0 mmol) in 5 ml of CH₂Cl₂ dropwise. After stirring for 5

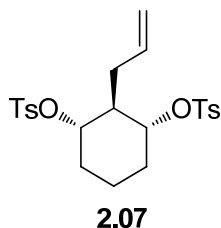
hours at 0°C, the reaction mixture was quenched by addition of saturated aqueous Na₂S₂O₃ (2 ml) and stirred for 15 min at r.t. After addition of saturated aqueous NaHCO₃ (5 ml), the mixture was separated and the aqueous layer was extracted by CH₂Cl₂ thoroughly. The combined organic layer was dried over MgSO₄, filtered and concentrated in vacuo. The crude product was purified by flash chromatography (Hex/EA = 3:1~3:2) to give epoxide alcohol (0.19 g, 82%) as a colorless oil. ¹H NMR (400 MHz, CDCl₃): δ 3.99-4.02 (m, 1H), 3.31-3.35 (m, 2H), 1.80-1.87 (m, 2H), 1.45-1.56 (m, 3H), 1.24-1.28 (m, 1H).



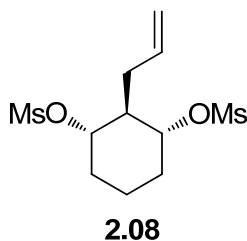
2.06

To a stirred suspension of copper (I) iodide (0.065 g, 0.34mmol) in 12 ml of anhydrous ether under nitrogen at -8°C was added allylmagnesium bromide in ether (1.0 M, 3.4 ml, 3.4 mmol). The black suspension was immediately cooled to -40°C, and epoxide alcohol **2.05** (0.13 g, 1.1 mmol) in 1 ml of anhydrous ether was added slowly. The brown homogeneous solution was then stirred at -40°C for 4 hours and a 2:1 mixture (3 ml) of sat. aqueous NH₄Cl and 28% NH₃·H₂O was added. The organic layer was separated and the aqueous layer (blue color) was extracted with CH₂Cl₂ (5×5 ml). The combined organic layer was dried over Na₂SO₄, filtered and concentrated in vacuo to give the crude product, which is a 1,2- and 1,3-diol mixture. This crude product was dissolved in THF (10 ml) and H₂O (10 ml), and then NaIO₄ (0.2 g) was added at r.t. The resulting solution was stirred for 3 hours and then diluted with DCM (10 ml). After separation of the organic phase, the water layer was thoroughly extracted by DCM and the combined organic phases were dried over MgSO₄, filtered and concentrated to give the aldehyde and 1,3-diol mixture. The crude product was purified by flash chromatography (Hex/EA =

5:1~1:3) to give epoxide alcohol **2.06** (0.09 g, 50%) as a colorless oil. ^1H NMR (400 MHz, CDCl_3): δ 5.90-6.00 (m, 1H), 5.15 (d, $J = 16$ Hz, 1H), 5.07 (d, $J = 8$ Hz, 1H), 3.49-3.54 (m, 2H), 2.38-2.41 (m, 2H), 1.83-1.88 (m, 3H), 1.56-1.60 (m, 1H), 1.30-1.40 (m, 3H). ^{13}C NMR (100 MHz, CDCl_3): δ 137.16, 116.61, 71.48, 50.02, 33.27, 21.02, 18.55.



To a solution of the diol **2.06** (3.9 g, 0.025 mol) in pyridine (35 ml) was added TsCl (16.66 g, 0.087 mol), and the reaction mixture was stirred at r.t. for 24 hours. The pyridine was removed in vacuo and the residue was purified by flash chromatography (Hex/EA = 5:1) to give the tosylate (9.9 g, 85%) as white solid. ^1H NMR (400 MHz, CDCl_3): δ 7.77 (d, $J = 8.3$ Hz, 4H), 7.32 (d, $J = 8.3$ Hz, 4H), 5.45-5.50 (m, 1H), 4.97 (d, $J = 10.2$ Hz, 1H), 4.91 (d, $J = 17.0$ Hz, 1H), 4.36-4.42 (m, 2H), 2.44 (s, 6H), 2.12-2.13 (m, 2H), 1.97-1.98 (m, 2H), 1.70-1.86 (m, 2H), 1.41-1.45 (m, 2H), 1.22-1.25 (m, 2H). ^{13}C NMR (100 MHz, CDCl_3): δ 144.69, 134.62, 132.89, 129.79, 127.62, 118.75, 80.27, 45.92, 30.92, 30.74, 21.61, 18.40.

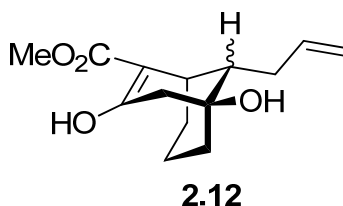


To a stirred solution of the diol **2.06** (0.3 g, 1.9 mmol) and Et_3N (1.2 ml, 8.8 mmol) in 3.2 ml of CH_2Cl_2 in an ice bath under nitrogen, was added dropwise MsCl (0.36 ml, 4.6 mmol). The resulting solution was stirred for 1 hour at 0°C , sat. NH_4Cl was then added and the mixture was extracted with CH_2Cl_2 . The combined organic phases were washed with brine, dried (MgSO_4)

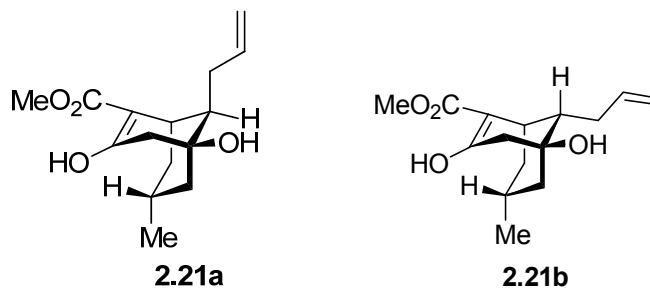
and concentrated to give the crude product, which was purified by flash chromatography (Hex/EA = 1:1) to give the mesylate (0.52 g, 87%) as white solid. ^1H NMR (400 MHz, CDCl_3): δ 5.83-5.87 (m, 1H), 5.18-5.23 (m, 2H), 4.52-4.58 (m, 2H), 3.04 (s, 6H), 2.38-2.40 (m, 2H), 2.19-2.24 (m, 2H), 2.00-2.04 (m, 1H), 1.80-1.84 (m, 1H), 1.62-1.65 (m, 3H).

2.6.3 General Procedure for the Robinson Annulations

To the freshly prepared sodium methoxide (1.1 equiv.) in methanol (0.55 M) was added ethyl acetoacetate or acetoacetamide or 3-oxobutanenitrile (1.1 equiv.) and the enone substrate (1.0 equiv.) under nitrogen. The resulting solution was heated under reflux for 84 hours. The mixture was cooled down to room temperature and then the methanol was removed under vacuum. The concentrated mixture was neutralized by 3N HCl to pH = 6 and then extracted with CH_2Cl_2 . The organic layer was dried (MgSO_4) and concentrated in vacuo led to crude product which could be purified using column chromatography (SiO_2).



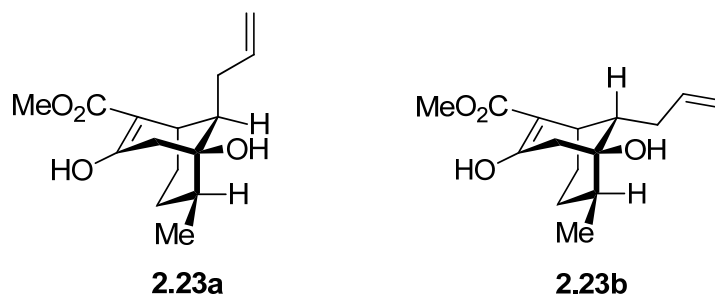
Column chromatography (1:5 ethyl acetate:hexane) yielded the product as a pale yellow oil (yield: 54%). The product was obtained as an inseparable mixture of diastereomers. ^1H NMR (400 MHz, CDCl_3): δ 12.11 (s, 1H), 5.78-5.86 (m, 1H), 5.06-5.15 (m, 2H), 3.75 (s, 3H), 2.89-2.99 (m, 1H), 2.46-2.57 (m, 3H), 2.17-2.23 (m, 1H), 1.78-1.82 (m, 3H), 1.52-1.69 (m, 4H), 1.22-1.28 (m, 1H). ^{13}C NMR (100 MHz, CDCl_3): δ 171.75, 171.71, 137.54, 116.10, 101.38, 70.55, 51.36, 45.82, 45.34, 35.14, 32.03, 30.07, 21.79, 18.61. Some of the characteristic peaks of the minor component: ^1H NMR (400 MHz, CDCl_3): δ 12.17 (s). HRMS (ESI): m/z calcd. for ($\text{C}_{14}\text{H}_{20}\text{O}_4+\text{Na}^+$): 275.1254; found: 275.1256.



Diastereomers **2.21a** and **2.21b** (total yield: 42%) were separated by column chromatography (7:1 hexane:ethyl acetate). The major diastereomer **2.21b** was a crystalline solid that could be further purified by recrystallization from petroleum ether.

2.21a: ^1H NMR (400 MHz, CDCl_3): δ 12.14 (s, 1H), 5.76-5.87 (m, 1H), 4.97-5.05(m, 2H), 3.76 (s, 3H), 2.94-2.95 (m, 1H), 2.33-2.50 (m, 4H), 2.00-2.18 (m, 1H), 1.79-1.82 (m, 2H), 1.56-1.65(m, 3H), 0.98-1.28 (m, 3H), 0.88 (d, $J = 6.2$ Hz, 3H). ^{13}C NMR (100 MHz, CDCl_3): δ 172.38, 171.69, 137.73, 116.18, 97.95, 71.36, 51.78, 51.52, 47.59, 40.41, 39.05, 33.84, 31.43, 25.96, 21.48. HRMS (ESI): m/z calcd. for ($\text{C}_{15}\text{H}_{22}\text{O}_4+\text{H}^+$): 267.1591; found: 267.1586.

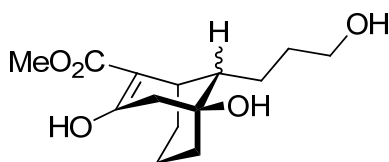
2.21b: ^1H NMR (400 MHz, CDCl_3): δ 12.06 (s, 1H), 5.78-5.84 (m, 1H), 5.11 (d, $J = 17\text{Hz}$, 1H), 5.06 (d, $J = 10\text{Hz}$, 1H), 3.75 (s, 3H), 2.87 (s, 1H), 2.50-2.55 (m, 3H), 2.08-2.16 (m, 1H), 1.76-1.79 (m, 1H), 1.62-1.68 (m, 2H), 1.51-1.55 (m, 1H), 1.32-1.38 (m, 2H), 1.18-1.22 (m, 1H), 0.90 (d, $J = 6.4$ Hz, 3H). ^{13}C NMR (100 MHz, CDCl_3): δ 171.72, 171.45, 137.57, 116.28, 102.24, 71.32, 51.47, 46.02, 45.02, 44.36, 32.44, 31.15, 30.34, 25.29, 21.70. HRMS (ESI): m/z calcd. for ($\text{C}_{15}\text{H}_{22}\text{O}_4+\text{H}^+$): 267.1591; found: 267.1592.



Diastereomers **2.23a** and **2.23b** (total yield: 31%) were separated by column chromatography (7:1 hexane:EtOAc). The major diastereomer **2.23b** was a crystalline solid that could be further purified by recrystallization from petroleum ether.

2.23a: ^1H NMR (400 MHz, CDCl_3): δ 12.11 (s, 1H), 5.71-5.76 (m, 1H), 4.90-4.94 (m, 2H), 3.68 (s, 3H), 2.89-2.92 (m, 1H), 2.44-2.48 (m, 2H), 2.15-2.42 (m, 2H), 1.70-1.83 (m, 2H), 1.42-1.52(m, 4H), 1.20-1.33 (m, 2H), 0.92 (d, $J = 6.5$ Hz, 3H). ^{13}C NMR (100 MHz, CDCl_3): δ 172.41, 171.81, 137.89, 115.96, 96.97, 73.02, 51.42, 49.03, 44.25, 33.85, 31.52, 30.44, 28.31, 24.62, 14.88. HRMS (ESI): m/z calcd. for ($\text{C}_{15}\text{H}_{22}\text{O}_4+\text{H}^+$): 267.1591; found: 267.1588.

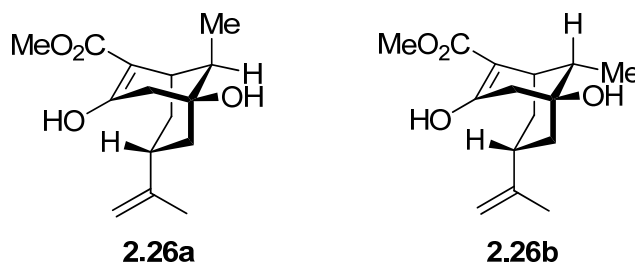
2.23b: ^1H NMR (400 MHz, CDCl_3): δ 12.09 (s, 1H), 5.76-5.83 (m, 1H), 5.10 (d, $J = 16$ Hz, 1H), 5.07 (d, $J = 7.8$ Hz, 1H), 3.73 (s, 3H), 2.87-2.88 (m, 1H), 2.69-2.75 (m, 1H), 2.49-2.54 (m, 1H), 2.15-2.24 (m, 2H), 1.79-1.84 (m, 2H), 1.61-1.66 (m, 2H), 1.44-1.48 (m, 1H), 1.24-1.27 (m, 1H), 1.13-1.23 (m, 1H), 0.93 (d, $J = 6.6$ Hz, 3H). ^{13}C NMR (100 MHz, CDCl_3): δ 171.78, 171.52, 137.74, 116.25, 101.32, 72.83, 51.42, 46.52, 39.13, 35.94, 32.48, 30.01, 27.70, 23.33, 14.85. HRMS (ESI): m/z calcd. for ($\text{C}_{15}\text{H}_{22}\text{O}_4+\text{Na}^+$): 289.1410; found: 289.1416.



2.25

Column chromatography (1:3~1:1 ethyl acetate:hexane) yielded the product as a colorless oil (yield: 43%). The product was obtained as an inseparable mixture of diastereomers. ^1H NMR (400 MHz, CDCl_3): δ 12.03 (s, 1H), 3.87 (br s., 2H), 3.68 (s, 3H), 3.54-3.60 (m, 2H), 2.80-2.81 (m, 1H), 2.40-2.52 (m, 2H), 1.60-1.88 (m, 4H), 1.34-1.45 (m, 6H), 1.17 (d, $J = 12$ Hz, 1H). ^{13}C NMR (100 MHz, CDCl_3): δ 171.91, 171.74, 101.37, 70.68, 61.96, 51.41, 45.79, 45.05, 34.87, 32.40, 30.56, 22.02, 21.22, 18.54. Some of the characteristic peaks of the minor component: ^1H

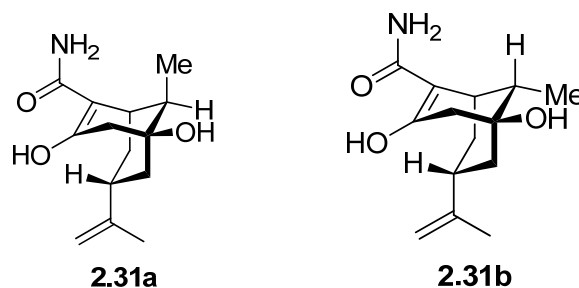
NMR (400 MHz, CDCl₃): δ 12.09 (s). HRMS (ESI): m/z calcd. for (C₁₄H₂₂O₅+H⁺): 271.1540; found: 271.1541.



Diastereomers **2.26a** and **2.26b** (total yield: 56%) were separated by column chromatography (6:1 hexane:EtOAc). The major diastereomer **2.26b** was a crystalline solid that could be further purified by recrystallization from petroleum ether.

2.26a: ¹H NMR (400 MHz, CDCl₃): δ 12.14 (s, 1H), 4.70 (s, 1H), 4.68 (s, 1H), 3.76 (s, 3H), 2.87-2.88 (m, 1H), 2.53-2.55 (m, 1H), 2.48-2.49 (m, 1H), 2.33-2.37 (m, 1H), 1.84-1.89 (m, 1H), 1.68-1.83 (m, 6H), 1.24-1.42 (m, 2H), 0.96 (d, J = 6.8 Hz, 3H). ¹³C NMR (100 MHz, CDCl₃): δ 172.37, 171.70, 148.34, 109.27, 97.80, 71.34, 51.53, 47.61, 42.30, 39.79, 38.23, 37.20, 35.43, 21.03, 12.92. HRMS (ESI): m/z calcd. for (C₁₅H₂₂O₄+H⁺): 267.1591; found: 267.1594.

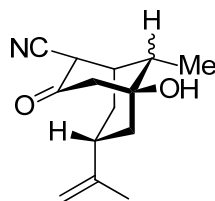
2.26b: ¹H NMR (400 MHz, CDCl₃): δ 12.06 (s, 1H), 4.70 (s, 2H), 3.75 (s, 3H), 2.83-2.84 (m, 1H), 2.56 (s, 2H), 2.12-2.19 (m, 1H), 1.89-1.90 (m, 1H), 1.51-1.67 (m, 7H), 1.38-1.41 (m, 1H), 1.09 (d, J = 7.0 Hz, 3H). ¹³C NMR (100 MHz, CDCl₃): δ 171.72, 171.60, 148.50, 109.24, 102.20, 71.20, 51.50, 45.64, 39.84, 39.59, 37.60, 35.84, 27.40, 20.97, 11.90. HRMS (ESI): m/z calcd. for (C₁₅H₂₂O₄+H⁺): 267.1591; found: 267.1593.



Diastereomers **2.31a** and **2.31b** (total yield: 80%) were separated by column chromatography (2:1~1:1 hexane:EtOAc). The major diastereomer **2.31b** was obtained as a crystalline solid.

2.31a: ^1H NMR (400 MHz, CDCl_3): δ 14.15 (s, 1H), 5.46 (s, 2H), 4.73 (s, 1H), 4.70 (s, 1H), 2.50-2.55 (m, 2H), 2.23-2.38 (m, 2H), 1.88-1.91 (m, 1H), 1.70-1.78 (m, 6H), 1.38-1.53 (m, 3H), 1.24-1.28 (m, 1H), 1.01 (d, $J = 6.8$ Hz, 3H). ^{13}C NMR (100 MHz, CDCl_3): δ 173.95, 171.85, 147.94, 109.56, 96.75, 71.12, 47.40, 42.58, 40.11, 38.66, 38.27, 35.30, 21.04, 13.05. HRMS (ESI): m/z calcd. for ($\text{C}_{14}\text{H}_{21}\text{NO}_3+\text{H}^+$): 252.1594; found: 252.1602.

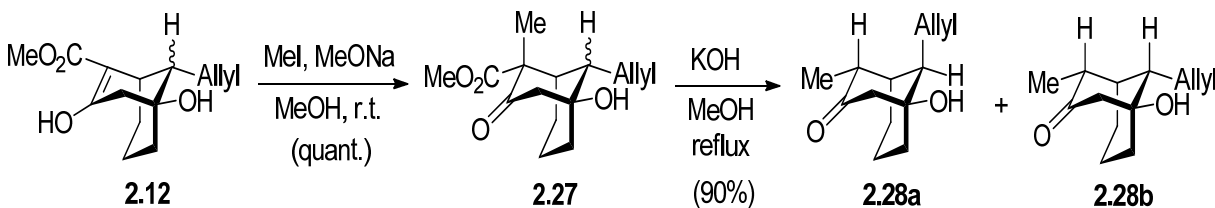
2.31b: ^1H NMR (400 MHz, CDCl_3): δ 14.08 (s, 1H), 5.54 (s, 2H), 4.73 (s, 1H), 4.71 (s, 1H), 2.47-2.57 (m, 2H), 2.20-2.24 (m, 1H), 1.78-1.98 (m, 1H), 1.57-1.70 (m, 7H), 1.19-1.43 (m, 3H), 1.12 (d, $J = 7.0$ Hz, 3H). ^{13}C NMR (100 MHz, CDCl_3): δ 173.22, 171.82, 148.11, 109.51, 101.27, 70.94, 45.97, 40.07, 39.41, 37.63, 37.32, 27.41, 20.98, 12.14. HRMS (ESI): m/z calcd. for ($\text{C}_{14}\text{H}_{21}\text{NO}_3+\text{Na}^+$): 274.1414; found: 274.1415.



2.32

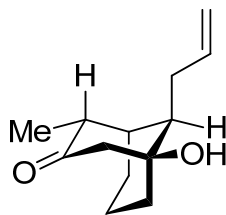
Column chromatography (1:2~1:1 ethyl acetate:hexane) yielded the product as a pale yellow oil (yield: 54%). The product was obtained as an inseparable mixture of diastereomers. ^1H NMR (400 MHz, CDCl_3): δ 4.81 (s, 1H), 4.76 (s, 1H), 2.43-2.54 (m, 6H), 2.35-2.38 (m, 1H), 1.70-1.77 (m, 5H), 1.19-1.26 (m, 1H), 1.11 (d, $J = 6.5$ Hz, 3H). ^{13}C NMR (100 MHz, CDCl_3): δ 209.26, 198.18, 146.10, 115.51, 110.80, 48.41, 46.80, 46.21, 43.86, 43.24, 32.58, 29.40, 20.12, 11.29. Some characteristic peaks of the minor component: ^1H NMR (400 MHz, CDCl_3): δ 0.95 (d, $J = 6.5$ Hz). HRMS (ESI): m/z calcd. for ($\text{C}_{14}\text{H}_{19}\text{NO}_2+\text{Na}^+$): 256.1308; found: 256.1320.

2.6.4 Preparation of Compounds 2.28a and 2.28b



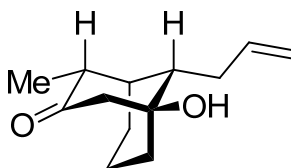
To the freshly prepared sodium methoxide (0.036 g Na, 1.56 mmol) in 2.0 ml of MeOH was added compound **2.12** (0.36 g, 1.40 mmol) in MeOH (0.8 ml) and then MeI (0.26 ml, 4.24 mmol). The resulting solution was stirred at r.t. overnight and then the MeOH was removed. Ethyl acetate and water were added to the residue and the organic layer was separated. The water phase was extracted with ethyl acetate. The combined organic phase was washed with brine, dried (MgSO₄), filtered and concentrated to give the product **2.27** (0.38 g, quant.) as a pale yellow oil, which is pure enough for the next step. ¹H NMR (400 MHz, CDCl₃): δ 5.76-5.82 (m, 1H), 4.97-5.15 (m, 2H), 3.72 (s, 3H), 2.51-2.68 (m, 3H), 2.18-2.22 (m, 2H), 1.74-1.79 (m, 2H), 1.49-1.63 (m, 6H), 1.33-1.45 (m, 1H), 1.22-1.27 (m, 2H). ¹³C NMR (62.5 MHz, CDCl₃): δ 207.58, 172.24, 136.56, 116.71, 71.72, 60.28, 59.32, 53.41, 51.87, 42.25, 41.60, 34.30, 30.20, 23.40, 22.04, 19.03, 14.01. Some of the characteristic peaks of the minor component: ¹³C NMR (62.5 MHz, CDCl₃): δ 206.37, 171.80, 137.53, 115.97. HRMS (ESI): *m/z* calcd. for (C₁₅H₂₂O₄+Na⁺): 289.1410; found: 289.1417.

To a solution of the substrate **2.27** (6.826 g, 0.026 mol) in 26 ml of MeOH was added 26 ml of 3.0 M aqueous KOH (0.078 mol). The solution was refluxed for 24 hours. After cooled down to r.t., the methanol in the solution was removed in vacuo. The resulting water phase was acidified to pH 0 and stirred for five minutes, and then extracted with DCM. The organic layer was dried (MgSO₄), filtered and concentrated. Column chromatography (Hex/EA = 3:1) yielded the product **2.28a** and **2.28b** (4.80 g, ratio=1:1, total yield: 90%) as colorless oil.



2.28a

^1H NMR (400 MHz, CDCl_3): δ 5.76-5.86 (m, 1H), 5.03-5.10 (m, 2H), 2.74-2.78 (m, 1H), 2.58-2.62 (m, 1H), 2.38-2.42 (m, 2H), 2.07-2.18 (m, 3H), 1.76-1.86 (m, 3H), 1.52-1.60 (m, 2H), 1.21-1.34 (m, 2H), 1.08-1.19 (m, 1H), 1.02 (d, $J = 6.7$ Hz, 3H). ^{13}C NMR (100 MHz, CDCl_3): δ 212.09, 137.19, 116.51, 73.67, 50.49, 48.41, 42.62, 41.00, 38.94, 31.11, 27.27, 20.07, 11.82. HRMS (ESI): m/z calcd. for ($\text{C}_{13}\text{H}_{20}\text{O}_2 + \text{H}^+$): 209.1536; found: 209.1533.



2.28b

^1H NMR (400 MHz, CDCl_3): δ 5.78-5.88 (m, 1H), 5.05-5.13 (m, 2H), 2.58-2.66 (m, 2H), 2.34-2.54 (m, 3H), 2.12-2.23 (m, 2H), 1.95-2.04 (m, 2H), 1.70-1.79 (m, 1H), 1.63-1.66 (m, 1H), 1.46-1.52 (m, 4H), 1.06 (d, $J = 6.8$ Hz, 3H). ^{13}C NMR (100 MHz, CDCl_3): δ 211.94, 137.43, 116.44, 73.13, 56.38, 49.07, 48.47, 39.06, 34.63, 30.85, 19.38, 18.70, 12.12. HRMS (ESI): m/z calcd. for ($\text{C}_{13}\text{H}_{20}\text{O}_2 + \text{Na}^+$): 231.1356; found: 231.1351.

2.6.5 General Procedure for Thermodynamic Control Reaction

To a solution of the substrate (1 equiv.) in MeOH (1M) was added the equal volume of x M aqueous KOH (x equiv., for the corresponding equiv., see the thesis). The solution was refluxed for 24 hours. After cooled down to r.t., the methanol in the solution was removed in vacuo. The resulting water phase was acidified to pH = 0 and stirred for a few minutes, and then extracted with DCM (for substrate **2.31**, using chloroform to extract and added a little bit MeOH to the

combined organic phases). The organic layer was dried (MgSO₄), filtered and concentrated to afford the crude product, which could be purified using column chromatography (SiO₂).

2.6.6 General Computational Consideration

All calculations were carried out with DFT method as implemented in GAUSSIAN 03.^[19] All structures were optimized by the B3LYP/6-31G(d) method. The stationary points were characterized by harmonic analysis. For all the transition structures, the vibration related to the imaginary frequency corresponds to the nuclear motion along the reaction coordinate. Intrinsic reaction coordinate (IRC) calculations were performed to ensure that the transition structures connect related intermediates correctly. Unless specifically mentioned, the discussed Gibbs free energy (ΔG), the enthalpy (ΔH), and the zero-point corrected energy (ΔE_0) were computed at 298 K in the gas phase by using the B3LYP/6-31G(d) method.

2.6.7 Spectral Data

Spectral data are shown from the next page.

2.7 References

- [1] a) F. A. Marques, C. A. Lenz, F. Simonelli, B. H. L. N. S. Maia, A. P. Vellasco and M. N. Eberlin, *J. Nat. Prod.* **2004**, *67*, 1939-1941; b) M. J. Taschner and A. Shahripour, *J. Am. Chem. Soc.* **1985**, *107*, 5570-5572; c) L. A. Paquette, A. G. Schaefer and J. P. Springer, *Tetrahedron* **1987**, *43*, 5567-5582; d) S. J. Spessard and B. M. Stoltz, *Org. Lett.* **2002**, *4*, 1943-1946; e) T. Amagata, K. Minoura and A. Numata, *J. Nat. Prod.* **2006**, *69*, 1384-1388; f) P. Moosophon, S. Kanokmedhakul, K. Kanokmedhakul and K. Soyong, *J. Nat. Prod.* **2009**, *72*, 1442-1446.
- [2] a) A. Gambacorta, G. Fabrizi and P. Bovicelli, *Tetrahedron* **1992**, *48*, 4459-4464; b) I. Yamawaki, S. W. Bukovac and A. Sunami, *Chem. Pharm. Bull.* **1994**, *42*, 2365-2369; c) J. Aleu, R. Hernandez-Galan, J. R. Hanson, P. B. Hitchcock and I. G. Collado, *J. Chem. Soc., Perkin Trans. 1* **1999**, 727-730; d) A. Srikrishna and D. Vijaykumar, *J. Chem. Soc., Perkin Trans. 1* **1999**, 1265-1271; e) R. H. Mach, B. Yang, L. Wu, R. J. Kuhner, B. R. Whirrett and T. West, *Med. Chem. Res.* **2001**, *10*, 339-355; f) W. H. Chu, J. B. Xu, D. Zhou, F. Zhang, L. A. Jones, K. T. Wheeler and R. H. Mach, *Bioorg. Med. Chem.* **2009**, *17*, 1222-1231; g) C. Ronco, G. Sorin, F. Nachon, R. Foucault, L. Jean, A. Romieu and P. Y. Renard, *Bioorg. Med. Chem.* **2009**, *17*, 4523-4536.

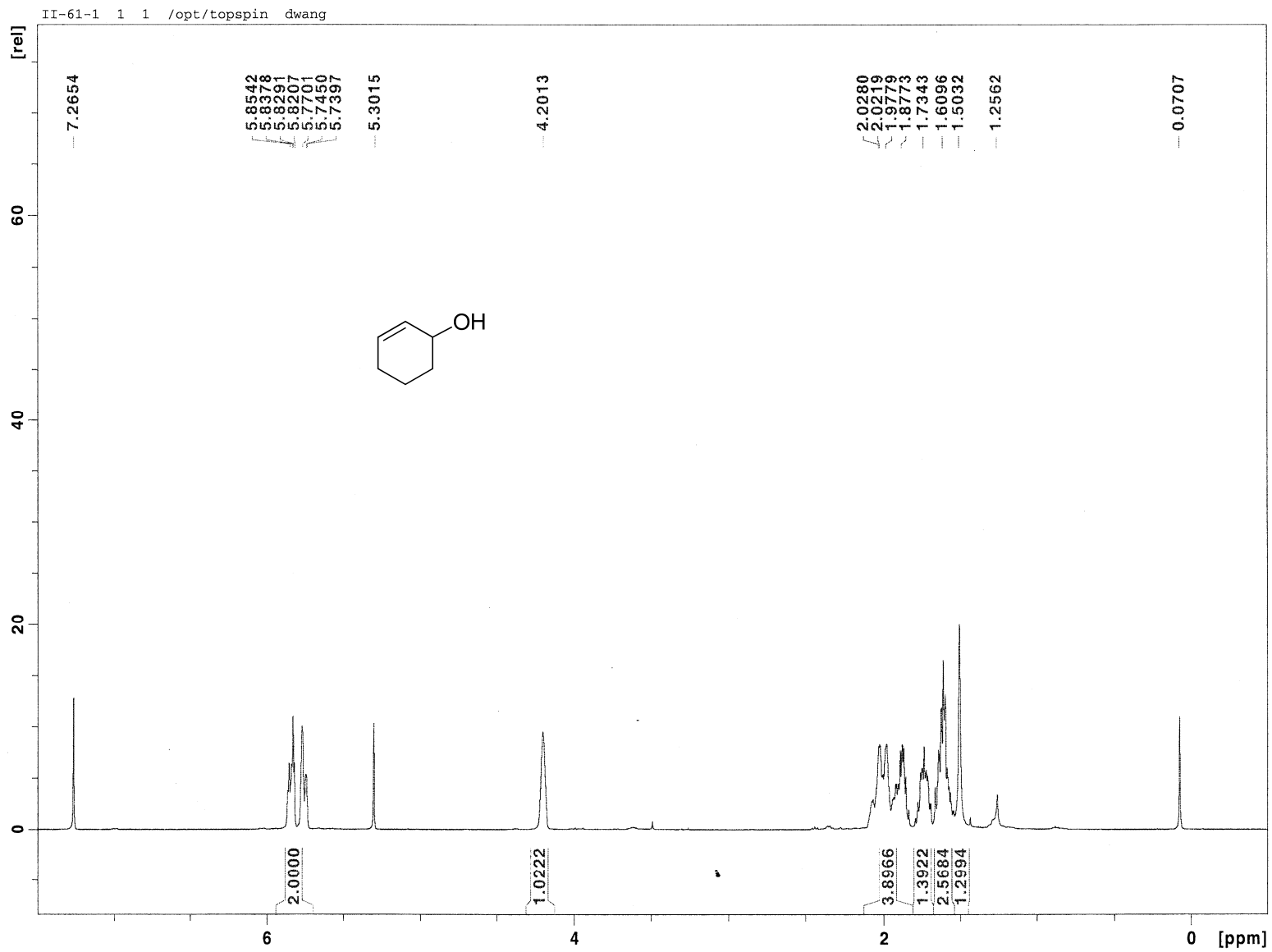


Figure 2.8 ^1H NMR (400 MHz, CDCl_3) of Cyclohexenol

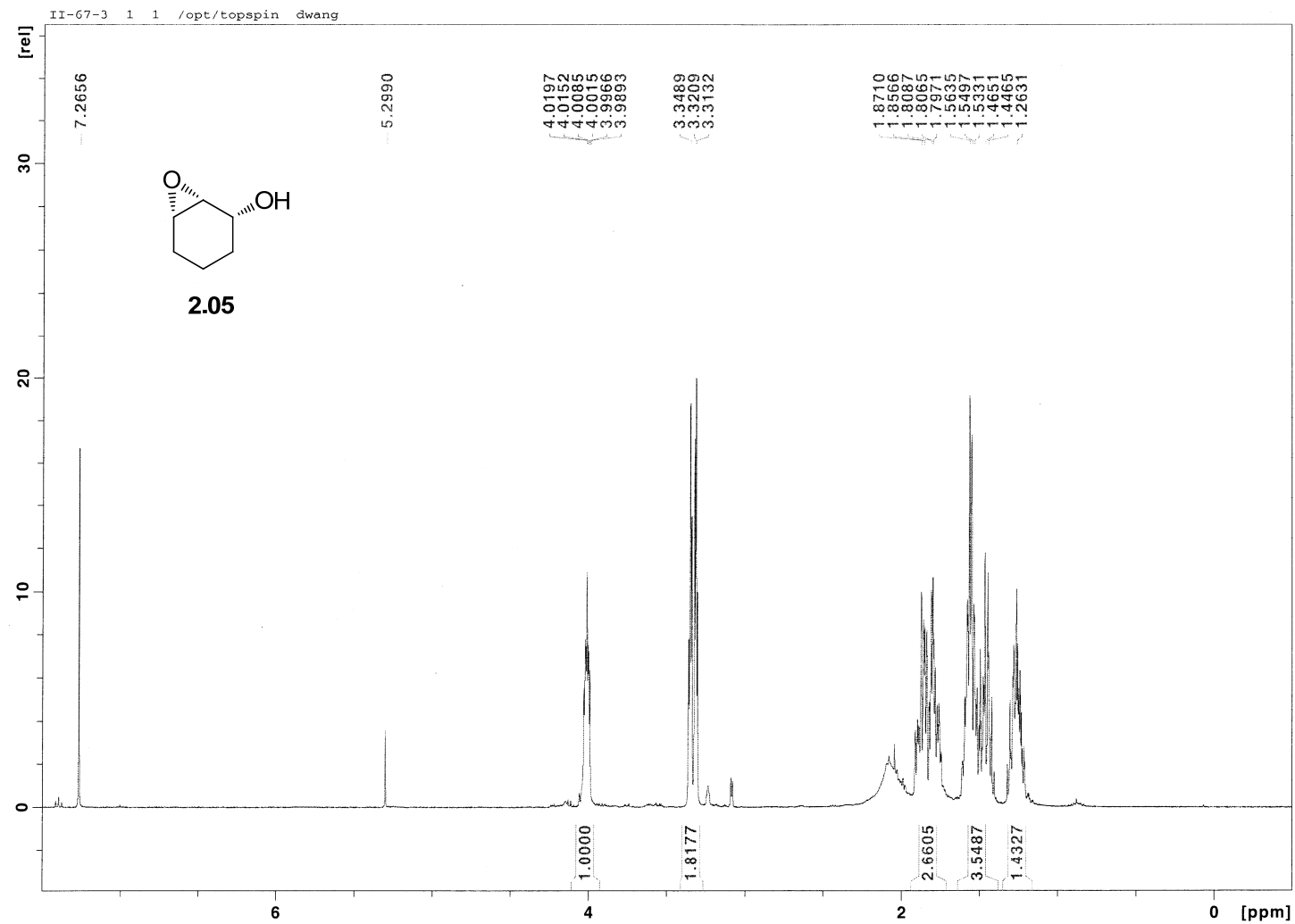


Figure 2.9 ^1H NMR (400 MHz, CDCl_3) of Compound 2.05

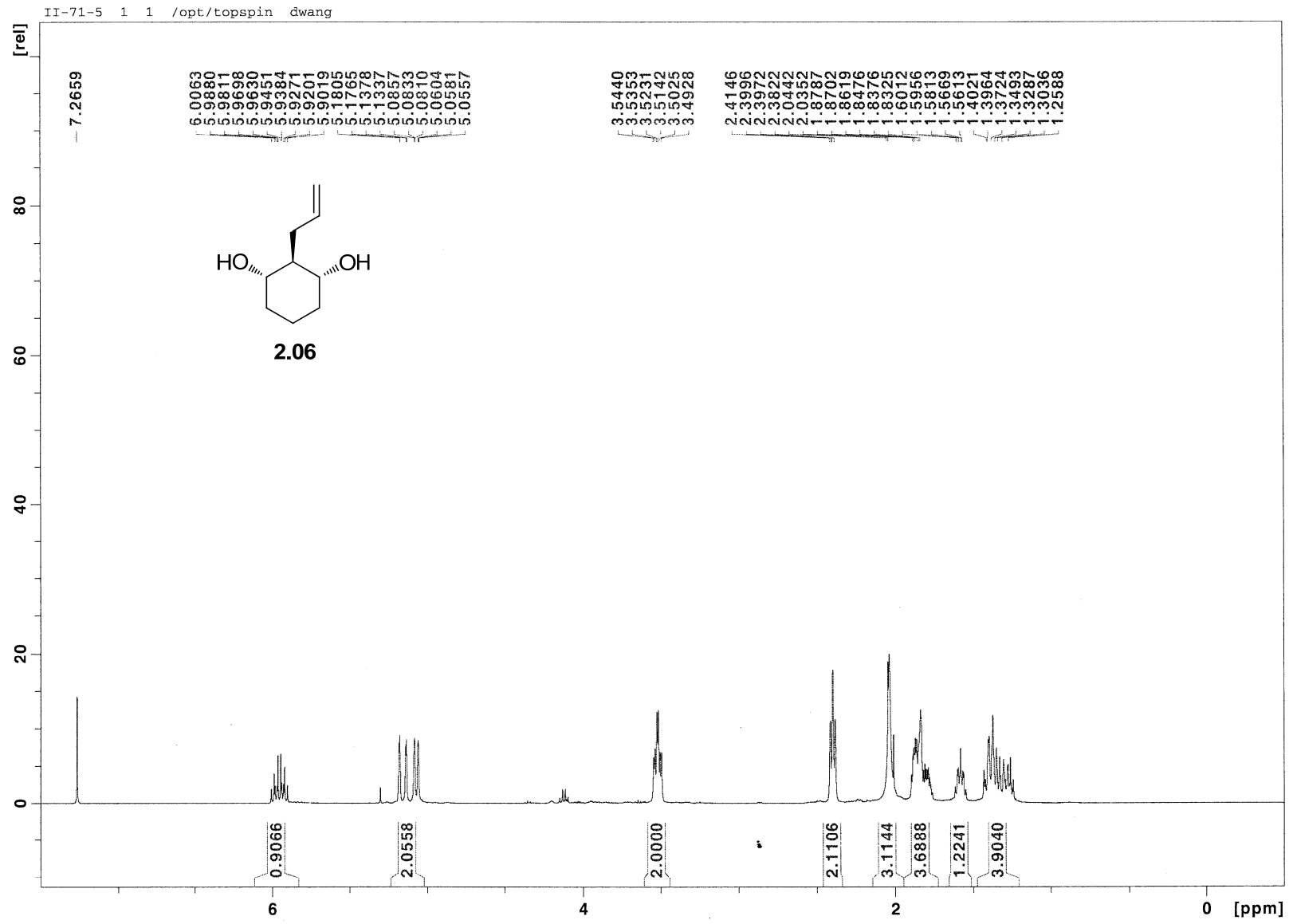


Figure 2.10 ^1H NMR (400 MHz, CDCl_3) of Compound 2.06

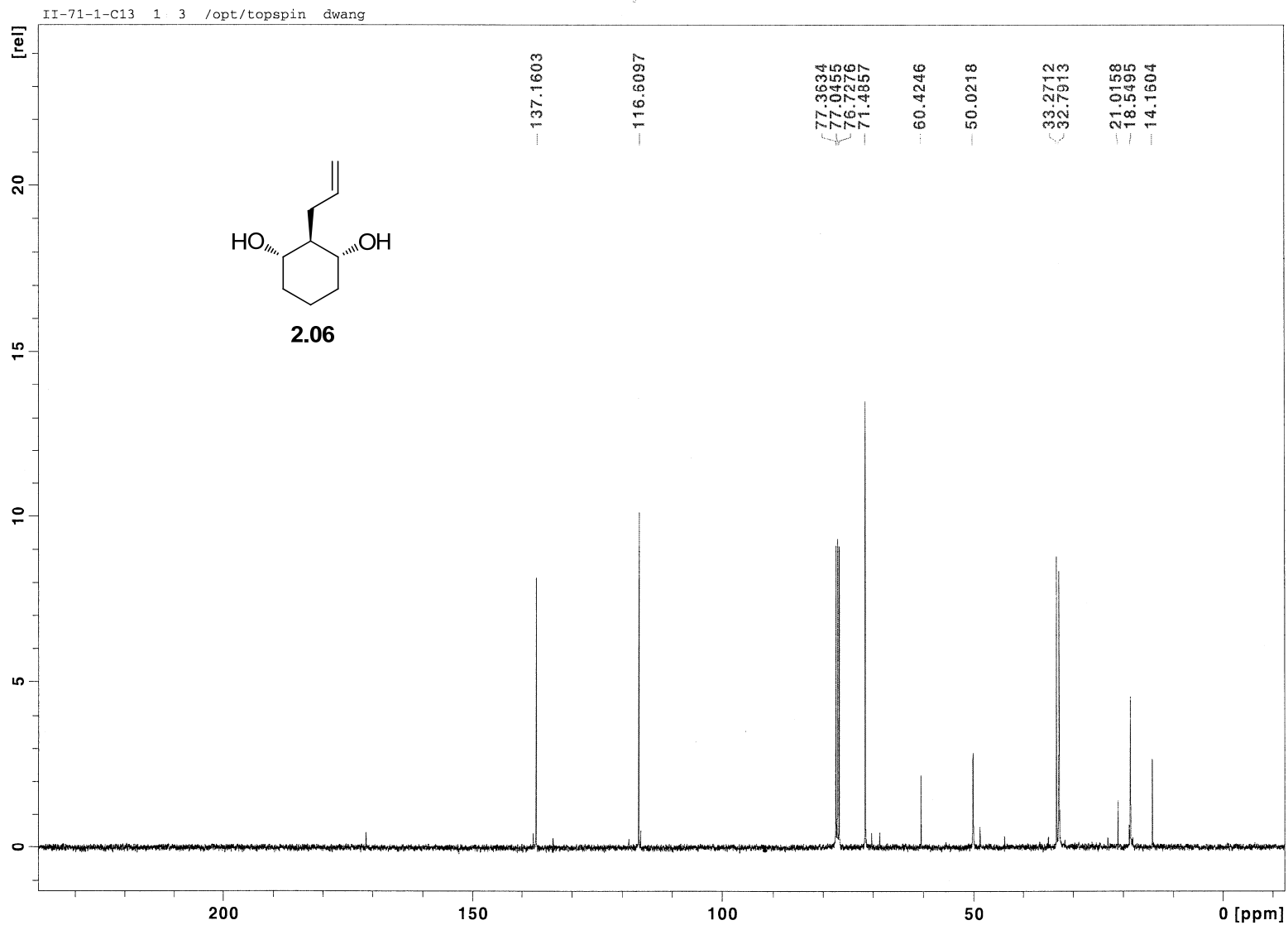


Figure 2.11 ^{13}C NMR (100 MHz, CDCl_3) of Compound 2.06

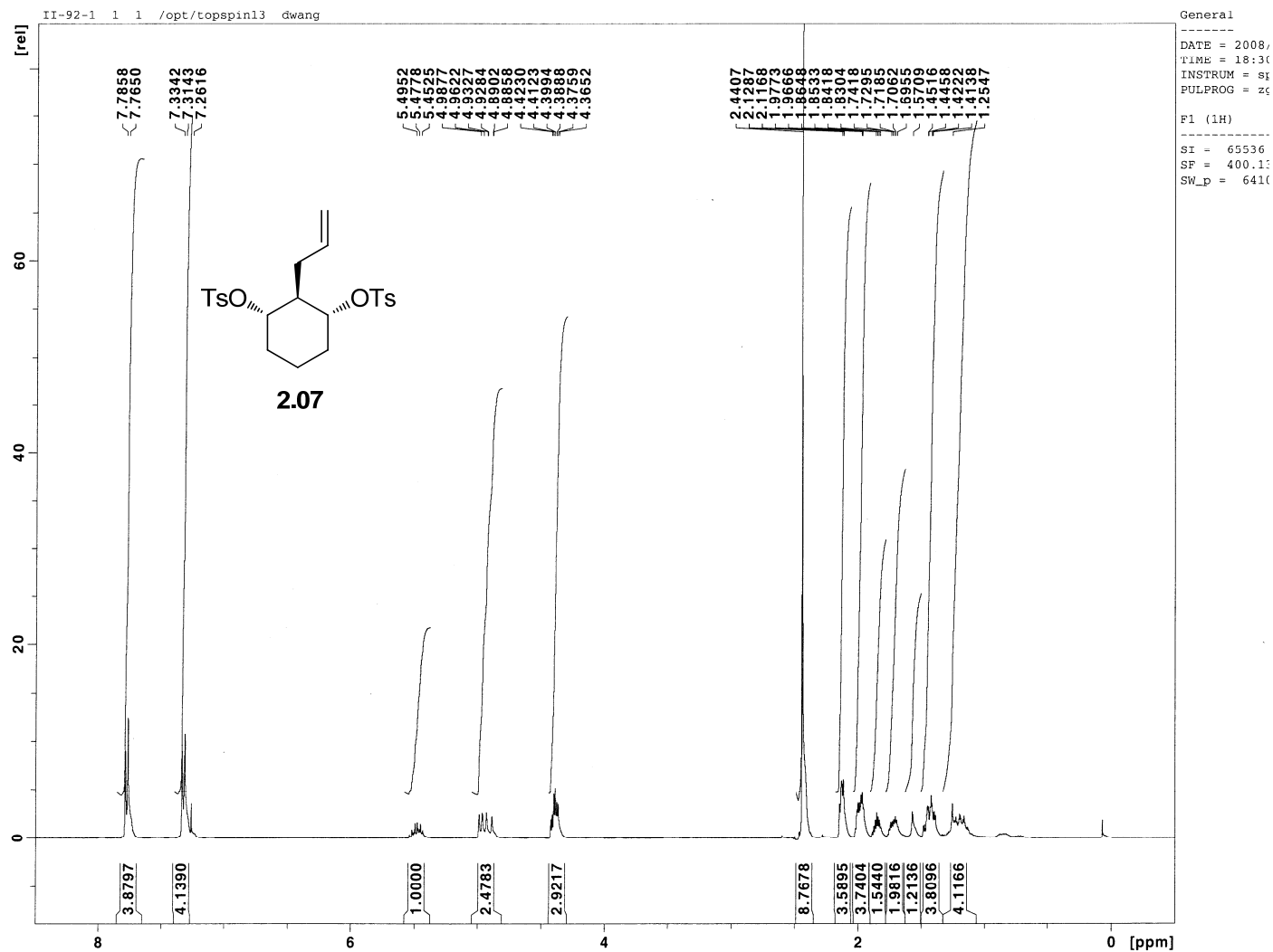


Figure 2.12 ^1H NMR (400 MHz, CDCl_3) of Compound 2.07

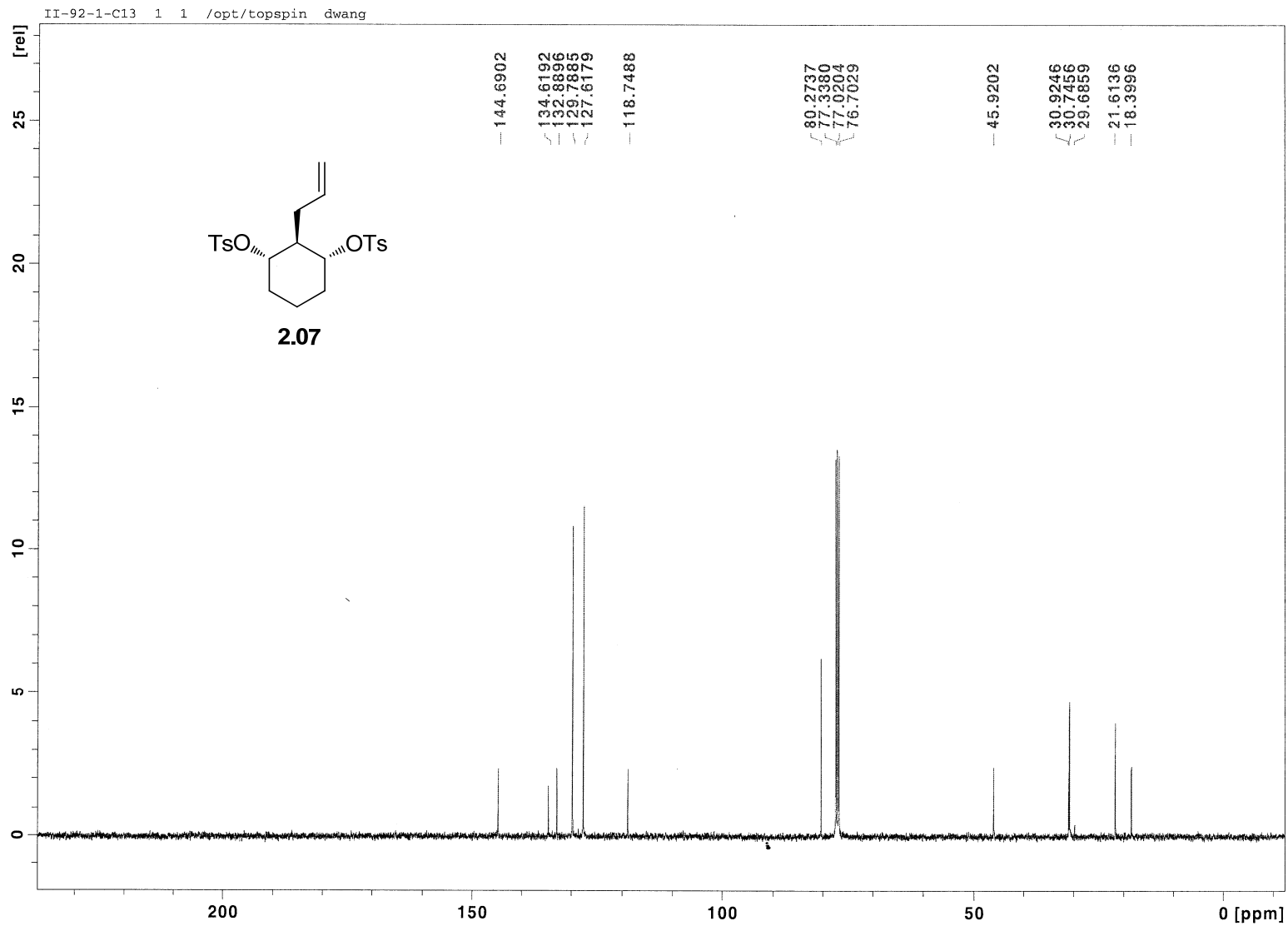


Figure 2.13 ^{13}C NMR (100 MHz, CDCl_3) of Compound 2.07

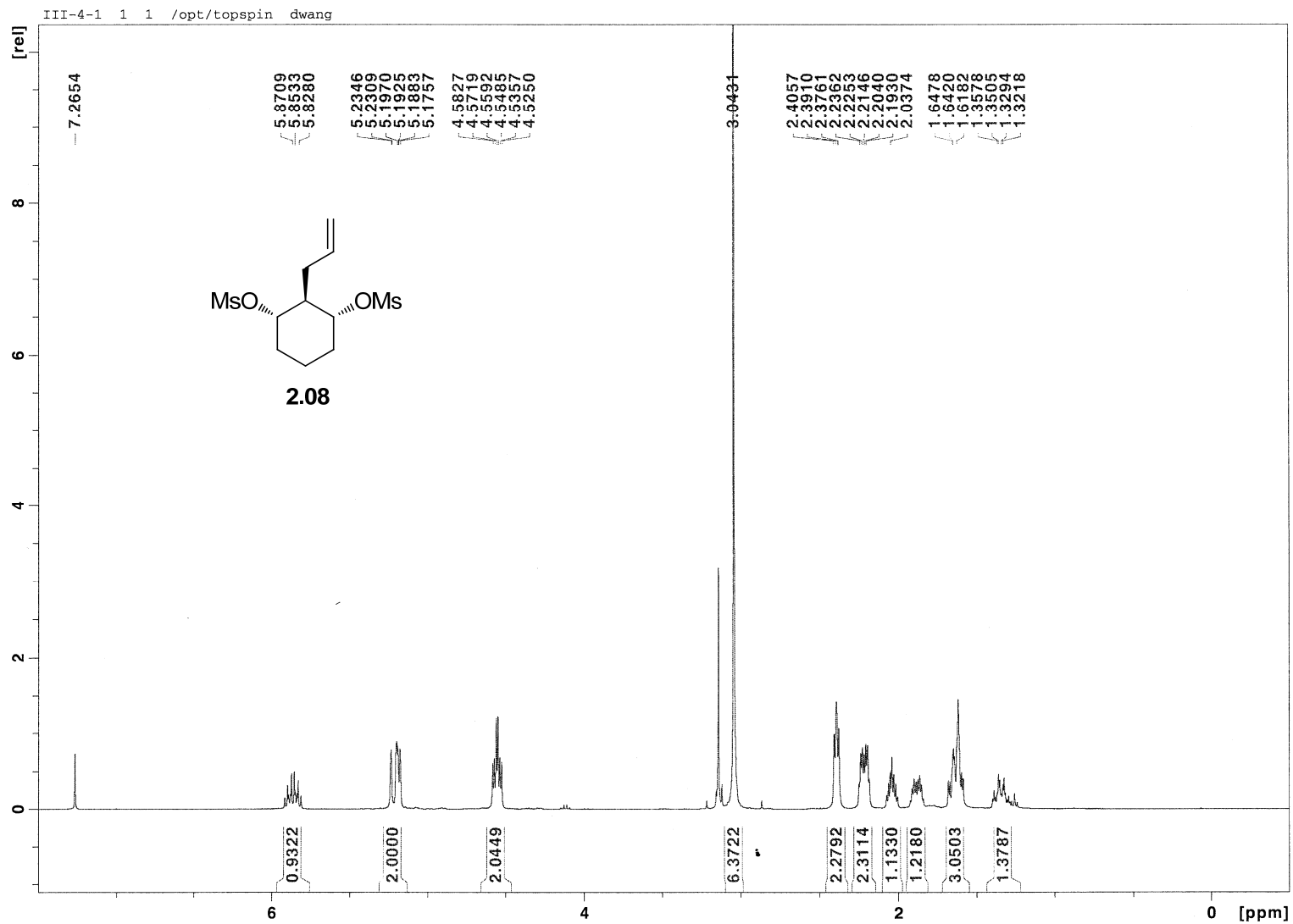


Figure 2.14 ^1H NMR (400 MHz, CDCl_3) of Compound 2.08

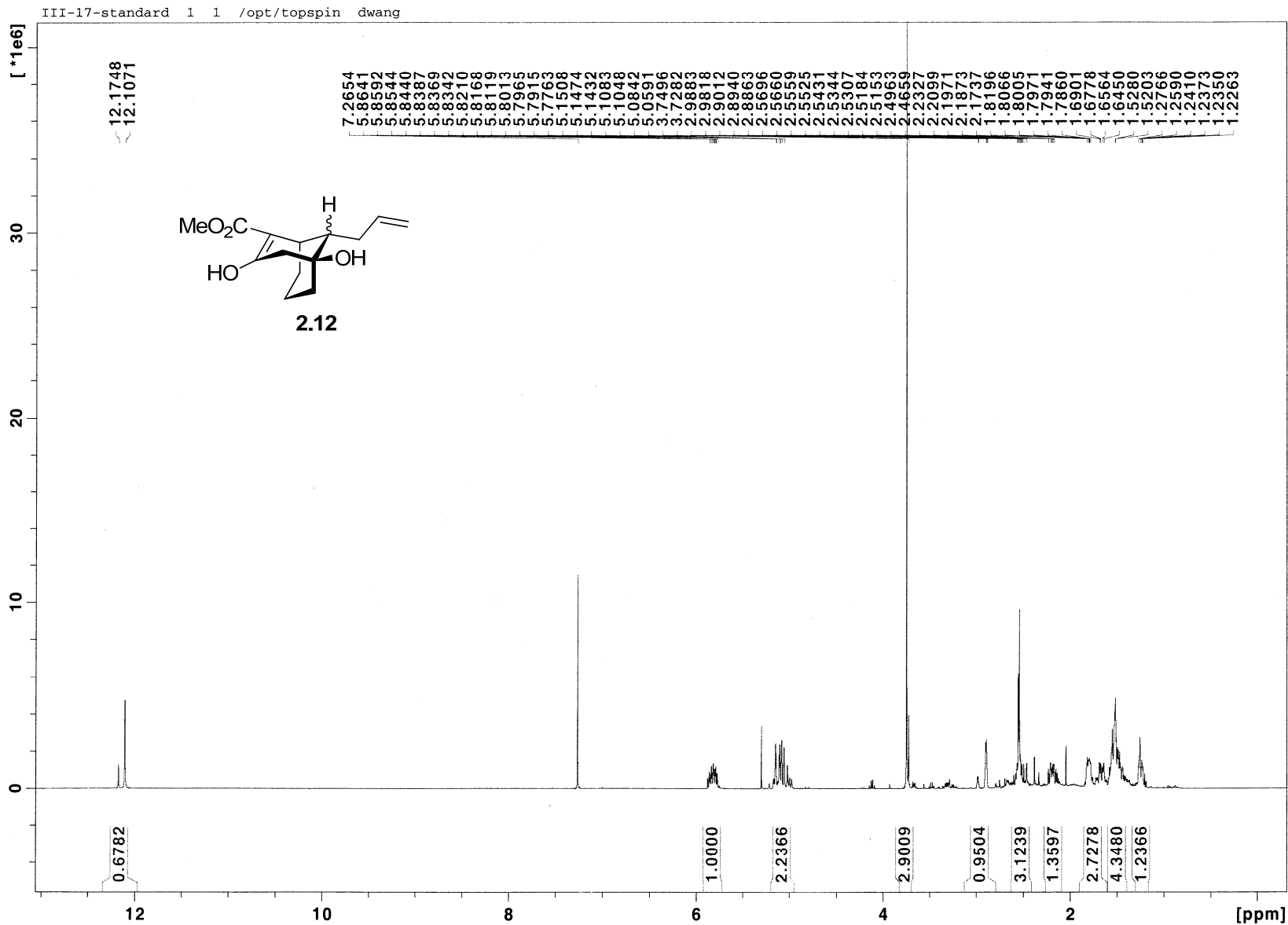


Figure 2.15 ^1H NMR (400 MHz, CDCl_3) of Compound 2.12

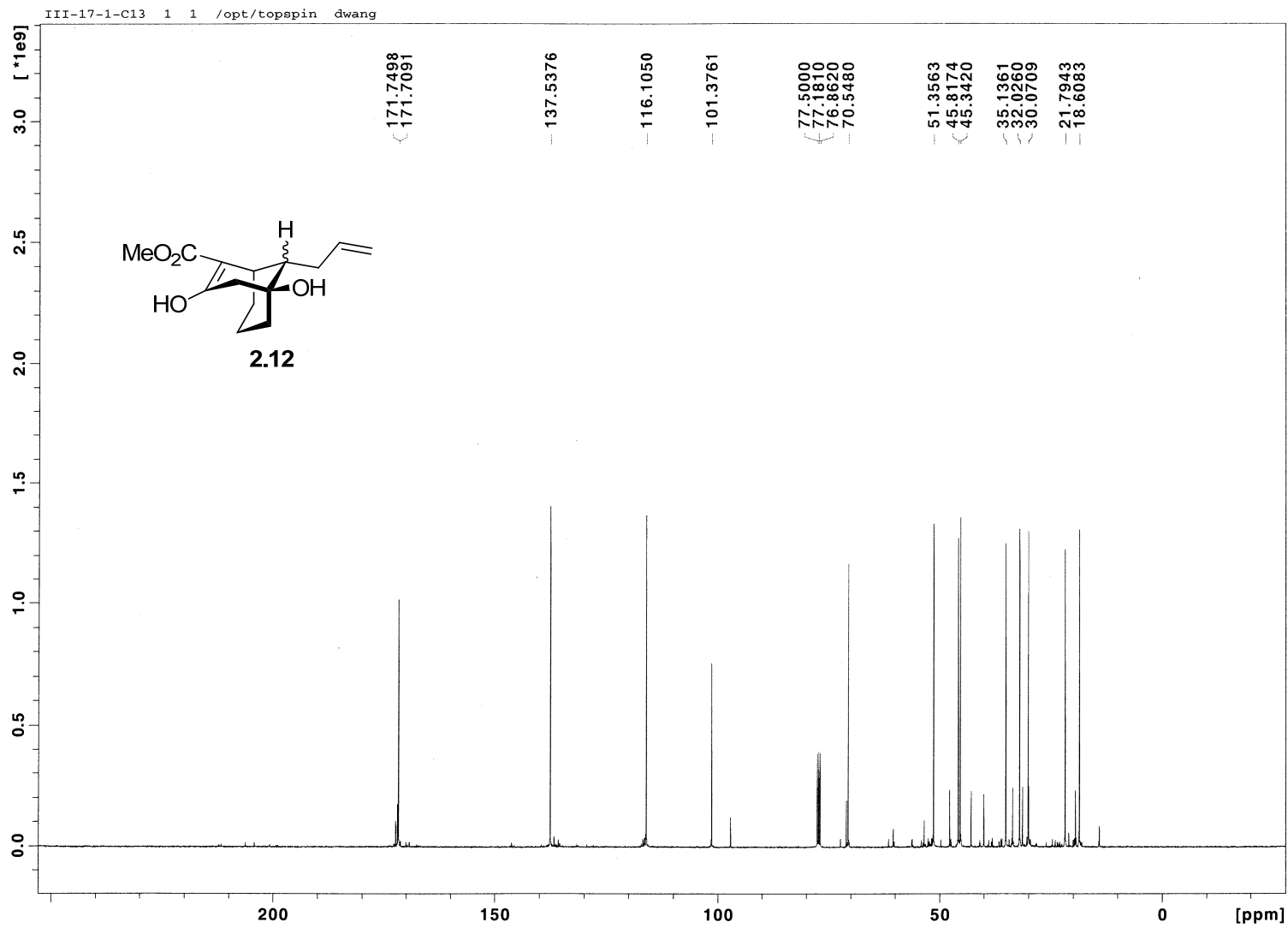


Figure 2.16 ¹³C NMR (100 MHz, CDCl₃) of Compound 2.12

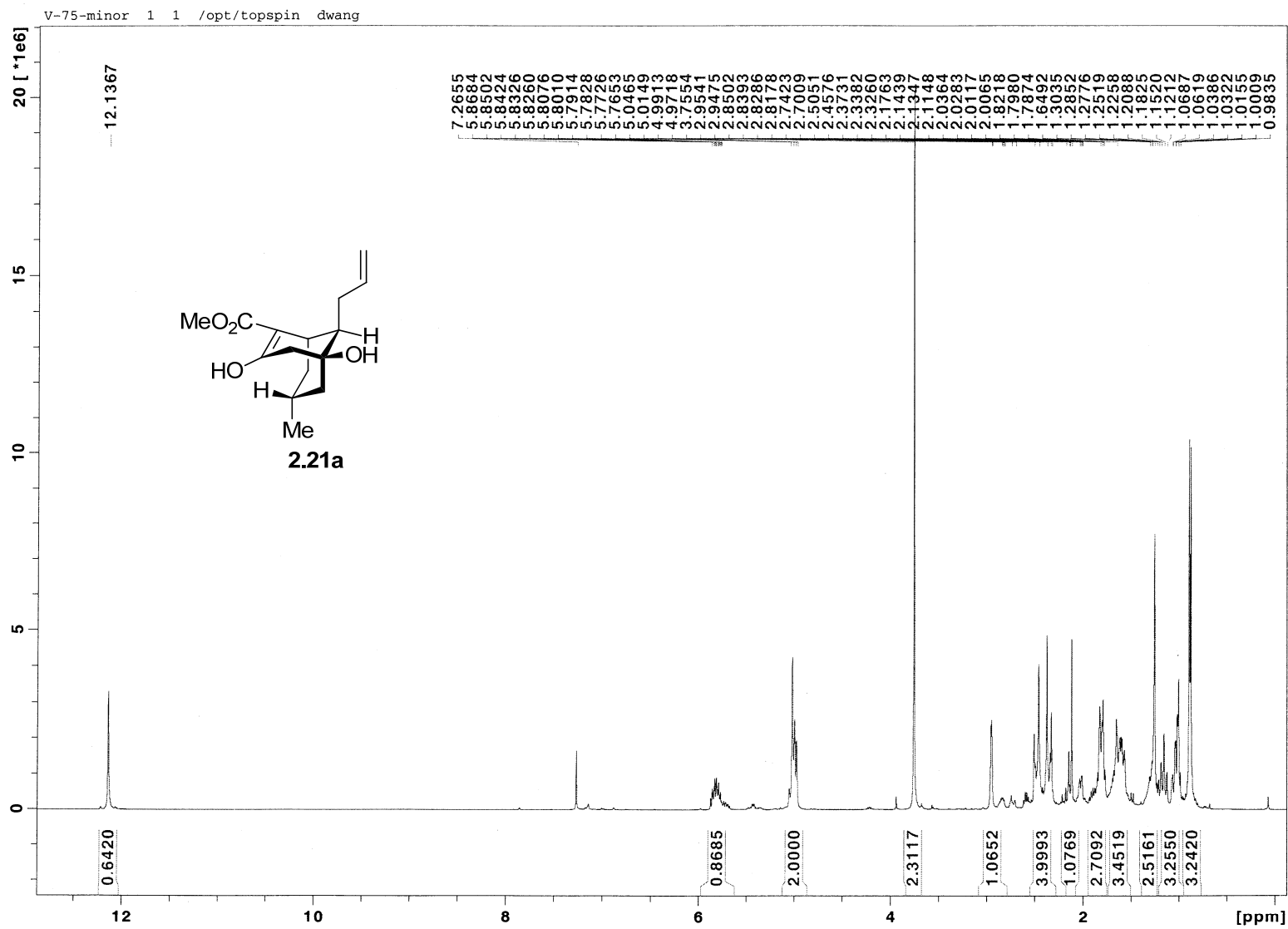


Figure 2.17 ^1H NMR (400 MHz, CDCl_3) of Compound 2.21a

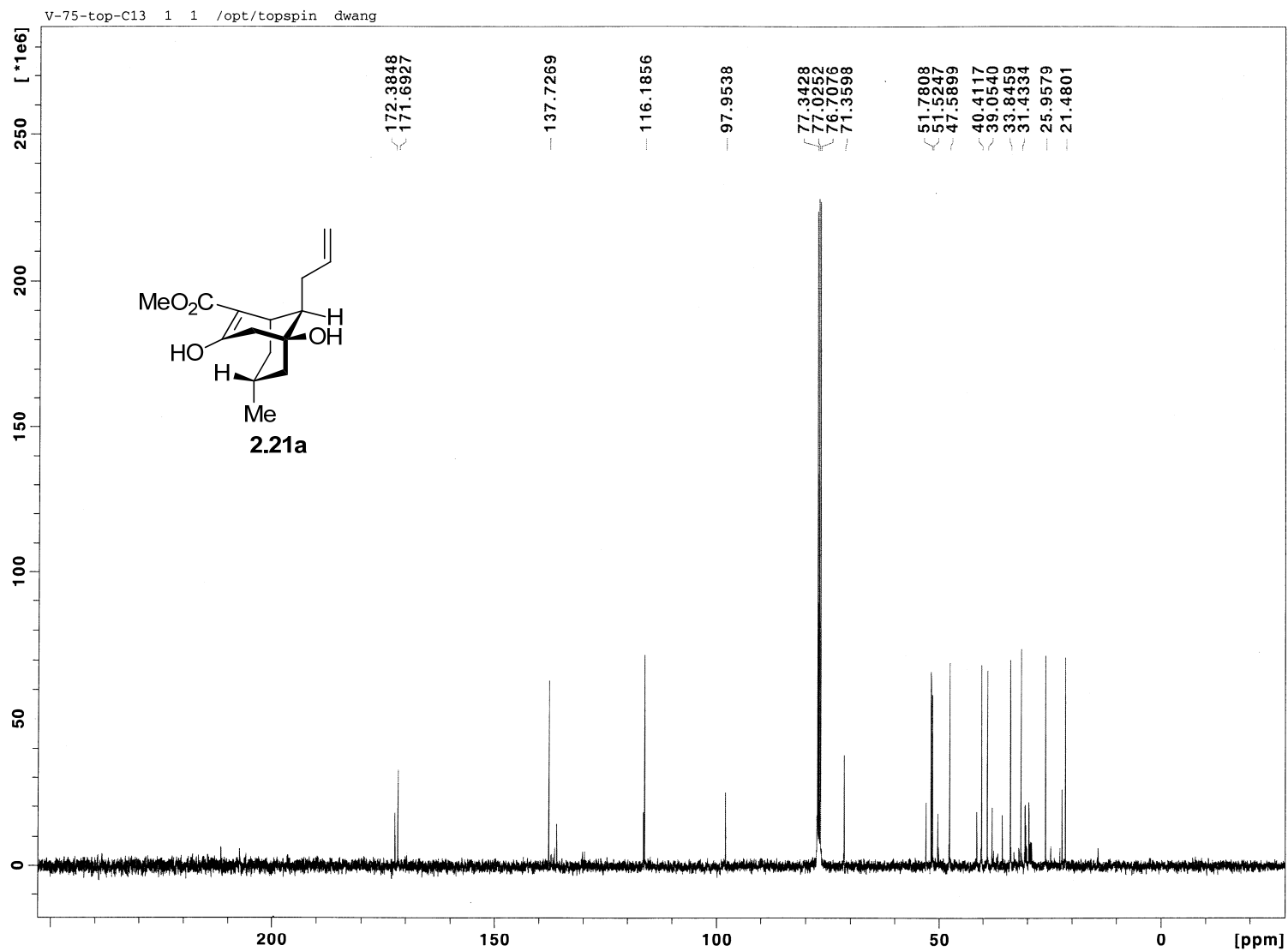


Figure 2.18 ^{13}C NMR (100 MHz, CDCl_3) of Compound 2.21a

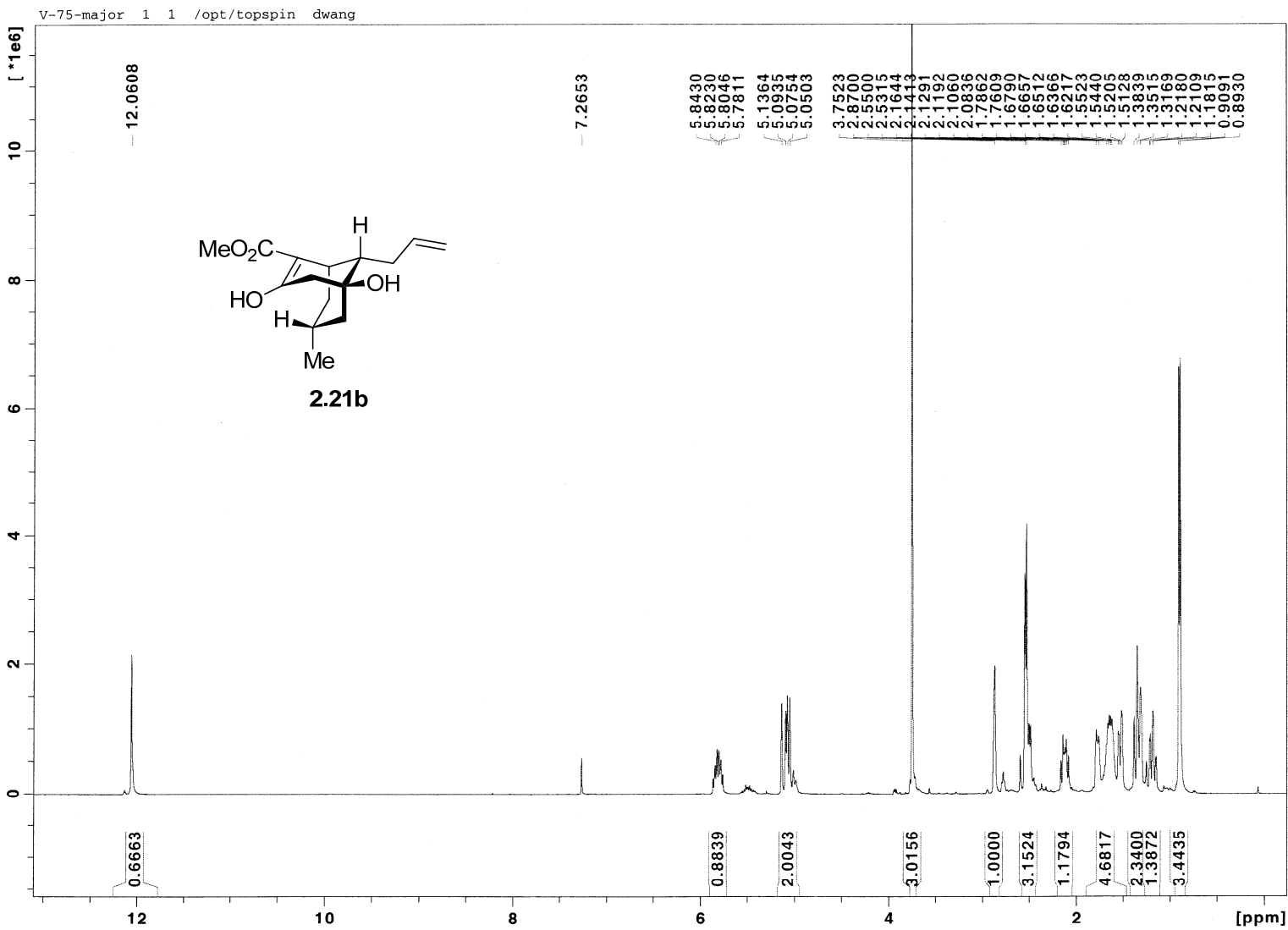


Figure 2.19 ¹H NMR (400 MHz, CDCl₃) of Compound 2.21b

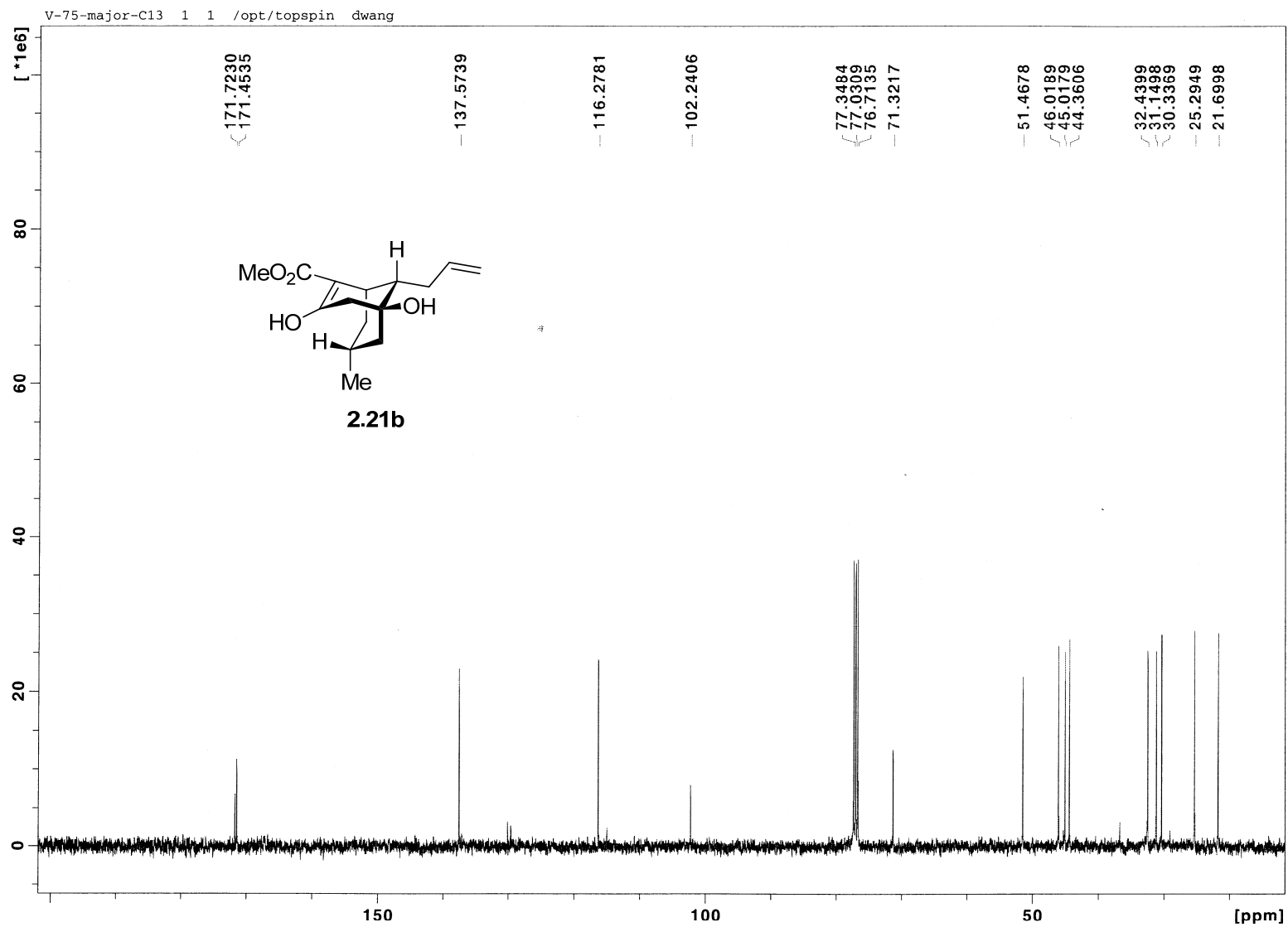


Figure 2.20 ¹³C NMR (100 MHz, CDCl₃) of Compound 2.21b

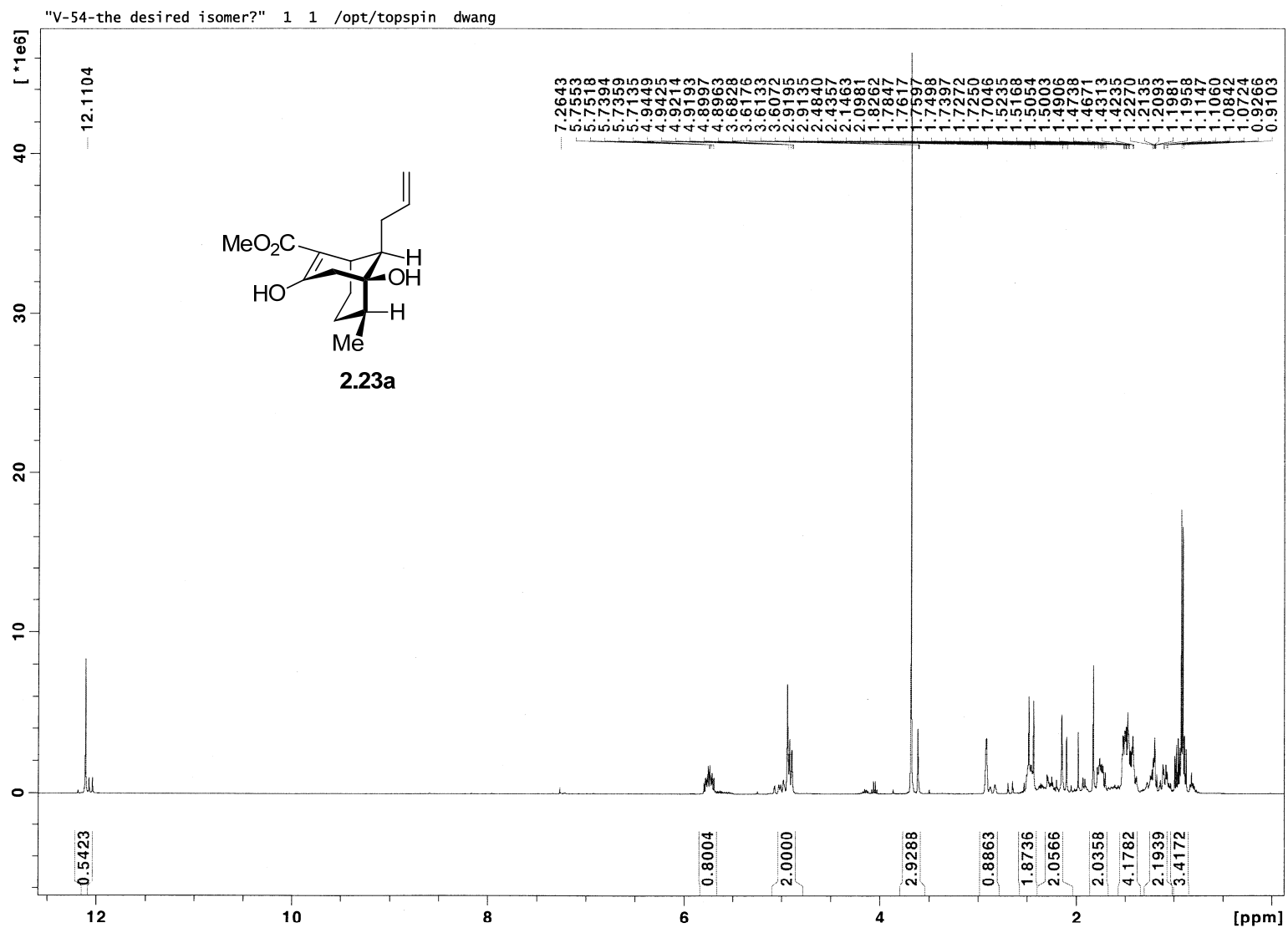


Figure 2.21 ^1H NMR (400 MHz, CDCl_3) of Compound 2.23a

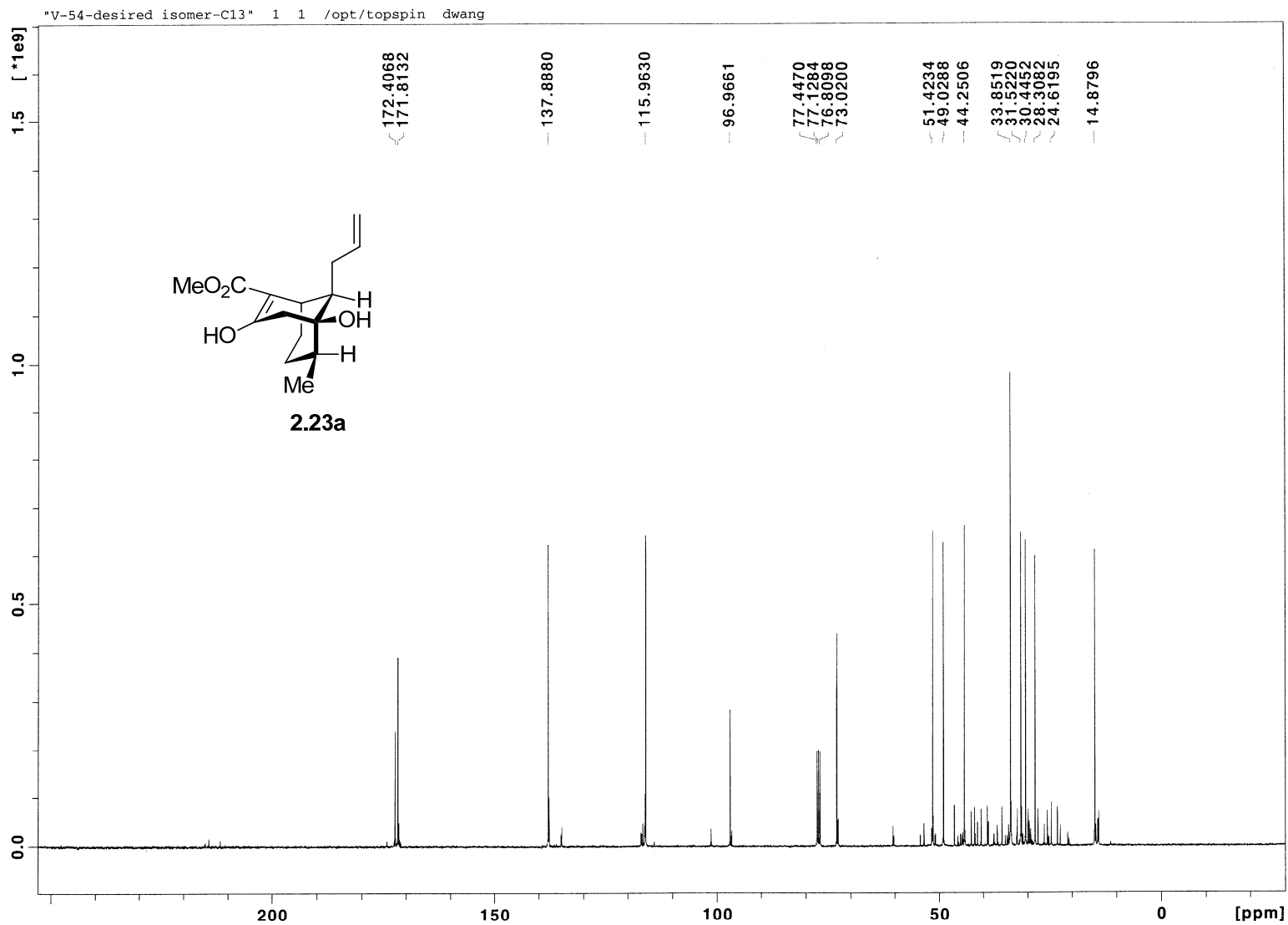


Figure 2.22 ¹³C NMR (100 MHz, CDCl₃) of Compound 2.23a

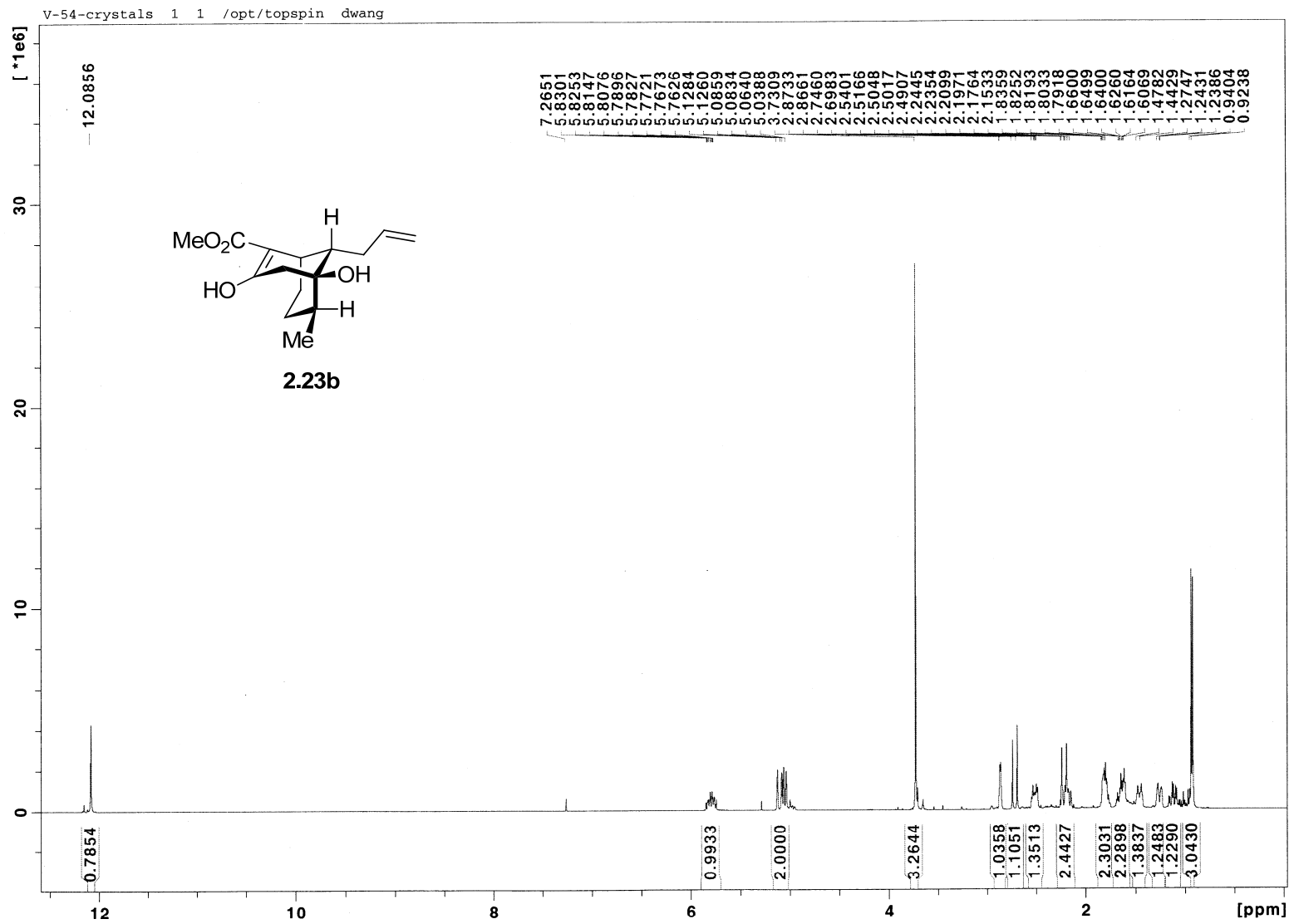


Figure 2.23 ¹H NMR (400 MHz, CDCl₃) of Compound 2.23b

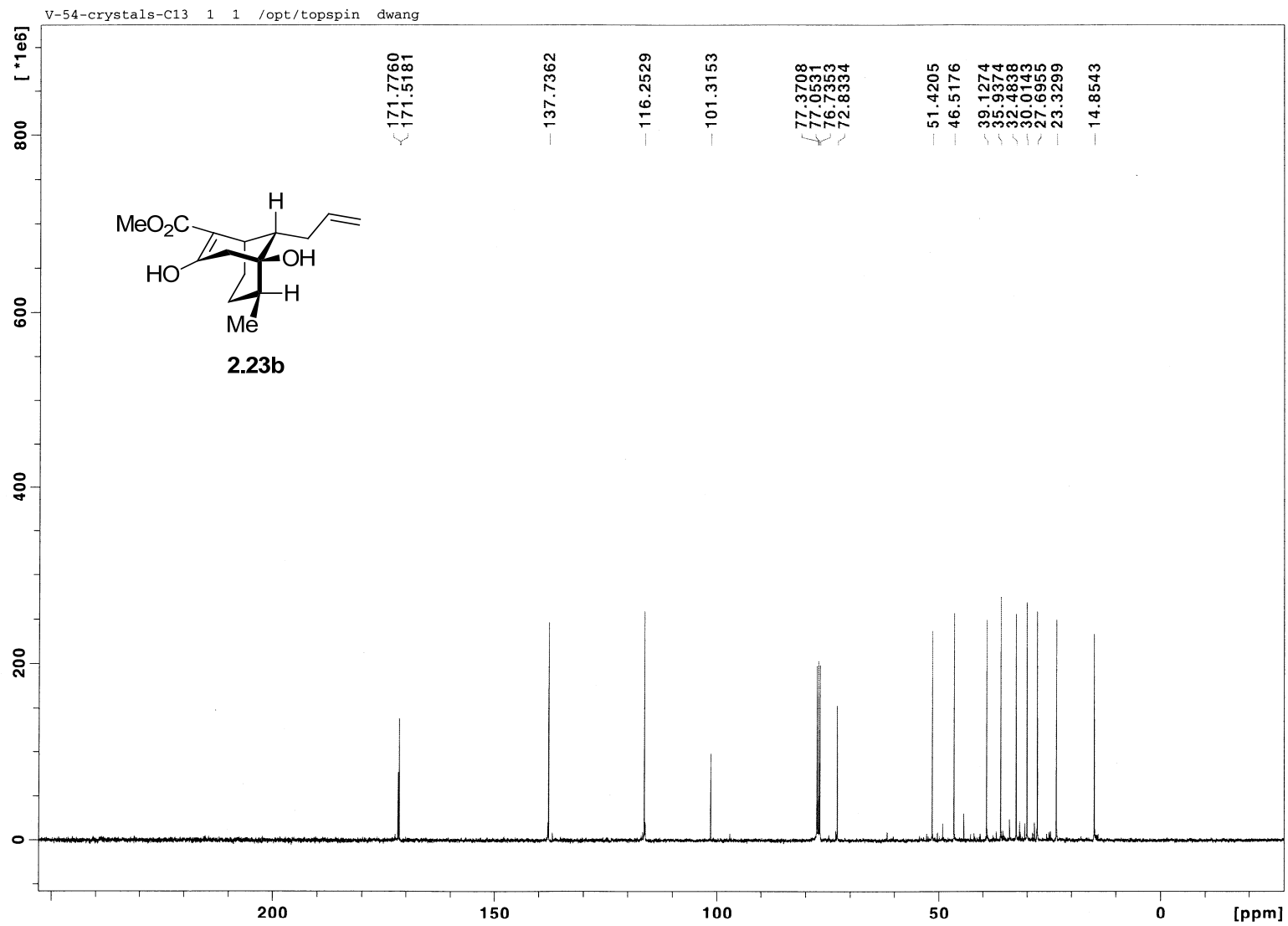


Figure 2.24 ^{13}C NMR (100 MHz, CDCl_3) of Compound 2.23b

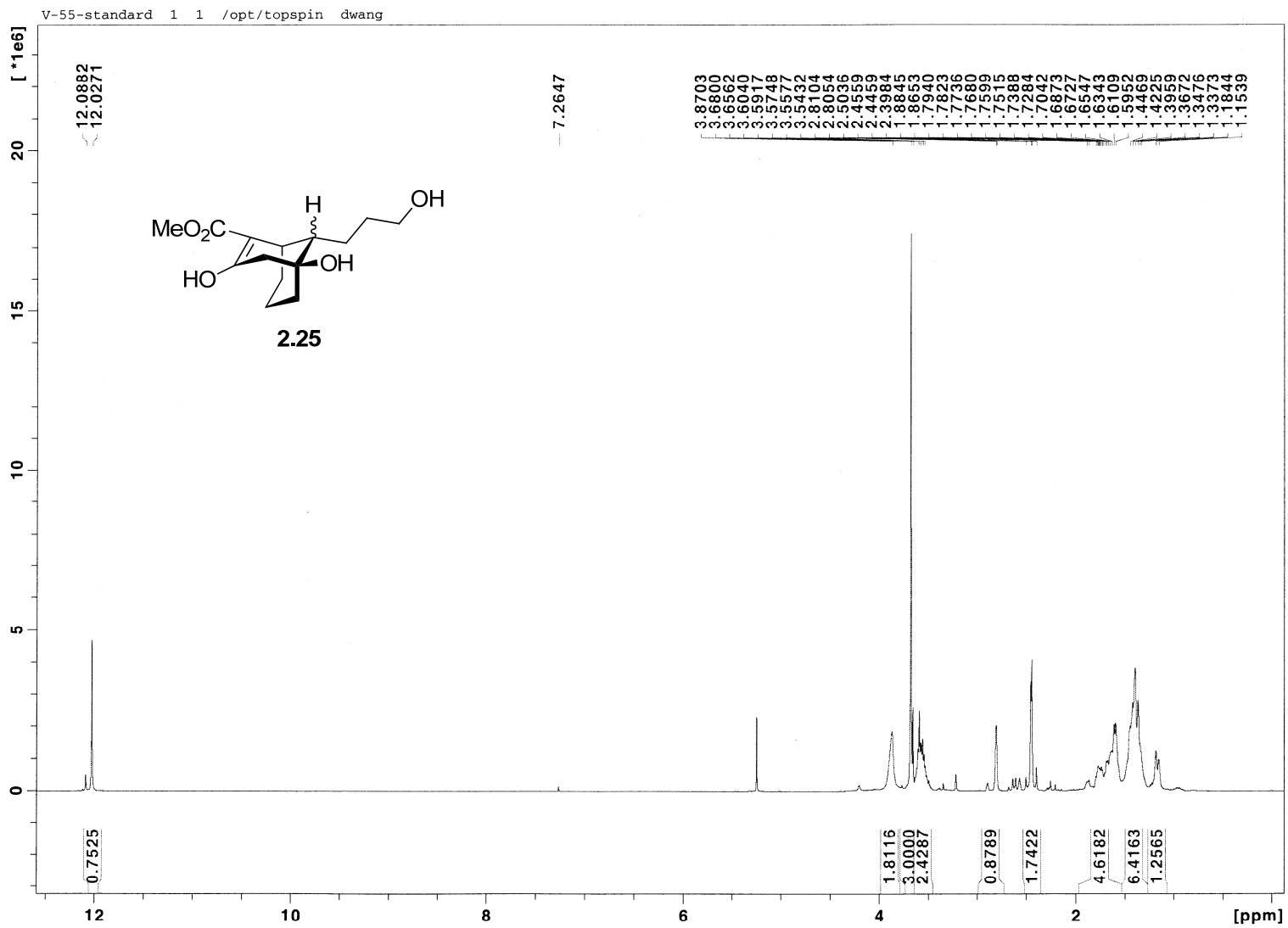


Figure 2.25 ^1H NMR (400 MHz, CDCl_3) of Compound 2.25

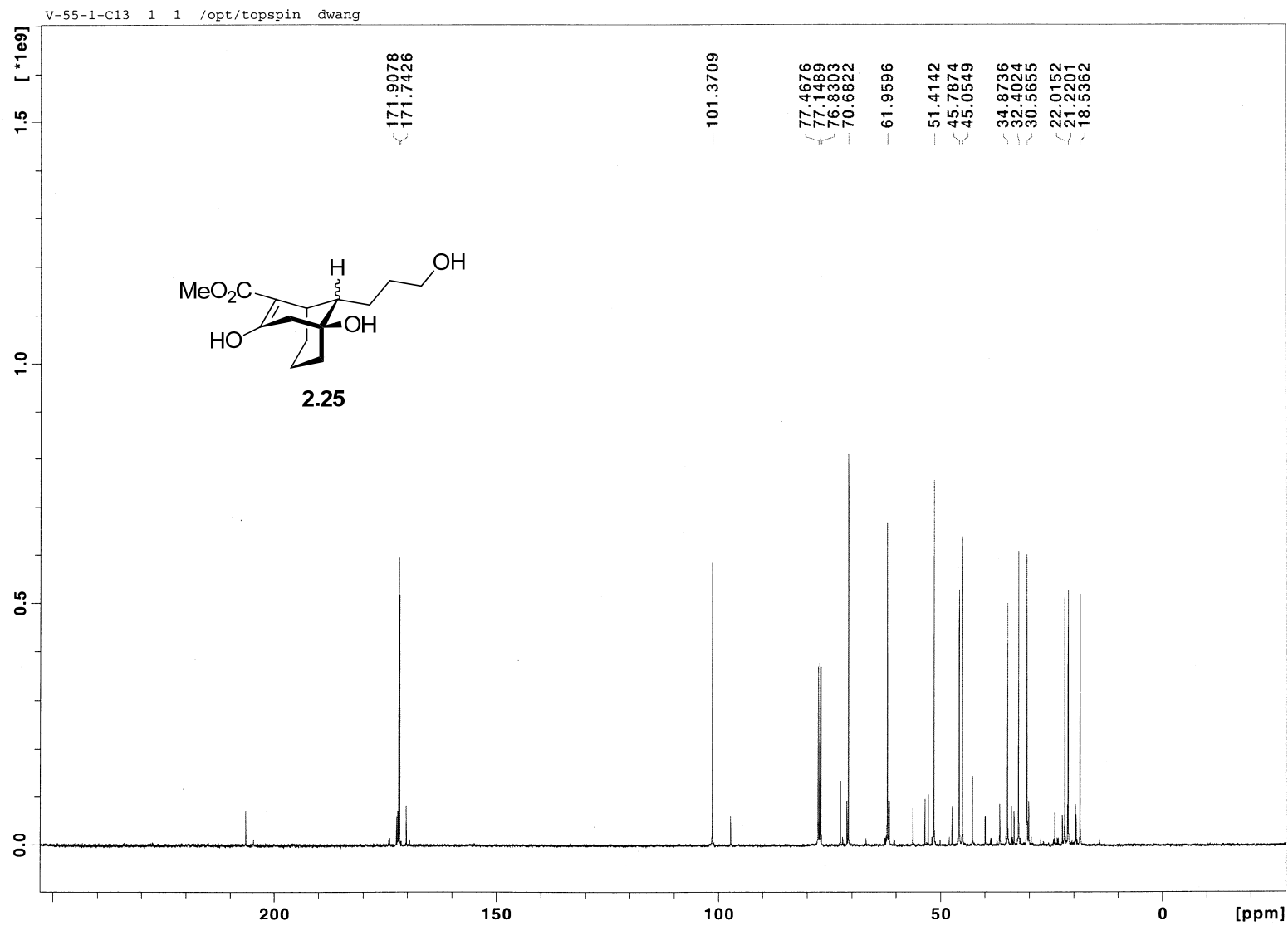


Figure 2.26 ^{13}C NMR (100 MHz, CDCl_3) of Compound 2.25

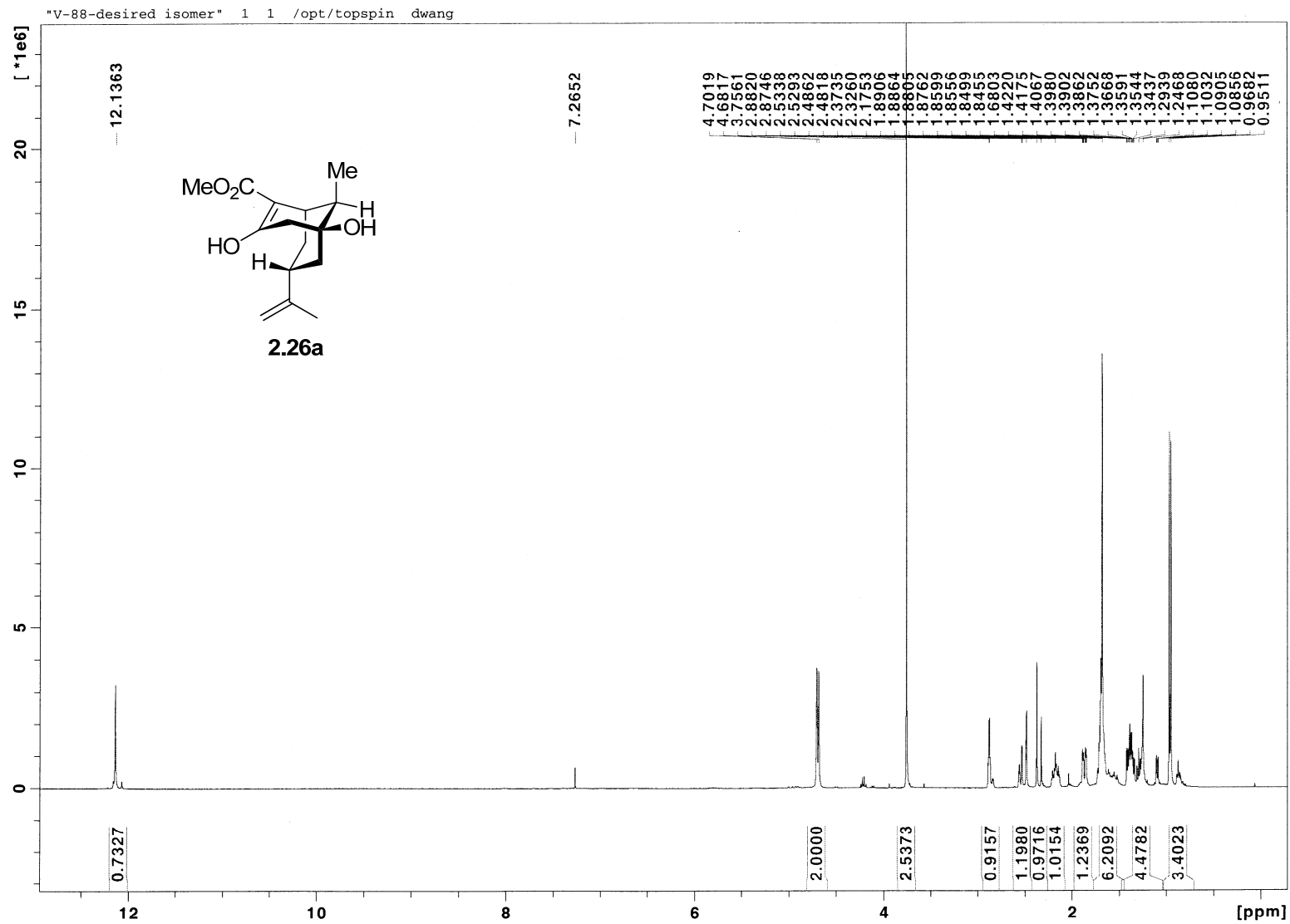


Figure 2.27 ^1H NMR (400 MHz, CDCl_3) of Compound 2.26a

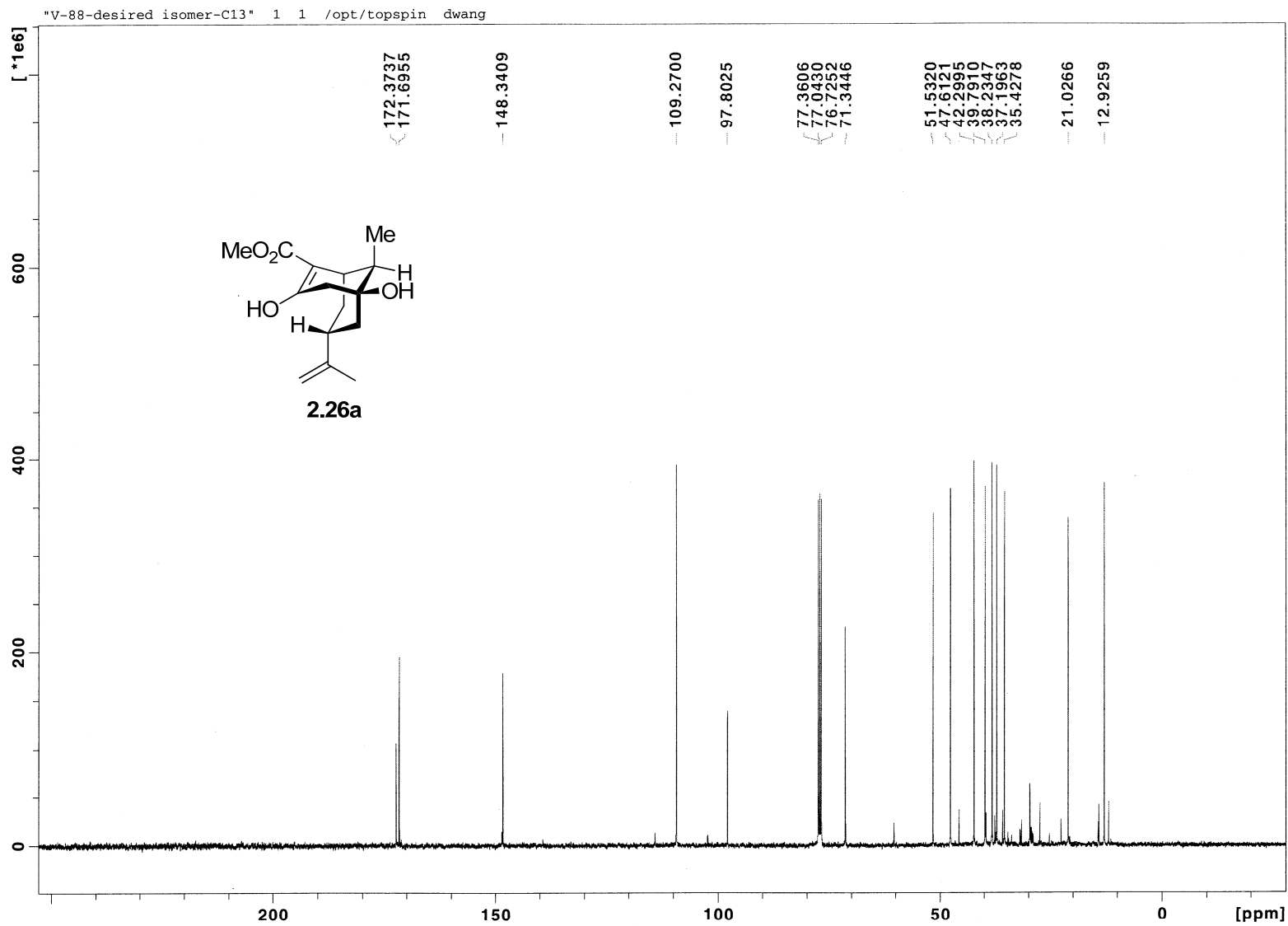


Figure 2.28 ^{13}C NMR (100 MHz, CDCl_3) of Compound 2.26a

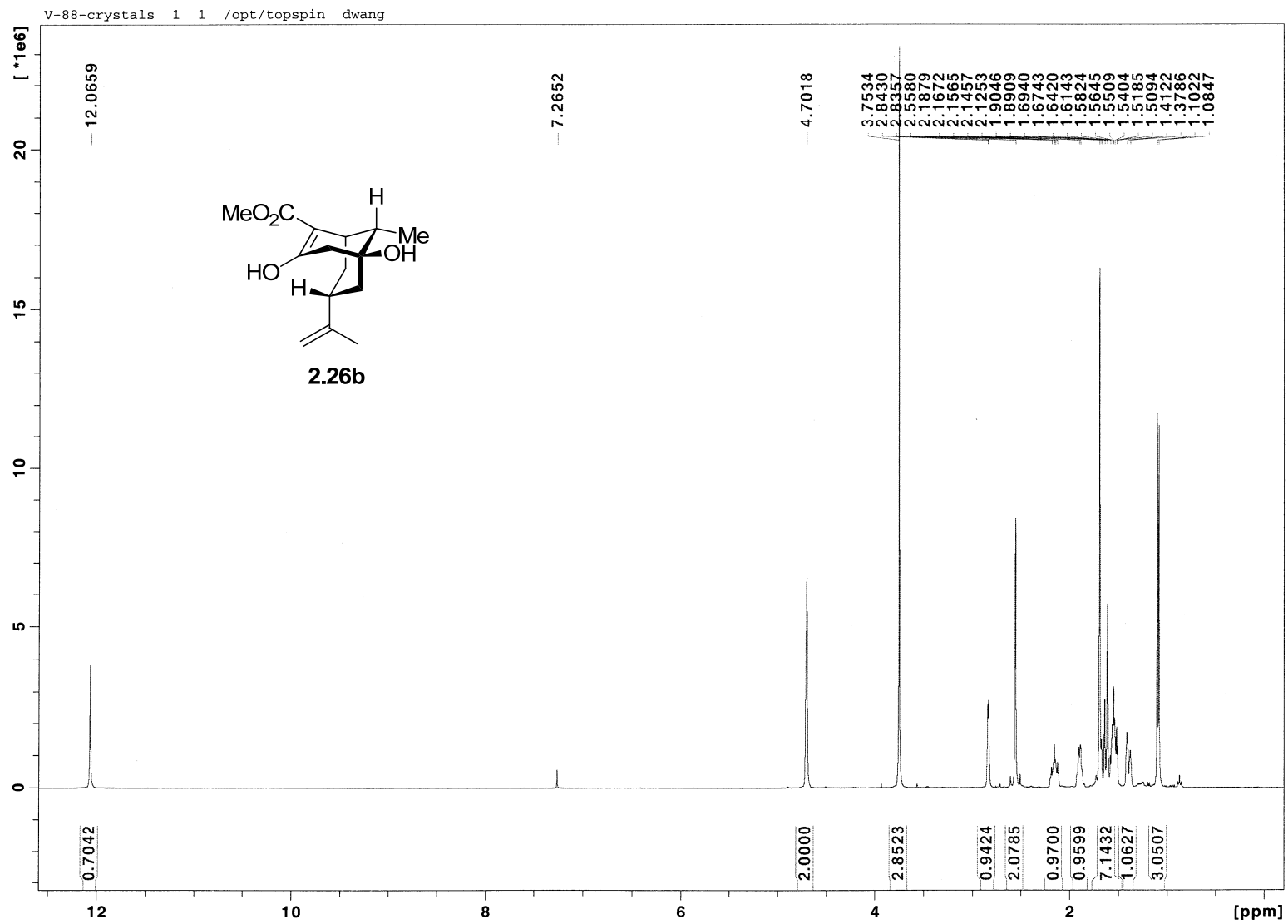


Figure 2.29 ^1H NMR (400 MHz, CDCl_3) of Compound 2.26b

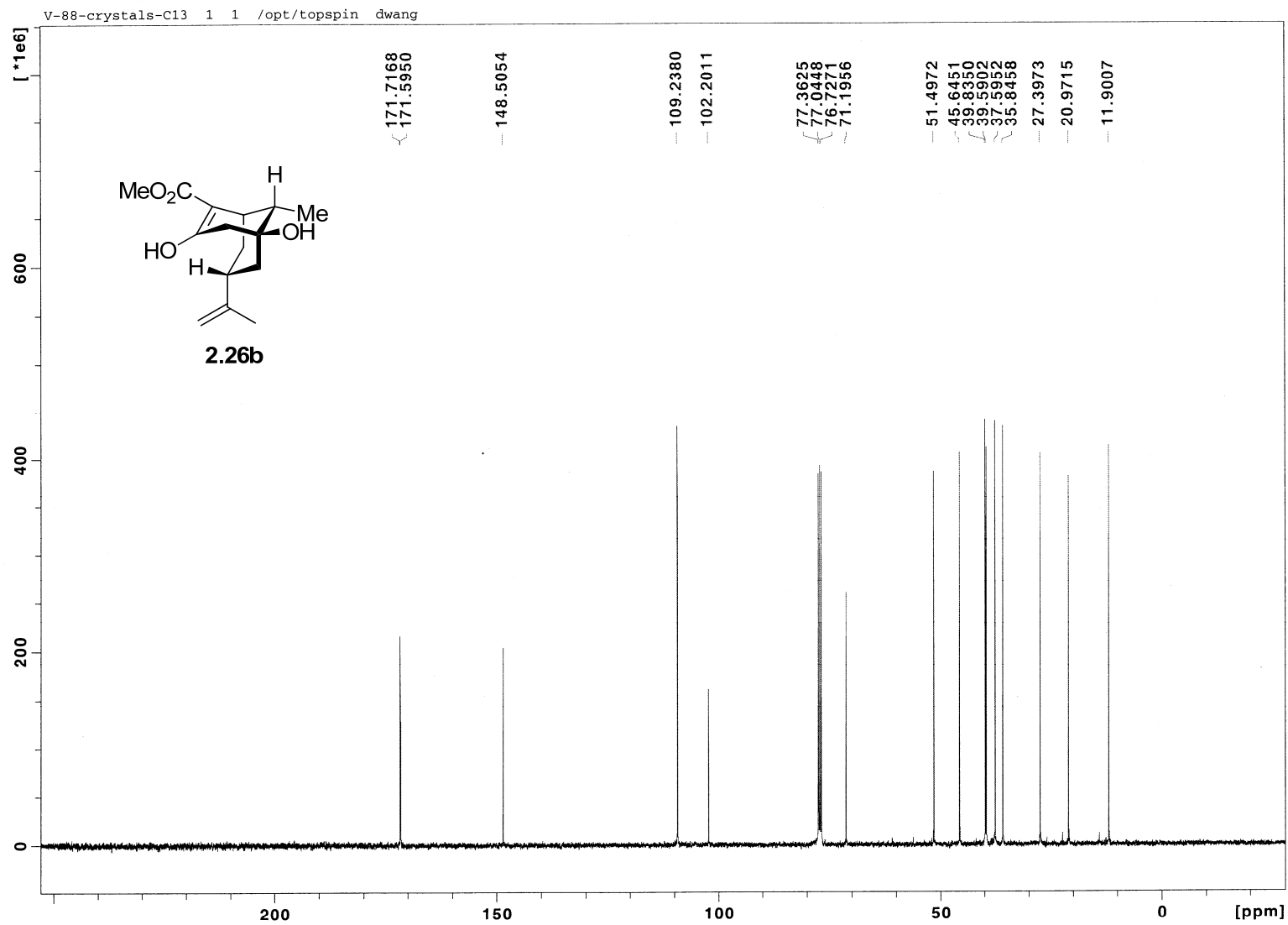


Figure 2.30 ¹³C NMR (100 MHz, CDCl₃) of Compound 2.26b

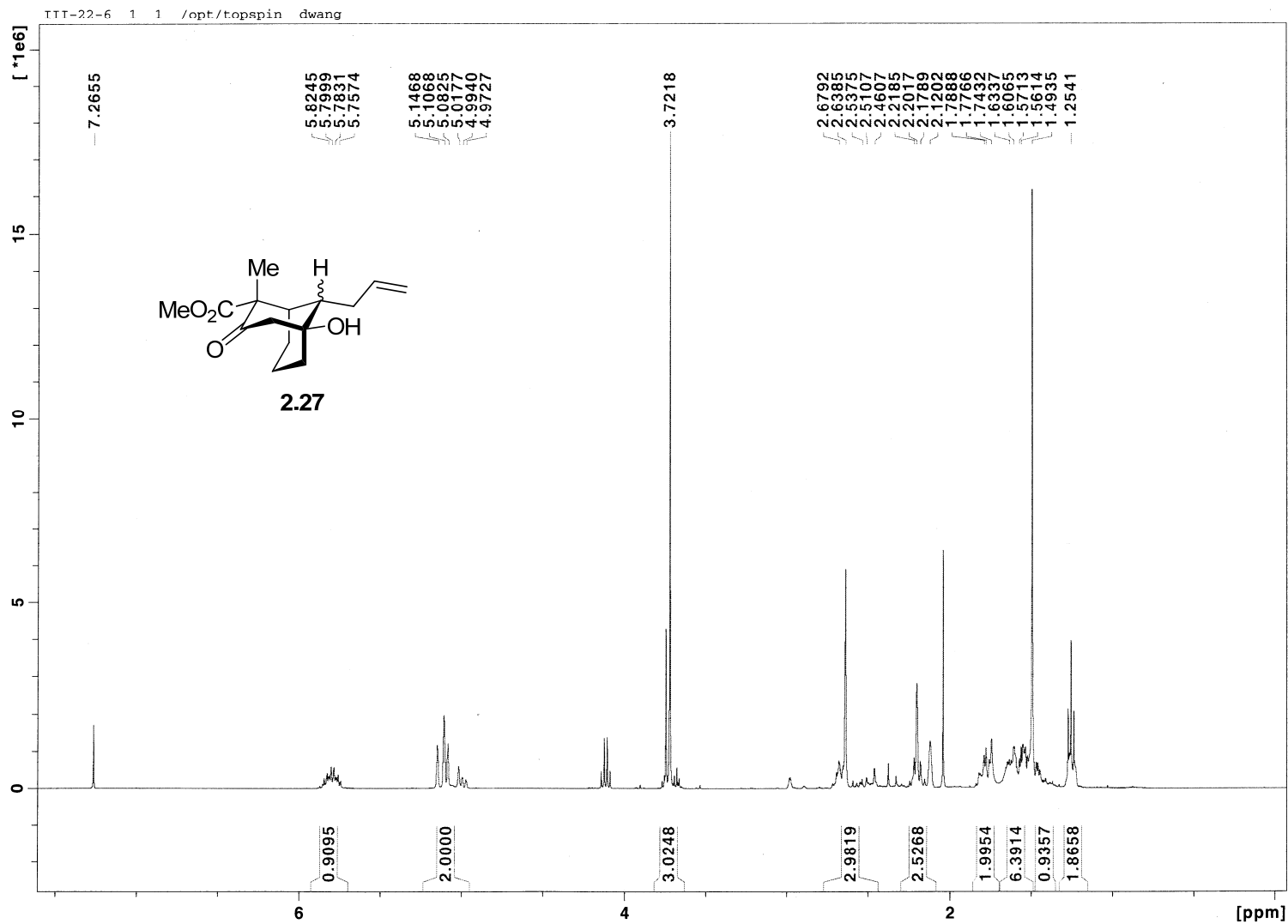


Figure 2.31 ^1H NMR (400 MHz, CDCl_3) of Compound 2.27

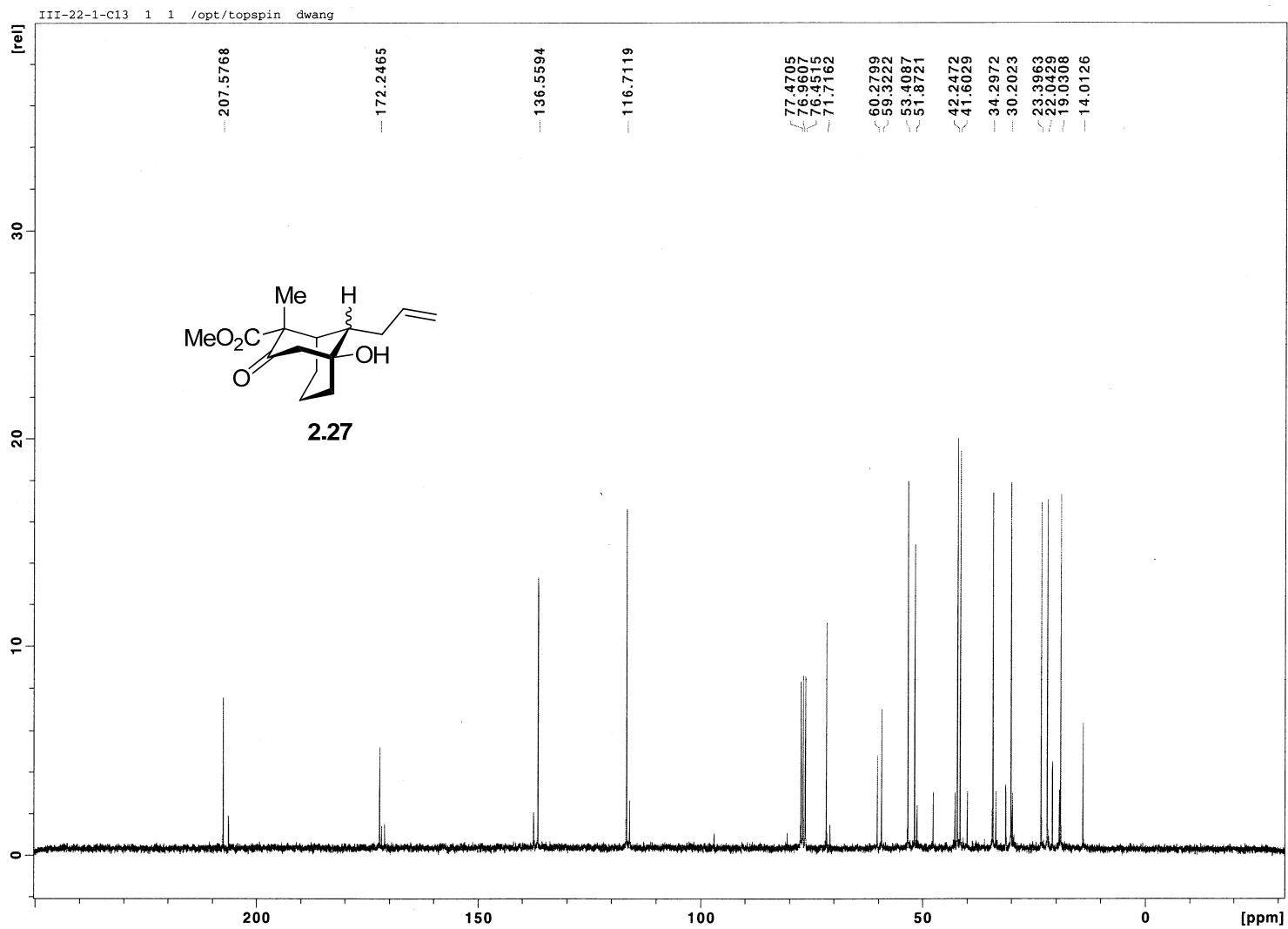


Figure 2.32 ^{13}C NMR (100 MHz, CDCl_3) of Compound 2.27

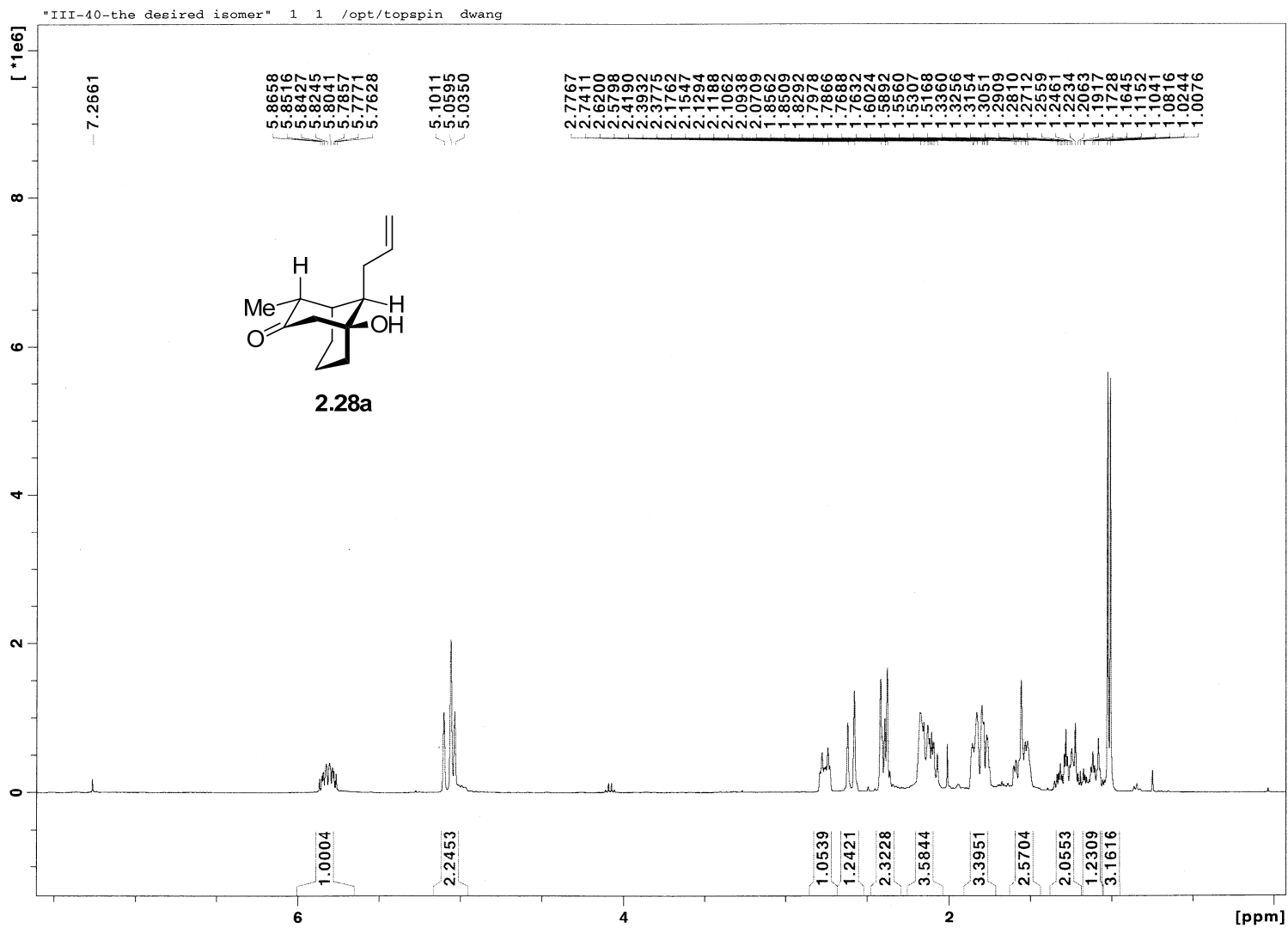


Figure 2.33 ^1H NMR (400 MHz, CDCl_3) of Compound 2.28a

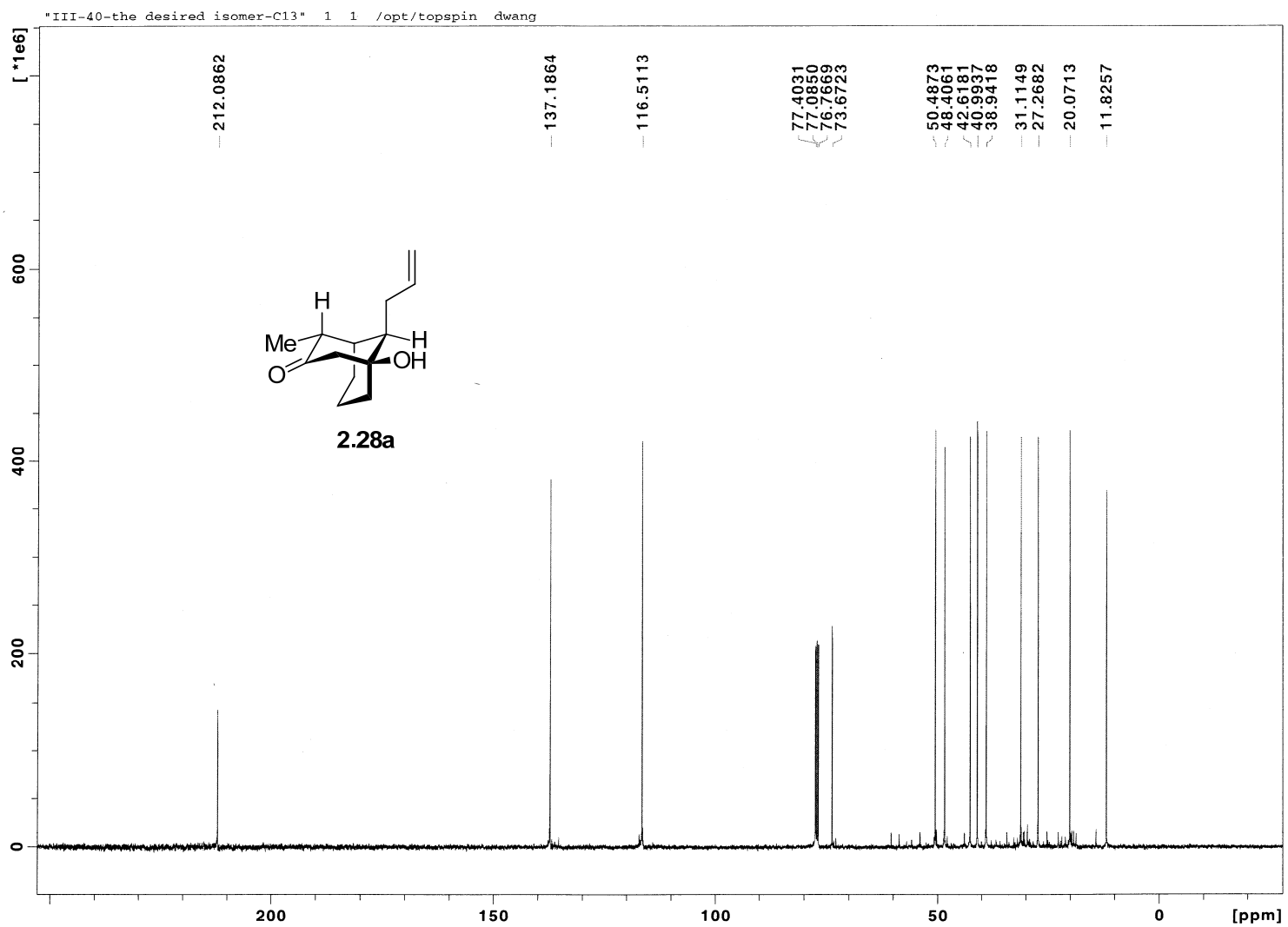


Figure 2.34 ^{13}C NMR (100 MHz, CDCl_3) of Compound 2.28a

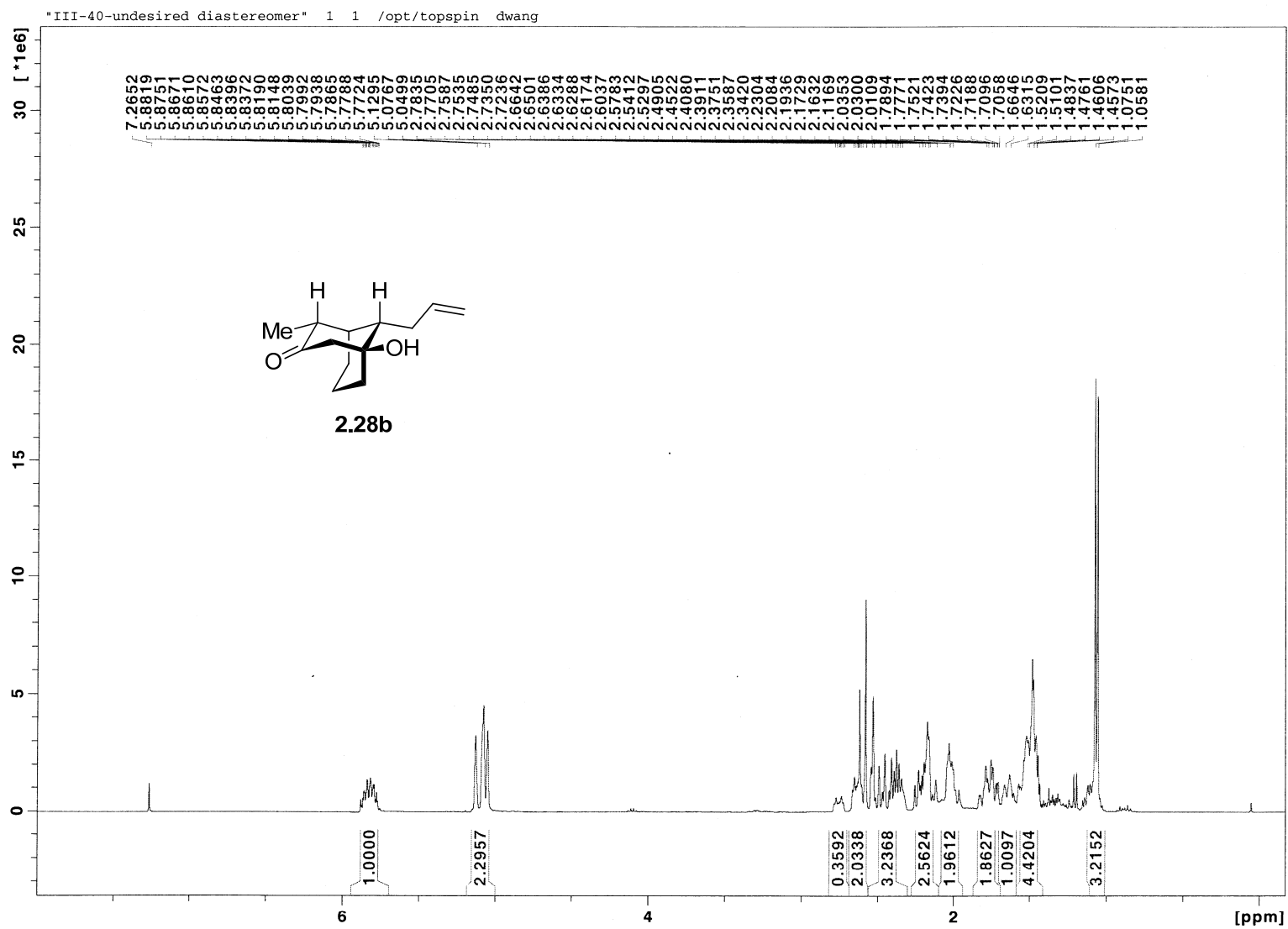


Figure 2.35 ^1H NMR (400 MHz, CDCl_3) of Compound 2.28b

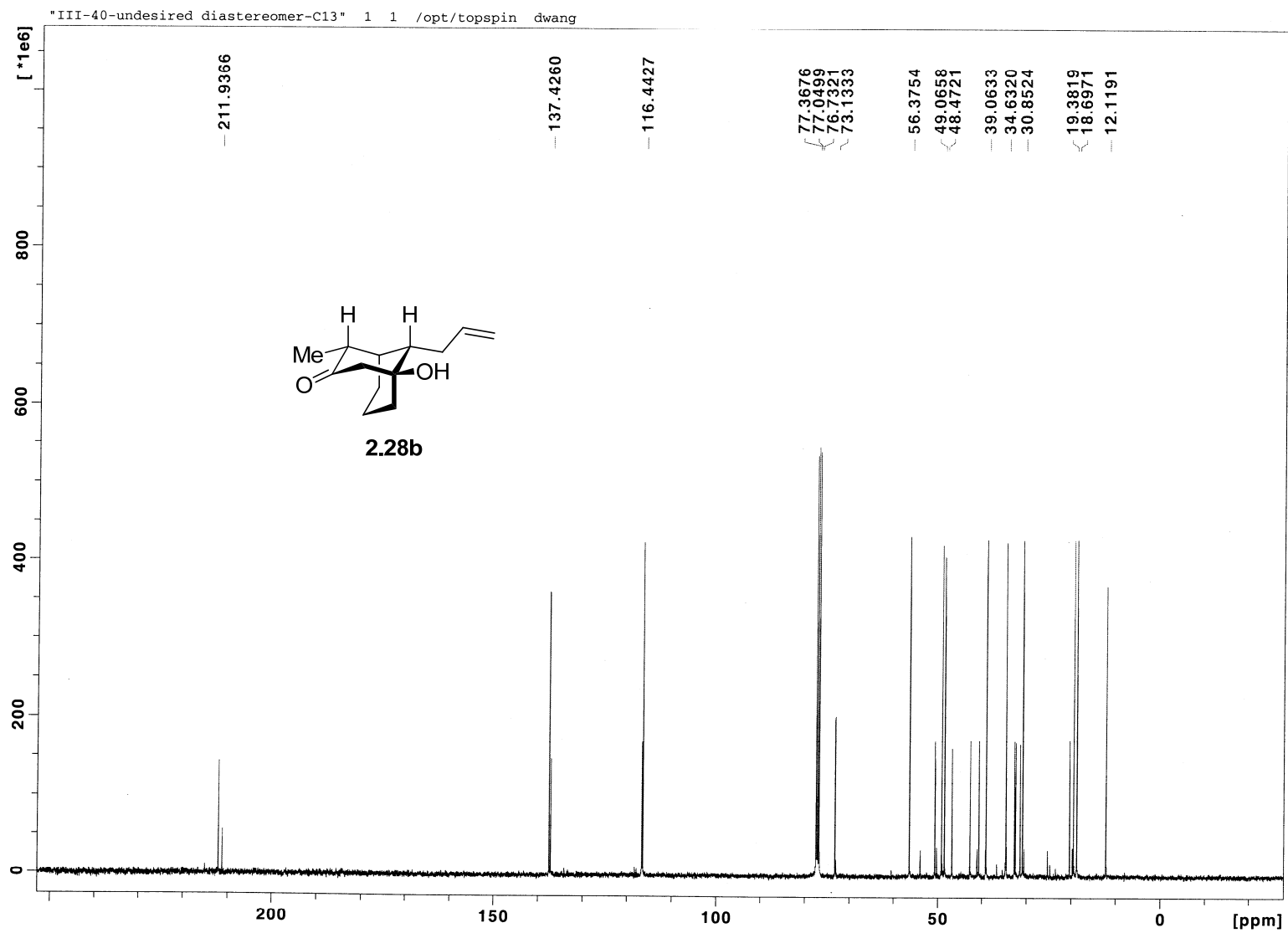


Figure 2.36 ^{13}C NMR (100 MHz, CDCl_3) of Compound 2.28b

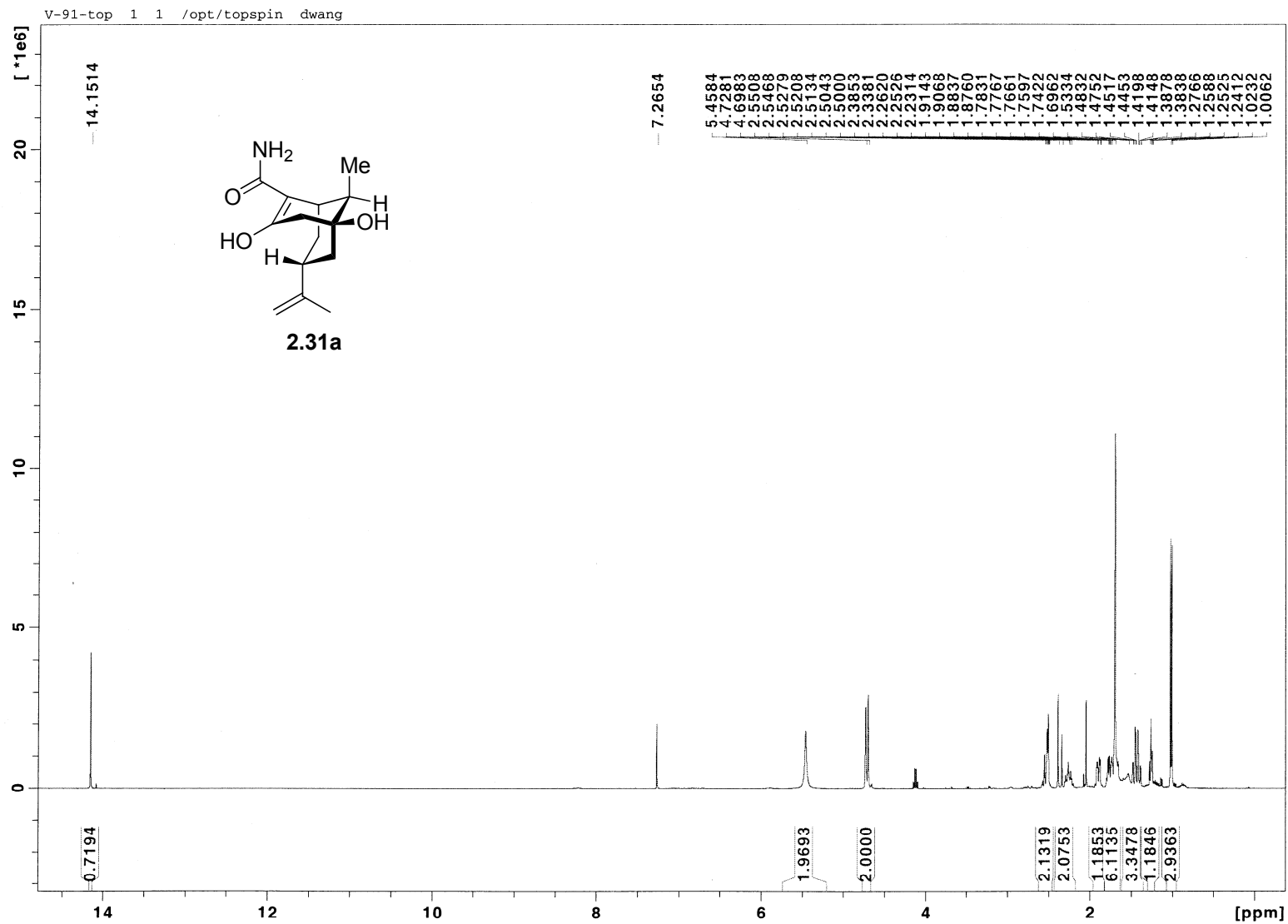


Figure 2.37 ^1H NMR (400 MHz, CDCl_3) of Compound 2.31a

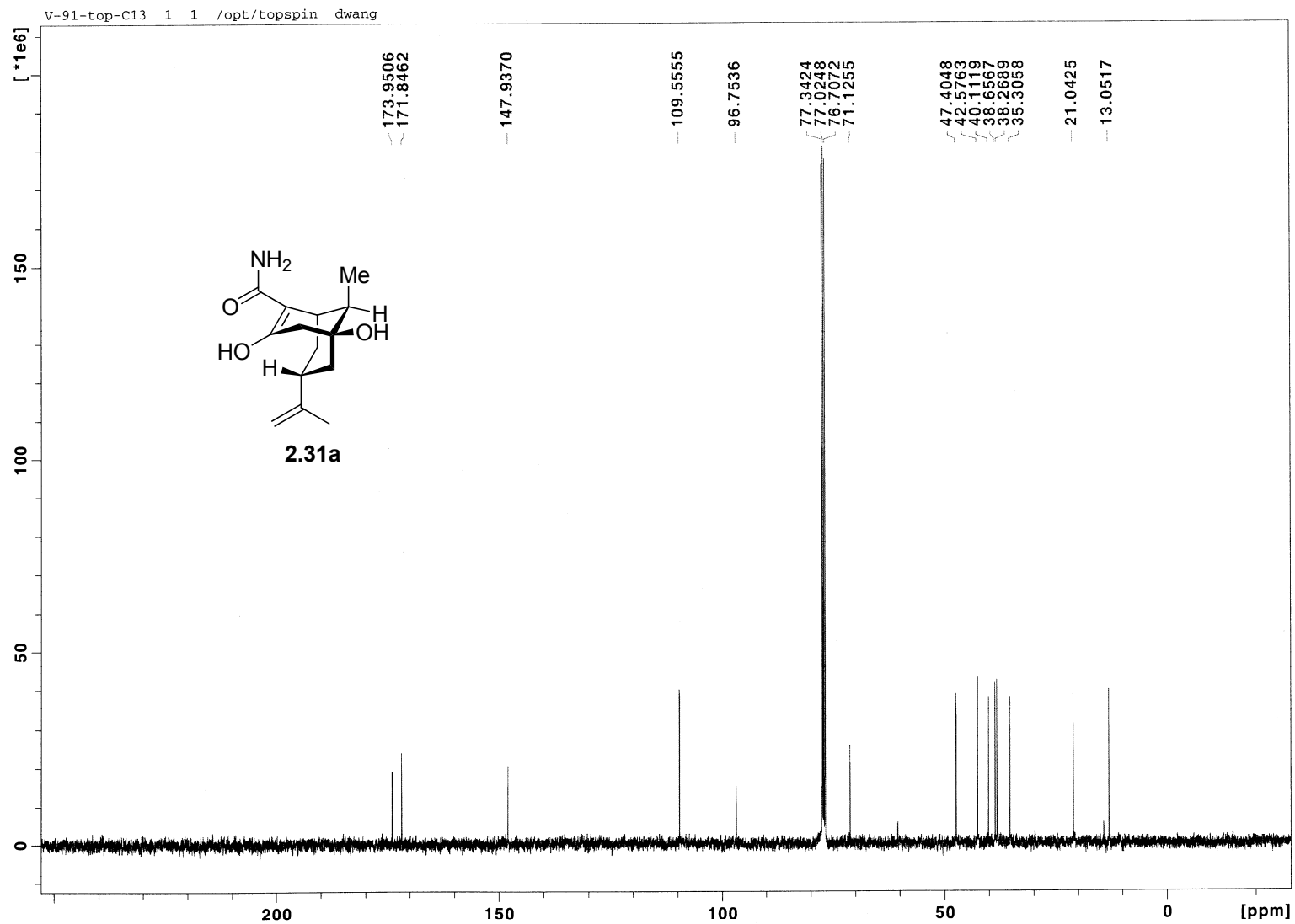


Figure 2.38 ^{13}C NMR (100 MHz, CDCl_3) of Compound 2.31a

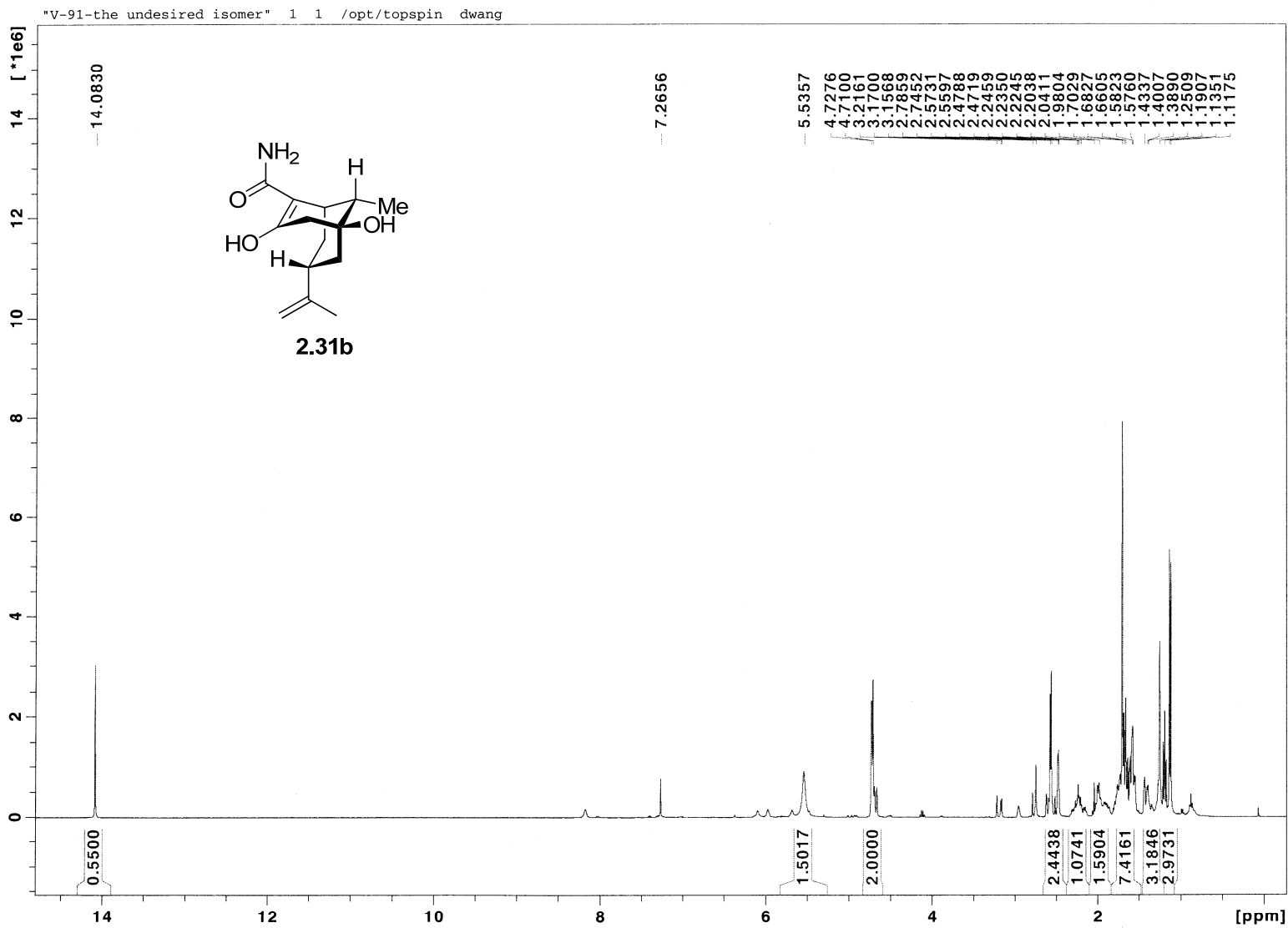


Figure 2.39 ^1H NMR (400 MHz, CDCl_3) of Compound **2.31b**

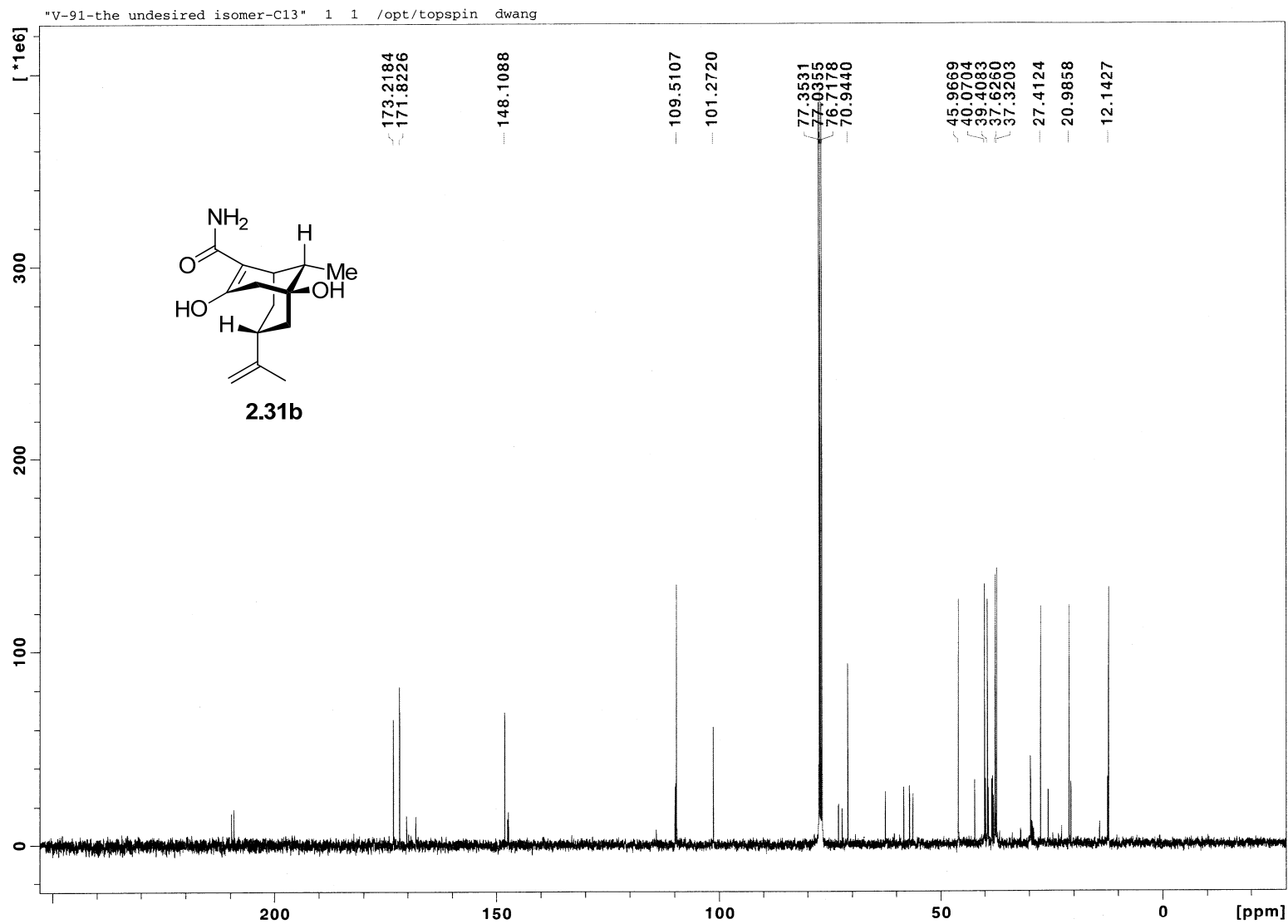


Figure 2.40 ^{13}C NMR (100 MHz, CDCl_3) of Compound 2.31b

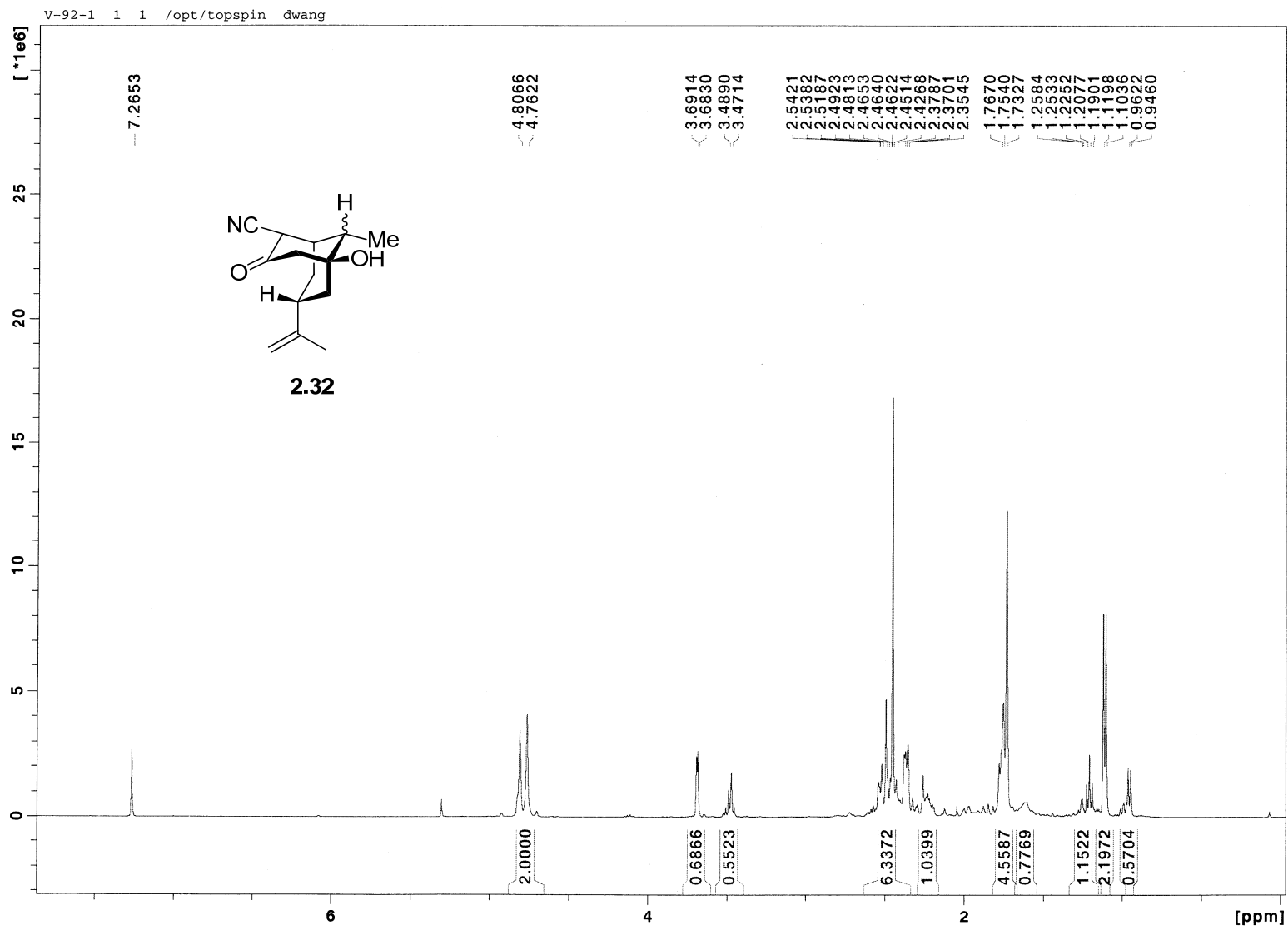


Figure 2.41 ^1H NMR (400 MHz, CDCl_3) of Compound 2.32

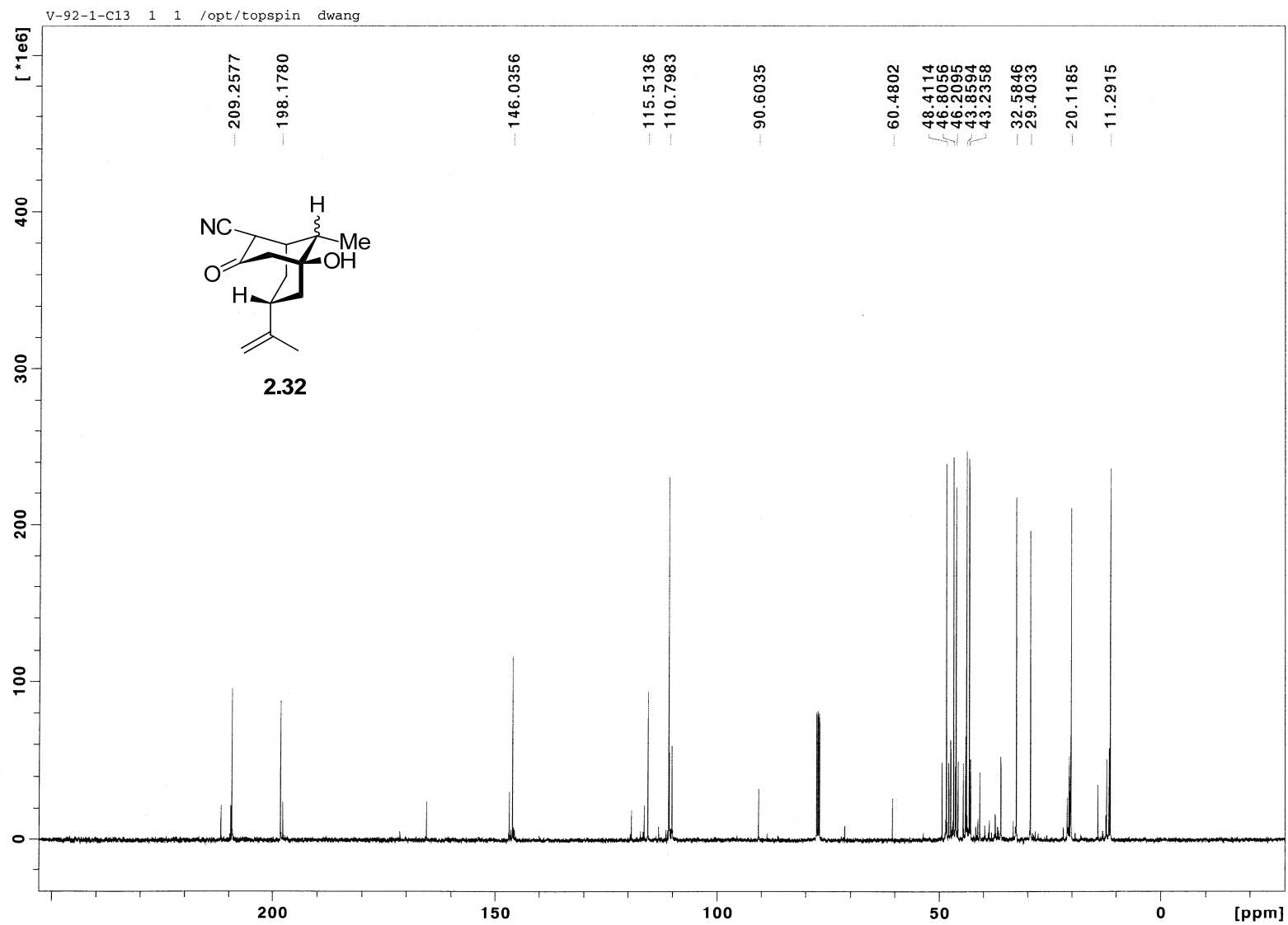


Figure 2.42 ¹³C NMR (100 MHz, CDCl₃) of Compound 2.32

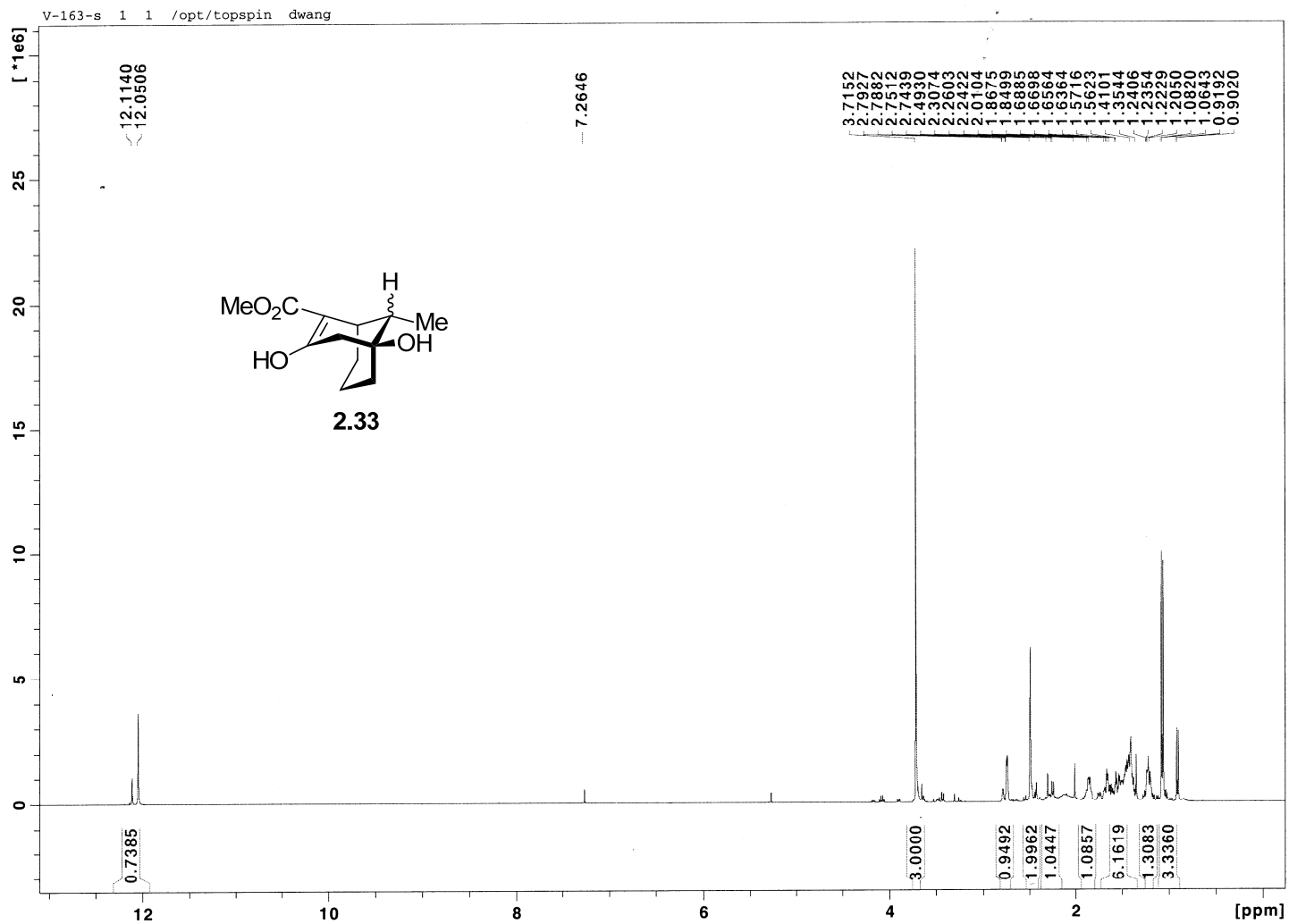


Figure 2.43 ^1H NMR (400 MHz, CDCl_3) of Compound 2.33

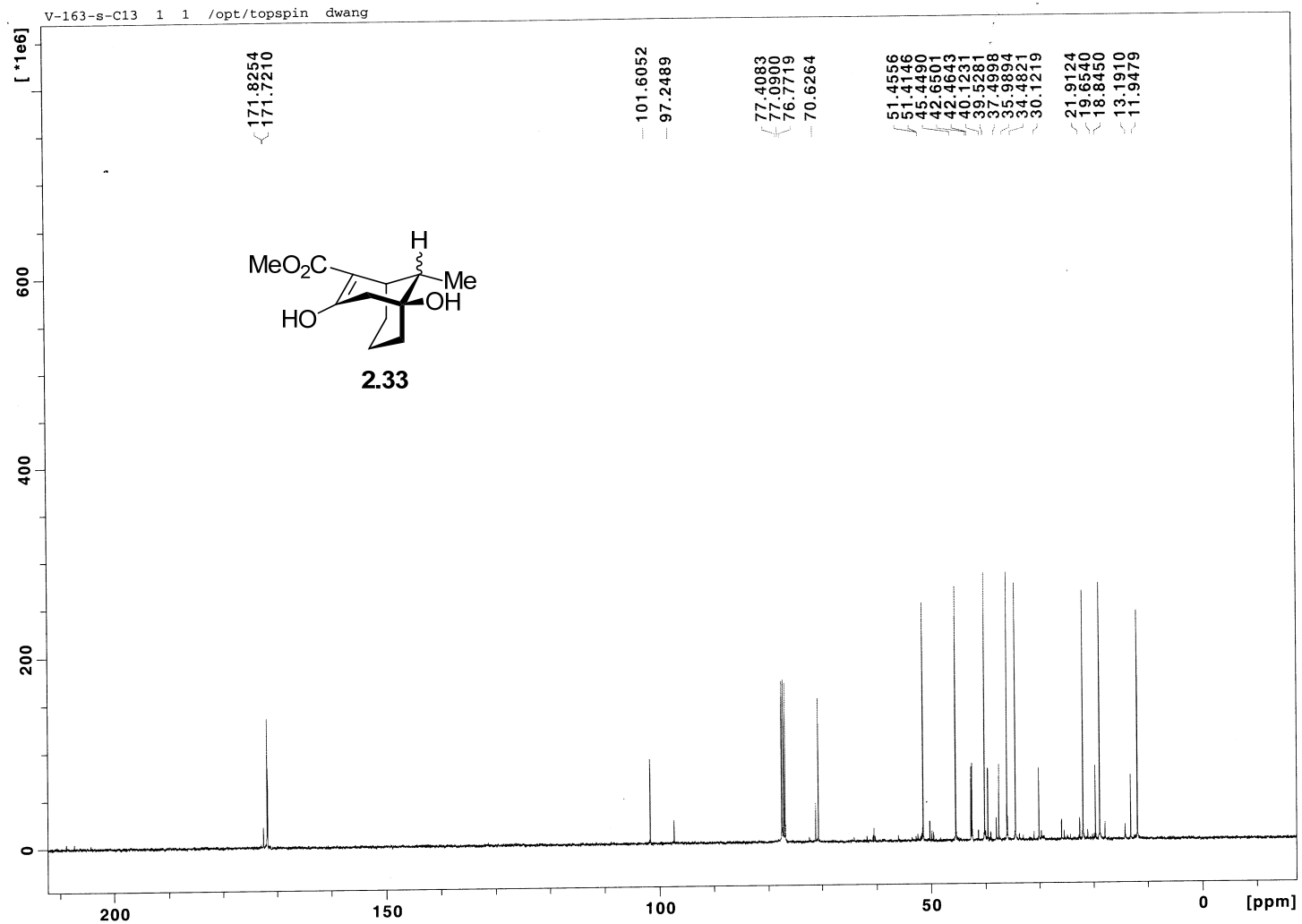


Figure 2.44 ^{13}C NMR (100 MHz, CDCl_3) of Compound 2.33

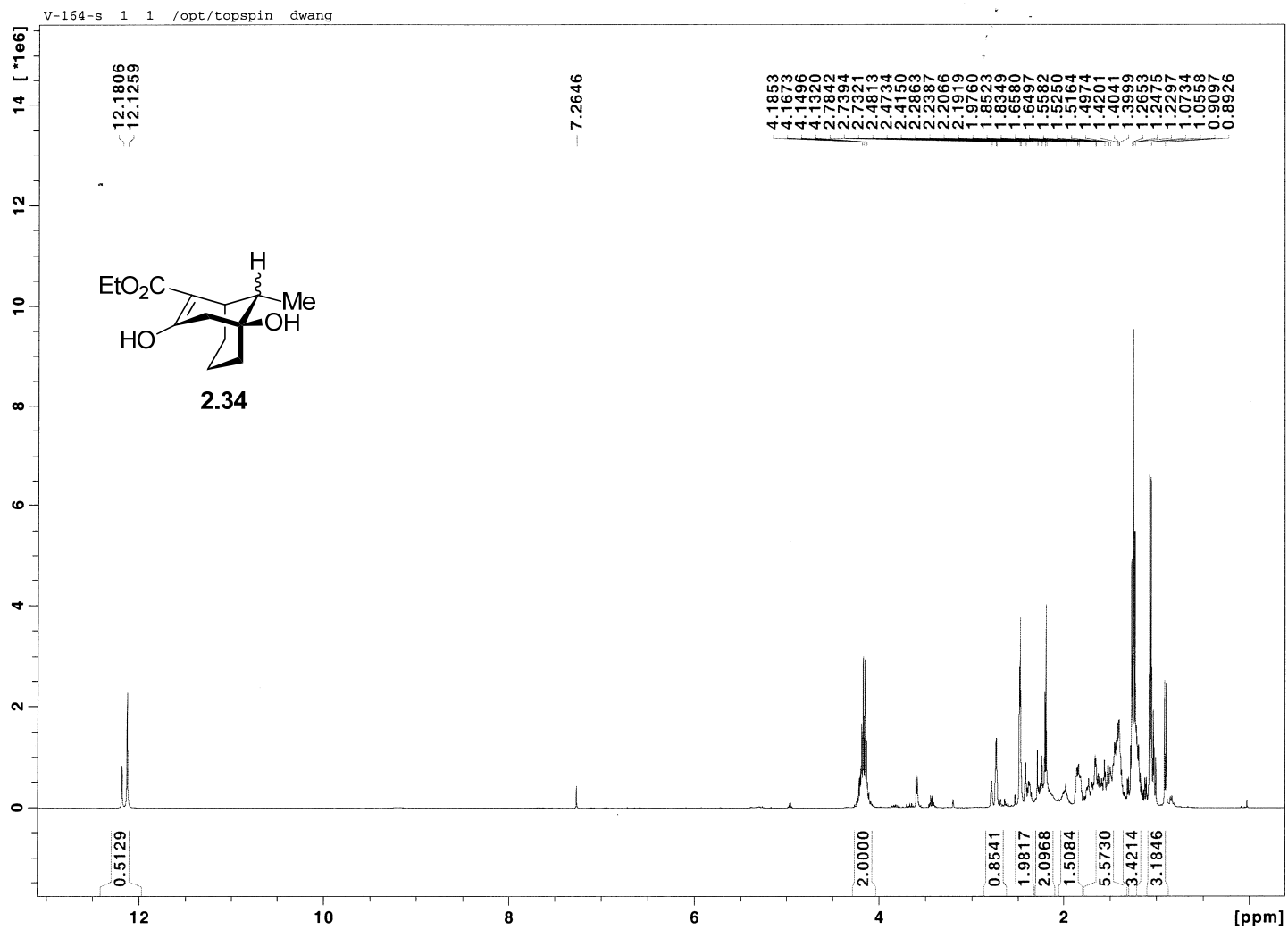


Figure 2.45 ^1H NMR (400 MHz, CDCl_3) of Compound 2.34

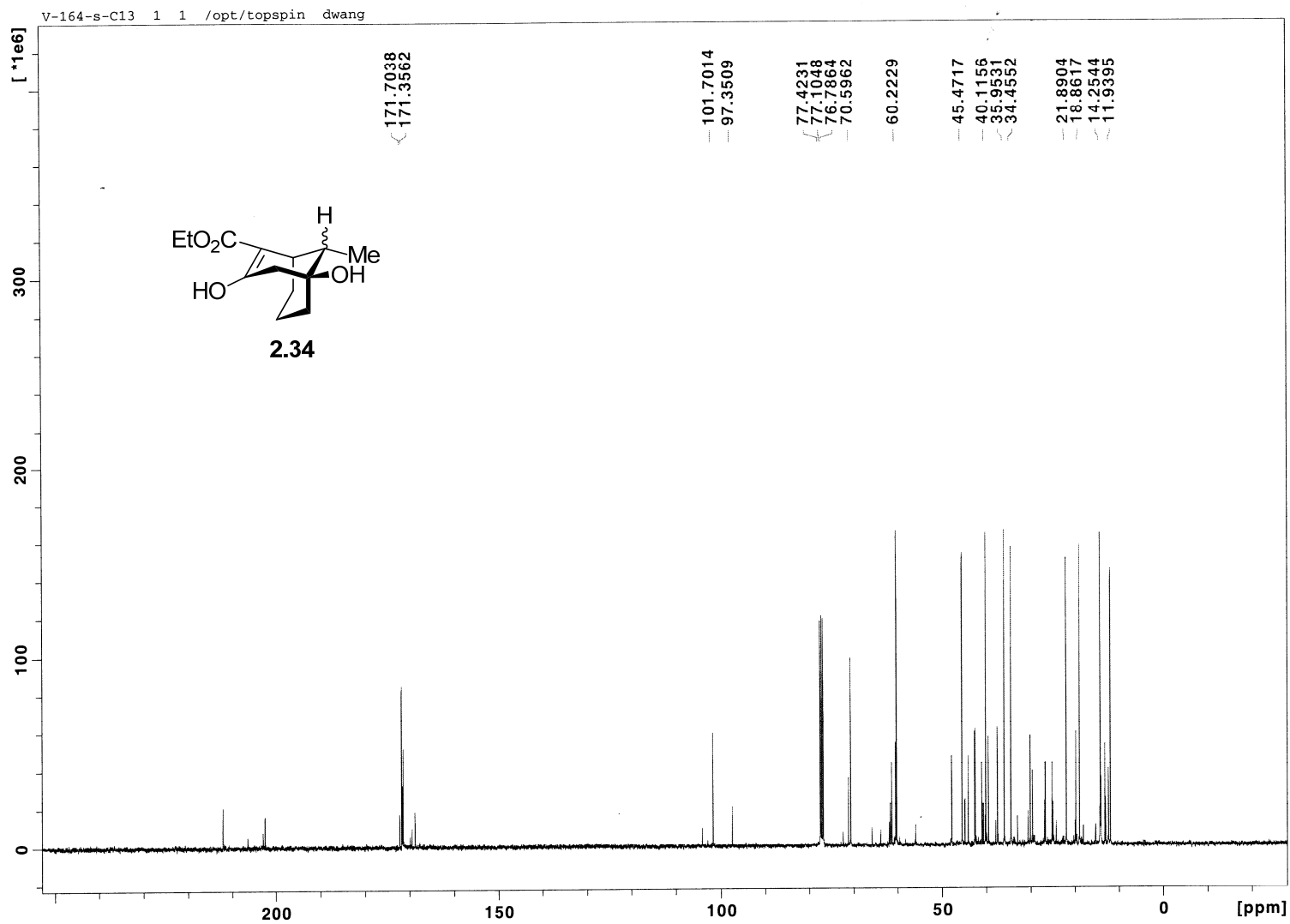


Figure 2.46 ^{13}C NMR (100 MHz, CDCl_3) of Compound 2.34

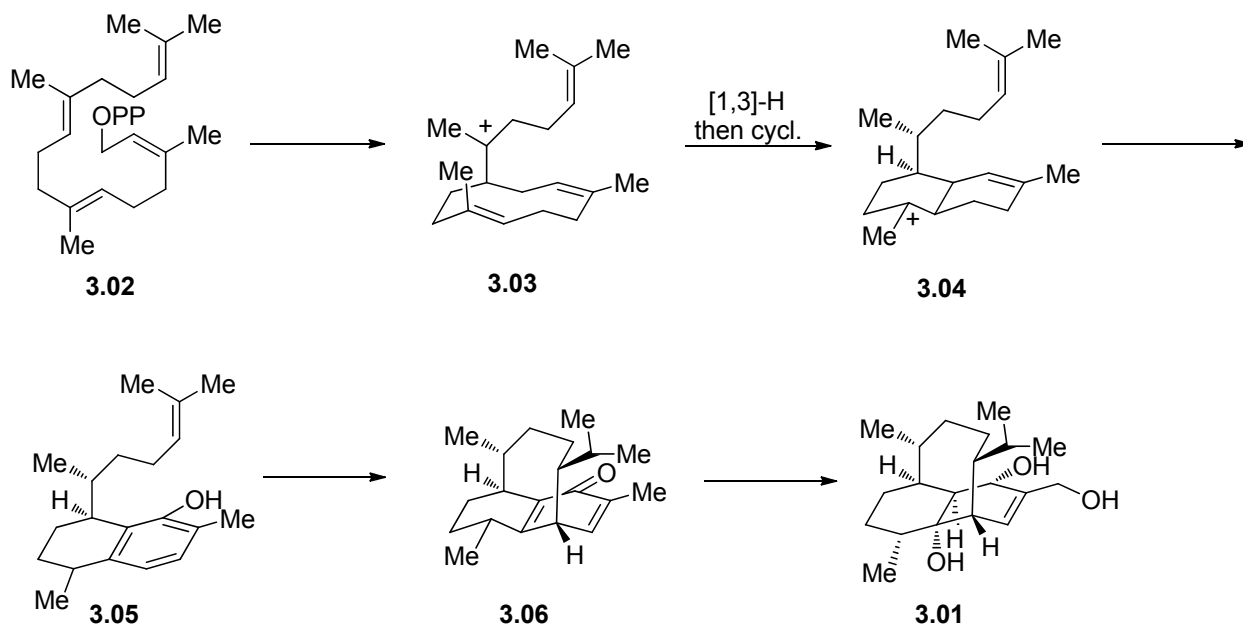
- [3] J. A. Peters, J. M. A. Baas, B. Vandegraaf, J. M. Vandertoorn and H. Vanbekkum, *Tetrahedron* **1978**, *34*, 3313-3323.
- [4] a) R. Chakraborti, B. C. Ranu and U. R. Ghatak, *J. Org. Chem.* **1985**, *50*, 5268-5271; b) K. C. Nicolaou, J. A. Pfefferkorn, G. Q. Cao, S. Kim and J. Kessabi, *Org. Lett.* **1999**, *1*, 807-810; c) K. Aoyagi, H. Nakamura and Y. Yamamoto, *J. Org. Chem.* **1999**, *64*, 4148-4151; d) J. K. F. Geirsson, S. Jonsson and J. Valgeirsson, *Bioorg. Med. Chem.* **2004**, *12*, 5563-5569; e) S. Bertelsen, R. L. Johansen and K. A. Jorgensen, *Chem. Commun.* **2008**, 3016-3018; f) Y. Kuninobu, J. Morita, M. Nishi, A. Kawata and K. Takai, *Org. Lett.* **2009**, *11*, 2535-2537; g) Y. L. Zhao, L. Chen, S. C. Yang, C. Tian and Q. Liu, *J. Org. Chem.* **2009**, *74*, 5622-5625; For reviews, see: h) J. A. Peters, *Synthesis* **1979**, 321-336; i) E. Butkus, *Synlett* **2001**, 1827-1835.
- [5] a) I. Uchida, T. Ando, N. Fukami, K. Yoshida, M. Hashimoto, T. Tada, S. Koda and Y. Morimoto, *J. Org. Chem.* **1987**, *52*, 5292-5293; b) T. Ando, Y. Tsurumi, N. Ohata, I. Uchida, K. Yoshida and M. Okuhara, *J. Antibiot.* **1988**, *41*, 25-30; c) T. Ando, K. Yoshida and M. Okuhara, *J. Antibiot.* **1988**, *41*, 31-35.
- [6] a) J. E. Baldwin, *J. Chem. Soc., Chem. Commun.* **1976**, 734-736; b) J. E. Baldwin and M. J. Lusch, *Tetrahedron* **1982**, *38*, 2939-2947.
- [7] A. H. Hoveyda, D. A. Evans and G. C. Fu, *Chem. Rev.* **1993**, *93*, 1307-1370.
- [8] a) J. M. Chong, D. R. Cyr and E. K. Mar, *Tetrahedron Lett.* **1987**, *28*, 5009-5012; b) F. Azzena, F. Calvani, P. Crotti, C. Gardelli, F. Macchia and M. Pineschi, *Tetrahedron* **1995**, *51*, 10601-10626; c) F. Azzena, P. Crotti, L. Favero and M. Pineschi, *Tetrahedron* **1995**, *51*, 13409-13422; d) D. F. Taber, J. H. Green and J. M. Geremia, *J. Org. Chem.* **1997**, *62*, 9342-9344; e) D. Rodriguez, M. Mulero and J. A. Prieto, *J. Org. Chem.* **2006**, *71*, 5826-5829.
- [9] D. W. Theobald, *Tetrahedron* **1969**, *25*, 3139-3144.
- [10] a) G. A. Kraus and Y. S. Hon, *J. Am. Chem. Soc.* **1985**, *107*, 4341-4342; b) G. A. Kraus and Y. S. Hon, *Heterocycles* **1987**, *25*, 377-386.
- [11] P. G. Baraldi, A. Barco, S. Benetti, G. P. Pollini and V. Zanirato, *Tetrahedron Lett.* **1984**, *25*, 4291-4294.
- [12] B. D. Chong, Y. I. Ji, S. S. Oh, J. D. Yang, W. Baik and S. Koo, *J. Org. Chem.* **1997**, *62*, 9323-9325.
- [13] F. A. Marques, C. A. Lenz, F. Simonelli, B. Maia, A. P. Vellasco and M. N. Eberlin, *J. Nat. Prod.* **2004**, *67*, 1939-1941.
- [14] G. W. Kabalka, S. Yu and N. S. Li, *Tetrahedron Lett.* **1997**, *38*, 5455-5458.
- [15] A mixture of **2.27a** and **2.27b** was prepared by methylation of the corresponding mixture of **2.12a** and **2.12b**.

- [16] a) C. J. V. Scanio and R. M. Starrett, *J. Am. Chem. Soc.* **1971**, *93*, 1539-1540; b) J. E. Telschow and W. Reusch, *J. Org. Chem.* **1975**, *40*, 862-865; c) R. E. Gawley, *Synthesis* **1976**, 777-794.
- [17] a) C. T. Lee, W. T. Yang and R. G. Parr, *Phys. Rev. B* **1988**, *37*, 785-789; b) A. D. Becke, *J. Chem. Phys.* **1993**, *98*, 5648-5652.
- [18] a) K. Fukui, *J. Phys. Chem.* **1970**, *74*, 4161-4163; b) K. Fukui, *Acc. Chem. Res.* **1981**, *14*, 363-368; c) C. Gonzalez and H. B. Schlegel, *J. Phys. Chem.* **1990**, *94*, 5523-5527.
- [19] GAUSSIAN 03 full reference: Gaussian 03, Revision D.02, M. J. Frisch, G. W. Trucks, H. B. Schlegel, G. E. Scuseria, M. A. Robb, J. R. Cheeseman, J. A. Montgomery, Jr., T. Vreven, K. N. Kudin, J. C. Burant, J. M. Millam, S. S. Iyengar, J. Tomasi, V. Barone, B. Mennucci, M. Cossi, G. Scalmani, N. Rega, G. A. Petersson, H. Nakatsuji, M. Hada, M. Ehara, K. Toyota, R. Fukuda, J. Hasegawa, M. Ishida, T. Nakajima, Y. Honda, O. Kitao, H. Nakai, M. Klene, X. Li, J. E. Knox, H. P. Hratchian, J. B. Cross, V. Bakken, C. Adamo, J. Jaramillo, R. Gomperts, R. E. Stratmann, O. Yazyev, A. J. Austin, R. Cammi, C. Pomelli, J. W. Ochterski, P. Y. Ayala, K. Morokuma, G. A. Voth, P. Salvador, J. J. Dannenberg, V. G. Zakrzewski, S. Dapprich, A. D. Daniels, M. C. Strain, O. Farkas, D. K. Malick, A. D. Rabuck, K. Raghavachari, J. B. Foresman, J. V. Ortiz, Q. Cui, A. G. Baboul, S. Clifford, J. Cioslowski, B. B. Stefanov, G. Liu, A. Liashenko, P. Piskorz, I. Komaromi, R. L. Martin, D. J. Fox, T. Keith, M. A. Al-Laham, C. Y. Peng, A. Nanayakkara, M. Challacombe, P. M. W. Gill, B. Johnson, W. Chen, M. W. Wong, C. Gonzalez, and J. A. Pople, Gaussian, Inc., Wallingford CT, 2004.

CHAPTER 3 AN APPROACH TO THE SYNTHESIS OF VINIGROL VIA TWO-CARBON RING EXPANSION STRATEGY

3.1 Background and Significance

The diterpenoid vinigrol (**3.01**) was isolated in 1987 from fungal strain *Virgaria nigra* F-5408 by Hashimoto and co-workers.^[1] An evaluation of the biological activity of vinigrol shows antihypertensive and platelet aggregation-inhibiting properties.^[1b, 1c] Furthermore, vinigrol has shown to function as a potential tumor necrosis factor (TNF) antagonist agent,^[2] and could therefore be useful for the treatment of inflammation and a host of autoimmune disease responses. Moreover, TNF antagonists are thought to slow the progression of AIDS, and are therefore considered especially valuable.^[3]



Scheme 3.1 Proposed Biosynthesis of Vinigrol

It has been proposed by Corey that vinigrol arises biosynthetically from the common diterpene building block geranylgeranyl pyrophosphate (**3.02**) following the sequence shown in Scheme 3.1.^[4] The pyrophosphate **3.02** is believed to undergo an enzyme-assisted cyclization to arrive at the ten-membered ring intermediate **3.03**. Subsequent [1,3]-hydride shift and cyclization

yield compound **3.04**, which is oxidized to provide phenol derivative **3.05**. Oxidative cyclization of **3.05** installs the final ring and provides tricycle **3.06**.^[5] Additional oxidation state adjustments of tricycle **3.06** ultimately give rise to **3.01**.

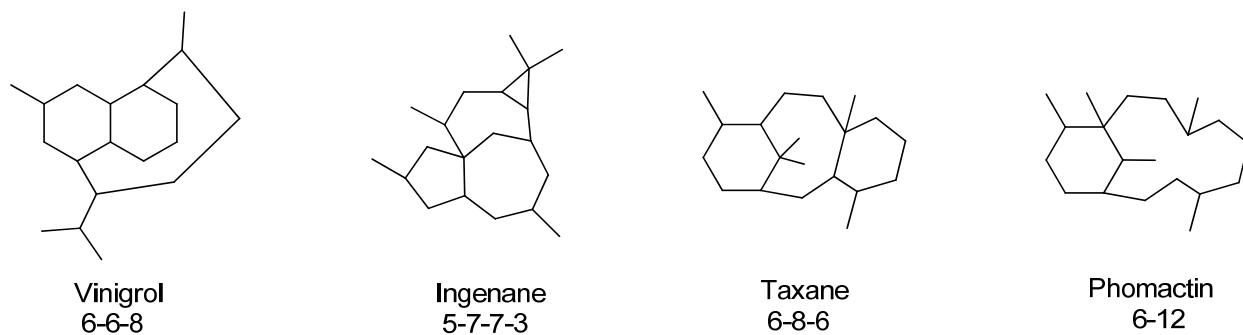
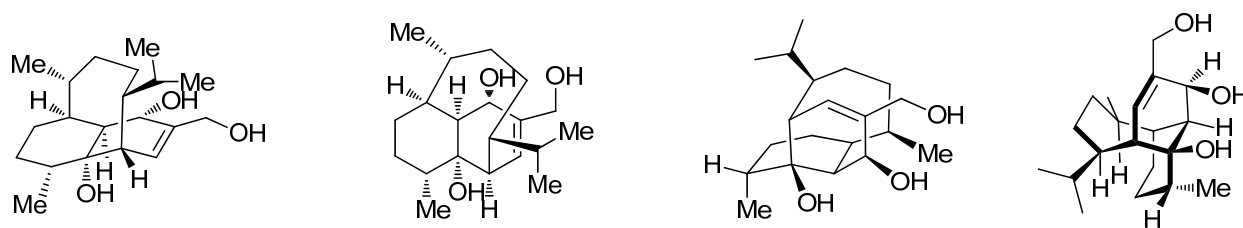


Figure 3.1 Historically Challenging Carbogenic Ring Systems in Terpene Synthesis



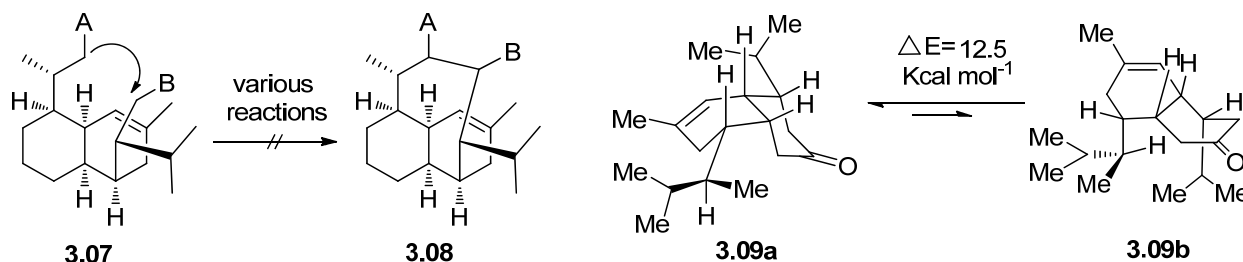
Scheme 3.2 Views of Vinigrol (3.01)

From a chemical standpoint, the provocative structure of vinigrol features an unprecedented decahydro-1,5-butanonaphthalene carbon skeleton that is not found in any other natural product. As such, it holds a special place alongside other historically challenging diterpene systems, such as the ingenanes, taxanes, and phomactins (see Figure 3.1).^[6] Although **3.01** is relatively small in size (molecular weight < 325 Da), the presence of eight contiguous stereocenters and multiple sites of oxygenation make it a particularly challenging synthetic problem, which can be analyzed from several seemingly different topological viewpoints (Scheme 3.2). Due to the promising biological properties of vinigrol and its unique terpene framework, innovative strategies toward the total synthesis of vinigrol are being pursued by at least ten organic research groups.^[4, 7] Over the past 24 years, more than 20 papers, six doctoral

dissertations and three reviews^[8] describing synthetic efforts toward vinigrol have been published, including four syntheses capable of preparing the skeleton of vinigrol, and one completed total synthesis. Each approach is presented in detail in the following sections.

3.2 Previous Synthetic Approaches to Vinigrol

3.2.1 Paquette's Attempt Based on a *cis*-Decalin Framework

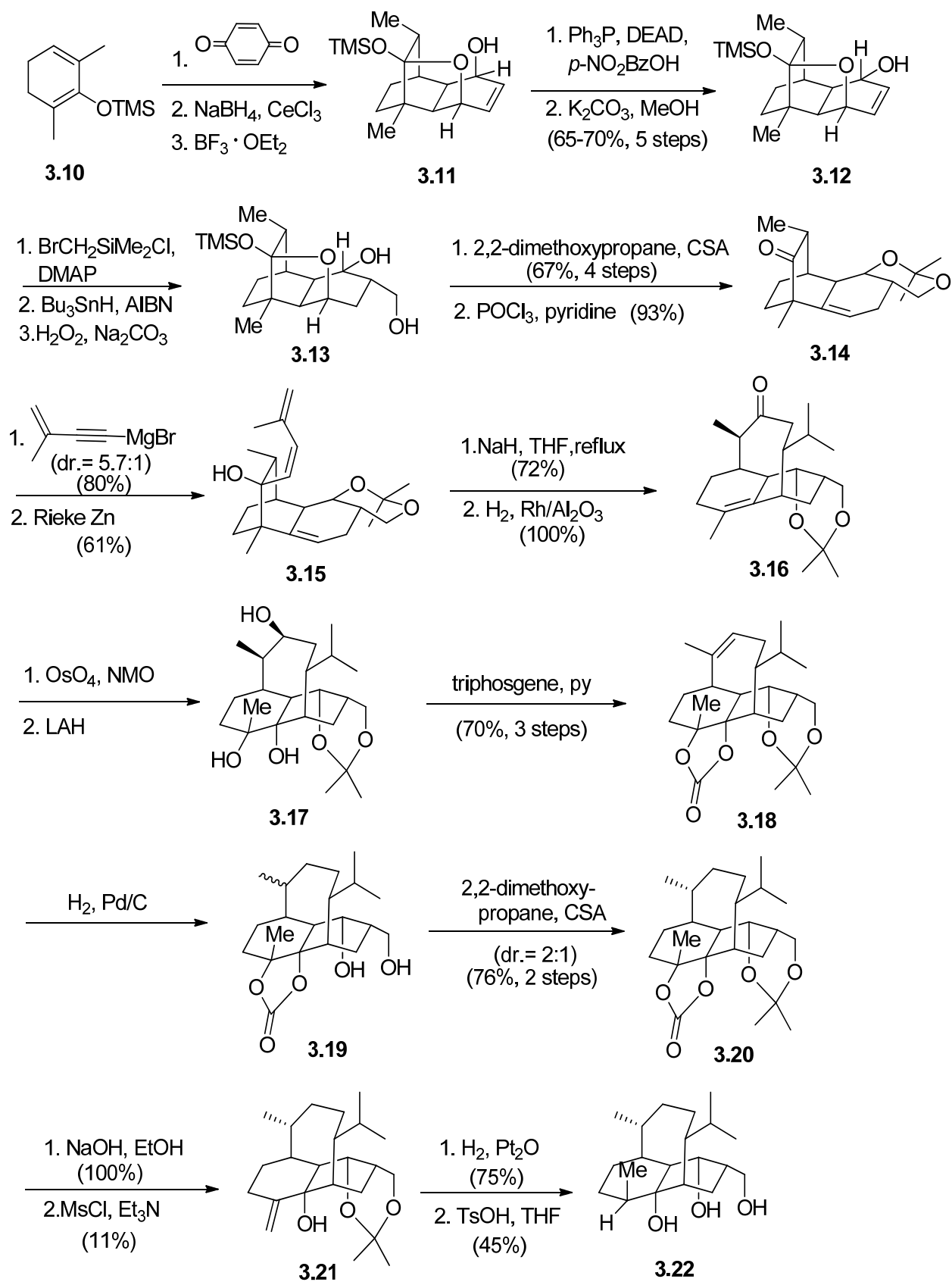


Scheme 3.3 Inherent Challenge of Building the Ring System of Vinigrol from a *cis*-Decalin

Paquette *et al.* have published efforts toward the synthesis of vinigrol.^[7l, 7o-q] Their continuous efforts have vividly demonstrated the difficulty in forming the bridging eight-membered ring of vinigrol from a pre-existing *cis*-decalin framework (**3.07** to **3.08**). A variety of approaches (Scheme 3.3), including intramolecular alkylation, Ring-Closing Metathesis, incorporating a lactone bridge as a conformational lock, ring-contraction, etc., have been explored without success. Their calculations on related model compounds point to a largely unfavorable equilibrium between two conformers ($\Delta E \approx 12.5 \text{ kcal mol}^{-1}$), with the major conformer (**3.09a**) lacking the proximity needed for ring closure.

3.2.2 Hanna's Approach toward Vinigrol

Hanna's group reported the most advanced vinigrol intermediate so far.^[7a, 7c, 7f, 7k, 7ab] Their strategy centered on an oxy-Cope rearrangement to provide the tricyclic core of vinigrol. As shown in Scheme 3.4, their synthesis commenced with the readily available silyl enol ether **3.10**, which was transformed to the mixed trimethylsilyl ketal **3.11** in three steps. The alcohol **3.11** was

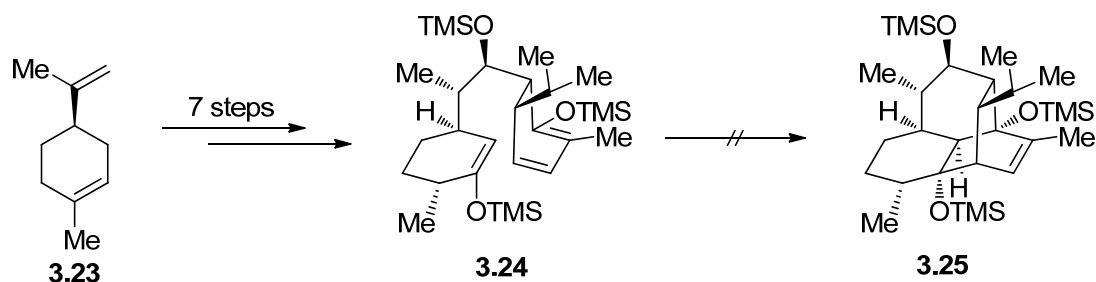


Scheme 3.4 Hanna's Approach to Vinigrol

submitted to Mitsunobu inversion, followed by cleavage of the resulting ester to yield **3.12**. Silylation of the alcohol **3.12** and subjecting to standard radical-generating conditions followed by Tamao oxidation furnished the diol **3.13**. Protection of the diol with 2,2-dimethoxypropane followed by dehydration delivered the key tricyclic ketone **3.14**.

Next, the ketone **3.14** was treated with Grignard reagent to form a separable mixture of endo and exo alcohols. Chemoselective reduction of the triple bond afforded the oxy-Cope precursor **3.15**, which was readily converted to the tricyclic skeleton **3.16** with the desired stereocenters after oxy-Cope reaction and hydrogenation. The tricyclic ketone **3.16** was then exposed to osmium tetroxide and LiAlH_4 , furnishing the triol **3.17**. Treatment of the triol **3.17** with triphosgene led to the cyclic carbamate **3.18**. Next, the carbamate **3.18** was hydrogenated to give an inseparable mixture of **3.19**, which was protected by 2,2-dimethoxypropane to afford a 2:1 separable mixture of **3.20**. Hydrolysis of the cyclic carbamate **3.20** followed by elimination gave a mixture of five products which were separated by careful column chromatography on silica gel to afford the alkene **3.21**. Finally, hydrogenation and deprotection afforded the triol **3.22**, which is an epi-C-8-dihydrovinigrol.

3.2.3 Corey's Attempt toward Vinigrol

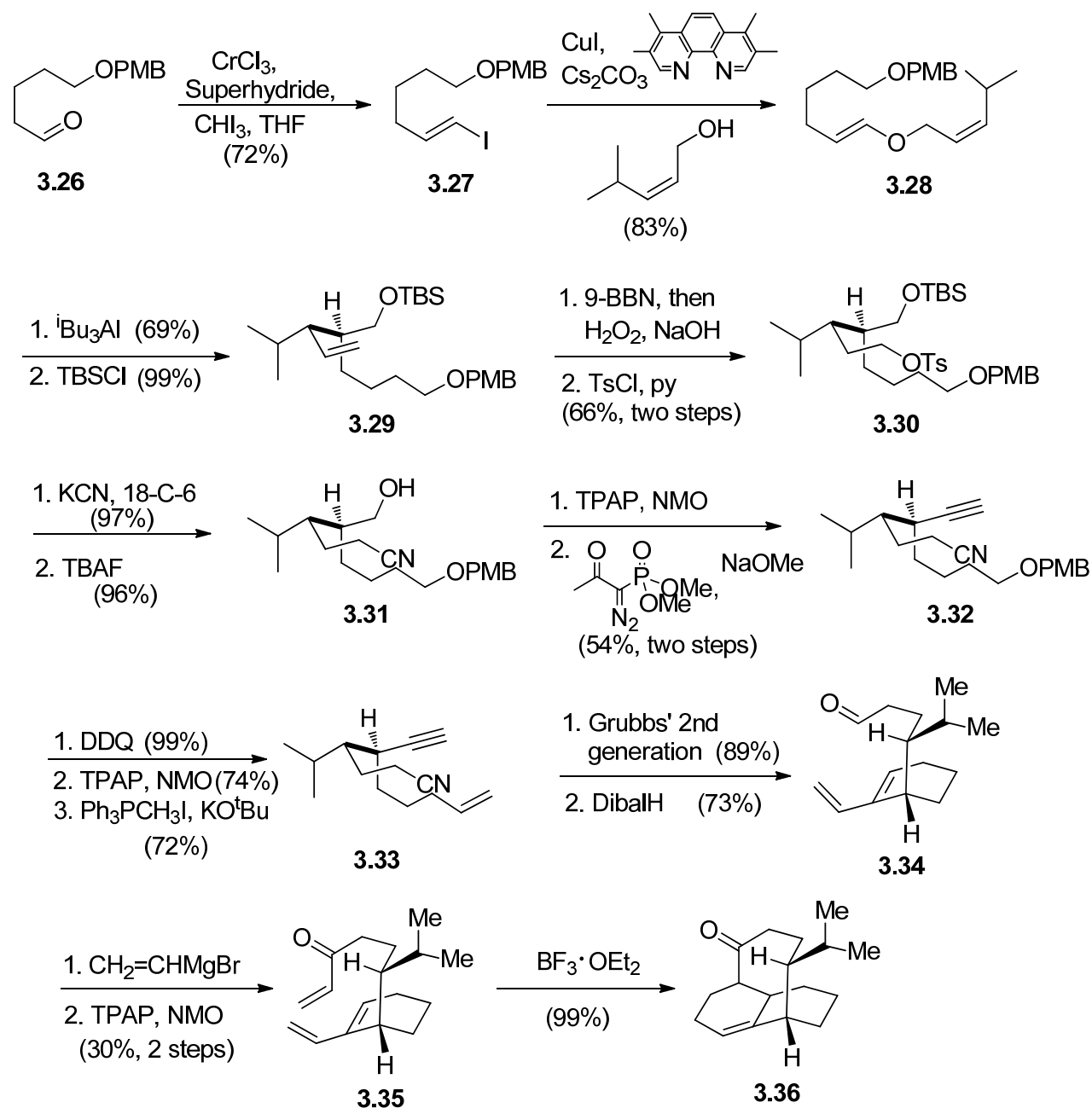


Scheme 3.5 Corey's Attempt to Vinigrol

The Corey group aimed to assemble the tricyclic core by a late stage intramolecular Diels-Alder reaction (Scheme 3.5).^[4] To this end, (R)-limonene (**3.23**) was elaborated to triene **3.24**

over seven steps. However, the final Diels-Alder cycloaddition has remained elusive under various conditions and modifications on the triene.

3.2.4 Barriault's Approach toward Vinigrol



Scheme 3.6 Barriault's Approach to Vinigrol

An alternative Diels-Alder disconnection was devised by Barriault *et al.* in 2007, though their previous synthesis based on other strategies was unsuccessful.^[7m, 7n, 7r, 7s, 8a] Their strategy

was to build up the tricyclic core by planning the Diels-Alder reaction earlier in the anticipated sequence.

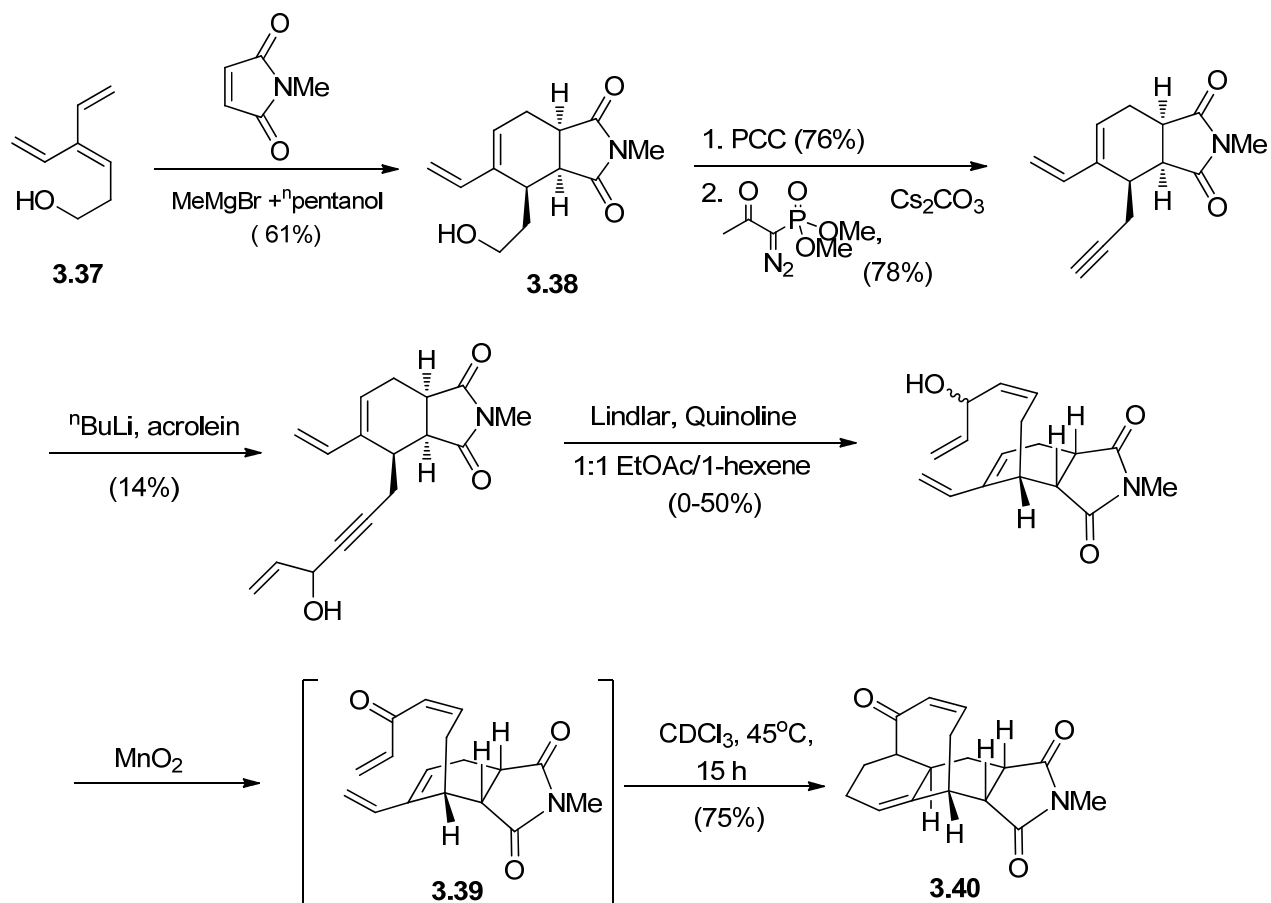
Their approach began with the known aldehyde **3.26**, which was transformed to the vinyl iodide **3.27** by a Takai olefination. Subsequent Buchwald's copper(I)-mediated coupling of **3.27** with the allylic alcohol led to the enol ether **3.28**. Treatment of the vinyl allyl ether **3.28** with triisobutylaluminum effected both the Claisen rearrangement and the reduction in a single step, affording the hydroxyalkene, which was further protected to give the silyloxy ether **3.29**. Next, a three step functional manipulation and removal of the silyl ether delivered the alcohol **3.31**. A TPAP oxidation followed by a modified version of Ohira's protocol led to the alkyne **3.32** as the sole diastereomer in 54% yield over two steps. Conversion of **3.32** to **3.33** was performed via DDQ removal of the PMB group, TPAP oxidation of the resulting alcohol, and Wittig olefination under Conia conditions.

Then, the enyne metathesis was effected by Grubb's 2nd generation catalyst followed by reduction of the nitrile group to yield **3.34**. The enone **3.35** was obtained by a three-step functional manipulation. Finally, the intramolecular Diels-Alder reaction took place smoothly to give the cycloadduct **3.36** when the triene **3.35** was treated with BF₃·OEt₂ in dichloromethane at -78°C.

3.2.5 Fallis's Approach toward Vinigrol

Fallis's group successfully prepared the skeleton of vinigrol based on a similar intramolecular Diels-Alder reaction.^[7^t] Their synthesis commenced with the homoallylic cross-conjugated trieneol **3.37**, which could be readily prepared from 1,3-propanediol in six steps. A Lewis acid catalyzed and self-assembled Diels-Alder reaction from the trieneol **3.37** with *N*-methylmaleimide afforded the monoadduct **3.38** with diastereo-, regio-, and chemoselective control. Further manipulations of **3.38** led to the enone **3.39**. The cyclization of the Diels-Alder

precursor **3.39** was particularly facile, and no added catalyst was required. On a preparative scale, heating **3.39** in deuteriochloroform provided quantitative conversion to the tricyclic core of vinigrol, **3.40**.

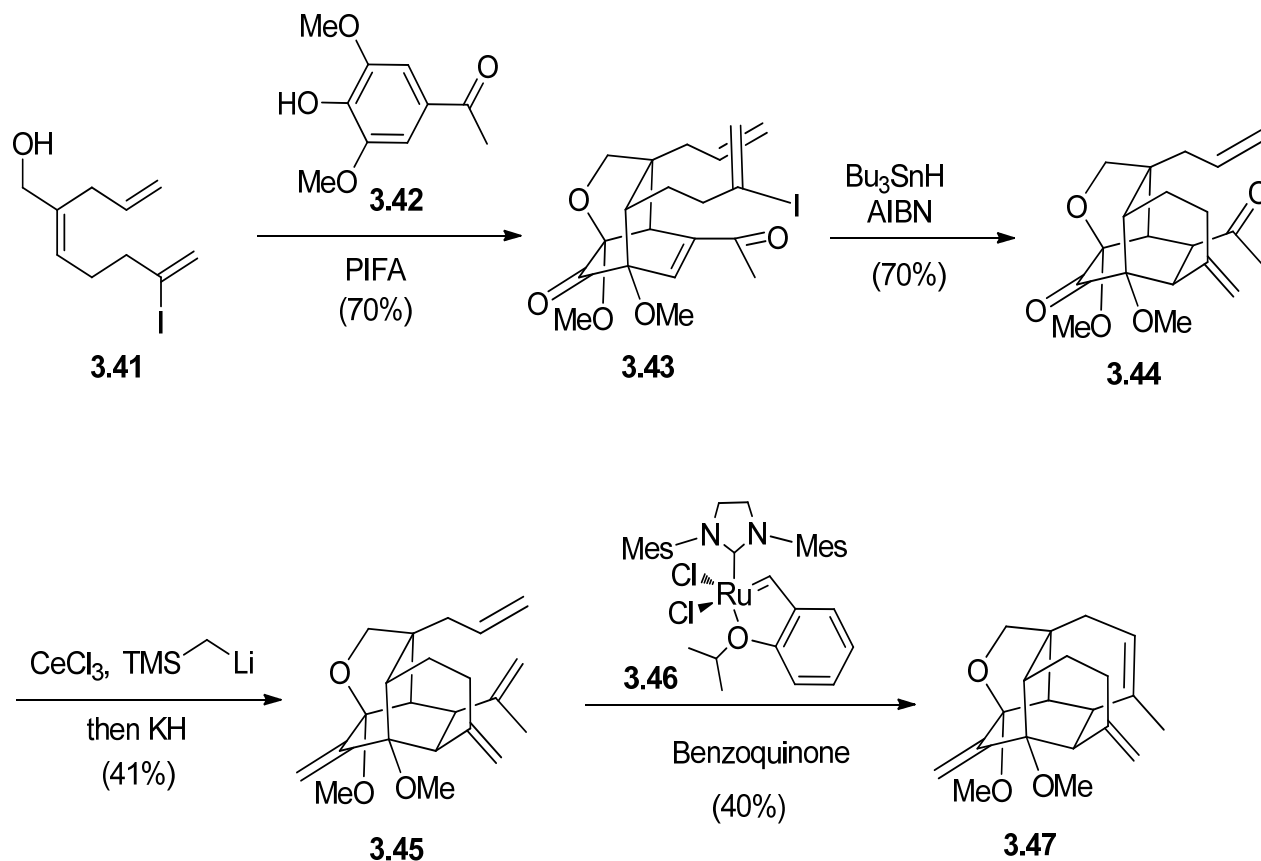


Scheme 3.7 Fallis's Approach to Vinigrol

3.2.6 Njardarson's Approach toward Vinigrol

Njardarson's group recently reported a highly expedient and convergent synthetic approach toward the total synthesis of vinigrol.^[7w-y] They prepared the core of vinigrol from commercially available ketone **3.42** in only four steps. The key features involve an oxidative dearomatization/Diels-Alder reaction sequence between allylic alcohol **3.41** and phenol **3.42** in the presence of iodobenzene bis(trifluoroacetate) to furnish the cycloadduct **3.43**. Then, a radical cyclization took place under standard conditions to form the *exo*-ketone **3.44**, which was

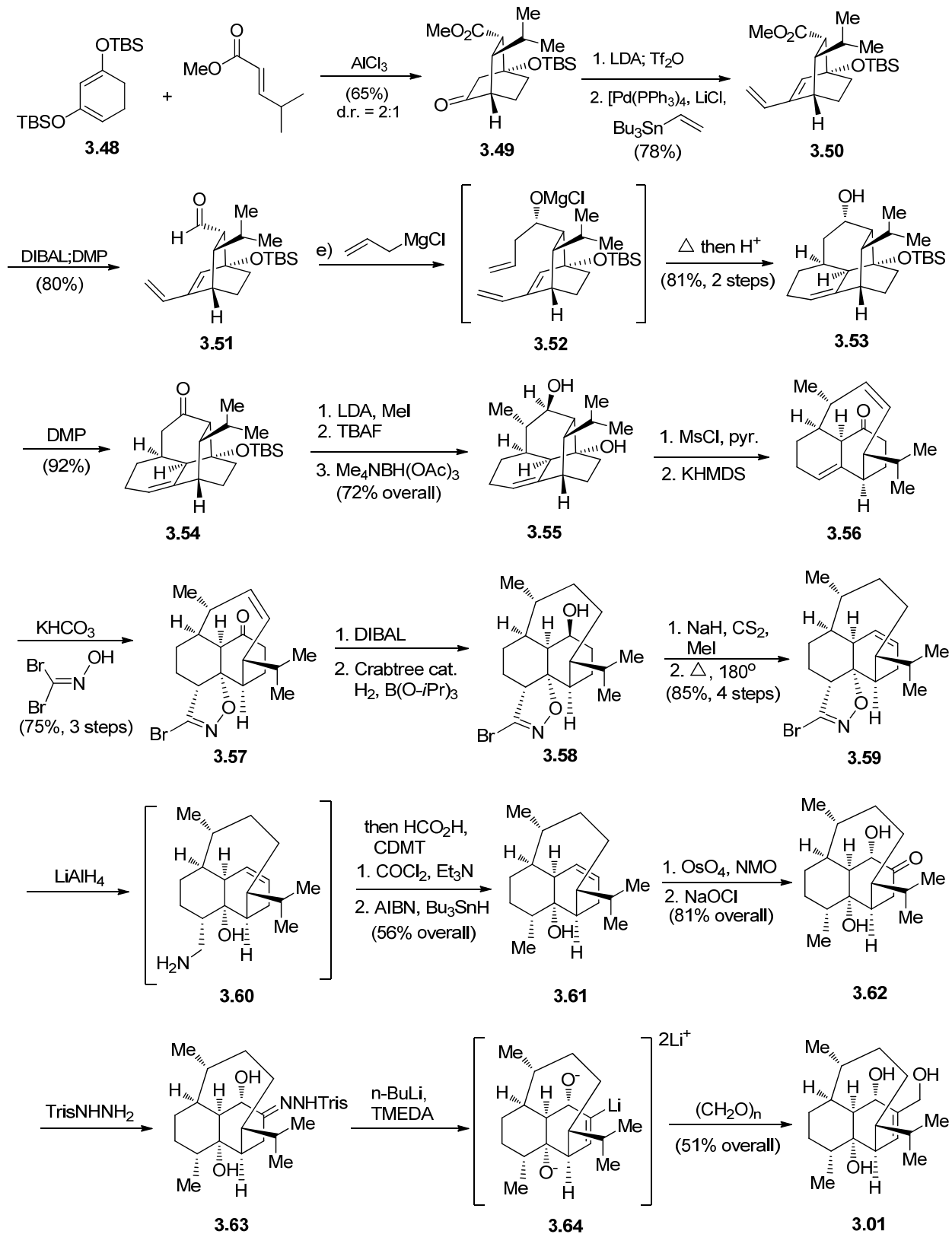
successfully bis-olefinated using the Peterson olefination protocol to afford the tetraene **3.45**. Finally, despite significant steric hindrance, the tetraene **3.45** could be cyclized using the Grubbs-Hoveyda catalyst **3.46** in the presence of benzoquinone to deliver the pentacyclic compound **3.47**, which is close to the core structure of vinigrol (see Scheme 3.2 to compare the structure of **3.47** and vinigrol).



Scheme 3.8 Njardarson's Approach to Vinigrol

3.2.7 Baran's Total Synthesis of Vinigrol

In 2008, Baran's group reported a very concise (9 steps), high-yield route (20% overall yield) to the skeleton of vinigrol based on an inter- and intramolecular Diels-Alder reactions followed by Grob fragmentation^[7u]. They are able to apply this concise route to the total synthesis of vinigrol later by a 23-step route in 3% overall yield.^[7z, 7aa] This study remains the only completed total synthesis of vinigrol to date.



Scheme 3.9 Baran's Total Synthesis of Vinigrol

Their synthesis commenced with the commercially available diene **3.48** and (*E*)-methyl 4-methyl-2-pentenoate, which were converted to the bicyclic ketone **3.49** via an endo-selective Diels-Alder reaction. Triflation of **3.49** and subsequent Stille coupling formed requisite diene **3.50** in 78% yield. After an oxidation state adjustment, allyl magnesium bromide was added to the corresponding aldehyde (d.r. = 6:1) **3.51** producing an intermediate alkoxide **3.52**, which was directly heated to 105 °C to initiate the intramolecular Diels-Alder reaction followed by aqueous workup to furnish tetracycle **3.53**. Next, the alcohol **3.53** was oxidized by DMP to give ketone **3.54**, an intermediate available in decagram quantities in seven steps from commercially available materials. The C-9 methyl group was installed by alkylation (LDA, MeI), and, following silyl group removal (TBAF), the adjacent alcohol stereochemistry was established using Evans's Me₄NBH(OAc)₃-mediated, hydroxyl-directed reduction to deliver **3.55** as a single diastereomer in 72% yield over the three-step sequence. Next, mesylation of **3.55** and treatment with KHMDS smoothly afforded the vinigrol core structure **3.56** via a mild Grob fragmentation.

Their next target focused on the installation of the C-8 methyl and C-8a hydroxyl group, which proved to be challenging due to the *cis* orientation. A dipolar [3+2] cycloaddition was effected by exposure of **3.56** to bromonitrile oxide, which was generated *in situ* from dibromoformaldoxime and KHCO₃, leading to the formation of **3.57** as a single isomer both chemo- and stereoselectively. Ketone reduction with DIBAL followed by directed olefin hydrogenation furnished **3.58**. Xanthate formation and subsequent Chugaev elimination afforded olefin **3.59** in 85% overall yield (4 steps from **3.57**). Then, the desired tertiary alcohol **3.61** was obtained by unveiling the bromoisoxazole **3.59** by the Saegusa deamination sequence: (1) reduction with LAH and immediate formylation of the crude amine **3.60**, (2) dehydration to a primary isonitrile, and (3) reduction with Bu₃SnH in the presence of AIBN in 56% overall yield.

In the final stage, dihydroxylation of **3.61** with OsO₄ and chemoselective oxidation of the resulting diol gave α -hydroxy ketone **3.62** in 81% overall yield. Finally, a Shapiro reaction took place by treatment of the trisylhydrazone **3.63** with ⁿBuLi and TMEDA followed by formaldehyde to deliver vinigrol, presumably through the trianionic species **3.64**.

3.3 Retrosynthetic Analysis

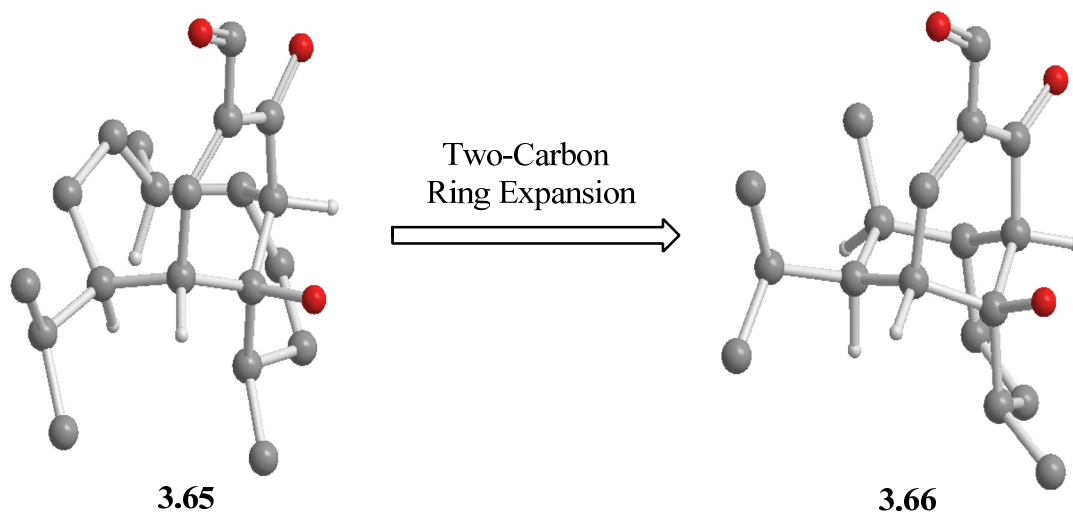
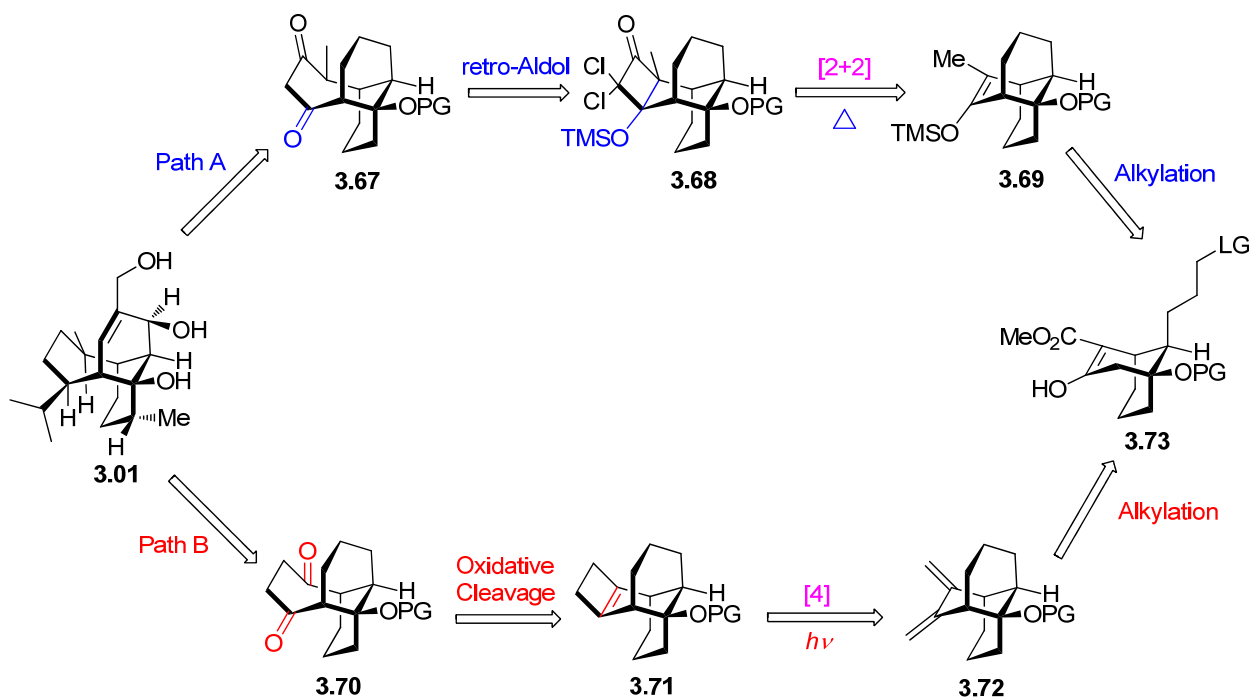


Figure 3.2 Retrosynthetic Analysis Enlightened by the X-ray Crystal Structure

As can be seen from the crystal structure of the oxidized product of vinigrol (**3.65**)^[1a], there seems to be a four-membered ring within the bridging eight-membered ring (Figure 3.2). Enlightened by this ‘four-membered ring’, we proposed preparing vinigrol from its six-membered ring analogue **3.66** centered upon a two-carbon ring expansion strategy.

In order to avoid the *cis*-decalin framework in approaching the bridging eight-membered ring of vinigrol, we envisioned that the bridging eight-membered ring could be constructed by another easily accessed tricyclic compound, **3.69** or **3.72**, based on a two-carbon ring expansion strategy (Scheme 3.10). There are two possible pathways in applying this strategy. In path A, the tricyclic adduct **3.67** could be prepared from enol ether **3.69** by a [2+2] cycloaddition with dichloroketene followed by a retro-aldol reaction. In path B, the 1,4-dicarbonyl tricyclic **3.70**

could be obtained by an oxidative cleavage of the cyclobutene **3.71**, which could in turn be accessed from the conjugated diene **3.72** via electrocyclic reaction. Both the tricyclic **3.69** and **3.72** could be constructed by an intramolecular alkylation of the bicyclo[3.3.1]nonane **3.73**. According to Baldwin, such a 6-exo-tet cyclization should prove favorable.^[9] The advantage of this retrosynthetic plan is that we have two possible pathways to build vinigrol, and both pathways result in the same starting material.

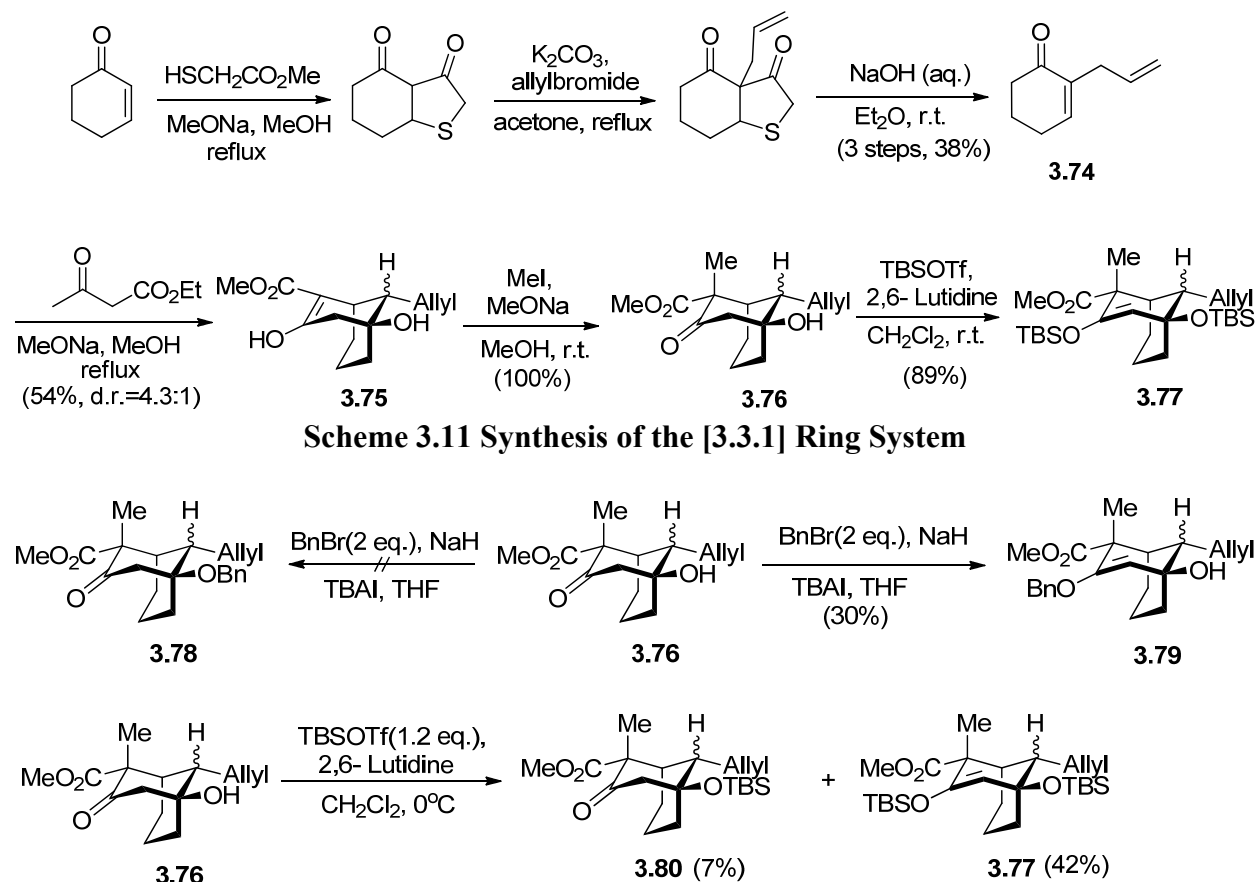


Scheme 3.10 Retrosynthetic Analysis of Vinigrol (3.01)

3.4 Gram Scale Synthesis of the Tricyclic Precursor of Vinigrol

3.4.1 First Generation Approach to the Tricyclic Precursor

Following known procedure,^[10] enone **3.74** was prepared in three consecutive steps by masking the double bond of 2-cyclohexenone (Scheme 3.11). As described in Chapter 2, the bicyclo[3.3.1]nonane **3.75** was readily assembled as an inseparable diastereomeric mixture from **3.74** by a Robinson annulation. Methylation of **3.75** afforded bicyclic ketone **3.76** in quantitative yield.

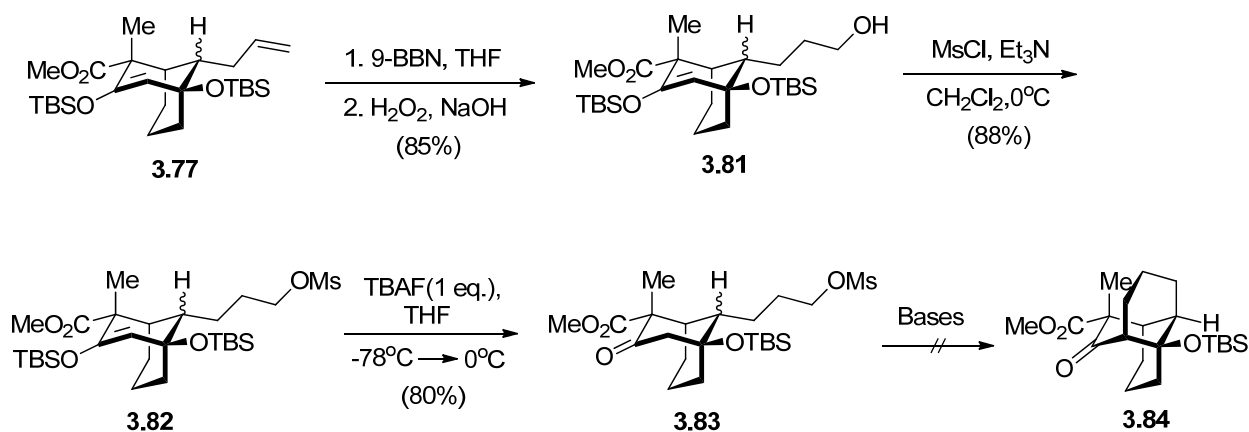


Scheme 3.12 The Easily Enolizable Carbonyl Group

The carbonyl group of bicyclic ketone **3.76** was found to be extremely enolizable. Protection of the tertiary hydroxy group of **3.76** by excess benzyl bromide in the presence of sodium hydride and TBAI in THF did not afford the desired benzyl ether **3.78**. The benzyl enol ether **3.79** was formed instead (Scheme 3.12). A similar problem was encountered with siloxyl ether protection. If **3.76** was treated with little excess (1.2 eq.) of TBSOTf, the doubly protected compound **3.77** was formed as the major product (42%, Scheme 3.12). In comparison, when **3.76** was treated with large excess (2.2 eq.) of TBSOTf, **3.77** was formed as the sole product in good yield (Scheme 3.11).

Next, chemoselective hydroboration of the allyl double bond of **3.77** followed by oxidation produced the alcohol **3.81** (Scheme 3.13). Then, mesylation of the alcohol **3.81** with MsCl in

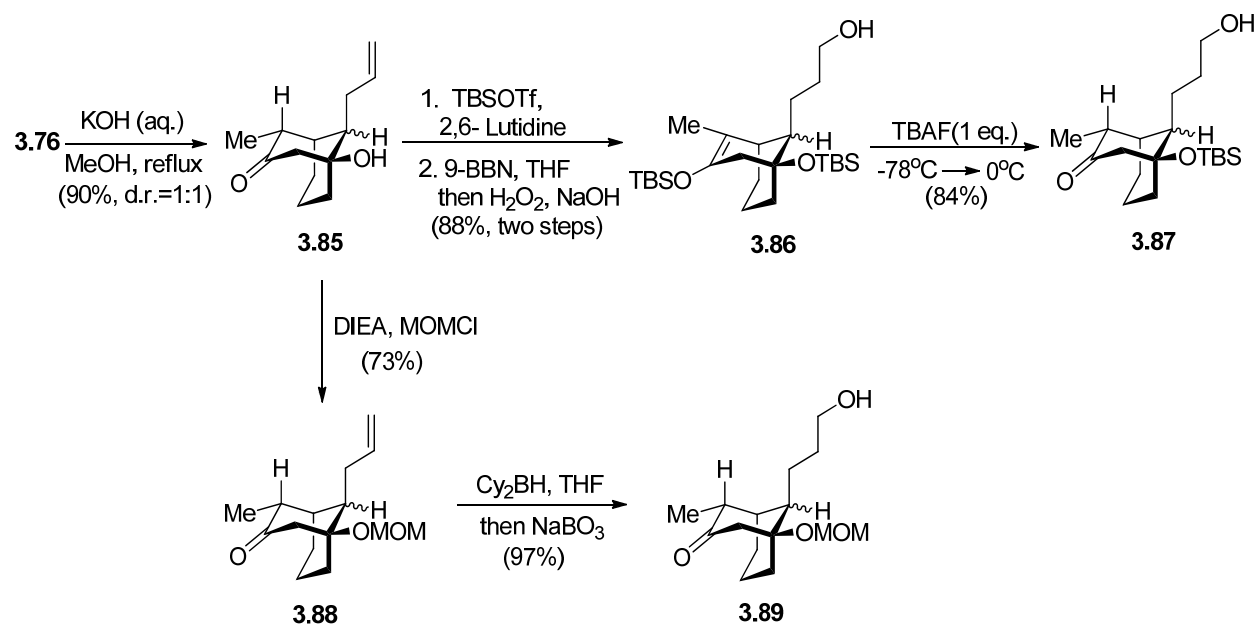
dichloromethane followed by chemoselective removal of the enol ether TBS group furnished mesylate **3.83**. Having mesylate **3.83** in hand, we turned our attention to the intramolecular alkylation. Unfortunately, our preliminary attempts at the preparation of the tricyclic **3.84** were fruitless, even though various reaction conditions were explored. Although the mesylate **3.83** was a mixture of diastereomers with the unreactive isomer as the major component, some cyclization product was expected. The ketone mesylate **3.83** was recovered upon treatment with milder bases, while decomposed products were detected upon treatment with harsher bases. The reluctance of this ring closure may be due to the strain energy associated with 1,3-diaxial repulsion.



Scheme 3.13 Initial Efforts toward the Synthesis of the Tricyclic System

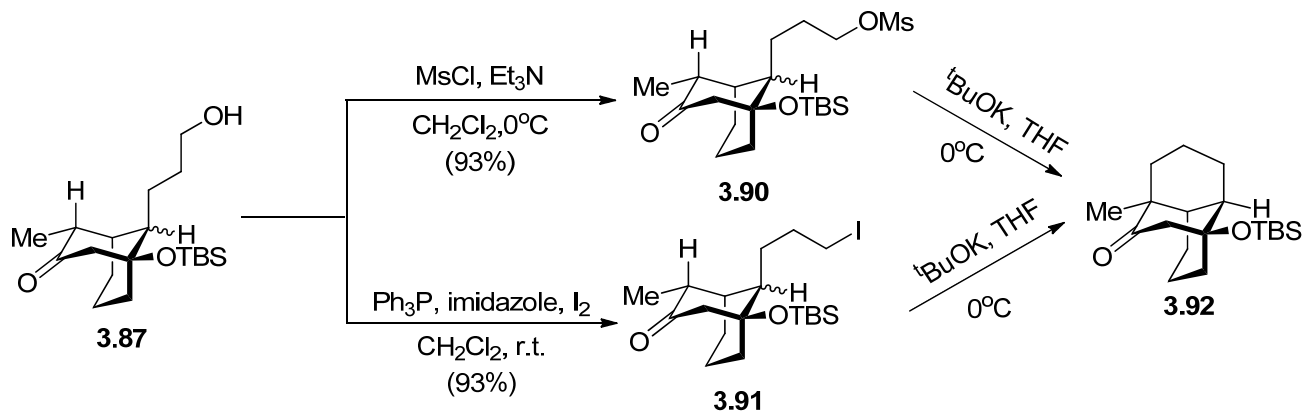
3.4.2 Revised Approach to the Tricyclic Precursor

Bearing in mind the severe 1,3-diaxial repulsion, it was considered a wise decision to remove the extra methyl ester group in an earlier step in the modified synthesis (Scheme 3.14). As described in Chapter 2, decarboxylation of **3.76** with large excess aqueous KOH gave the epimerized product **3.85** as a diastereomeric mixture of 1:1 ratio. As in previous studies, TBS protection, hydroboration-oxidation and chemoselective removal of the enol ether TBS group offered us the primary alcohol **3.87** (Scheme 3.14).



Scheme 3.14 Synthesis of the Tricyclic Precursor

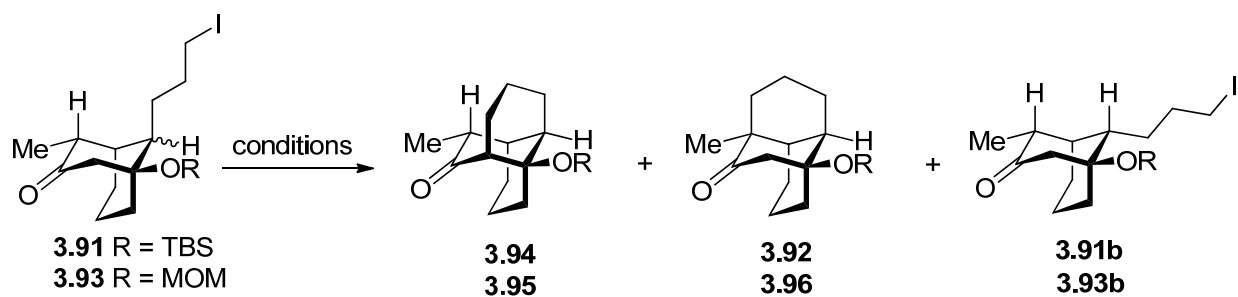
In an effort to explore the role of protective groups in the synthesis of the tricyclic compound, the MOM ether **3.88** was obtained by mixing the ketone alcohol **3.85** with MOMCl in the presence of DIEA (Scheme 3.14). Next, chemoselective hydroboration-oxidation of the allyl double bond was achieved to furnish the primary alcohol **3.89** in 97% yield by treating MOM ether **3.88** with dicyclohexylborane followed by oxidative workup.^[11] It is worth noting that the borane reagent is crucial to achieve excellent selectivity. Both 9-BBN and BH_3 react preferentially with the carbonyl group of **3.88**.



Scheme 3.15 The Intramolecular Alkylation

Next, mesylation of the alcohol **3.87** produced mesylate **3.90**, which was treated with potassium tert-butoxide to afford the undesired regio-isomeric tricyclic **3.92** as the sole product (Scheme 3.15). In an effort to perform the intramolecular alkylation, we decided to convert the primary alcohol **3.87** to iodide, which would act as a better leaving group. Iodination of the alcohol afforded the iodide **3.91**. To our surprise, when iodide **3.91** was exposed to potassium tert-butoxide, the same tricyclic **3.92** was detected. These results indicate that only the thermodynamic enolate can be formed using ^tBuOK as the base.

Table 3.1 Regioisomer Distribution in the Cyclization Reaction



Entry	Substrate	Base	Temperature	Ratio ^a	Total yield ^b
1	3.91	LDA	-78 °C	N.A.	No Reaction
2	3.91	LDA	-40 °C	2.3:1	100%
3	3.91	LDA	0 °C	2.0:1	75%
4	3.91	LiTMP	-40 °C	N.A.	No Reaction
5	3.91	LiTMP	-15 °C	3.8:1	100%
6	3.91	LiTMP	0 °C	3.5:1	77%
7	3.93	LDA	0 °C	1.5 : 1	90%

^a The ratio of the two regioisomeric products is based on the ¹H NMR of crude product

^b This is the yield of the two regioisomeric products based on the reactive substrate

This cyclization reaction was carefully studied. In order to obtain the desired tricyclic, we tried LDA, a kinetically faster base at low temperature. Surprisingly, no reaction was detected w-

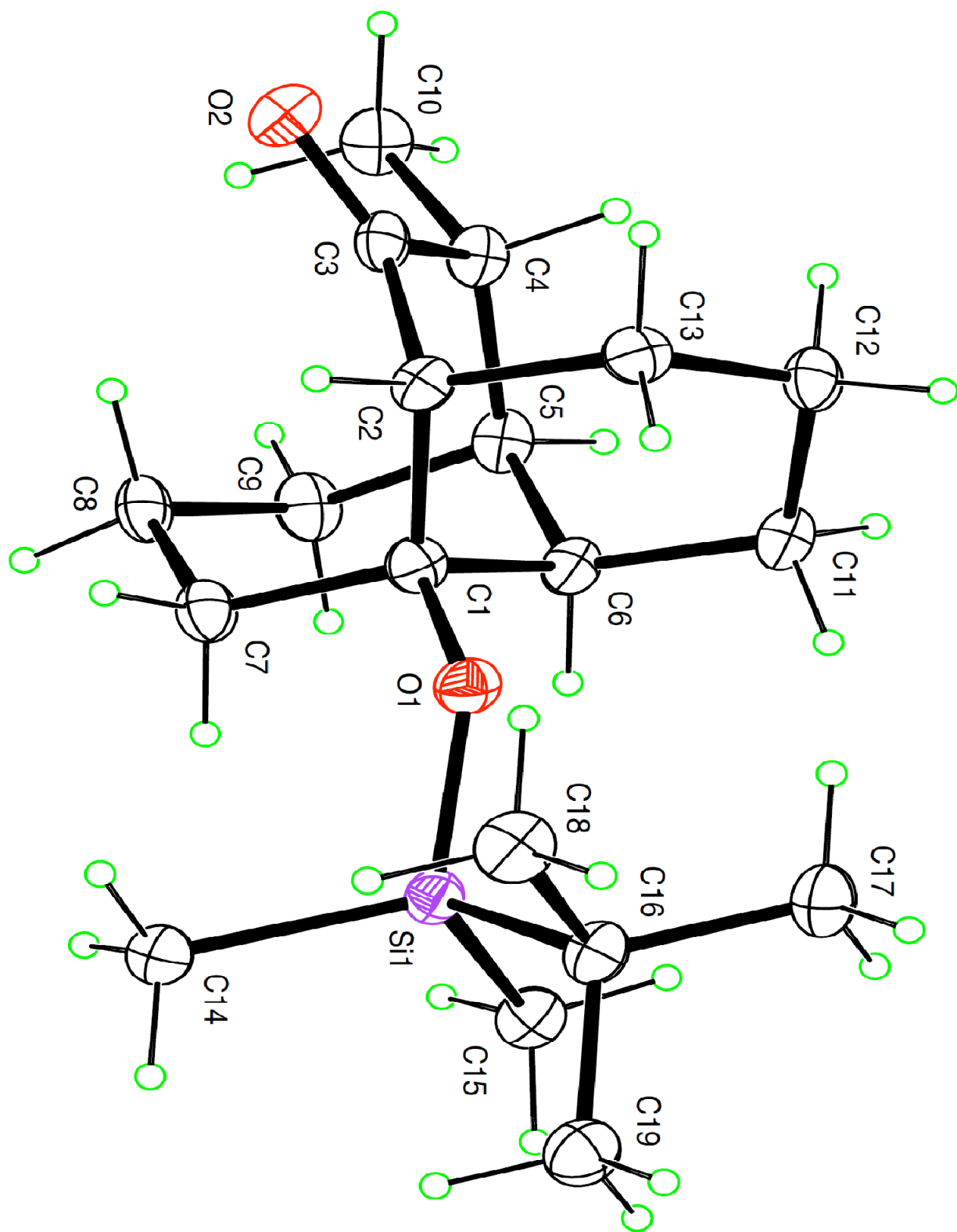
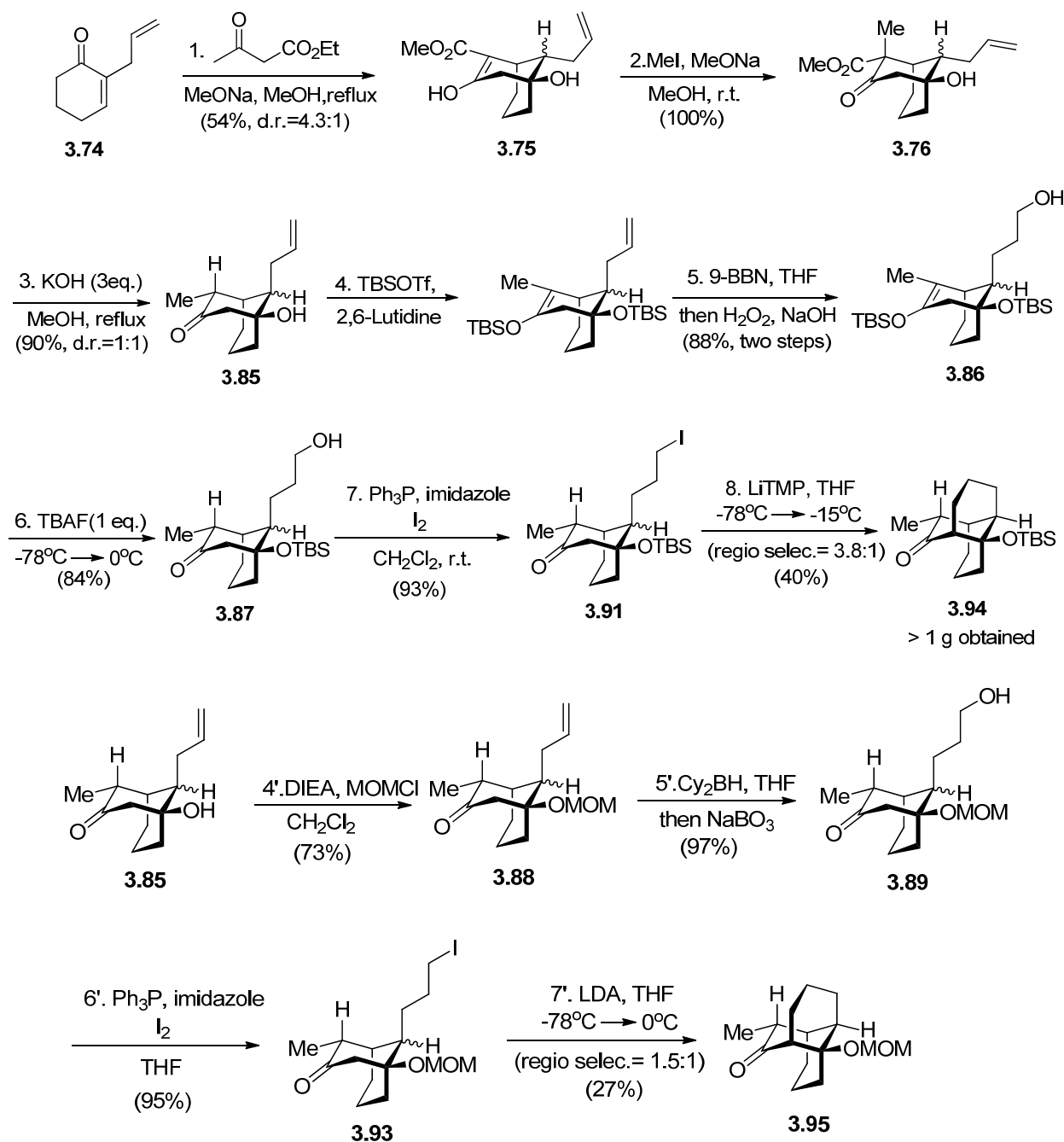


Figure 3.3 ORTEP Plot of Tricyclic Precursor 3.94



Scheme 3.16 Synthesis of the Tricyclic Precursor of Vinigrol (3.01)

When iodide **3.91** was treated with LDA at -78°C (Table 3.1, entry 1). Gratefully, the desired tricyclic **3.94** was formed as the major product (ratio = 2.3:1) when the reaction temperature was increased to -40°C (entry 2). And we were able to isolate the two regioisomeric products **3.92**, **3.94** and the unreactive starting material **3.91b**. As expected, the ratio dropped as the temperature

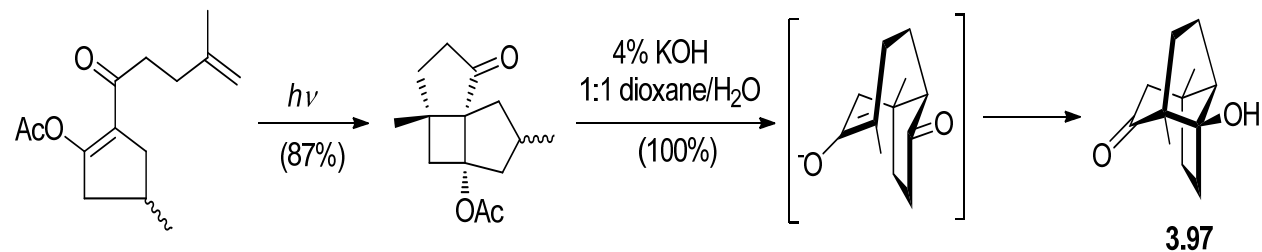
increased. At 0 °C, both the ratio and the yield were reduced (entry 3). The optimized condition was to use the more hindered base LiTMP and maintain the reaction temperature at -15 °C (entry 5). Substrate MOM ether **3.93** showed poorer selectivity in comparison with TBS ether **3.91** (entry 7).

It is worth noting that no reaction occurred when **3.91** was treated with LiTMP at -40°C (entry 4), whereas the reaction was finished in one hour at the same temperature using LDA. This result indicates that the formation of enolate rather than the alkylation step is the rate determining step.

In summary, efforts toward the synthesis of the unusual tricyclic precursor of vinigrol (**3.01**) are described. More than one gram of this tricyclic **3.94** has been successfully prepared (Scheme 3.16), and the structure has been unambiguously assigned according to its crystal structure (Figure 3.3). A Robinson annulation and an intramolecular alkylation allow the rapid construction of the core ring system in eight steps (based on TBS protection) with an average yield of 78%, and seven steps (based on MOM protection) with an average yield of 70%, respectively (Scheme 3.16). This route is a potential approach to the synthesis of vinigrol.

3.5 A Potential Synthesis of the Tricyclic Precursor

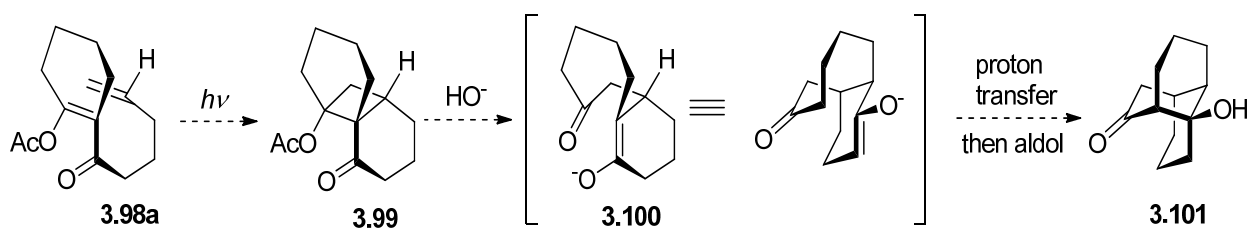
3.5.1 De Mayo Photoannulations



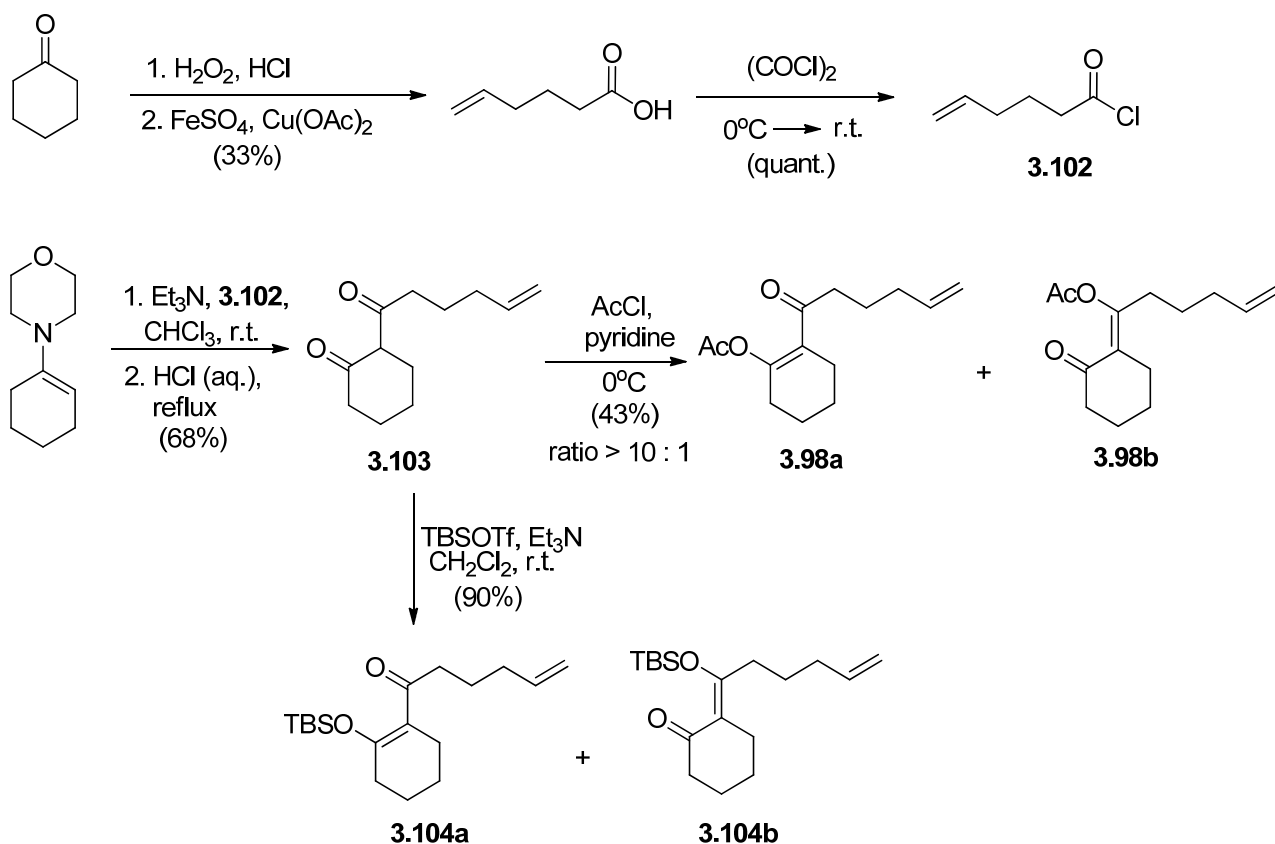
Scheme 3.17 Seto's Synthesis of Tricyclic Compound Using De Mayo Photoannulations

During Seto's synthesis of the bicyclo[5.4.0]undecanes,^[12] the tricyclic **3.97** was prepared by De Mayo photoannulations (enone [2+2] photocycloaddition followed by a Grob

fragmentation, Scheme 3.17).^[13] Enlightened by this sequence, we designed a potential concise route to our tricyclic intermediate **3.101** as outlined in Scheme 3.18.



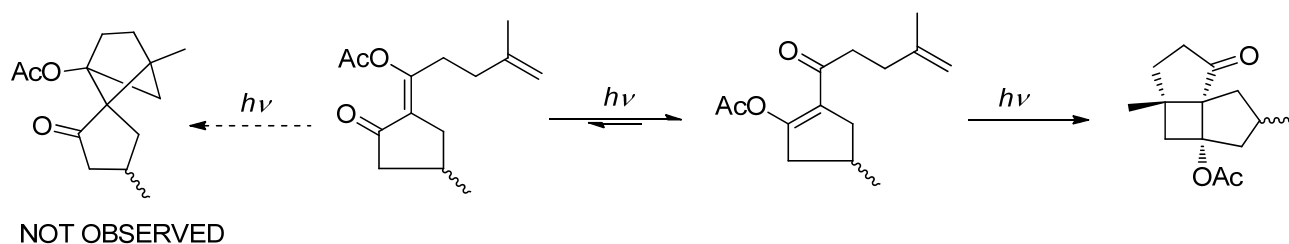
Scheme 3.18 A Potential Approach to the Tricyclic Precursor



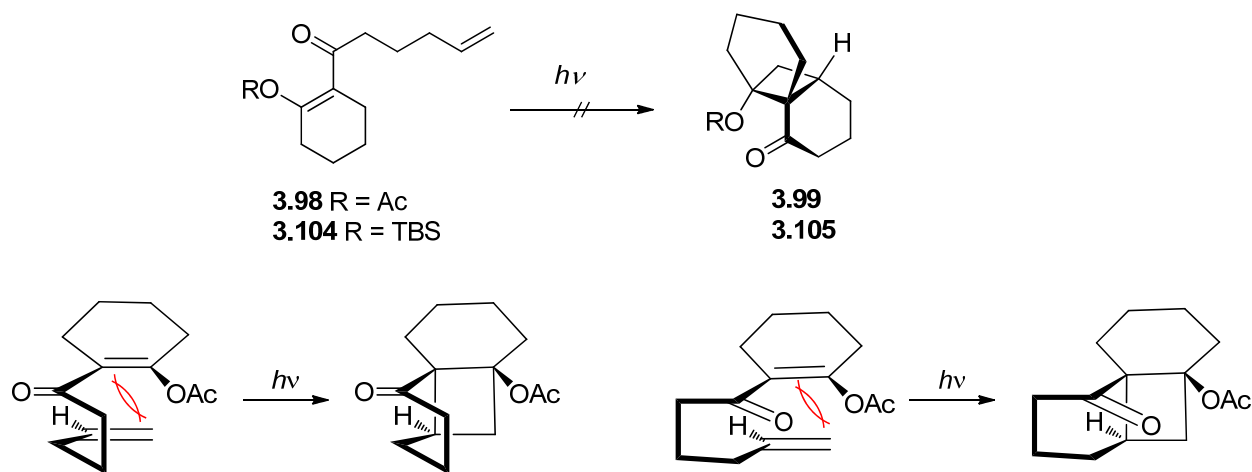
Scheme 3.19 Synthesis of the Photoannulation Precursor

When **3.98a** is irradiated by UV light, an intramolecular [2+2] cycloaddition takes place within **3.98** to yield **3.99** with both high regio- and stereo-control. Under basic conditions, the acetate of **3.99** will be hydrolyzed followed by a retro-aldol to form the intermediate **3.100**. After proton transfer process, an aldol reaction will occur leading to the target tricyclic **3.101**.

As shown in Scheme 3.19, acid chloride **3.102** was readily prepared from 5-hexenoic acid, which had been synthesized from cyclohexanone following a known procedure.^[14] Then, 1-morpholinocyclohexene was coupled with the acid chloride **3.102** to afford the diketone **3.103** by standard procedure. Treatment of ketone **3.103** with acetyl chloride in the presence of pyridine led to the acetate enol ether mixture **3.98a** and **3.98b**. ¹H NMR indicated a 10:1 ratio of the two regioisomers (major component undetermined). Similarly, a mixture of the TBS enol ether **3.104a** and **3.104b** (ratio = 3.6:1, indicated by ¹H NMR and major component undetermined) were obtained by treating ketone **3.103** with TBSOTf in the presence of triethylamine.



Scheme 3.20 Photo Fries Rearrangement of Two Isomers Reported by Seto



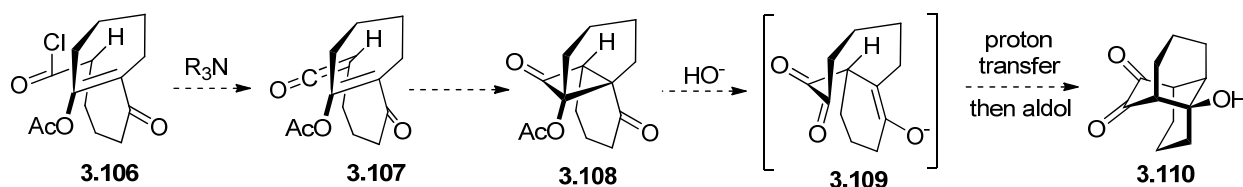
Scheme 3.21 Unsuccessful Intramolecular Photo [2+2] Reaction and Possible Reason

According to the literature,^[12b, 12c] only the endo enol ether (**a** series compounds) are reactive in the [2+2] cycloaddition (Scheme 3.20). Additionally, the two regioisomers interconvert with each other under photo conditions, presumably through a Photo-Fries

Rearrangement.^[15] Therefore, the regioisomeric mixture will not be a problem. When either **3.98** or **3.104** is irradiated by UV light, only the desired photoadduct product will be formed.

With the photoaddition precursors **3.98** and **3.104** in hand, we focused on the key step--- the enone-olefin [2+2] cycloaddition step. Unfortunately, both the ketone **3.98** and **3.104** were completely recovered without any detectable amount of the photoadduct (Scheme 3.21). We believe that the decreased reactivity of **3.98** and **3.104** in comparison with their five-membered ring analogue is due to steric hindrance (Scheme 3.21). This reaction is currently under study.

3.5.2 A Potential Synthesis of the Precursor by Thermal [2+2]

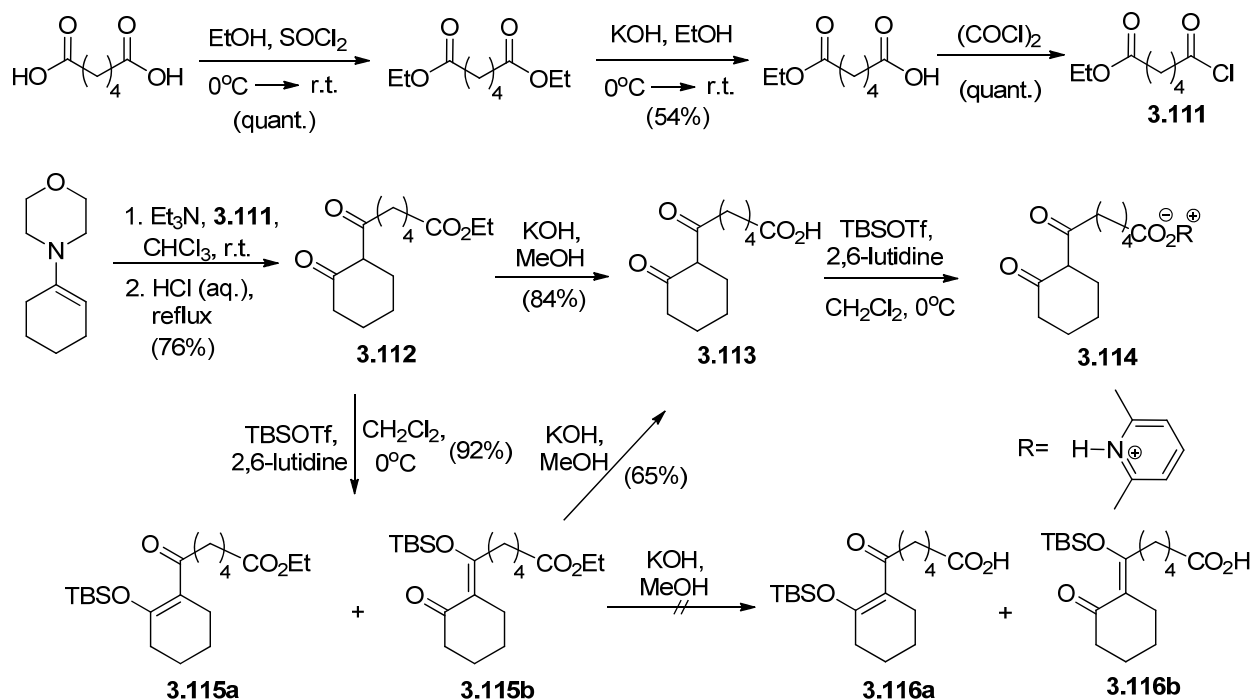


Scheme 3.22 Another Potential Approach to the Tricyclic Precursor

In replacing the previous route using photo [2+2] condition with thermal [2+2] via ketene, we realized that the tricyclic skeleton could also be built by another potential route. As outlined in Scheme 3.22, treatment of acid chloride **3.106** with amine bases results in the formation of ketene **3.107** *in situ*, which will undergo an intramolecular [2+2] cycloaddition to furnish the tricyclic **3.108**. Finally, under basic conditions, the acetate **3.108** will be hydrolyzed followed by a retro-aldol to afford the intermediate **3.109**. After proton transfer process, an aldol reaction will take place, leading to the tricyclic **3.110**, which is a potential precursor of vinigrol skeleton.

Similar to the previous synthesis, diketone **3.112** was readily prepared from 1-morpholinocyclohexene and mono acid chloride **3.111** (Scheme 3.23), which was obtained according to the literature.^[16] Hydrolysis of **3.112** gave the carboxylic acid **3.113** (Scheme 3.23). Unfortunately, it turns out that the enol ether **3.116** is difficult to prepare. When the carboxylic acid **3.113** was treated with excess amount of TBSOTf in the presence of 2,6-lutidine under

standard conditions, only the amine salt **3.114** was detected. We tried to circumvent the problem by forming the TBS enol ether first. Although we did get the TBS enol ether **3.115** in high yield, **3.115** was readily hydrolyzed under basic conditions to give **3.113** instead of **3.116**. This problem may be due to the incompatibility of the two functional groups: carboxylic acid and enol ether. Currently, in order to avoid the problem, we are trying to prepare the ketene **3.107** by some other method, like Wolff Rearrangement.^[17]



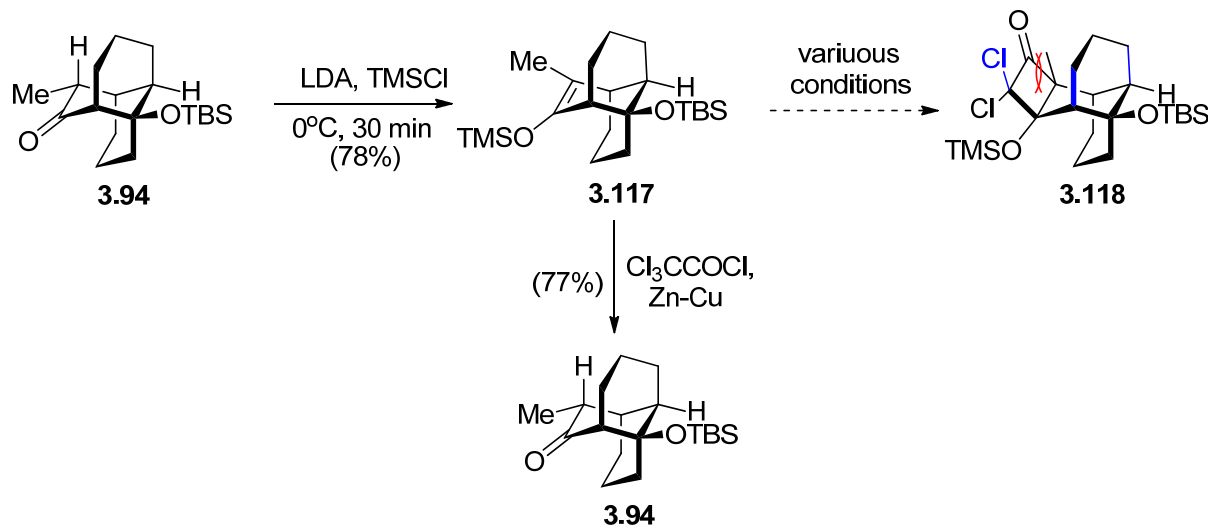
Scheme 3.23 Synthetic Effort to Prepare the Thermal[2+2] Precursor

3.6 Efforts toward the Skeleton of Vinigrol Based on Thermal [2+2] Reactions

3.6.1 Initial Attempt for the Cycloaddition Reaction

As shown in Scheme 3.24, TMS enol ether **3.117** was readily formed once ketone **3.94** was treated with TMSCl in the presence of LDA at 0°C . With the enol ether **3.117** in hand, we initiated studies on the [2+2] ring expansion to test the applicability of this strategy. Unfortunately, our preliminary attempts at the [2+2] cycloaddition with dichloroketene did not afford the desired tetracyclic **3.118**, even though a number of different reaction conditions had

been explored (see Table 3.2). Our attempt involved utilizing the improved procedure reported by Hassner: preparation of dichloroketene in the presence of the enol ether and adding the trichloroacetyl chloride to the reaction mixture very slowly in order to avoid the polymerization of ketene itself.^[18] We also tried to do the reaction under ultrasound condition, which has been known to promote the cycloaddition of ketenes with olefins.^[19]



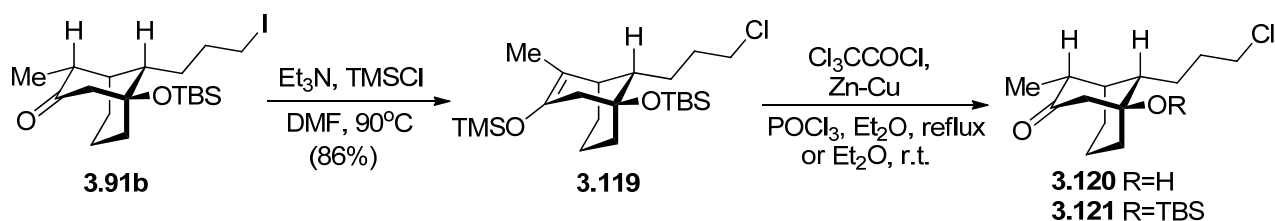
Scheme 3.24 Efforts to Prepare the Tricyclic Core of Vinigrol by Ketene Addition

Table 3.2 Attempted [2+2] Cycloaddition Conditions toward the Tetracyclic 3.118

Entry	Reaction Conditions	Additive	Products
1	Cl ₃ CCOCl, Zn-Cu, Et ₂ O, r.t.	None	3.94
2	Cl ₃ CCOCl, Zn-Cu, Et ₂ O, reflux	None	3.94
3	Cl ₃ CCOCl, Zn-Cu, Et ₂ O, reflux	POCl ₃	3.94
4	Cl ₃ CCOCl, Zn, Et ₂ O, sonication at r.t.	None	3.94
5	Cl ₂ CHCOCl, Et ₃ N, Et ₂ O, r.t.	None	No reaction

However, the TMS enol ether **3.117** did not react with dichloroketene, which was prepared *in situ* from trichloroacetyl chloride and zinc powder^[18] (Table 3.2, entries 1-4) or from dichloroacetyl chloride and triethyl amine^[20] (Table 3.2, entry 5). Instead of the tetracyclic **3.118**

we want, formation of ketone **3.94** was observed (entries 1-4), presumably due to the formation of zinc chloride. It has been reported that phosphorus oxychloride could complex with the zinc chloride, resulting in the removal of the zinc chloride out of the reaction system.^[21] However, this did not avoid hydrolyzing the enol ether in the reaction (entry 3). This failed result may be due to the severe 1,3-diaxial repulsion between the chlorine and the cyclohexane ring (Scheme 3.24).



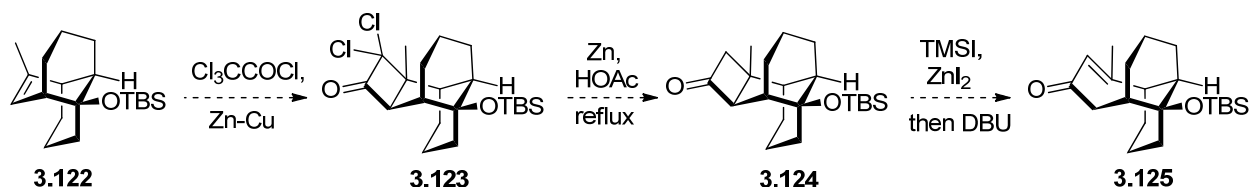
Scheme 3.25 Studies toward the [2+2] Cycloaddition with the Bicyclic Enol Ether

Bearing in mind the severe 1,3-diaxial repulsion in the cycloaddition reaction, we decided to tackle this hurdle early rather than at a late stage of the synthesis. With the unreactive iodide **3.91b** in hand, the enol ether **3.119** was readily obtained by mixing **3.91b** with TMSCl in the presence of Et₃N in DMF at 90°C, and the iodine was replaced by chlorine in the same step (Scheme 3.25). Next, the cycloaddition was carefully studied. To our surprise, although the bicyclic chloride **3.119** is much less hindered than the tricyclic analogue **3.117**, either hydroxy ketone **3.120** or the siloxy ether ketone **3.121** was formed as the major product under standard ketene formation conditions. These results indicate that these types of enol ethers tend to be hydrolyzed and are unreactive toward ketene cycloaddition.

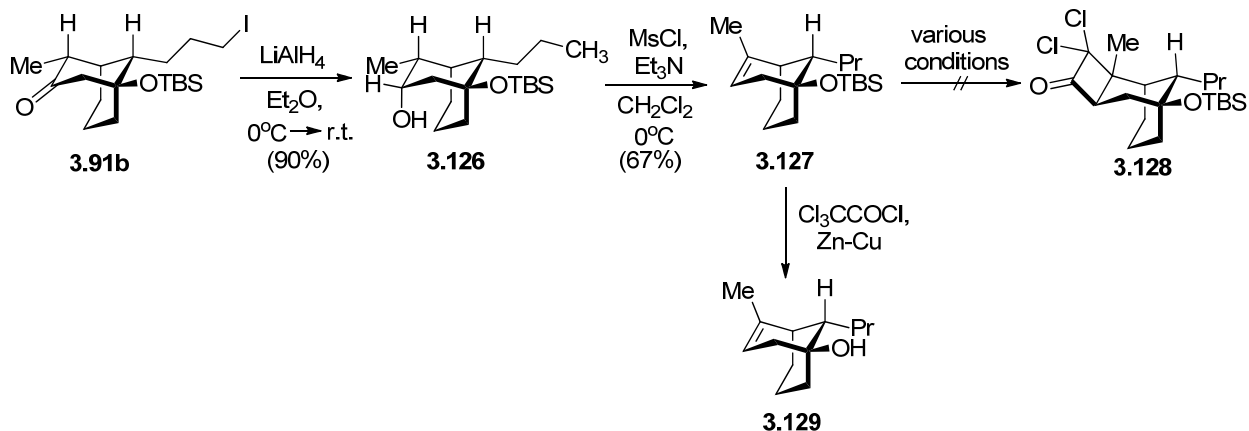
3.6.2 Revised Cycloaddition Reaction with Neutral Olefins

Although enol ethers are much more reactive toward ketene addition than neutral olefins based upon electronic effects, enol ethers are more hindered than neutral olefins. Therefore, we turned our attention to olefin analogues of the tricyclic precursors. As outlined in Scheme 3.26,

tetracyclic **3.123** will be formed from olefin **3.122** by ketene cycloaddition. Next, dechlorination of **3.123** by zinc and acetic acid produces the ketone **3.124**,^[22] whose cyclobutanone ring will be cleaved by TMSI in the presence of zinc iodide followed by elimination with DBU to furnish the enone **3.125**, the tricyclic core of vinigrol.^[23]



Scheme 3.26 Synthetic Plan to Prepare the Core of Vinigrol



Scheme 3.27 Studies toward the [2+2] Cycloaddition with the Bicyclic Olefin

To this end, the iodide **3.91b** was converted to the alcohol **3.126** stereoselectively by LAH reduction of both the ketone and the iodide in one step (Scheme 3.27). Next, alcohol **3.126** was mesylated by MsCl in the presence of Et₃N in DCM at 0°C to give a mesylate, which was eliminated *in situ* to afford the olefin **3.127**. With the olefin **3.127** in place, we studied the cycloaddition reaction carefully. Unfortunately, our preliminary attempts did not show any fruitful result, although a number of different reaction conditions were explored (Table 3.3). The first attempt we utilized was the improved procedure reported by Brady: using a high dilution technique in order to avoid the self dimerization of ketene (Table 3.3, entry 1)^[24]. We also tried

to avoid the deprotection of the TBS ether by adding POCl₃ or DME (entry 2 and 3), which are known to be capable of complexing with the zinc salts formed in the reaction.^[21] However, as can be seen in Table 3.3, either the deprotected olefin **3.129** (entries 1-3) was formed, or recovery of the starting material **3.127** (entries 4-5) was detected. The reason for these unsuccessful cycloadditions may be due to the steric hindrance of the six-membered ring in the context of the molecule, though simple six-membered ring is known to be reactive to dichloroketene.

Table 3.3 Attempted [2+2] Cycloaddition Conditions toward the Tetracyclic 3.128

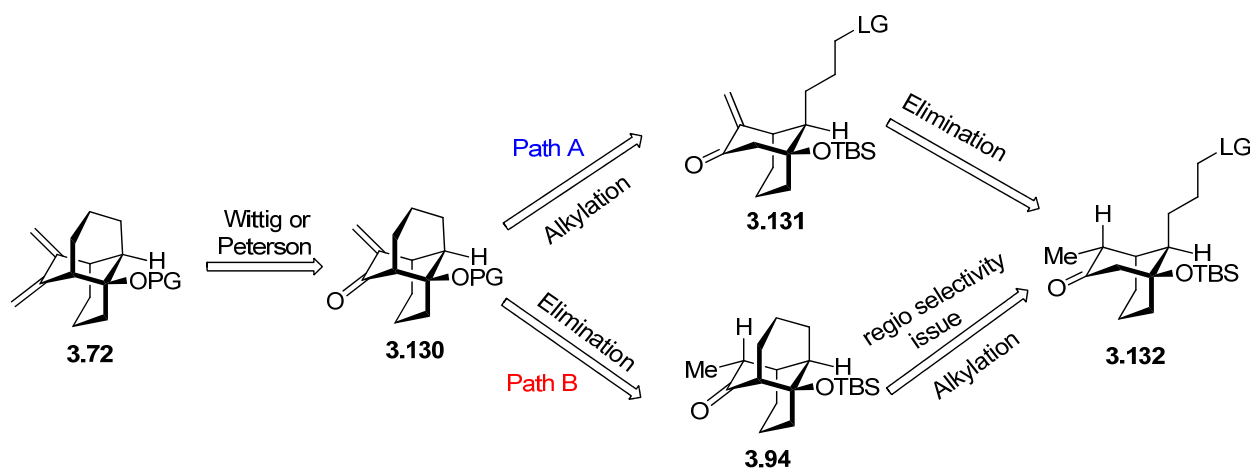
Entry	Reaction Conditions	Additive	Substrate Concentration	Products
1	Cl ₃ CCOCl, Zn-Cu, Et ₂ O, reflux	None	0.05 M	3.129
2	Cl ₃ CCOCl, Zn-Cu, Et ₂ O, reflux	DME	0.1 M	3.129
3	Cl ₃ CCOCl, Zn-Cu, Et ₂ O, reflux	POCl ₃	0.05 M	3.129
4	Cl ₃ CCOCl, Zn-Cu, Et ₂ O, r.t.	None	0.05 M	No reaction
5	Cl ₃ CCOCl, Zn, Et ₂ O, sonication at r.t.	None	0.1 M	No reaction

3.7 Efforts toward the Skeleton of Vinigrol Based on Electrocyclic Reactions

With the failure in making the skeleton of vinigrol via thermal [2+2] reaction, we turned our attention to the alternative route----prepare the target by an electrocyclic ring closure reaction (see Scheme 3.10). As revealed in Scheme 3.28, the conjugated diene **3.72** can be generated via the classic Wittig or Peterson olefination reaction from the tricyclic enone **3.130**, which in turn would arise from either bicyclic enone **3.131** or tricyclic ketone **3.94** by two possible routes.

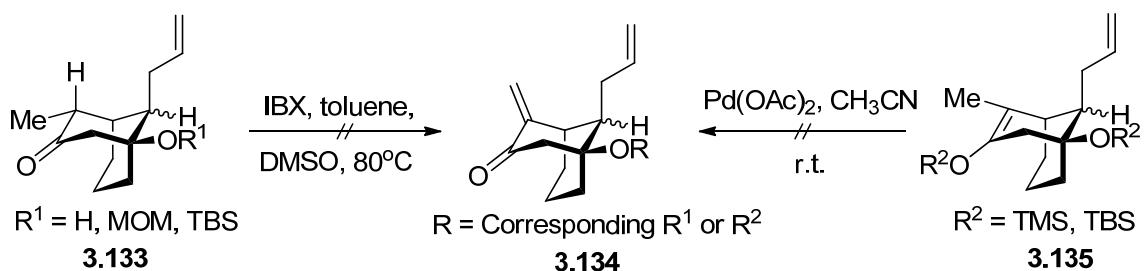
In path A, α -elimination of the ketone **3.132** followed by an intramolecular alkylation would furnish the tricyclic enone **3.130**. In path B, by reversing the order of path A, the tricyclic

enone **3.130** would arise from the same substrate **3.132** by an intramolecular alkylation followed by the α -elimination of the ketone **3.94**, which has been obtained from our previous synthesis. In comparing the two pathways, while we have obtained the tricyclic ketone **3.94** in the previous synthesis, we had a regioselective issue that needs to be solved in the alkylation step. In path A, this alkylation problem will be circumvented by utilizing the bicyclic enone **3.131** under kinetic conditions (only one possible enolate could be formed in this case). Therefore, we decided to explore path A first.



Scheme 3.28 Retrosynthetic Analysis of the Conjugated Diene

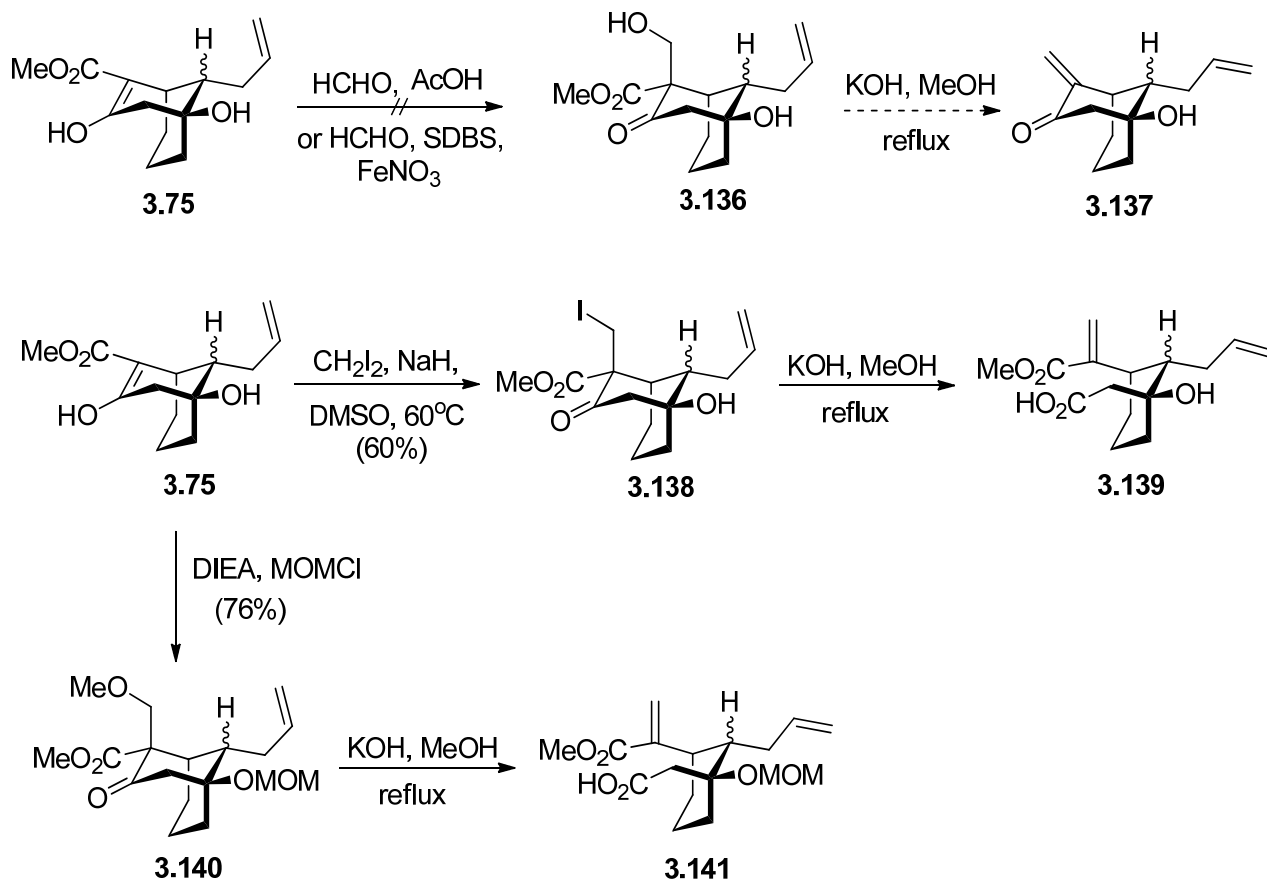
3.7.1 Efforts to Prepare the Bicyclic Enone



Scheme 3.29 Studies toward the Bicyclic Enone by Direct Elimination

With the ketone **3.133** or enol ether **3.135** readily prepared from the substrate **3.85** (see Scheme 3.14), we tried to do the direct dehydrogenation first. However, both of the two standard procedures were unsuccessful (Scheme 3.29). When ketone **3.133** was treated with IBX in hot

DMSO^[25], complex mixtures were detected. Whereas when the enol ether **3.135** was treated with palladium(II) acetate,^[26] no reaction occurred resulting in the complete recovery of the starting material.



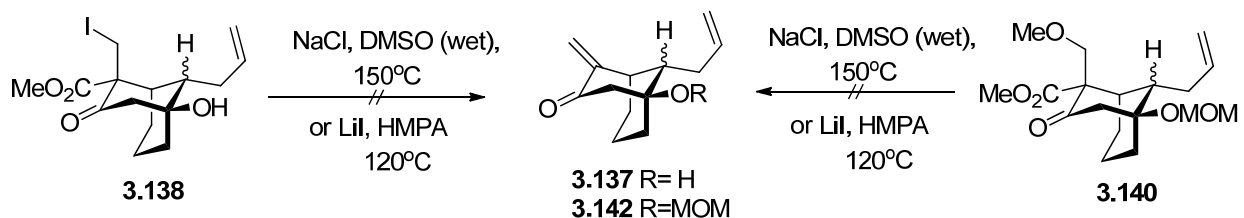
Scheme 3.30 Initial Attempt to Prepare the Bicyclic Enone

Then, we focused on an aldol or aldol-like reaction aimed at introducing an extra carbon with a good leaving group to the β -keto ester **3.75**. Initially, no reaction was detected when **3.75** was treated with formaldehyde under various conditions (Scheme 3.30), but then, iodide **3.138** was formed in 60% yield when **3.75** was treated with diiodomethane in the presence of sodium hydride in hot DMSO. Next, we planned to do the decarboxylation and elimination reactions in a single operation by treating iodide **3.138** under base catalyzed hydrolysis conditions. However, instead of the desired enone **3.137**, a good amount of the carboxylic acid **3.139** was identified.

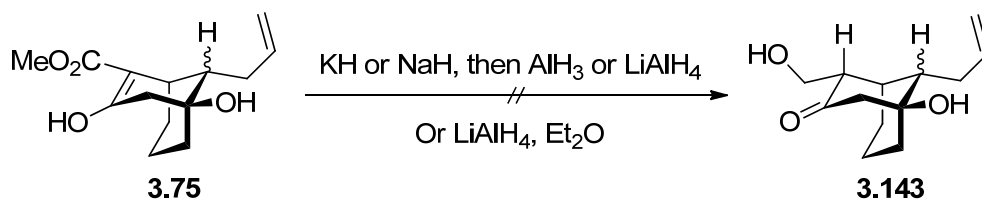
The reaction likely proceeded by a retro Dieckmann condensation followed by an elimination of the iodide.

Considering the tendency of elimination of iodides, we synthesized MOM ether **3.140** with MOM groups introduced to both the β -keto ester group and the tertiary hydroxyl group (Scheme 3.30). However, we were surprised to find that the elimination of the MOM group was observed to give the carboxylic acid **3.141**. The strain release of the bicyclic precursor, which has the 1,3-diaxial repulsion within the system, may be the driving force for the tendency of the elimination to form the ring opened compounds.

In order to avoid this elimination, we tried to remove the ester group under neutral conditions by Krapcho dealkoxy carbonylation.^[27] However, only decomposition products were detected after heating either **3.138** or **3.140** with the inorganic salts and the organic solvent (Scheme 3.31).



Scheme 3.31 Attempted Krapcho Dealcoxy Carbonylation

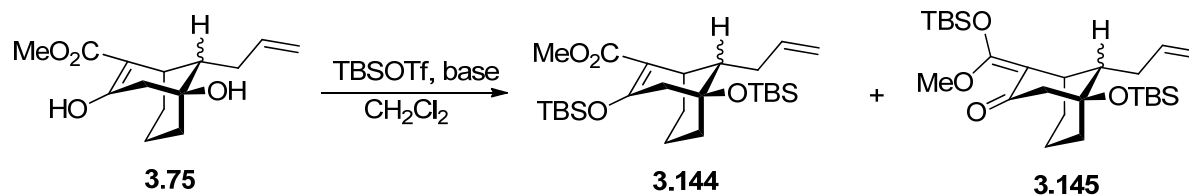


Scheme 3.32 Attempted Selective Reduction of the Ester Group

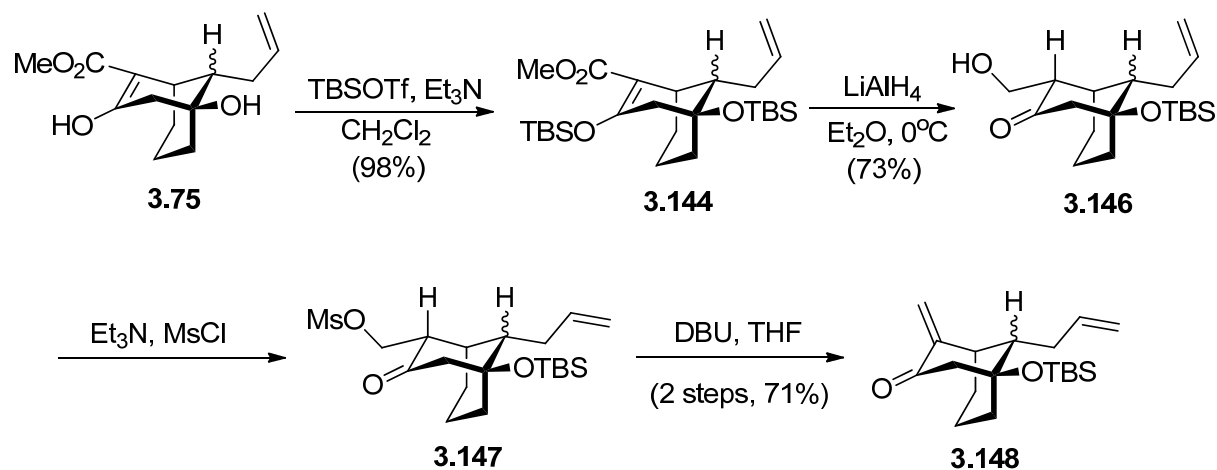
Next, we turned our attention to the selective reduction of the ester group of the β -keto ester of **3.75**. It has been reported that aluminum hydride can selectively reduce the ester group in enolate salts of highly enolizable β -keto esters without attacking the enolate anion.^[28] In this

case, when **3.75** was treated by different bases followed by the reducing reagents, no reaction could be detected (Scheme 3.32).

Table 3.4 Regioisomer Distribution in Forming the Enol Ether



Entry	Reaction Condition	Percent of 3.144	Total yield
1	2,6-Lutidine, 0°C, 2 hs	50%	90%
2	2,6-Lutidine, r.t., 3 hs	83%	100%
3	Et ₃ N, r.t., 10 hs	100%	98%

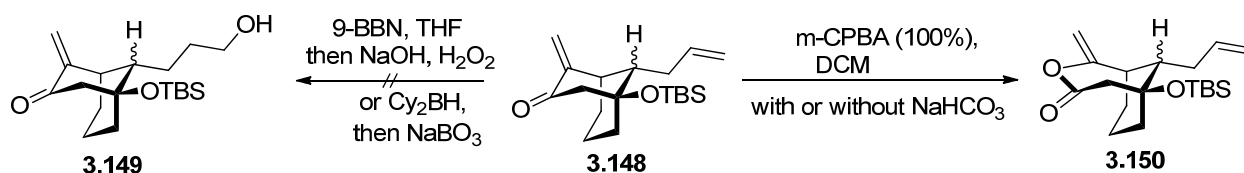


Scheme 3.33 Successful Synthesis of the Bicyclic Enone

Then we considered the possibility of locking the enol form of **3.75** by mixing it with silicon reagents. Since we also need to protect the hydroxyl group of **3.75**, we chose to use TBSOTf. When **3.75** was mixed with TBSOTf in the presence of triethyl amine, the silyl enol ether with the protected hydroxyl product **3.144** was formed in 98% yield (Table 3.4, entry 3). We found that both the base and the temperature are crucial for the regioselectivity (Table 3.4). It

seems that triethylamine promotes the formation of the desired isomer **3.144**. Also, the higher the temperature is, the more distribution of **3.144** there will be.

Next, reduction of both the enol ether and the ester was accomplished in one step by treating **3.144** with LAH at 0°C to afford the desired α -hydroxyl ketone **3.146**, which was converted to the bicyclic enone **3.148** by mesylation and elimination (Scheme 3.33).

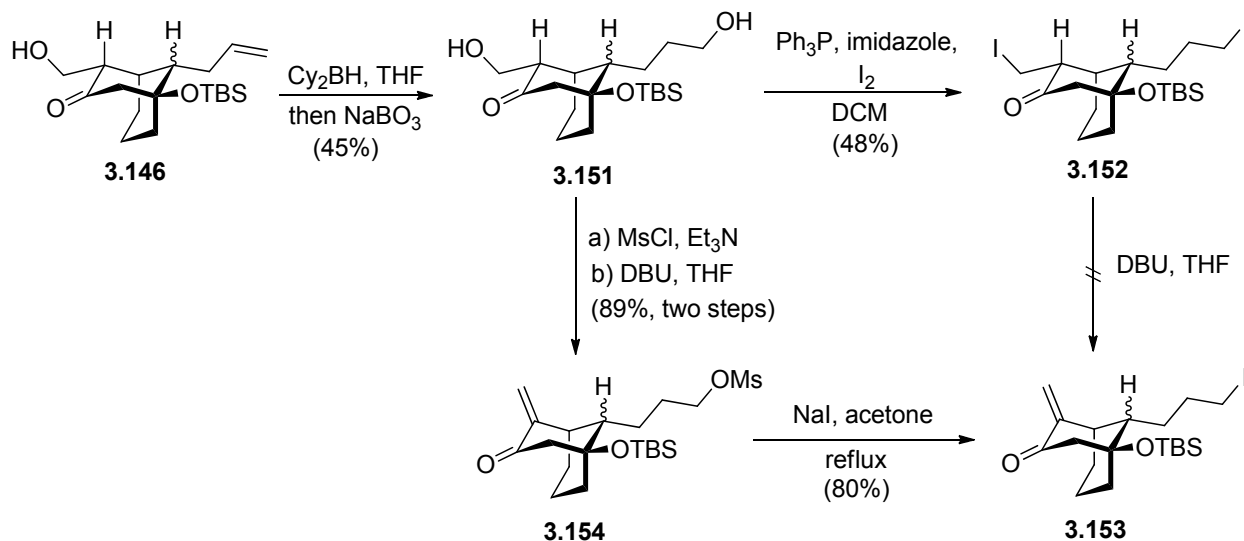


Scheme 3.34 Attempt Functionalization of the Allylic Double Bond

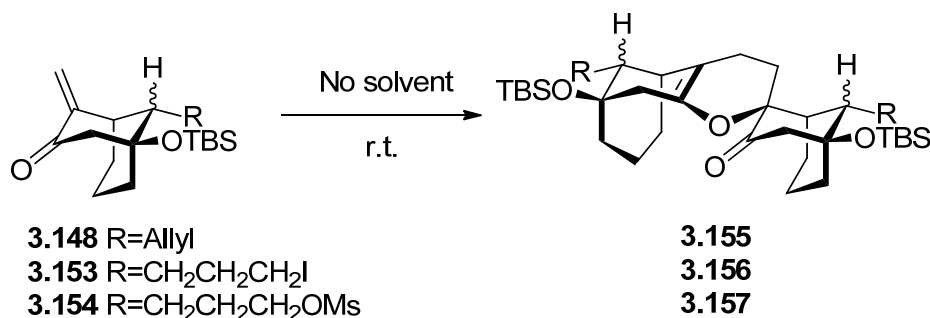
With the enone **3.148** in hand, we were focused on the functionalization of the terminal double bond. However, this enone turned out to be a tough compound to handle. In this scenario, the enone competes with the allyl double bond. Hydroboration of the enone **3.148** with 9-BBN followed by oxidation afforded a complex mixture, whose major component was identified to be the carbonyl reduced product (Scheme 3.34). Hydroboration of **3.148** with dicyclohexylborane followed by oxidation gave a mixture of alcohols including **3.146**, which was produced from the hydroboration of the enone carbon-carbon double bond. When **3.148** was treated with *m*-CPBA under standard conditions, instead of the epoxide we want, the lactone **3.150** was formed, presumably from a Baeyer-Villiger reaction. We tried to avoid this reaction by adding sodium bicarbonate into the reaction mixture, but the same lactone **3.150** was obtained (Scheme 3.34).

Bearing in mind the high reactivity of the enone, we realized that we needed to functionalize the terminal olefin before the enone was generated. Thus, the β -hydroxy ketone **3.146**, the precursor for the enone, was selected. It seems that the sequence of the transformation is critical. In the event, when **3.146** was treated with dicyclohexyl borane followed by sodium perborate afforded the diol **3.151**, which was transformed to the diiodide **3.152** under standard

conditions (Scheme 3.35). However, decomposed products were identified after mixing the diiodide **3.152** with DBU. To this end, the diol was converted to a dimesylate and chemoselectively eliminated the mesylate next to the carbonyl group by DBU, forming the bicyclic enone **3.154** in 89% yield. Mesylate **3.154** was further substituted by iodide to afford the desired iodide **3.153**, the precursor for cyclization (Scheme 3.35).



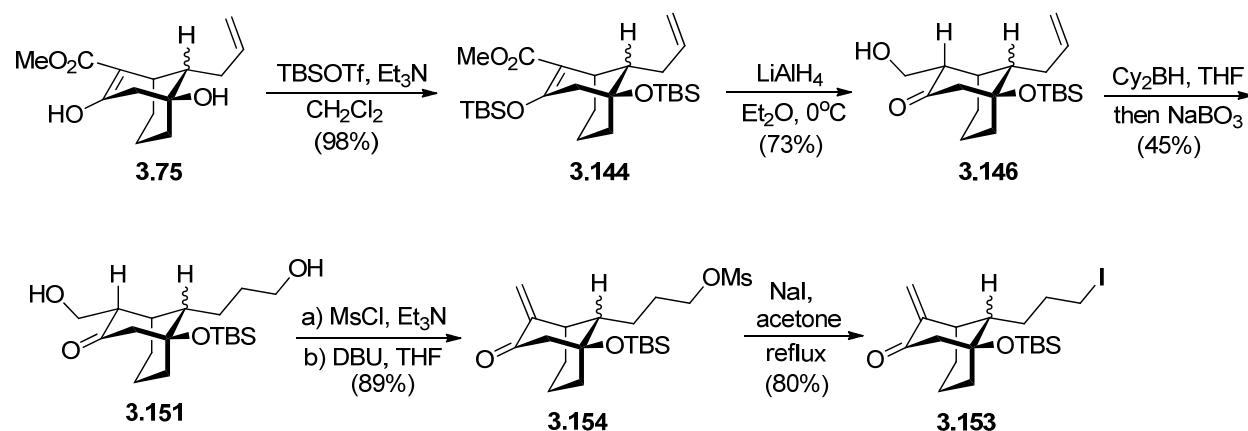
Scheme 3.35 Synthetic Effort to Prepare the Enone Iodide



Scheme 3.36 Self Dimerization of the Bicyclic Enone

It is worth noting that the bicyclic enones (**3.148**, **3.153** and **3.154**) are unstable. Without the presence of any solvent, they will self dimerize at room temperature presumably through a hetero Diels-Alder reaction in a regio- and stereoselective manner (Scheme 3.36). Indeed, this self dimerization of methylene ketone has been reported in the literature.^[29] Besides, this self

dimerization of the bicyclic enone can be prevented by storing the pure compound in a solution rather than neat.



Scheme 3.37 First Generation Synthesis of the Bicyclic Enone Iodide

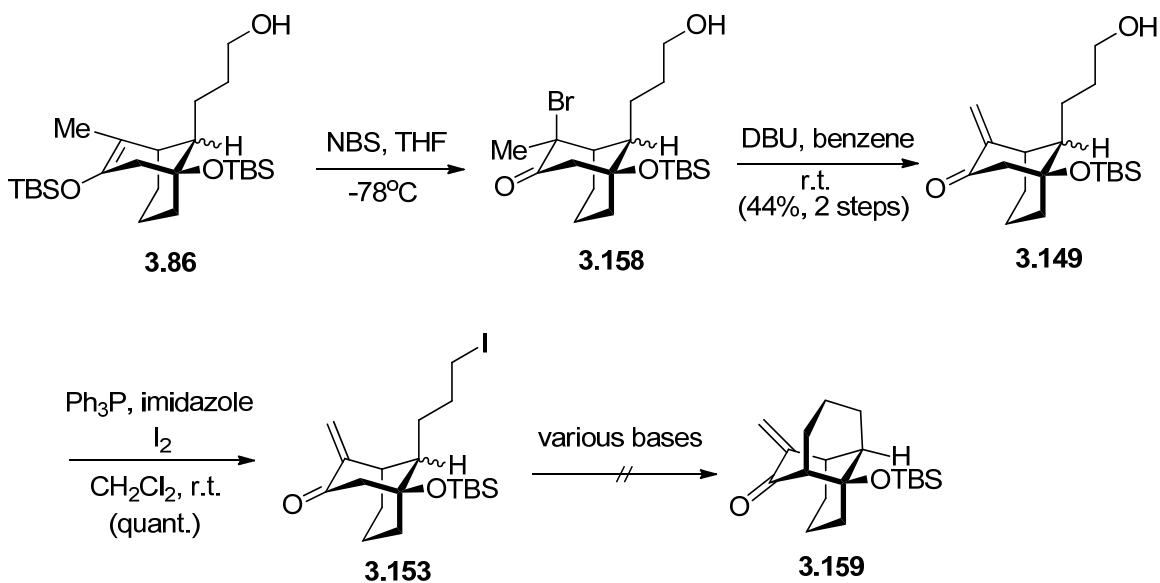
In summary, we have developed a concise route to the bicyclic enone **3.153**, which is a potential precursor of vinigrol (summarized in Scheme 3.37). Key elements of the sequence involve selective reduction of the ester group of β -keto ester by masking the ketone with TBS silyl ether and the sequence of functionalizing the terminal olefin.

3.7.2 An Alternative Route to Prepare the Bicyclic Enone

Although the above route to prepare the bicyclic enone **3.153** is efficient and high yielding, the obtained enone **3.153** is a diastereomeric mixture with the desired isomer as the minor component (ratio = 1:4.3) because we started the synthesis from bicyclo[3.3.1]nonane **3.75**. No epimerization occurred thereafter. Therefore, we developed a second route to access the enone, aiming to obtain the desired diastereomer as the major component. As outlined below (Scheme 3.38), the synthesis was commenced with the previously obtained TBS enol ether **3.86**, which was a 1:1 mixture of the two diastereomers at the bridgehead of bicyclo[3.3.1]nonane system.

This second generation route proved to be fruitful. The enone **3.149** was prepared with a 44% yield by exposure of the silyl enol ether **3.86** to NBS in THF at -78°C , followed by

elimination with DBU. Then, the enone **3.149** was converted to the iodide **3.153** by standard procedure.



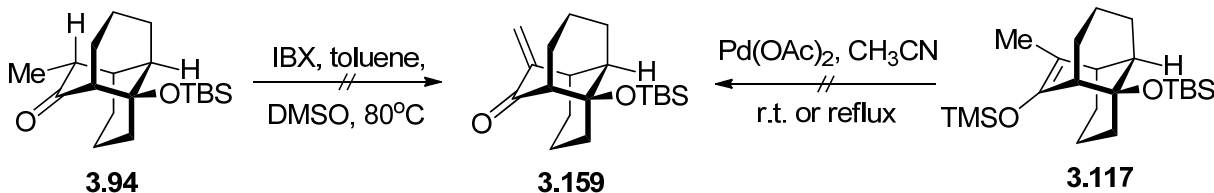
Scheme 3.38 Second Generation Synthesis of the Bicyclic Enone Iodide

Having the iodide **3.153** in hand, our next challenge was to close the third ring. Unfortunately, our preliminary attempts at the cyclization did not afford the desired tricyclic enone product **3.159**. At lower temperature, the starting material **3.153** was recovered, whereas elimination products were identified at higher temperature (Table 3.5). Although **3.153** is a mixture of the diastereomers (1:1 ratio), it is sufficient for us to test the applicability of the reaction. The reluctance of the bicyclic enone to cyclize may be caused by the reduced accessibility or reactivity of the cross-conjugated enolate.

Table 3.5 Attempted Enone Cyclization Reaction Conditions

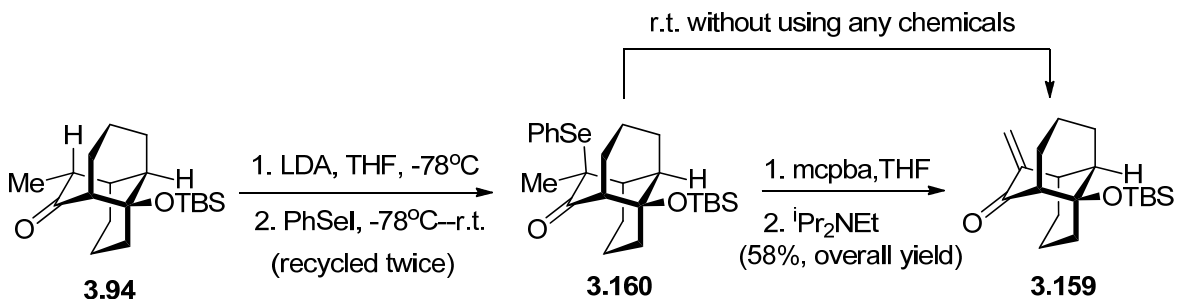
Entry	Reaction Condition	Result
1	KO ^t Bu, THF, 12 hs at 0°C	No reaction
2	LDA, HMPA, THF, 24 hs at 0°C	No reaction
3	LDA, HMPA, THF, 3 hs at r.t.	E2 elimination product formed

3.7.3 Efforts to Prepare the Tricyclic Enone



Scheme 3.39 Attempted Direct Dehydrogenation of the Tricyclic

We, therefore, decided to explore path B, cyclization first followed by elimination to access the tricyclic enone. Initial attempts to effect the direct unsaturation of the ketone **3.94** with IBX in hot DMSO^[25] resulted in multiple spots on TLC, without producing any major products (Scheme 3.39). The alternative route to access the enone by exposure of the corresponding TMS enol ether **3.117** to palladium acetate in acetonitrile^[26] proved unfruitful as well.

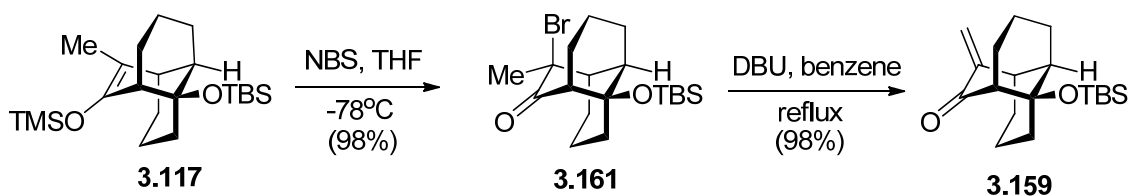


Scheme 3.40 Preparation of the Tricyclic Enone

In an effort to find a viable route to the tricyclic enone, a selenation of the ketone **3.94** followed by an oxidative elimination to introduce the resident olefin was suggested. Thus, the ketone **3.94** was selenated with LDA and PhSeI, which was generated *in situ* by treating diphenyl diselenide with iodine, to afford the selenide **3.160** with approximately 30% conversion (Scheme 3.40). And this was the optimized condition we found (only 20% conversion was observed if PhSeBr was used as the selenating reagent). Due to the low conversion of this step, we recycled the crude product with LDA and PhSeI one more time. The reluctance of **3.94** to undergo selenation may be due to the associated 1,3-diaxial repulsion.

Subsequent oxidation of the selenide **3.160** with *m*-CPBA followed by diisopropyl amine furnished the desired tricyclic enone **3.159** in 58% yield after two cycles of the first step (Scheme 3.40).

It is worth mentioning that **3.160** was found to eliminate to **3.159** at r.t. without any chemical treatment. The release of the steric strain may be the driving force for this elimination. Two possible mechanisms were suggested: either oxidation of **3.160** by air or homocleavage of the carbon-selenium bond via a radical pathway.



Scheme 3.41 An Alternative Route to Prepare the Tricyclic Enone

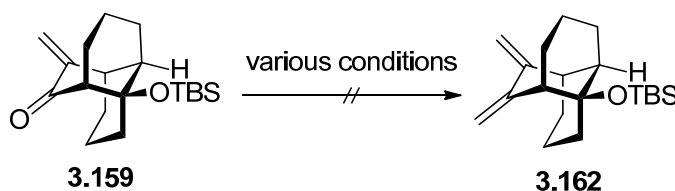
Although **3.159** has been successfully prepared, the above route requires the use of a large excess of very toxic selenium reagent, and the synthesis appears to be tedious (the first step needs to be recycled twice) and low yielding. An alternative route utilizing the previously obtained TMS enol ether **3.117** was explored. The enol ether **3.117** was smoothly converted to the bromide **3.161** by mixing with NBS in THF at -78°C for one hour (Scheme 3.41). The elimination step appears slower than the selenide route. A large excess base DBU (5.0 eq.) was needed, and the temperature was increased to reflux (no reaction was detected at r.t.) for 18 hours. This route to access the enone **3.159** was high yielding and convenient, though it required an additional step to prepare **3.117** from **3.94**.

3.7.4 Efforts to Prepare the Conjugated Diene

With the tricyclic enone **3.159** in hand, efforts were focused on the olefination of **3.159** to provide the conjugated diene **3.162**, the precursor for the electrocyclic ring closure reaction. However, it turns out that the carbonyl group of the enone **3.159** is unreactive. No reaction was

observed under either standard or modified Wittig reaction conditions (Table 3.6, entries 1-2). Decomposed products were detected when **3.159** was treated with deprotonated ylide (entry 3) or Petasis reagent (entry 4). Under Peterson olefination condition, multiple products without olefinic hydrogen (proved by ^1H NMR) were detected, indicating the formation of conjugate addition products (entry 5). This tendency for conjugate addition may be due to the high steric congestion of the enone carbonyl group. In order to minimize this steric issue, we added methyllithium, which is a very small nucleophile, to the reaction. Surprisingly, similar results were observed after **3.159** reacted with methyllithium (entry 6).

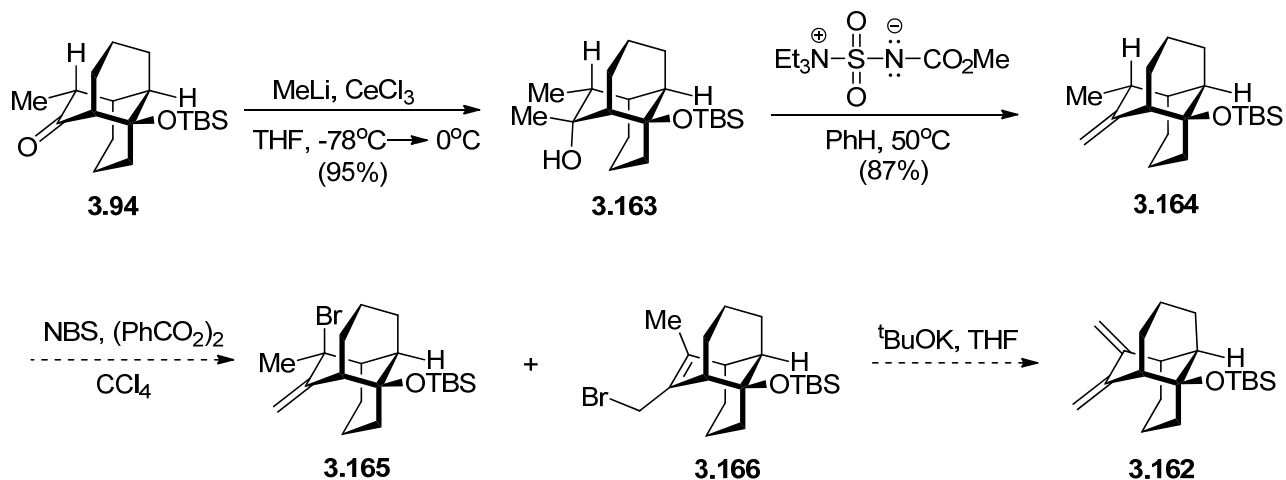
Table 3.6 Attempted Enone Olefination Conditions



Entry	Reaction Conditions	Results
1	$\text{Ph}_3\text{P}=\text{CH}_2$, THF, 0°C	No reaction
2	$\text{Ph}_3\text{P}=\text{CH}_2$, DMSO, 80°C	No reaction
3	$\text{Ph}_3\text{P}=\text{CHLi}$, THF, 0°C	Decomposed
4	Cp_2TiMe_2 , toluene, 65°C	Decomposed
5	TMSCH_2Li , CeCl_3 , THF, 0°C	Multiple products without the desired product
6	MeLi , Et_2O , -78°C	Multiple products including the conjugate addition product but no signs of the desired product

Considering the unreactive nature of the carbonyl group in the tricyclic enone system, we decided to convert this carbonyl group to an alkene earlier in the synthesis. In the event, the ketone **3.94** was smoothly converted to the alcohol **3.163** stereoselectively by mixing **3.94** with

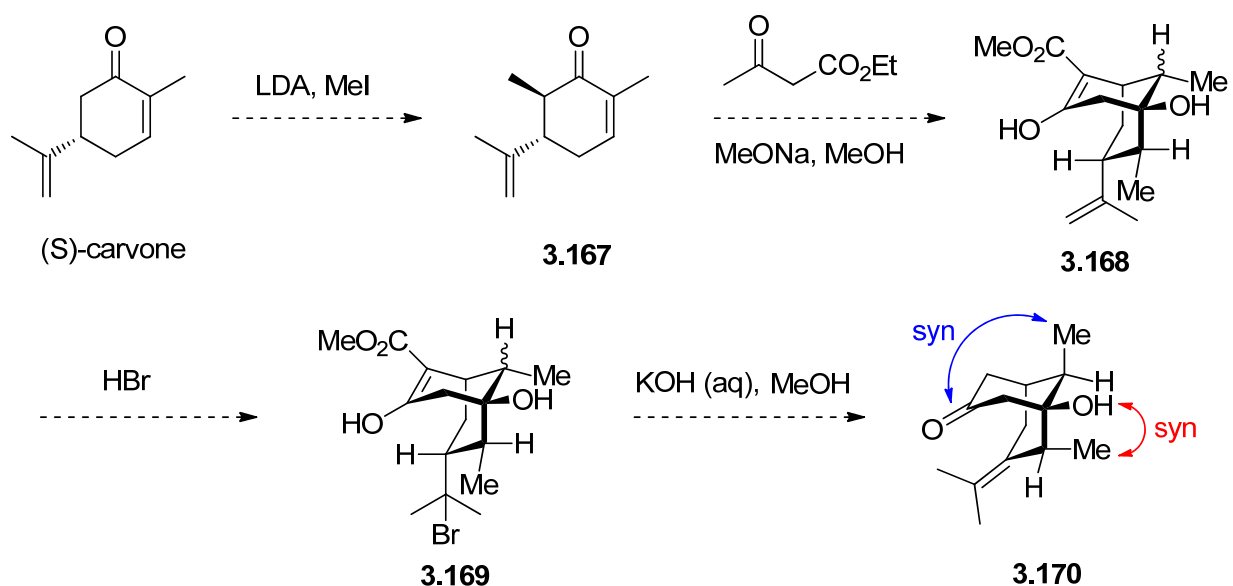
methylolithium in the presence of cerium (III) chloride in THF (Scheme 3.42). Then the alcohol **3.163** underwent a regioselective dehydration reaction to afford the alkene **3.164** by treating **3.163** with Burgess reagent. Next, allylic bromination of **3.164** with NBS will lead to the allylic bromides **3.165** and **3.166**. Subsequent elimination of the allylic bromides mixture will deliver the conjugated diene **3.162**. The last two steps are currently under study in our lab.



Scheme 3.42 Another Potential Route to the Conjugated Diene

3.8 Future Plan

In order to solve the syn relationship between the methyl and hydroxyl group in vinigrol, we come up with a model study as depicted in Scheme 3.43. The commercially available (S)-carvone is methylated to give **3.167**, which is subjected to base catalyzed Robinson annulation to afford **3.168**. Based on our previous experimental studies, **3.168** will be a mixture of diastereomers with the anti product as the major component. Treatment of **3.168** with HBr will afford, after decarboxylation, base catalyzed epimerization and elimination of the bromide in one step, the desired compound **3.170**. The syn relationship between the methyl and hydroxyl group is anticipated because of the unfavored $A^{1,3}$ strain associated with the anti isomer. And the bridgehead methyl group of the [3.3.1] system has to be syn to the carbonyl in order to avoid the 1,3-diaxial repulsion with the other methyl group.

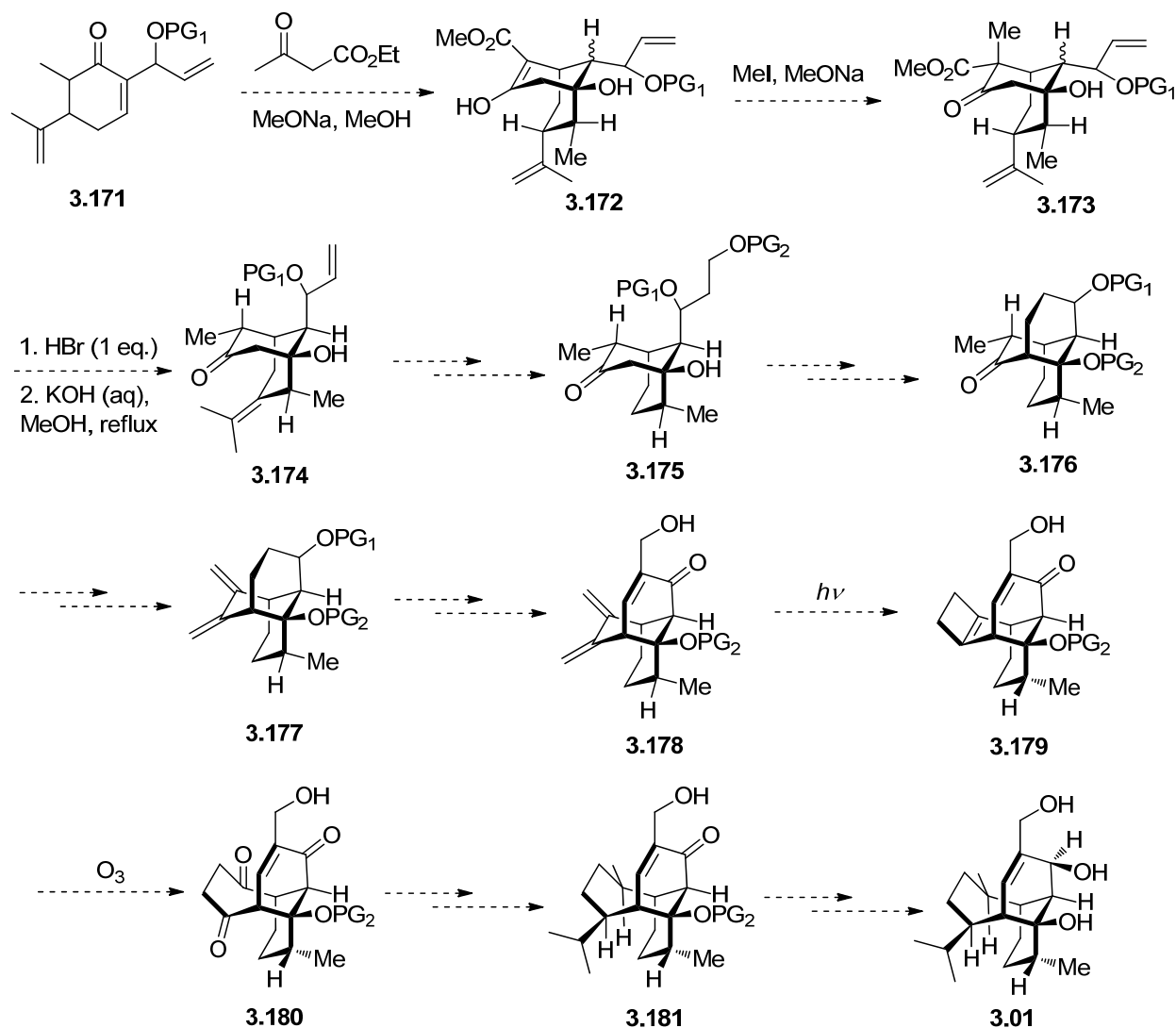


Scheme 3.43 A Model Study on the Stereocenters Formed in [3.3.1] System

If the model study is successful, we can elaborate it to the synthesis of vinigrol. As shown in Scheme 3.44, a Robinson annulation between **3.171** and acetoacetate will give **3.172** as a mixture in favor of the anti isomer. Methylation of **3.172** followed by chemoselective hydrobromination will afford, after decarboxylation, elimination and epimerization in one step, the desired compound **3.174**. Removal of the isopropylidene group will be the next target. Several steps of transformations, including protection of the carbonyl group to a cyclic acetal, chemoselective hydroboration-oxidation of the allyl double bond, protection of the resulting alcohol, ozonolysis of the isopropylidene group, protection of the resulting carbonyl group with thiols, hydrogenolysis of the resulting dithio acetal and deprotection of the cyclic acetal, will furnish **3.175**.

Next, similar transformations as our previous synthesis, containing deprotection of the hydroxyl group, conversion of the alcohol to iodide and alkylation, will secure the tricyclic **3.176**, which could be converted to the conjugated diene **3.177** according to our previous experimental studies. Enone **3.178** can be obtained by deprotection of the hydroxyl group of **3.177**, oxidation,

elimination with IBX and Baylis-Hillman reaction with formaldehyde. Next, an electrocyclic reaction followed by ozonolysis will furnish the diketone **3.180**, which can be transformed to **3.181** through chemoselective Wittig reaction and stereoselective hydrogenation of the resulting double bonds. Finally, deprotection of the hydroxyl group of **3.181** followed by a stereoselective reduction will afford vinigrol.



Scheme 3.44 Potential Synthesis of Vinigrol

3.9 Conclusion

Efforts toward the total synthesis of vinigrol (**3.01**) have been described. It has been realized that vinigrol can be built by two potential pathways starting from the same tricyclic

precursor based on a two-carbon ring expansion strategy. The tricyclic precursor has been efficiently prepared in gram scale utilizing the Robinson annulation, base catalyzed epimerization and intramolecular alkylation as the pivotal steps.

It was hoped that the thermal [2+2] reaction with dichloroketene would generate the bridging eight-membered ring. Unfortunately, this step remains in vain presumably due to steric congestion. We are exploring an alternative route using the tricyclic enone as the electrocyclic reaction precursor. Although the bicyclic enone has been synthesized in high yield via either indirect or direct pathways, the intramolecular cyclization remains elusive.

Finally, the tricyclic enone can be obtained from the tricyclic precursor via either a selenation- or a bromination-elimination sequence. Further transformation involving olefination, electrocyclic reaction and oxidative cleavage to generate the bridging eight-membered ring would complete the synthesis of the vinigrol core.

3.10 Experimental Section

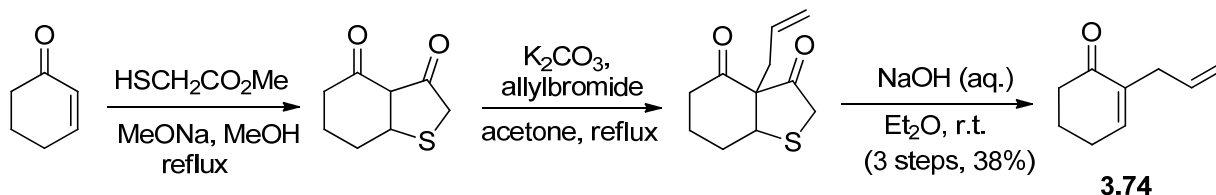
3.10.1 General Considerations

Reactions were carried out in oven or flame-dried glassware under a nitrogen atmosphere, unless otherwise noted. All solvents were freshly distilled and dried by standard techniques just before use. Diethyl ether and THF were distilled from sodium/benzophenone. Methylene chloride (CH₂Cl₂), benzene (PhH), and diisopropylamine were distilled from calcium hydride. Anhydrous pyridine (Py), triethylamine, *N,N*-dimethylformamide (DMF), acetonitrile (MeCN), and dimethyl sulfoxide (DMSO) were purchased from Aldrich and used without purification. *n*-butyllithium (*n*BuLi) was purchased from Aldrich and titrated against 1,3-diphenyl-2-propanone *p*-toluenesulphonylhydrazone prior to use. Trimethylsilyl trifluoromethanesulfonate (TMSOTf) and trimethylsilyl chloride were distilled from calcium hydride. Except as indicated otherwise, all other reagents were purchased from Sigma-Aldrich, Acros, or Cambridge Isotope

Laboratories, Inc. and used as received. Reactions were monitored by thin layer chromatography (TLC) with 0.20-mm pre-coated silica gel plates (aluminum backing, Sorbent Technologies). Spots were detected by viewing under a UV light, putting into an iodine chamber, or coloring with charring after dipping in an anisaldehyde solution composed of acetic acid, sulfuric acid, and methanol. Silica gel for flash chromatography (particle size 0.032-0.063 mm) was supplied by Sorbent Technologies. Yields refer to chromatographically and spectroscopically pure compounds, unless otherwise stated.

^1H NMR spectra was recorded on a Bruker AV-400 (400 MHz ^1H) spectrometer in deuterated solvents using the solvent residual protons as an internal reference (CDCl_3 : 7.26 ppm ^1H) for ^1H NMR or using solvent carbons as an internal reference for ^{13}C NMR (CDCl_3 : 77.00 ppm, t for ^{13}C NMR). Chemical shifts (δ) are given in parts per million down from tetramethylsilane (TMS). Data for ^1H NMR spectra are reported as follows: chemical shift (δ ppm), multiplicity (s = singlet, d = doublet, t = triplet, q = quartet, quin = quintet, dd = doublet of doublets, m = multiplet, br = broad), coupling constant (Hz), and integration. High-resolution mass spectra (HRMS) were recorded on Agilent LC/MS 6210-TOF (Time-Of-Flight) mass spectrometer by electrospray ionization time of flight reflectron experiments.

3.10.2 Preparative Procedures



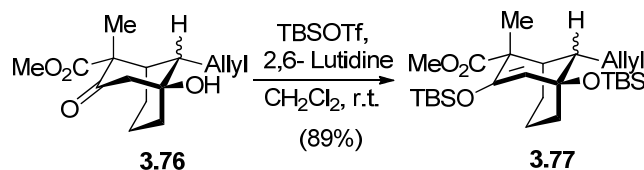
To 440 mL of a freshly prepared sodium methoxide in methanol solution (1.5 M, 0.66 mol) was added 54.9 ml of methyl thioglycolate (0.60 mol) dropwise at 0°C . To the resulting solution was then added a solution of 2-cyclohexen-1-one (58.0 g, 0.60 mol) in 130 ml of methanol. The solution was refluxed overnight. After removal of the solvent, the brown residue

was acidified by 3N HCl and extracted with DCM. The combined organic layers were dried and concentrated to give a reddish oil, which was taken on to the next step without further purification.

To a mechanically stirred solution of the above product in 550 ml of acetone was added potassium carbonate (125.4 g, 0.9 mol) and allyl bromide (78.5 ml, 0.9 mol). The resulting solution was refluxed overnight. The inorganic salts were separated by filtration through sintered glass funnel. The filtrate was concentrated and taken on to the next step without further purification.

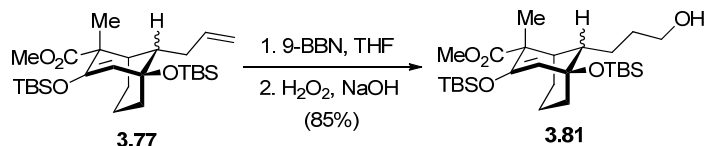
To the above concentrated product was added 608 ml of ether and then 243 ml of a 5.0 M aqueous sodium hydroxide solution at room temperature. After stirring for five hours, the solution was separated. The aqueous layer was extracted with ether (3×200 ml). The combined organic layers were dried (MgSO₄), filtered and concentrated. The crude residue was purified by flash chromatography on silica gel (Hex/EA = 7:1) yielded the titled compound (31.2 g, three steps yield: 38%) as a pale yellow oil. ¹H NMR (400 MHz, CDCl₃): δ 6.72-6.74 (t, J= 4 Hz, 1H), 5.76-5.86 (m, 1H), 5.02-5.06 (m, 2H), 2.94-2.96 (m, 2H), 2.42-2.45 (m, 2H), 2.35-2.37 (m, 2H), 1.96-2.00 (m, 2H).

See **Chapter 2** for the preparation of **3.75** and **3.76**.

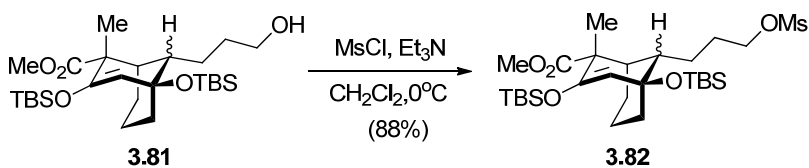


To an ice-cold solution of the ketone **3.76** (1.1 g, 4.13 mmol) in 20 ml of dry CH₂Cl₂ was added 2,6-lutidine (1.77 g, 16.5 mmol) and TBSOTf (2.40 g, 9.09 mmol) sequentially, dropwise and the resulting reaction mixture was stirred at r.t. for 3 hours. Then the mixture was poured into 30 ml of saturated NaHCO₃ at 0°C. The solution was extracted thoroughly with CH₂Cl₂, and

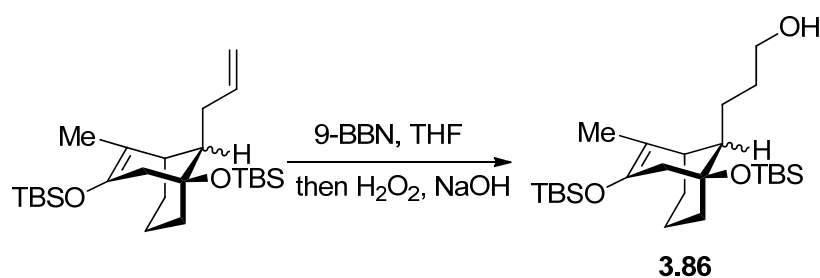
the organic extracts were dried over Na₂SO₄ and filtered. Removal of the solvent under reduced pressure followed by column with hexane as the eluent to give the product **3.77** (1.82 g, 89%) as colorless oil. ¹H NMR (400 MHz, CDCl₃): δ 5.64-5.74 (m, 1H), 4.94-5.03 (m, 2H), 4.72 (s, 1H), 3.63 (s, 3H), 2.54-2.58 (m, 1H), 2.00-2.05 (m, 1H), 1.84-1.89 (m, 3H), 1.30-1.70 (m, 8H), 0.88 (s, 9H), 0.87 (s, 9H), 0.19 (d, J = 4 Hz, 6H), 0.09 (d, J = 4 Hz, 6H).



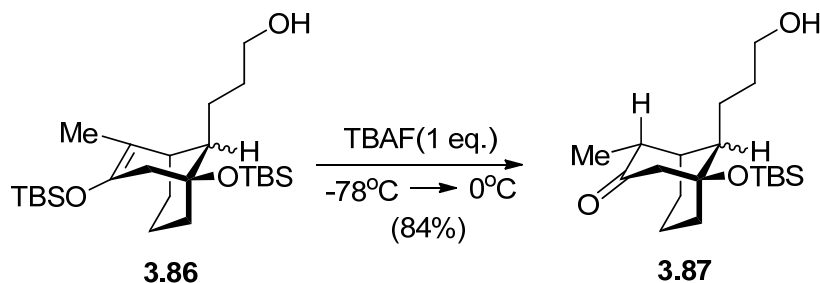
A solution of the substrate **3.77** (0.87 g, 1.76 mmol) in 8.8 ml of THF was cooled to 0 °C, and a solution of 9-BBN in THF (0.5 M, 3.5 ml, 1.76 mmol) was added dropwise under nitrogen. The solution was slowly (about 2 hours) warmed to r.t. and stirred for 3 hours at r.t. (the reaction was judged complete by TLC). The reaction mixture was opened to air and NaOH solution (3 M, 3.5 ml, 10.6 mmol) was added. The mixture was cooled to 0 °C and H₂O₂ (1.5 ml, 30% max., 14 mmol) was added dropwise followed by MeOH (1 ml). The resulting mixture was warmed to r.t. and stirred for an additional 3 hours. Then the organic solvent was moved in vacuo, and the residue was diluted with ethyl acetate and washed with saturated NaHCO₃ and brine. The organic layer was dried over MgSO₄, filtered, concentrated and purified by silica gel chromatography (Hex/EA = 5:1) to give the product (0.77 g, 85%) as colorless oil. ¹H NMR (250 MHz, CDCl₃): δ 4.70 (s, 1H), 3.63 (br s, 5H), 1.60-1.80 (m, 8H), 1.35-1.44 (m, 7H), 0.87 (s, 9H), 0.85 (s, 9H), 0.18 (s, 6H), 0.07 (s, 6H). ¹³C NMR (62.5 MHz, CDCl₃): δ 175.27, 151.89, 111.80, 75.33, 63.04, 53.34, 51.06, 43.64, 42.26, 32.43, 30.88, 25.72, 25.47, 22.95, 22.50, 20.76, 19.85, 18.07, 17.83, -1.99, -2.34, -4.31, -5.40.



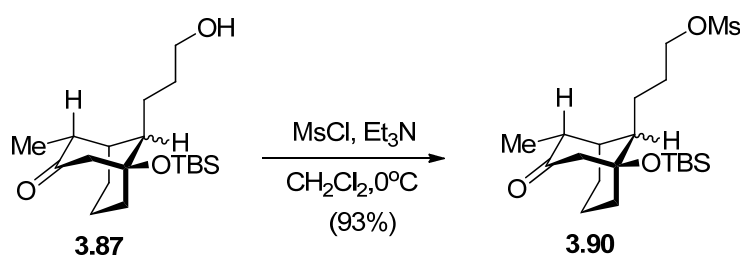
A procedure analogous to that used for **3.77** afforded the product (5.6 g, 89% as using 3.0 g of the SM) as colorless oil. ^1H NMR (400 MHz, CDCl_3): δ 5.72-5.82 (m, 1H), 4.97-5.06 (m, 2H), 2.54-2.57 (m, 1H), 2.23-2.27 (m, 1H), 2.02-2.14 (m, 1H), 1.60-1.70 (m, 2H), 1.50-1.55 (m, 8H), 1.27 (br s, 3H), 0.96 (s, 9H), 0.87 (s, 9H), 0.15 (d, $J = 6$ Hz, 6H), 0.08 (d, $J = 7$ Hz, 6H). ^{13}C NMR (100 MHz, CDCl_3): δ 142.19, 138.78, 115.14, 114.20, 74.31, 48.50, 46.30, 38.49, 36.18, 30.10, 25.86, 19.98, 19.36, 18.24, 18.15, 14.83, -1.80, -1.91, -3.59, -3.85. HRMS (ESI): m/z calcd. for $(\text{C}_{25}\text{H}_{48}\text{O}_2\text{Si}_2+\text{H}^+)$: 437.3266; found: 437.3260.



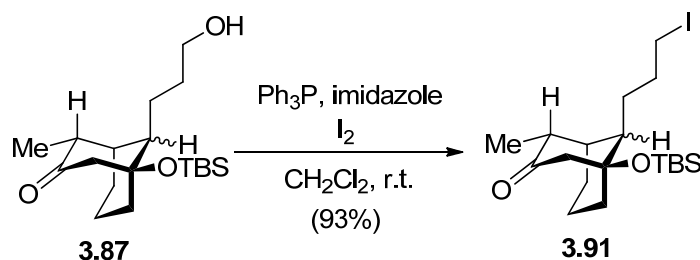
A procedure analogous to that used for **3.81** afforded the alcohol (4.47 g, 99% as using 4.34 g of the SM) as colorless oil. ^1H NMR (400 MHz, CDCl_3): δ 3.60-3.69 (m, 2H), 2.40-2.41 (m, 1H), 2.33-2.37 (m, 2H), 1.40-1.80 (m, 11H), 1.35 (br s, 3H), 0.96 (s, 9H), 0.86 (s, 9H), 0.14 (d, $J = 6$ Hz, 6H), 0.07 (d, $J = 6$ Hz, 6H). ^{13}C NMR (100 MHz, CDCl_3): δ 142.41, 142.26, 114.04, 109.80, 75.17, 74.64, 63.54, 63.49, 49.07, 48.46, 46.53, 43.51, 43.18, 40.99, 39.28, 36.22, 31.54, 31.45, 28.38, 25.90, 25.66, 22.76, 21.21, 20.31, 20.26, 19.33, 18.23, 18.16, 15.25, 14.91, -1.79, -1.83, -3.56, -3.67, -3.85. HRMS (ESI): m/z calcd. for $(\text{C}_{25}\text{H}_{50}\text{O}_3\text{Si}_2+\text{H}^+)$: 455.3371; found: 455.3360.



A procedure analogous to that used for **3.83** afforded the **3.87** (2.8 g, 84% as using 4.47 g of the SM) as colorless oil. ^1H NMR (400 MHz, CDCl_3): δ 3.70 (t, $J = 5$ Hz, 2H), 2.64-2.68 (m, 1H), 2.40-2.58 (m, 2H), 2.37-2.38 (m, 1H), 1.85-1.87 (m, 2H), 1.73-1.76 (m, 2H), 1.45-1.56 (m, 6H), 1.10-1.30 (m, 1H), 1.08 (d, $J = 7$ Hz, 3H), 0.86 (s, 9H), 0.08 (s, 6H). ^{13}C NMR (100 MHz, CDCl_3): δ 212.45, 75.96, 62.96, 57.01, 49.98, 48.92, 40.98, 38.76, 34.85, 31.34, 27.26, 25.72, 21.89, 19.35, 18.84, 18.02, 11.85, -1.91. HRMS (ESI): m/z calcd. for $(\text{C}_{19}\text{H}_{36}\text{O}_3\text{Si}+\text{Na}^+)$: 363.2326; found: 363.2332.

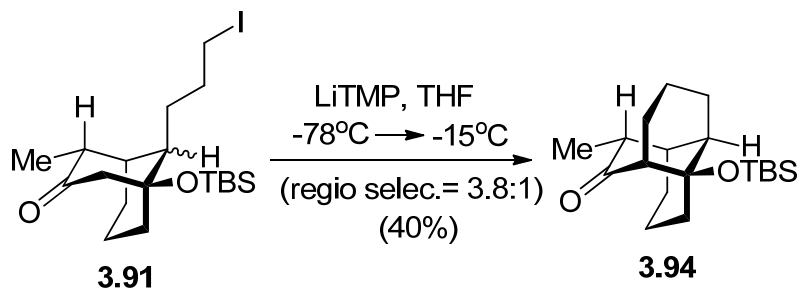


A procedure analogous to that used for **3.82** afforded mesylate **3.90** (1.48 g, 93% as using 1.3 g of the SM) as colorless oil. ^1H NMR (400 MHz, CDCl_3): δ 4.28 (br s, 2H), 3.02 (s, 3H), 2.50-2.69 (m, 2H), 1.70-2.10 (m, 7H), 1.24-1.58 (m, 6H), 1.08 (t, $J = 7$ Hz, 3H), 0.87 (s, 9H), 0.09 (s, 6H).



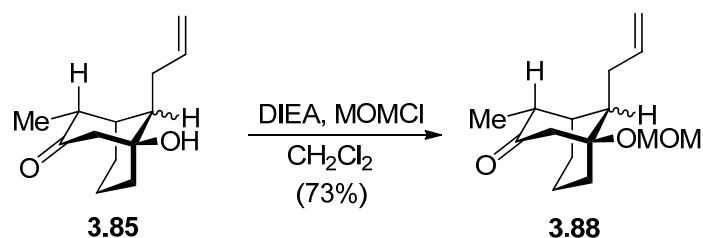
To dry DCM (28 ml) was added in this order: triphenylphosphine (2.18 g, 8 mmol), imidazole (0.56 g, 8 mmol) and iodine (2.11 g, 8 mmol). A solution of the alcohol **3.87** (2.35 g, 7 mmol) in 7 ml of dry DCM was added and the mixture was stirred at room temperature for two hours. Then the solvent was removed in vacuo and the product was purified by passing it through a column (Hex/EA = 20:1) to afford the product **3.91** (2.9 g, 93%) as pale yellow crystalline

solid. ^1H NMR (400 MHz, CDCl_3): δ 3.20-3.26 (m, 2H), 2.65-2.68 (m, 1H), 2.34-2.49 (m, 2H), 2.11-2.15 (m, 1H), 1.96-1.98 (m, 2H), 1.73-1.85 (m, 3H), 1.46-1.56 (m, 4H), 1.22-1.24 (m, 1H), 1.05 (d, $J = 7$ Hz, 3H), 0.88 (s, 9H), 0.09 (s, 6H). ^{13}C NMR (100 MHz, CDCl_3): δ 211.86, 76.48, 51.40, 49.17, 42.65, 41.12, 39.06, 32.01, 27.31, 27.26, 25.89, 20.08, 19.03, 11.94, 6.96, -1.77. HRMS (ESI): m/z calcd. for $(\text{C}_{19}\text{H}_{35}\text{IO}_2\text{Si}+\text{H}^+)$: 451.1524; found: 451.1499.

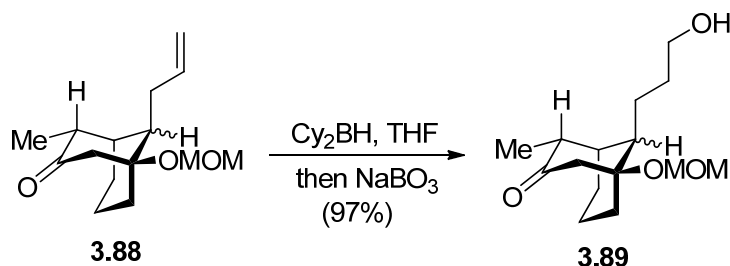


To a solution of dry TMP (1.14 ml, 6.56 mmol) in 7.0 ml of THF was added n butyllithium solution (1.6 M, 4.1 ml, 6.56 mmol) slowly at -78°C under N_2 and increased the temperature to 0°C . After 15 minutes stirring at 0°C , the mixture was cooled to -78°C . A solution of the substrate **3.91** (1.97 g, 4.37 mmol) in 27 ml of THF was added dropwise to the mixture at -78°C , and the resulting mixture was slowly warmed to -15°C during the next one hour, and stirring was continued overnight. Saturated aqueous NH_4Cl (10 ml) was added and diluted with 50 ml of ether, separated. The organic layer was washed with water (2×8 ml), brine (10 ml), dried over MgSO_4 , filtered and concentrated under reduced pressure. The crude product NMR indicated that the ratio of two isomers is around 3.8:1. The residue was purified by column (Hex:EA = 30:1) to give the unreactive isomer **3.91b** (0.80 g) and the desired tricyclic product **3.94** (0.56 g, 40%) as white crystalline solid. ^1H NMR (400 MHz, CDCl_3): δ 2.64-2.70 (m, 1H), 2.40-2.47 (m, 3H), 2.19-2.39 (m, 1H), 1.78-1.83 (m, 3H), 1.58-1.76 (m, 1H), 1.52-1.56 (m, 5H), 1.38-1.42 (m, 1H), 1.23-1.30 (m, 1H), 1.07 (d, $J = 7$ Hz, 3H), 0.92 (s, 9H), 0.11 (d, $J = 7$ Hz, 6H). ^{13}C NMR (100 MHz, CDCl_3): δ 216.76, 75.09, 57.95, 45.48, 44.10, 42.31, 41.47, 28.02, 26.09, 25.64, 24.45,

19.65, 18.65, 18.57, 12.40, -1.59, -1.77. HRMS (ESI): m/z calcd. for $(C_{19}H_{34}O_2Si+H^+)$: 323.2401; found: 323.2396.

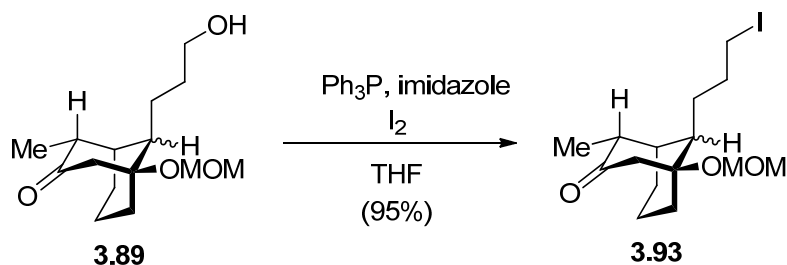


To a stirred solution of the ketone **3.85** (1.23 g, 5.9 mmol) in 100 ml of dichloromethane/diisopropyl ethylamine (1:1) at 0°C was added dropwise MOMCl (4.5 ml, 59 mmol). After stirring 24 hours at r.t., the reaction mixture was diluted with 50 ml of DCM and the organic layer was washed with 50 ml of 3N HCl. The aqueous washes were back extracted with DCM (3×50 ml), and the combined organic layers were washed with brine, dried (MgSO₄), filtered and concentrated. The residue was chromatographed on silica gel (Hex/EA = 10:1) yielded the titled compound (1.08 g, 73%) as pale yellow oil. ¹H NMR (400 MHz, CDCl₃): δ 5.76-5.83 (m, 1H), 5.05- 5.12 (m, 2H), 4.79 (d, J = 7.0 Hz, 1H), 4.70 (d, J = 7.0 Hz, 1H), 3.37 (s, 3H), 2.71-2.79 (m, 1H), 2.60-2.68 (m, 2H), 2.36-2.39 (m, 1H), 2.09-2.22 (m, 2H), 1.48-1.75 (m, 6H), 1.20-1.33(m, 1H), 1.08 (d, J = 7.0 Hz, 3H). HRMS (ESI): m/z calcd. for $(C_{15}H_{24}O_3+Na^+)$: 275.1618; found: 275.1630.



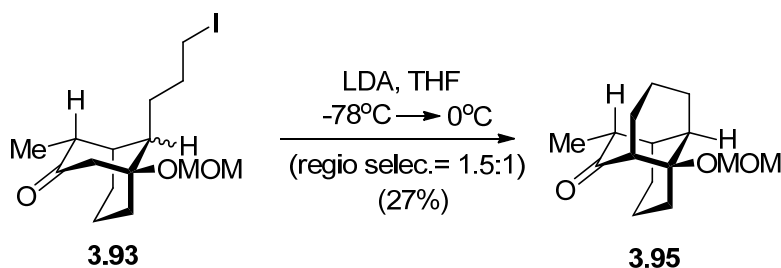
Borane-tetrahydrofuran (1.0 M in THF, 0.46 ml, 0.46 mmol) was placed in a dry, nitrogen-flushed, round-bottomed flask, which was then immersed in an ice-water bath. Cyclohexene (0.093 ml, 0.92 mmol) was added dropwise and the mixture stirred at 0°C for one

hour. The substrate **3.88** (116 mg, 0.46 mmol) in 0.3 ml of THF was then added to the slurry of dicyclohexylborane in THF. The cooling bath was removed and the mixture stirred for two hours at r.t. Oxidation was achieved by adding $\text{NaBO}_3 \cdot 4\text{H}_2\text{O}$ (0.212 g, 1.38 mmol) and water (0.5 ml) and stirring was continued at r.t. for two more hours. The product was extracted into ether (3×3 ml), dried (MgSO_4), filtered and concentrated. The residue was chromatographed on silica gel (Hex/EA = 1:1) yielded the title compound (120 mg, 97%) as colorless oil. ^1H NMR (250 MHz, CDCl_3): δ 4.70 (d, $J = 7.0$ Hz, 1H), 4.64 (d, $J = 7.0$ Hz, 1H), 3.61 (t, $J = 6.0$ Hz, 2H), 3.29 (s, 3H), 2.56-2.65 (m, 3H), 2.32-2.34 (m, 1H), 2.12 (br s, 1H), 1.80-2.00 (m, 1H), 1.63-1.79 (m, 4H), 1.41-1.45 (m, 4H), 1.15-1.19 (m, 1H), 1.01 (d, $J = 6.8$ Hz, 3H). ^{13}C NMR (62.5 MHz, CDCl_3): δ 211.92, 89.94, 78.16, 62.50, 55.17, 53.35, 48.70, 46.65, 38.91, 31.35, 30.80, 21.88, 18.97, 18.65, 12.08. HRMS (ESI): m/z calcd. for $(\text{C}_{15}\text{H}_{26}\text{O}_4 + \text{Na}^+)$: 293.1723; found: 293.1730.

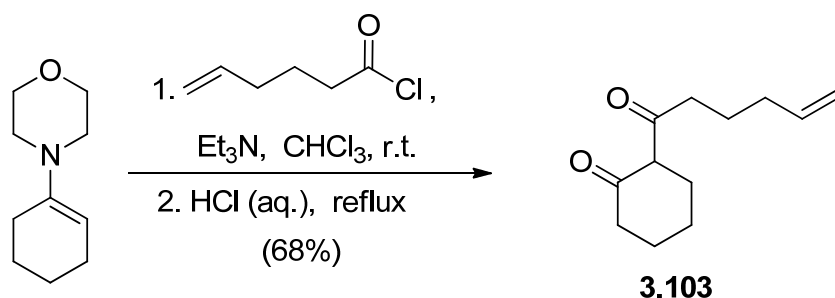


The alcohol **3.89** (94 mg, 0.35 mmol) was dissolved in THF (2.3 ml) and treated with imidazole (59.2 mg, 0.87 mmol) and triphenylphosphine (109.4 mg, 0.42 mmol). The mixture was cooled to 0 °C and iodide (106 mg, 0.42 mmol) was added in two portions (or added portionwise over 10 minutes). The reaction mixture was stirred at 0 °C for two and half hours, warmed to ambient temperature and stirred for an additional one hour. The reaction mixture was quenched with saturated sodium thiosulphate (0.16 ml) and water (0.33 ml) and then stirred for 30 minutes at ambient temperature, poured into water (1.6 ml) and extracted with ethyl acetate (2×3.2 ml). The combined organic layers were dried with MgSO_4 , filtered and concentrated in vacuo. The residue was chromatographed on silica gel (Hex/EA = 5:1) yielded the titled

compound (126 mg, 95%) as colorless oil. ^1H NMR (400 MHz, CDCl_3): δ 4.76 (d, $J = 7.50$ Hz, 1H), 4.70 (d, $J = 7.50$ Hz, 1H), 3.36 (s, 3H), 3.19-3.29 (m, 2H), 2.76 (d, $J = 15.0$ Hz, 1H), 2.65 (d, $J = 15.0$ Hz, 1H), 2.37-2.40 (m, 1H), 2.14 (br s, 1H), 1.86-2.02 (m, 4H), 1.72-1.74 (m, 2H), 1.48-1.54 (m, 4H), 1.21-1.24 (m, 1H), 1.08 (d, $J = 6.8$ Hz, 3H). ^{13}C NMR (100 MHz, CDCl_3): δ 211.57, 90.17, 78.00, 55.42, 53.56, 48.85, 46.64, 39.22, 32.33, 31.55, 27.26, 19.29, 18.79, 12.27, 7.10. HRMS (ESI): m/z calcd. for ($\text{C}_{15}\text{H}_{25}\text{IO}_3 + \text{Na}^+$): 403.0741; found: 403.0737.

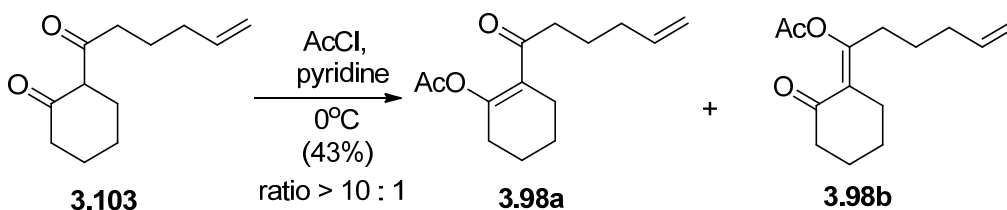


A procedure analogous to that used for **3.94** afforded the unreactive isomer **3.93b** (1.9 g) and the product (0.9 g, 27% as using 5.0 g of the SM) as colorless oil. ^1H NMR (400 MHz, CDCl_3): δ 4.70 (d, $J = 6.80$ Hz, 1H), 4.68 (d, $J = 6.80$ Hz, 1H), 3.35 (s, 3H), 2.69 (t, $J = 6.8$ Hz, 1H), 2.60 (br s, 1H), 2.20-2.28 (m, 3H), 1.92 (br s, 1H), 1.70-1.81 (m, 3H), 1.48-1.59 (m, 5H), 1.35-1.39 (m, 1H), 1.19-1.28 (m, 1H), 1.04 (d, $J = 6.6$ Hz, 3H). ^{13}C NMR (100 MHz, CDCl_3): δ 215.82, 89.76, 76.85, 55.52, 54.88, 45.73, 42.37, 41.32, 36.64, 27.84, 25.43, 24.12, 19.13, 18.66, 12.40. HRMS (ESI): m/z calcd. for ($\text{C}_{15}\text{H}_{24}\text{O}_3 + \text{H}^+$): 253.1798; found: 253.1789.

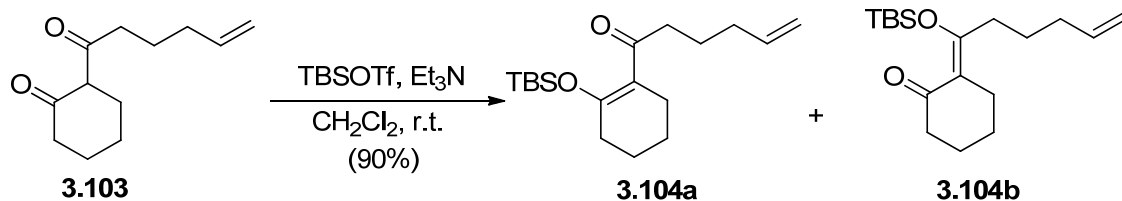


The enamine (1.39 ml, 8.27 mmol) was dissolved in 8.8 ml of dry chloroform and treated with triethyl amine (1.16 ml, 8.32 mmol). To the resulting mixture kept at 40°C was slowly

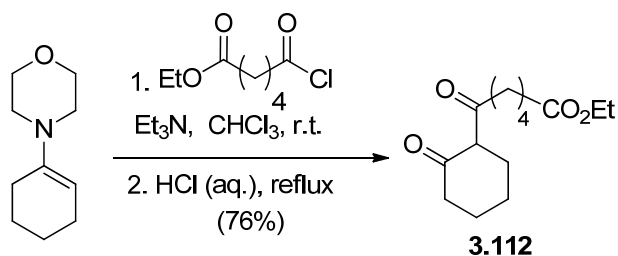
added a solution of 5-hexenoyl chloride (1.0 g, 7.54 mmol) in 6.6 ml of chloroform. After stirring at r.t. for further 12 hours, concentrated aqueous HCl (2.2 ml) and water (1.1 ml) were added. The resulting mixture was refluxed for five hours and the organic phase was washed with water until neutral. The combined aqueous phases were neutralized with aqueous NaOH and re-extracted with chloroform. The combined organic extracts were dried over MgSO₄, filtered and concentrated to leave a residue, which was chromatographed on silica gel (Hex/EA = 15:1) yielded the titled compound (1.0 g, 68%) as pale yellow oil. ¹H NMR (400 MHz, CDCl₃): δ 5.70-5.76 (m, 1H), 4.90-4.99 (m, 2H), 2.35 (t, J = 7.5 Hz, 2H), 2.25-2.26 (m, 4H), 2.01-2.07 (m, 2H), 1.61-1.68 (m, 7H). ¹³C NMR (100 MHz, CDCl₃): δ 201.17, 181.47, 137.98, 115.03, 106.64, 36.02, 33.18, 31.04, 23.71, 23.27, 22.81, 21.62.



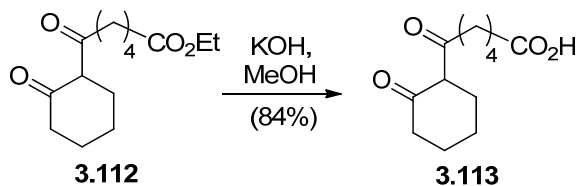
To a cold (0°C) stirred solution of the substrate (138 mg, 0.71 mmol) in dry pyridine (3.4 ml) under nitrogen was added acetyl chloride (0.076 ml, 1.07 mmol), and the resulting mixture was stirred at 0°C overnight. The mixture was poured into ice-cold aqueous HCl, and then extracted with ether. The combined organic extracts were washed with aqueous HCl then brine, dried (Na₂SO₄), filtered and evaporated. The residue was purified by column (Hex/EA = 10:1) to afford an inseparable mixture of **3.98a** and **3.98b** (72 mg, 43%, ratio = 10:1 as indicated by NMR) as colorless oil. Major component: ¹H NMR (400 MHz, CDCl₃): δ 5.73-5.80 (m, 1H), 4.95-5.02 (m, 2H), 2.54 (t, J = 7.4 Hz, 2H), 2.33-2.36 (m, 2H), 2.26-2.29 (m, 2H), 2.17 (s, 3H), 2.05 (q, J = 7.1 Hz, 2H), 1.64-1.72 (m, 7H). ¹³C NMR (100 MHz, CDCl₃): δ 201.01, 168.48, 153.27, 138.20, 125.76, 115.08, 41.45, 33.18, 28.62, 25.06, 22.78, 22.15, 21.73, 21.21.



A procedure analogous to that used for **3.77** afforded an inseparable mixture of **3.104a** and **3.104b** (0.23 g, 90% as using 0.16 g of the SM, ratio = 3.6 :1) as colorless oil. ^1H NMR (400 MHz, CDCl_3): δ 5.74-5.81 (m, 1H), 4.98 (d, $J = 17$ Hz, 1H), 4.92 (d, $J = 9.8$ Hz, 1H), 2.75 (t, $J = 7.5$ Hz, 2H), 2.24 (t, $J = 7.0$ Hz, 2H), 2.19 (t, $J = 7.0$ Hz, 2H), 2.04-2.06 (m, 2H), 1.62-1.70 (m, 4H), 1.52-1.54 (m, 2H), 0.93 (s, 9H), 0.21 (s, 6H). ^{13}C NMR (100 MHz, CDCl_3): δ 202.78, 158.67, 138.66, 117.95, 114.61, 43.16, 33.40, 32.17, 26.03, 24.78, 23.59, 22.96, 22.23, 18.62, -2.82.

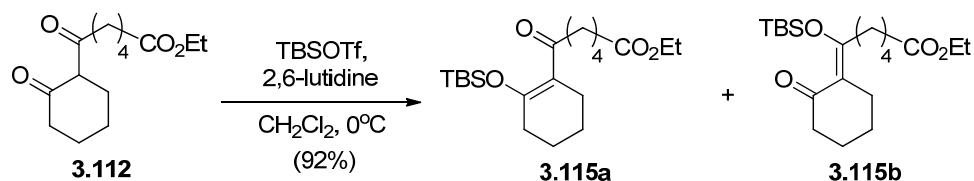


A procedure analogous to that used for **3.103** yielded the titled compound **3.112** (1.06 g, 76% as using 1.06 g of the acyl chloride) as colorless oil. ^1H NMR (400 MHz, CDCl_3): δ 4.06 (q, $J = 7.1$ Hz, 2H), 2.35-2.39 (m, 2H), 2.24-2.28 (m, 6H), 1.79-1.82 (m, 1H), 1.60-1.63 (m, 7H), 1.19 (t, $J = 7.1$ Hz, 3H). ^{13}C NMR (100 MHz, CDCl_3): δ 200.97, 181.43, 173.31, 106.64, 60.18, 36.45, 34.07, 30.99, 24.59, 23.71, 23.57, 22.78, 21.58, 14.17.

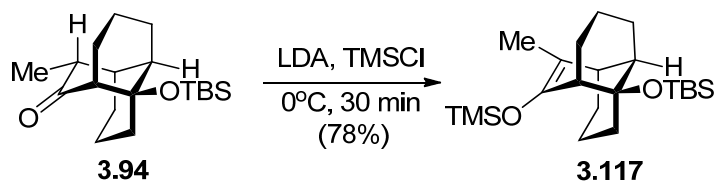


To a solution of the ester (0.186 g, 0.73 mmol) in 1.5 ml of methanol was added 1.5 ml of 1.1 N aqueous KOH. The resulting mixture was refluxed for three hours. After cooling down to

r.t., the methanol was removed under reduced pressure. The resulting aqueous phase was acidified to pH = 0, and extracted with chloroform, dried (MgSO₄), filtered and concentrated to give the product (0.138 g, 84%) as colorless oil. ¹H NMR (400 MHz, CDCl₃): δ 2.34-2.44 (m, 7H), 1.62-1.71 (m, 7H), 1.26-1.36 (m, 2H).

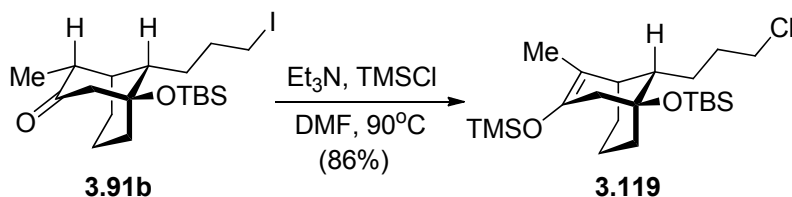


A procedure analogous to that used for **3.77** afforded an inseparable mixture of **3.115a** and **3.115b** (0.206 g, 92% as using 0.154 g of the SM, ratio \approx 5:1 as indicated by ¹H NMR) as colorless oil. Major component: ¹H NMR (250 MHz, CDCl₃): δ 4.13 (q, J = 7.1 Hz, 2H), 2.40-2.45 (t, J = 6.8 Hz, 2H), 2.31-2.33 (m, 6H), 1.65-1.69 (m, 8H), 1.26 (t, J = 7.1 Hz, 3H), 0.92 (s, 9H), 0.10 (s, 6H).

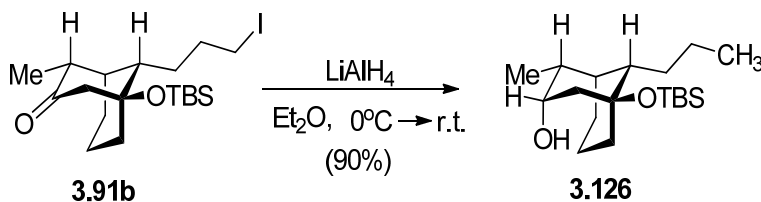


To a solution of dry diisopropylamine (0.12 ml, 0.85 mmol) in 0.85 ml of THF was added ⁿbutyllithium solution (2.5M, 0.34 ml, 0.85 mmol) slowly at -78 °C under N₂ and increased the temperature to 0 °C. After 15 minutes stirring at 0 °C, the mixture was cooled to -40 °C. A solution of the substrate **3.94** (0.249 g, 0.77 mmol) in 3.0 ml of THF was added dropwise to the mixture, followed by the addition of TMSCl (0.11 ml, 0.85 mmol). The temperature was increased to 0 °C and stirred for half an hour, and then partitioned between pentane and saturated aqueous NaHCO₃. The aqueous phase was extracted by pentane two more times. The organic layer was washed with brine, dried over Na₂SO₄, filtered and concentrated. Flash Column (pure hexane) afforded the product **3.117** (0.237 g, 78%) as colorless oil. ¹H NMR (400 MHz, CDCl₃):

δ 2.10 (br s, 1H), 2.00 (s, 3H), 1.75-1.78 (m, 1H), 1.40-1.70 (m, 10H), 1.23-1.30 (m, 3H), 0.91 (s, 9H), 0.21 (s, 9H), 0.10(s, 6H). ^{13}C NMR (100 MHz, CDCl_3): δ 142.20, 112.16, 74.68, 47.94, 44.55, 43.82, 41.64, 28.01, 27.06, 26.12, 22.82, 20.82, 18.58, 16.93, 13.81, 1.02, -1.51, -1.87.

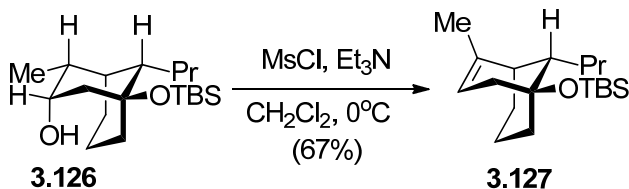


A 15 ml of two-necked round bottom flask was charged with the ketone **3.91b** (220 mg, 0.49 mmol) and anhydrous DMF (2.5 ml). Triethyl amine (0.16 ml, 1.2 mmol) was added, followed by dropwise addition of TMSCl (0.074 ml, 0.59 mmol) under nitrogen. The solution was then warmed to 90°C for eight hours. After cooling to r.t., the mixture was transferred to a separatory funnel, rinsing with 5 ml of hexanes. The organic layer was washed with water (3 \times 1 ml) and brine, dried (MgSO_4), filtered and concentrated. The residue was chromatographed on silica gel (Hex/EA = 20:1) yielded the titled compound (180 mg, 86%) as colorless oil. ^1H NMR (400 MHz, CDCl_3): δ 3.54-3.56 (m, 2H), 2.39 (d, $J = 17.0$ Hz, 1H), 2.24 (d, $J = 17.0$ Hz, 1H), 2.13-2.14 (m, 1H), 1.80-1.95 (m, 2H), 1.62-1.68 (m, 2H), 1.53-1.56 (m, 3H), 1.40-1.48 (m, 4H), 1.17-1.26 (m, 1H), 1.09 (d, $J = 6.8$ Hz, 1H), 0.86 (s, 9H), 0.20 (s, 9H), 0.07-0.09 (m, 6H).

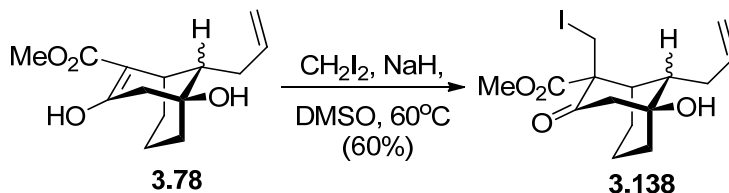


To a cold (0°C) stirred solution of the ketone **3.91b** (310 mg, 0.68 mmol) in anhydrous ether (6.8 ml) is added LAH solution (1.0 M in ether, 0.96 ml, 0.96 mmol) dropwise under nitrogen. The resulting reaction mixture is increased slowly (one hour) to r.t. and stirred at r.t. for two additional hours. The reaction is quenched by 0.05 ml of water, 0.05 ml of 15% NaOH

solution and 0.05 ml of water in this order, dried (MgSO_4), filtered and evaporated. The residue was chromatographed on silica gel (Hex/EA = 20:1) yielded the titled compound (203 mg, 90%) as colorless oil. ^1H NMR (400 MHz, CDCl_3): δ 3.98-4.04 (m, 1H), 2.42-2.47 (m, 1H), 1.94-1.95 (m, 2H), 1.70-1.76 (m, 1H), 1.52-1.68 (m, 3H), 1.44-1.50 (m, 2H), 1.30-1.34 (m, 7H), 1.11-1.20 (m, 2H), 1.00 (d, $J = 7.2$ Hz, 3H), 0.86 (s, 9H), 0.07 (s, 6H).

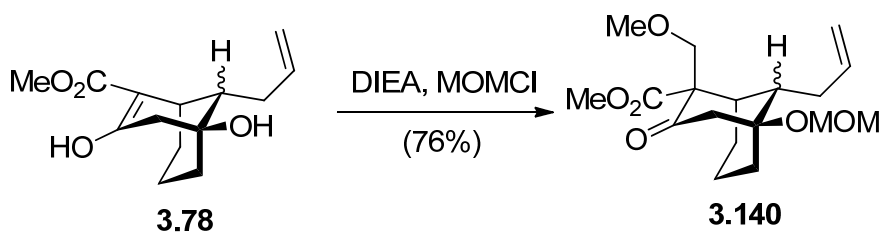


To a stirred solution of the alcohol **3.126** (0.19 g, 0.58 mmol) and Et_3N (0.31 ml, 2.21 mmol) in 1.9 ml of CH_2Cl_2 in an ice bath under nitrogen, was added dropwise MsCl (0.09 ml, 1.16 mmol). The resulting solution was stirred for 1 hour at 0°C , sat. aqueous NH_4Cl (1 ml) was then added and the mixture was extracted with CH_2Cl_2 (3×2 ml). The combined organic phase was washed with brine, dried (MgSO_4) and concentrated to give the crude product, which was purified by flash chromatography (hexanes) to yield the alkene (0.12 g, 67%) as colorless oil. ^1H NMR (400 MHz, CDCl_3): δ 5.34-5.35 (m, 1H), 2.30-2.35 (m, 1H), 2.19-2.23 (m, 2H), 1.71-1.74 (m, 3H), 1.63-1.64 (m, 3H), 1.42-1.52 (m, 7H), 1.21-1.28 (m, 4H), 0.94 (t, $J = 7.1$ Hz, 3H), 0.88 (s, 9H), 0.08 (s, 6H). ^{13}C NMR (100 MHz, CDCl_3): δ 136.70, 121.06, 74.00, 45.89, 44.19, 40.46, 36.67, 27.46, 25.90, 21.76, 21.37, 20.12, 19.48, 18.18, 14.56, -1.74, -1.81.

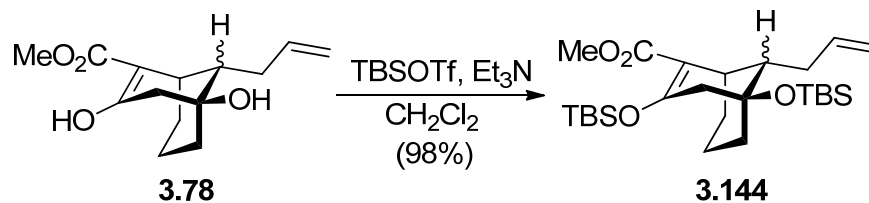


A solution of the substrate **3.78** (219 mg, 0.87 mmol) in DMSO (0.64 ml) was added dropwise to a suspension of NaH (24 mg, 0.96 mmol, 95% purity) in DMSO (1.1 ml), and the reaction mixture was stirred until hydrogen evolution had ceased. Then diiodomethane (0.7 ml,

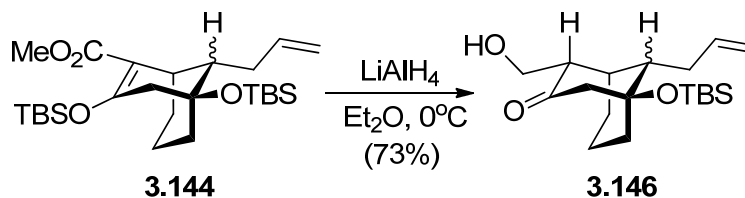
8.7 mmol) was added dropwise and the resulting mixture was warmed to 60 °C and kept stirring for five hours. The reaction was quenched by dropwise addition of water (3.6 ml) and extracted with 10% ether/hexane (3×5 ml). The combined organic layers were washed with brine (4 ml), dried (MgSO₄). The residue was chromatographed on silica gel (Hex/EA = 3:1 to 1:1) yielded the titled compound (204 mg, 60%) as colorless oil. ¹H NMR (400 MHz, CDCl₃): δ 5.78-5.86 (m, 1H), 5.09-5.15 (m, 2H), 3.76 (s, 3H), 3.71 (d, J = 10.6 Hz, 1H), 3.64 (d, J = 10.6 Hz, 1H), 2.37 (s, 1H), 2.16-2.23 (m, 2H), 2.03-2.11 (m, 1H), 1.72-1.82 (m, 1H), 1.39-1.64 (m, 6H), 1.23-1.24 (m, 2H). ¹³C NMR (100 MHz, CDCl₃): δ 201.93, 169.64, 136.48, 117.26, 72.29, 62.68, 54.03, 52.42, 43.34, 42.06, 34.16, 30.55, 22.06, 19.46, 7.44.



To a stirred solution of the substrate **3.78** (0.253 g, 1.0 mmol) in 16.6 ml of dichloromethane/ diisopropyl ethylamine (1:1) at 0°C was added dropwise MOMCl (1.5 ml, 20 mmol). After stirring two days at r.t., the reaction mixture was diluted with 20 ml of DCM and the organic layer was washed with 20 ml of 3N HCl. The aqueous washes were back extracted with DCM (3×20 ml), and the combined organic layers were washed with brine, dried (MgSO₄), filtered and concentrated. The residue was chromatographed on silica gel (Hex/EA = 3:1) afforded the titled compound (0.26 g, 76%) as colorless oil. ¹H NMR (400 MHz, CDCl₃): δ 5.74-5.84 (m, 1H), 5.01-5.11 (m, 2H), 4.76 (d, J = 7.4 Hz, 1H), 4.71 (d, J = 7.4 Hz, 1H), 3.71 (s, 3H), 3.48 (s, 3H), 3.37 (s, 3H), 2.95-2.96 (m, 1H), 2.81 (d, J = 18.0 Hz, 1H), 2.68 (d, J = 18.0 Hz, 1H), 2.50-2.54 (m, 1H), 2.18-2.22 (m, 1H), 1.86-1.89 (m, 1H), 1.39-1.62 (m, 7H), 1.22-1.1.28 (m, 1H).

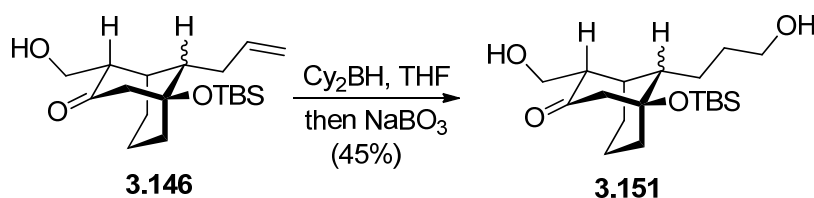


To a solution containing the ketone **3.78** (3.06 g, 12.1 mmol) and TBSOTf (6.1 ml, 26 mmol) in 150 ml of DCM was added dropwise triethyl amine (16.9 ml, 120 mmol). After stirring overnight at r.t., the mixture was hydrolyzed with a saturated NaHCO_3 solution. The mixture was then extracted with DCM and the combined organic layers were dried over MgSO_4 , filtered and concentrated. The residue was chromatographed on silica gel (Hex/EA = 20:1) afforded the titled compound (5.71 g, 98%) as colorless oil. ^1H NMR (400 MHz, CDCl_3): δ 5.74-5.84 (m, 1H), 4.94-5.09 (m, 2H), 3.68 (s, 3H), 2.92 (br s, 1H), 2.50-2.56 (m, 2H), 2.35-2.43 (m, 1H), 2.08-2.24 (m, 1H), 1.70-1.72 (m, 2H), 1.47-1.56 (m, 5H), 0.97 (s, 9H), 0.87 (s, 9H), 0.20 (d, $J = 5.2$ Hz, 6H), 0.08 (d, $J = 6.8$ Hz, 6H).

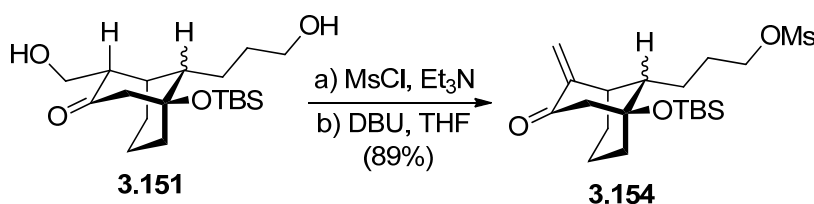


To a stirred cold solution of the substrate **3.144** (5.33 g, 11.1 mmol) in 28 ml of dry ether was added LAH solution (1.0 M in ether, 10.8 ml, 10.8 mmol) dropwise under nitrogen. The reaction mixture was stirred for 1.5 hours at 0°C , diluted with ether (28 ml), and quenched by dropwise addition of water (2.8 ml). The ice-water bath is removed, and the resulting gray suspension is allowed to reach r.t. and the mixture is stirred vigorously for an additional one hour. Then the mixture was diluted with 50 ml of ether. Anhydrous Na_2SO_4 (20 g) was added, the suspension is stirred for 30 minutes, and filtered. The filter cake is washed twice with ether. The solvent is removed under reduced pressure and the residue is purified by column (Hex/EA =

5:1) afforded the titled compound (2.73 g, 73%) as crystalline solid. ^1H NMR (400 MHz, CDCl_3): δ 5.72-5.82 (m, 1H), 5.04-5.09 (m, 2H), 3.97-4.03 (m, 1H), 3.45-3.51 (m, 1H), 2.71-2.80 (m, 1H), 2.65-2.69 (m, 2H), 2.51-2.57 (m, 2H), 2.29 (br s, 1H), 2.10-2.20 (m, 1H), 1.90-1.93 (m, 1H), 1.72-1.79 (m, 1H), 1.52-1.56 (m, 3H), 1.27-1.31 (m, 1H), 1.11-1.14 (m, 1H), 0.86 (s, 9H), 0.089 (d, $J = 5.4$ Hz, 6H). ^{13}C NMR (100 MHz, CDCl_3): δ 214.02, 137.29, 116.19, 75.29, 61.78, 57.19, 55.75, 48.90, 35.23, 34.60, 30.02, 25.62, 19.62, 19.47, 17.97, -1.98.



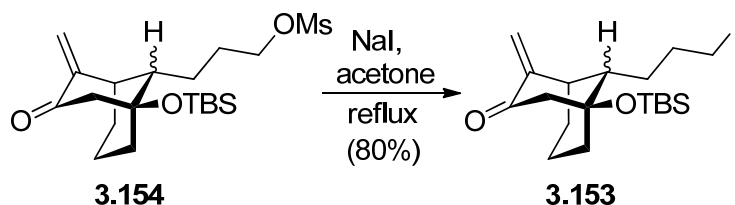
A procedure analogous to that used for **3.89** afforded the diol **3.151** (1.18 g, 45% as using 2.48 g of the SM) as colorless oil. ^1H NMR (400 MHz, CDCl_3): δ 4.00 (dd, $J_1 = 8.1$ Hz and $J_2 = 11.3$ Hz, 1H), 3.63-3.67 (m, 2H), 3.48 (dd, $J_1 = 4.3$ Hz and $J_2 = 11.3$ Hz, 1H), 2.64 (d, $J = 15.4$ Hz, 1H), 2.50-2.54 (m, 2H), 2.29 (s, 1H), 1.81-1.88 (m, 3H), 1.67-1.76 (m, 3H), 1.46-1.55 (m, 7H), 0.84 (s, 9H), 0.071 (d, $J = 3.8$ Hz, 6H). ^{13}C NMR (100 MHz, CDCl_3): δ 214.05, 75.78, 63.12, 61.81, 57.30, 55.86, 49.49, 36.05, 34.76, 31.33, 25.76, 21.63, 20.03, 19.58, 18.10, -1.83.



At 0°C , triethyl amine (1.85 ml, 13.2 mmol) was added to a solution of the diol **3.151** (0.788 g, 2.2 mmol) in 28 ml of dry DCM followed by dropwise addition of MsCl (0.69 ml, 8.8 mmol). The reaction mixture was slowly allowed to warm to r.t. in half an hour and then stirred at r.t. for 10 minutes. Sat. aqueous NH_4Cl solution (4.5 ml) was then added, and the mixture was then separated. The aqueous phase was extracted by DCM (2×10 ml) and the combined organic

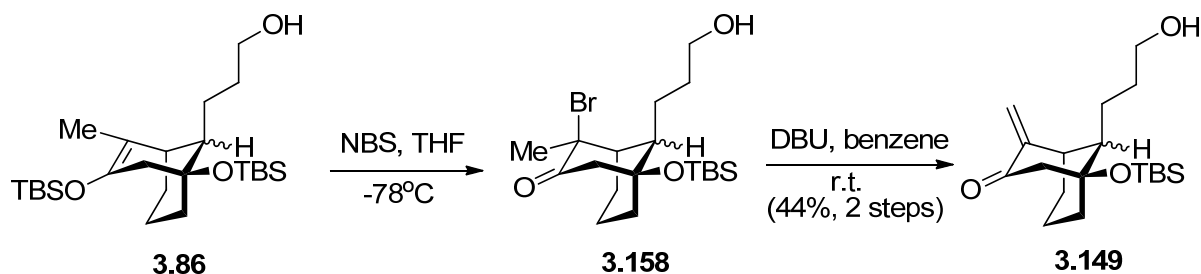
phase was dried over MgSO_4 , filtered and concentrated to give the dimesylate along with some inorganic salts.

DBU (0.7 ml, 4.7 mmol) was added to a solution of the dimesylate in 11 ml of THF at r.t. (yellow ppt. formed immediately). After being stirred at r.t. for 3 hours, the mixture was diluted with 50 ml of ethyl acetate and washed with 10 ml of 1N HCl and brine, dried over MgSO_4 , filtered and concentrated. Flash column chromatography on silica gel (Hex/EA = 3:1) of the residue afforded the product (0.82 g, 89%) as colorless oil. ^1H NMR (400 MHz, CDCl_3): δ 5.91 (s, 1H), 5.20 (s, 1H), 4.20-4.23 (m, 2H), 2.98 (s, 3H), 2.78-2.84 (m, 1H), 2.48-2.52 (m, 1H), 1.80-2.00 (m, 3H), 1.58-1.78 (m, 7H), 1.20-1.24 (m, 3H), 0.83 (s, 9H), 0.07 (s, 9H). ^{13}C NMR (100 MHz, CDCl_3): δ 199.70, 148.61, 121.16, 74.50, 69.95, 56.34, 46.89, 40.39, 37.38, 34.89, 27.92, 26.34, 25.77, 21.90, 19.32, 18.09, -1.84.



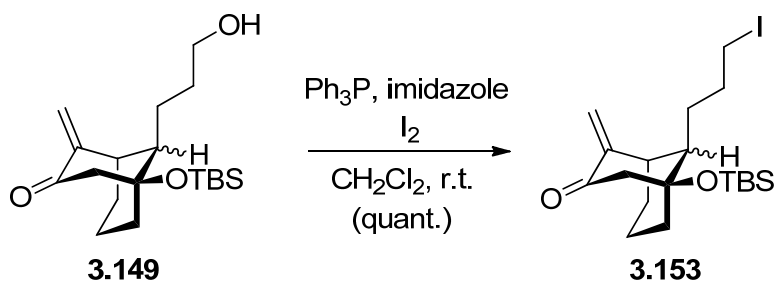
Sodium iodide (0.589 g, 3.9 mmol) was added to a solution of the mesylate (82 mg, 0.2 mmol) in 10 ml of acetone at r.t., and the resulting mixture was heated to reflux for 3 hours. The solution was cooled down to r.t. and the acetone was removed under vacuum. The residue was taken up in ether and water. The ethereal portion was washed with sat. sodium bisulfate solution and brine, dried (MgSO_4), filtered and concentrated to afford the crude product, which was purified by flash column on silica gel (Hex/EA = 20:1) to give the iodide (71 mg, 80%) as white crystalline solid. ^1H NMR (400 MHz, CDCl_3): δ 5.91 (s, 1H), 5.19 (s, 1H), 3.18-3.21 (m, 2H), 2.79 (d, $J = 17.9$ Hz, 1H), 2.47-2.54 (m, 1H), 1.80-1.95 (m, 2H), 1.73-1.78 (m, 4H), 1.45-1.60 (m, 4H), 1.18-1.22 (m, 4H), 0.84 (s, 9H), 0.08 (s, 6H). ^{13}C NMR (100 MHz, CDCl_3): δ 199.81,

148.73, 121.04, 74.48, 56.39, 46.45, 40.52, 34.90, 32.19, 26.99, 26.43, 25.87, 19.39, 18.12, 7.05, -1.76.

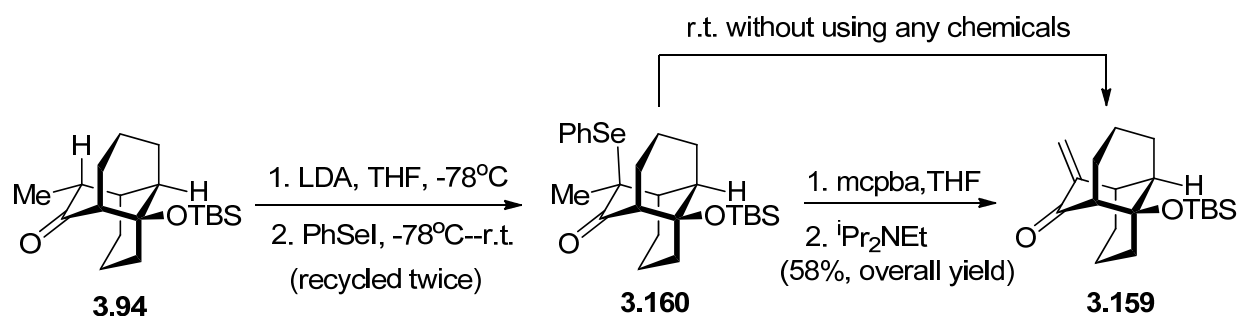


To a cold (-78°C) stirred solution of the substrate (3.09 g, 6.8 mmol) in 34 ml of dry THF was added a solution of NBS (1.451 g, 8.2 mmol) in 34 ml of dry THF under nitrogen, and the resulting mixture was stirred at -78°C for three hours. The mixture was then warmed to r.t. and poured into a separatory funnel containing ether. The mixture was washed with sat. NaHCO₃ solution and brine, dried (MgSO₄) and filtered to afford the bromide **3.158**.

DBU (1.6 ml, 10.7 mmol) was added to a solution of the bromide in 50 ml of benzene at r.t. (yellow ppt. formed immediately). After being stirred at r.t. for one hour, saturated aqueous NH₄Cl solution was added and the mixture was extracted with ether. The combined organic extracts were washed with brine, dried over Na₂SO₄, filtered and concentrated. Flash column chromatography on silica gel (Hex/EA = 3:1) of the residue afforded the product (1.0 g, 44%) as colorless oil. ¹H NMR (400 MHz, CDCl₃): δ 5.93-6.04 (m, 1H), 5.21-5.37 (m, 1H), 3.63-3.71 (m, 2H), 2.80-2.96 (m, 1H), 2.50-2.59 (m, 1H), 1.88-1.93 (m, 1H), 1.53-1.67 (m, 9H), 1.24-1.27 (m, 3H), 0.86-0.92 (m, 9H), 0.09-0.20 (m, 6H).



A procedure analogous to that used for **3.91** afforded the iodide **3.153** (1.3 g, 100% as using 1.0 g of the SM) as pale yellow oil.

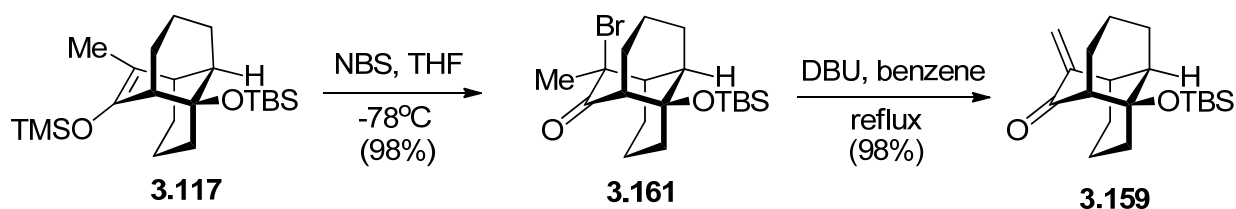


To the freshly prepared solution of LDA (1.86 mmol) in 1.8 ml of dry THF was added a solution of the substrate (0.3 g, 0.93mmol) in 1.0 ml of dry THF dropwise at -78°C under nitrogen. After 15 minutes stirring at -78°C , a solution of the PhSeI [this is made by adding iodine (1.63 g, 6.4 mmol) to a solution of Ph_2Se_2 (2.0 g, 6.4 mmol) in 5.0 ml of THF, stirring at r.t. for 15 minutes] was introduced and the resulting reaction mixture was warmed to r.t. and stirred overnight. Saturated aqueous NH_4Cl was added, and the mixture was extracted with ether. The combined organic extracts were dried (MgSO_4), filtered and concentrated to leave a residue which was purified by column chromatograph on silica gel (pure hexanes to Hex/EA = 40:1) to give a mixture of the selenide **3.160** and the unreactive starting material **3.94** (ratio $\approx 1:1$), which was recycled in the same reaction again.

To a cold (0°C) stirred solution of the selenide in 10 ml of chloroform was added *m*-CPBA (0.428 g, 1.9 mmol). The reaction mixture was stirred at 0°C for 15 minutes and then treated with diisopropyl ethyl amine (0.5 ml, 2.9 mmol) and increased to r.t. After 20 minutes, the mixture was diluted with 20 ml of ether. The organic layer was washed with a saturated aqueous solution of $\text{Na}_2\text{S}_2\text{O}_3$ (10 ml), saturated aqueous solution of NaHCO_3 (10 ml), dried over MgSO_4 , filtered and concentrated. The crude residue was chromatographed on silica gel (Hex/EA = 40:1) yielded the enone **3.159** (0.175 g, two steps yield: 58%) as colorless oil. ^1H

NMR (400 MHz, CDCl₃): δ 5.93 (s, 1H), 5.14 (s, 1H), 2.89 (s, 1H), 2.52 (s, 1H), 2.27-2.39 (m, 2H), 1.43-1.82 (m, 9H), 1.25-1.32 (m, 3H), 0.91 (s, 9H), 0.11 (d, J = 5.5 Hz, 6H). ¹³C NMR (100 MHz, CDCl₃): δ 204.96, 149.89, 118.66, 74.74, 57.08, 44.06, 43.97, 41.38, 36.44, 26.96, 26.65, 26.13, 19.87, 18.67, 17.18, -1.53, -1.75.

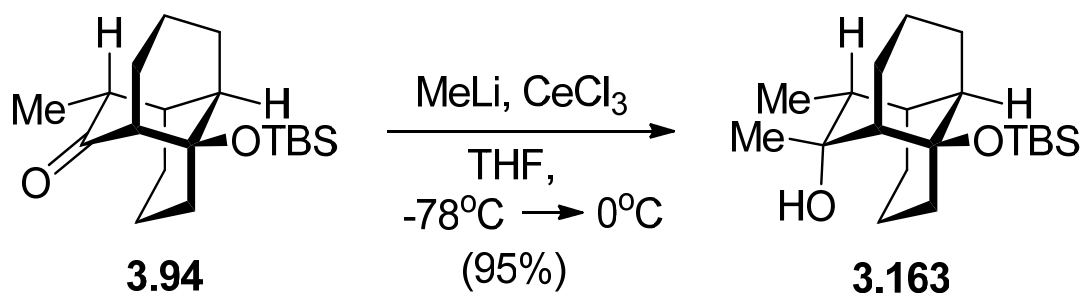
An alternative way to prepare the enone **3.159** is to leave the selenide **3.160** without any solvent at r.t. for two days, after which a flash column is applied to purify the product. A similar yield of **3.159** was identified.



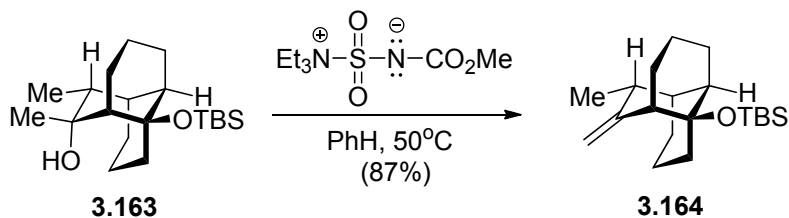
To a cold (-78°C) stirred solution of the substrate (0.21 g, 0.53 mmol) in 3 ml of dry THF was added a solution of NBS (0.47 g, 2.7 mmol) in 5 ml of dry THF under nitrogen, and the resulting mixture was stirred at -78°C for one hour. The mixture was then warmed to r.t. and poured into a separatory funnel containing ether. The mixture was washed with sat. NaHCO₃ solution and brine, dried (MgSO₄), filtered and concentrated. The crude residue was chromatographed on silica gel (Hex/EA = 40:1) yielded the bromide **3.161** (0.21 g, 98%). ¹H NMR (400 MHz, CDCl₃): δ 2.66-2.67 (m, 1H), 2.52-2.54 (m, 1H), 2.30-2.47 (m, 3H), 2.00-2.06 (m, 4H), 1.72-1.99 (m, 5H), 1.51-1.56 (m, 2H), 1.24-1.33 (m, 2H), 0.91 (s, 9H), 0.12 (d, J = 9.7 Hz, 6H). ¹³C NMR (100 MHz, CDCl₃): δ 211.43, 75.05, 58.68, 55.97, 49.08, 43.20, 41.16, 31.60, 29.06, 27.28, 26.02, 23.61, 19.33, 18.58, 15.19, -1.58, -1.77.

DBU (0.41 ml, 2.7 mmol) was added to a solution of the bromide (0.21 g, 0.52 mmol) in 5.5 ml of benzene at r.t. and the resulting mixture was heated to reflux for 18 hours. After cooled down to r.t., saturated aqueous NH₄Cl solution was added and the mixture was extracted with ether. The combined organic extracts were washed with brine, dried over Na₂SO₄, filtered and

concentrated. Flash column chromatography on silica gel (Hex/EA = 40:1) of the residue afforded the product (0.16 g, 98%) as colorless oil.



To a dry flask was added $\text{CeCl}_3 \cdot 7\text{H}_2\text{O}$ (3.67 g, 9.86 mmol) and a stir bar. The flask was placed under high vacuum and temperature was raised to 120-140 °C for one hour and then at 140-160 °C for two hours. The flask was then allowed to cool to r.t. and 18 ml of dry THF was added. After being mixed for 30 minutes, the slurry was cooled to -78 °C and MeLi solution (1.6 M, 5.5 ml, 8.80 mmol) was added dropwise and with vigorous stirring. After stirring for 15 minutes at -78 °C, the brown slurry was warmed to 0 °C and the ketone **3.94** (0.64 g, 1.97 mmol) in 7 ml of dry THF was added dropwise. The reaction was stirred at 0 °C for two hours. The workup was effected by adding TMEDA (1.5 ml, 9.86 mmol) and allowing the mixture to stir for 15 minutes. The solution was poured into saturated aqueous NaHCO_3 and DCM. The organic layer was separated and the aqueous layer was extracted by DCM three times. The combined organic layers were dried over Na_2SO_4 , filtered and concentrated in vacuo. Flash column chromatography on silica gel (Hex/EA = 20:1) of the residue afforded the product (0.64 g, 95%) as colorless oil. ^1H NMR (400 MHz, CDCl_3): δ 2.44-2.49 (m, 1H), 2.18-2.32 (m, 2H), 2.00-2.04 (m, 1H), 1.81-1.84 (m, 2H), 1.66-1.74 (m, 2H), 1.54-1.57 (m, 2H), 1.38-1.45 (m, 5H), 1.26-1.28 (m, 5H), 1.07 (s, 1H), 0.96 (d, $J = 7.2$ Hz, 3H), 0.91 (s, 9H), 0.11 (d, $J = 5.4$ Hz, 6H). ^{13}C NMR (100 MHz, CDCl_3): δ 76.07, 74.90, 52.72, 45.42, 44.05, 41.04, 39.66, 30.81, 27.85, 26.58, 26.27, 23.66, 20.00, 18.92, 12.03, -1.32, -1.61.



The alcohol **3.163** (0.64 g, 1.87 mmol) in 6 ml of dry benzene was added dropwise to a solution of Burgess reagent (0.63 g, 2.64 mmol) in 4 ml of dry benzene at r.t. under nitrogen. After the addition was complete, the temperature was raised to 50°C and maintained for one hour. After cooled down to r.t., water (4 ml) was added and the benzene layer was separated. The water layer was extracted with ether twice and the ether phase was combined with benzene, dried over MgSO₄, filtered and concentrated in vacuo. Flash column chromatography on silica gel (pure hexane) of the residue afforded the product (0.53 g, 87%) as colorless oil. ¹H NMR (400 MHz, CDCl₃): δ 4.67 (s, 1H), 4.60 (s, 1H), 2.85-2.87 (m, 1H), 2.27-2.45 (m, 3H), 1.68-1.89 (m, 7H), 1.34-1.55 (m, 3H), 1.22- 1.28 (m, 3H), 1.10 (d, J = 6.6 Hz, 3H), 0.92 (s, 9H), 0.12 (s, 6H). ¹³C NMR (100 MHz, CDCl₃): δ 159.00, 106.16, 75.08, 51.82, 44.88, 44.51, 42.26, 35.64, 31.60, 29.86, 28.90, 26.20, 21.51, 19.62, 16.20, 14.12, -1.50, -1.61.

3.10.3 Spectral Data

Spectral data are shown from the next page.

3.11 References

- [1] a) I. Uchida, T. Ando, N. Fukami, K. Yoshida, M. Hashimoto, T. Tada, S. Koda and Y. Morimoto, *J. Org. Chem.* **1987**, *52*, 5292-5293; b) T. Ando, Y. Tsurumi, N. Ohata, I. Uchida, K. Yoshida and M. Okuhara, *J. Antibiot.* **1988**, *41*, 25-30; c) T. Ando, K. Yoshida and M. Okuhara, *J. Antibiot.* **1988**, *41*, 31-35.
- [2] D. B. Norris, Depledge, P., Jackson, A. P. WO 9107953 (Ed. P. I. Appl.), **1991**.
- [3] H. Nakajima, Yamamoto, N., Kaisi, T. JP 07206668 (Ed. J. K. T. Koho), Japan, **1995**.
- [4] S. N. Goodman. Ph.D. Thesis, Harvard University, **2000**.
- [5] M. Akhtar and J. N. Wright, *Nat. Prod. Rep.* **1991**, *8*, 527-551.

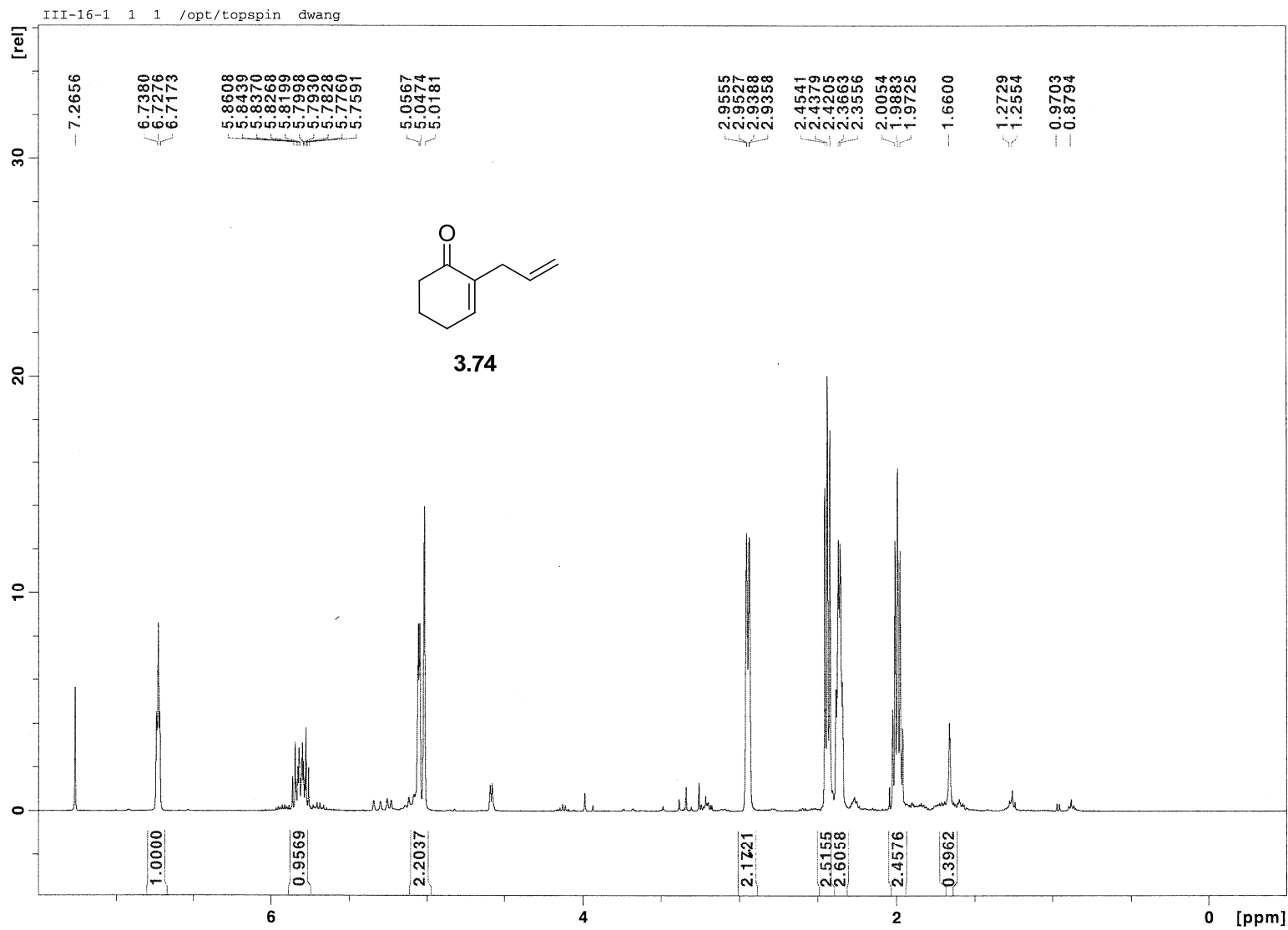


Figure 3.4 ^1H NMR (400 MHz, CDCl_3) of Compound 3.74

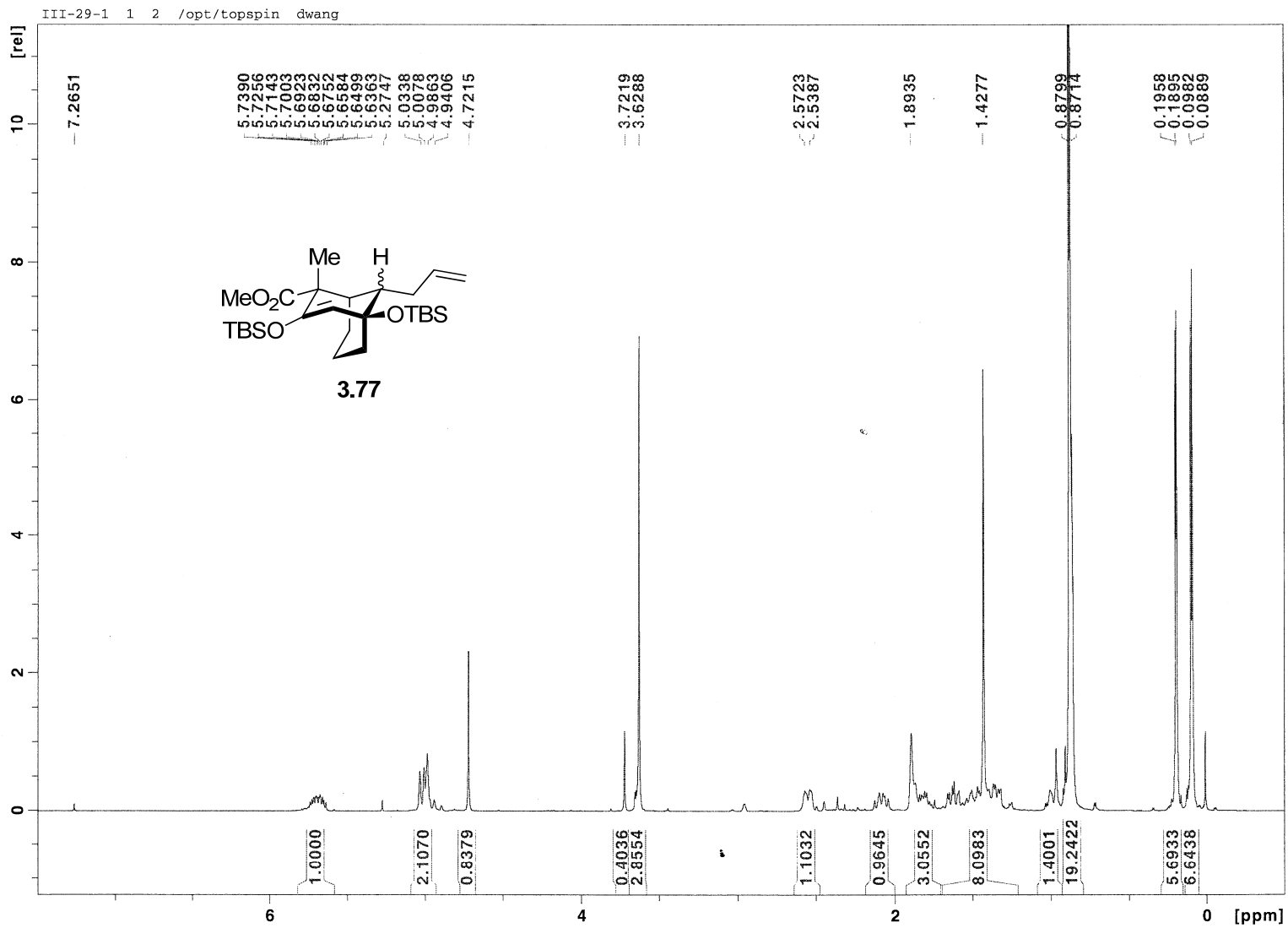


Figure 3.5 ^1H NMR (400 MHz, CDCl_3) of Compound 3.77

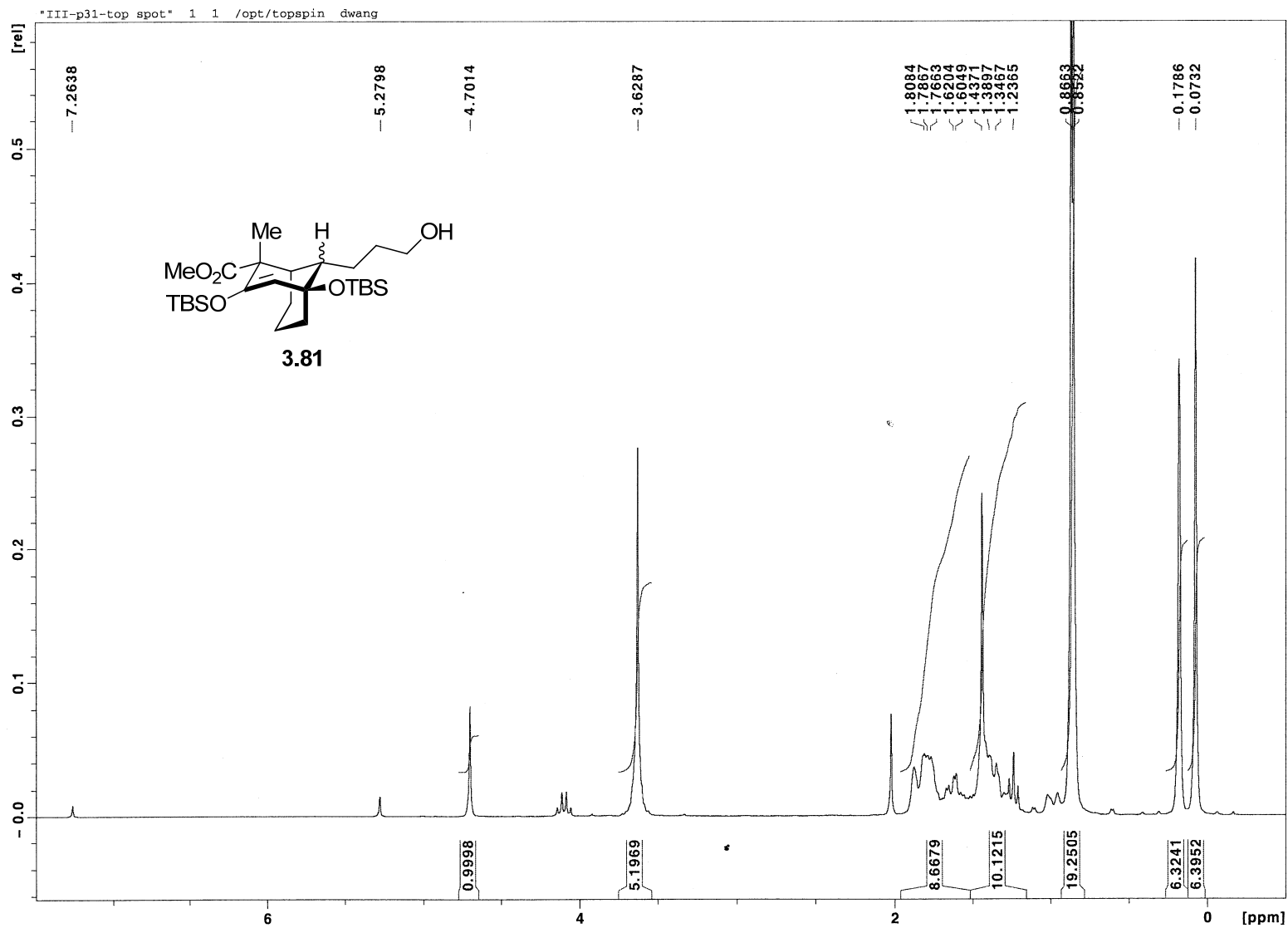


Figure 3.6 ¹H NMR (400 MHz, CDCl₃) of Compound 3.81

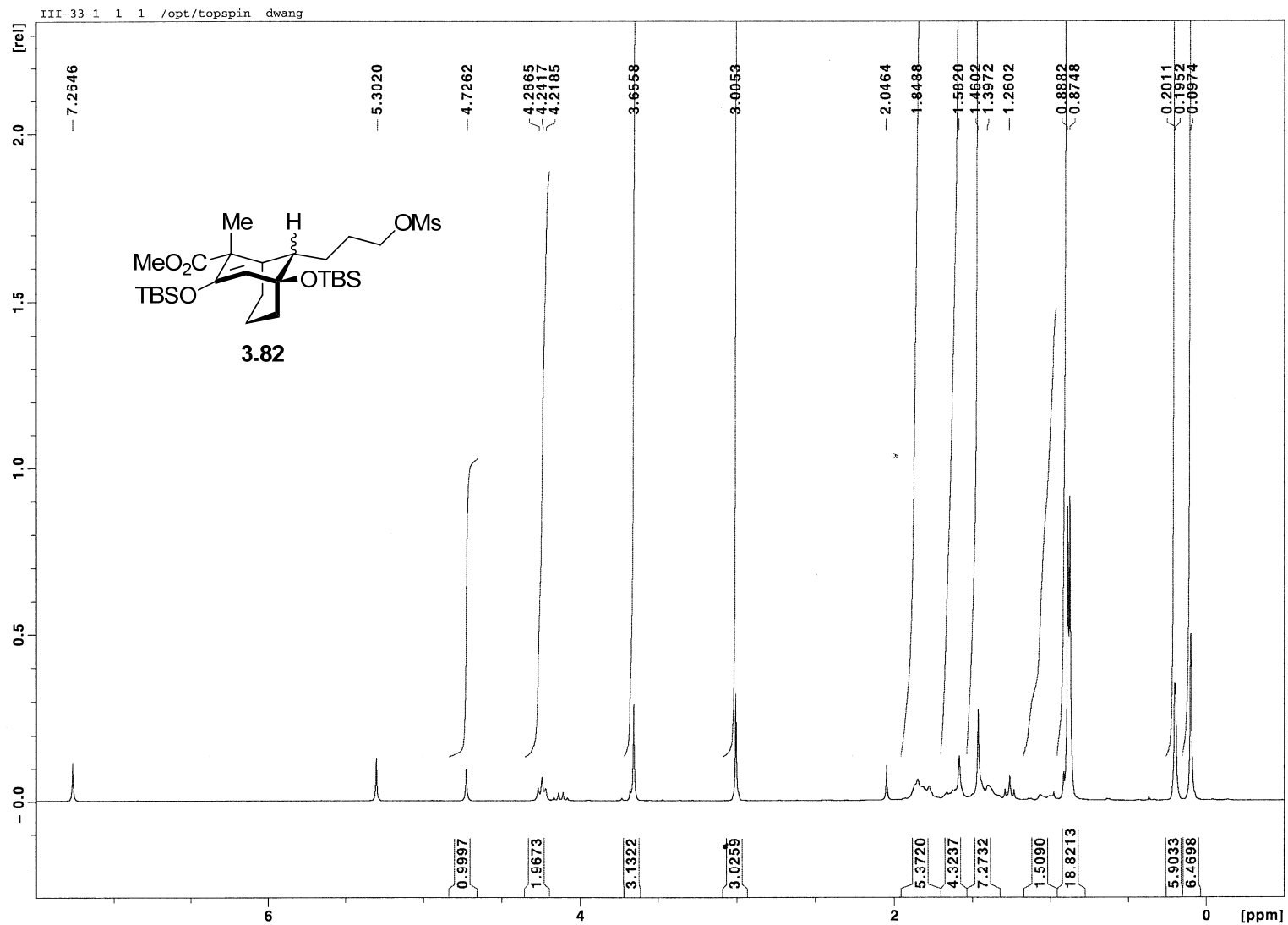


Figure 3.7 ¹H NMR (400 MHz, CDCl₃) of Compound 3.82

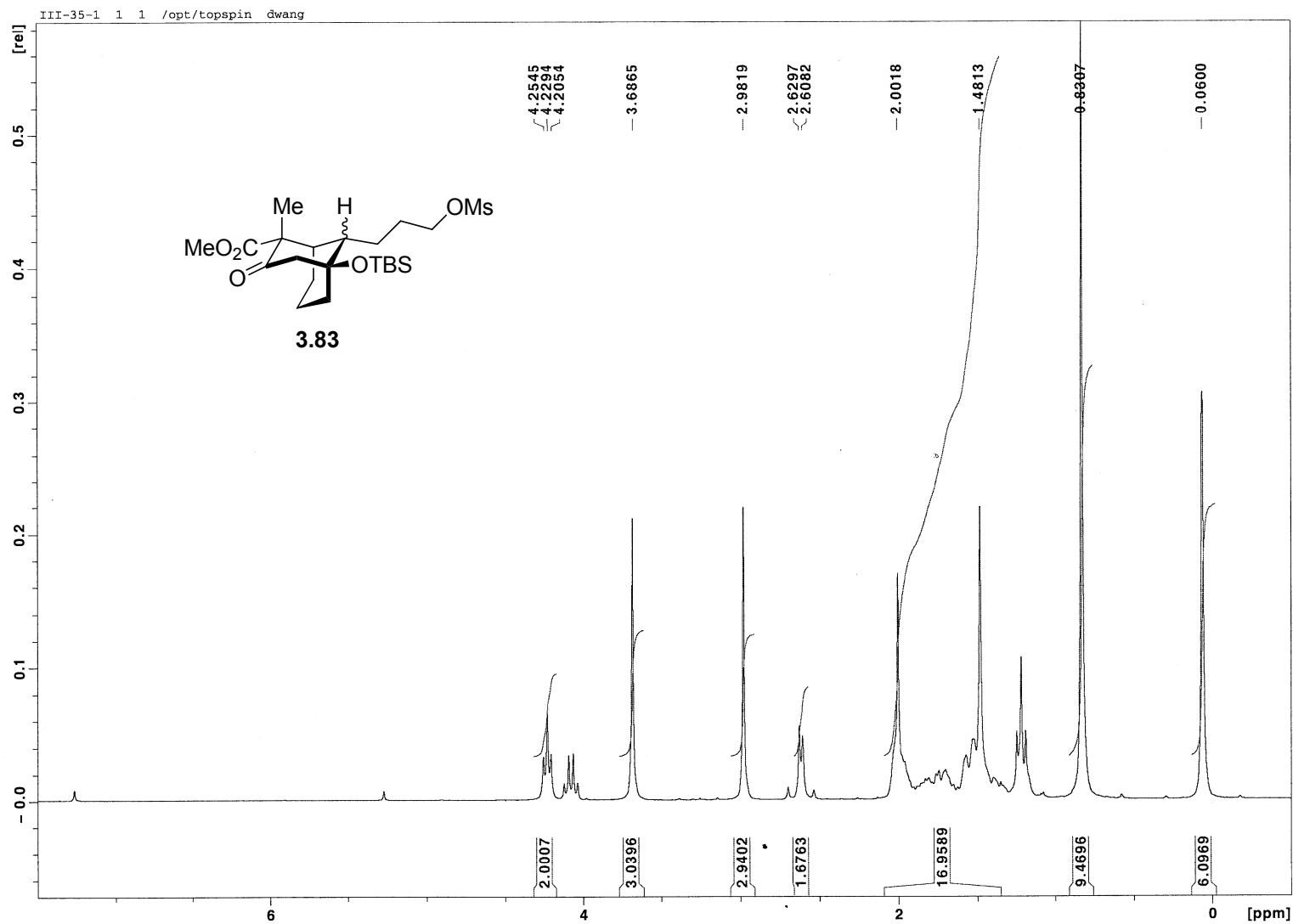


Figure 3.8 ¹H NMR (250 MHz, CDCl₃) of Compound 3.83

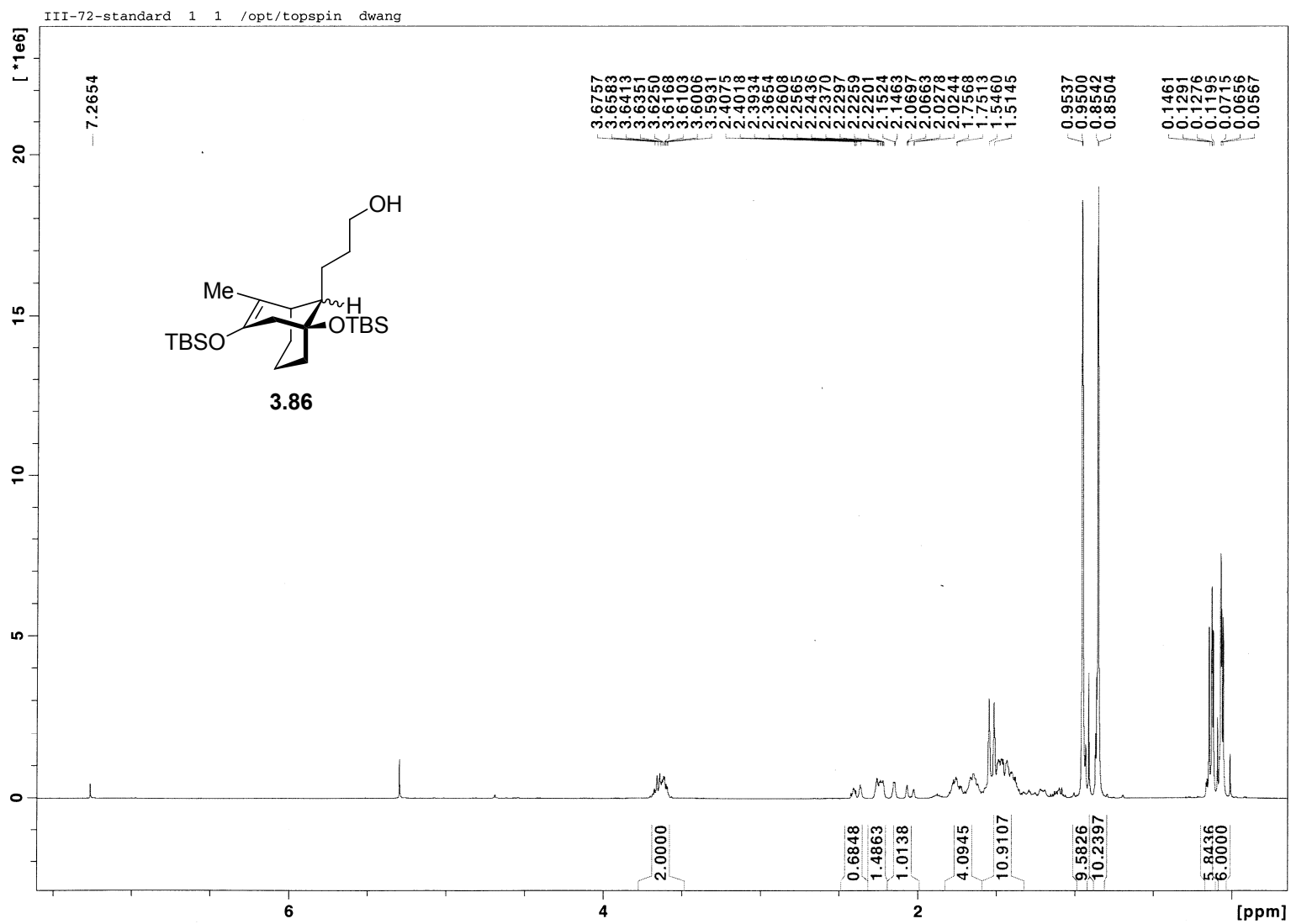


Figure 3.11 ^1H NMR (400 MHz, CDCl_3) of Compound 3.86

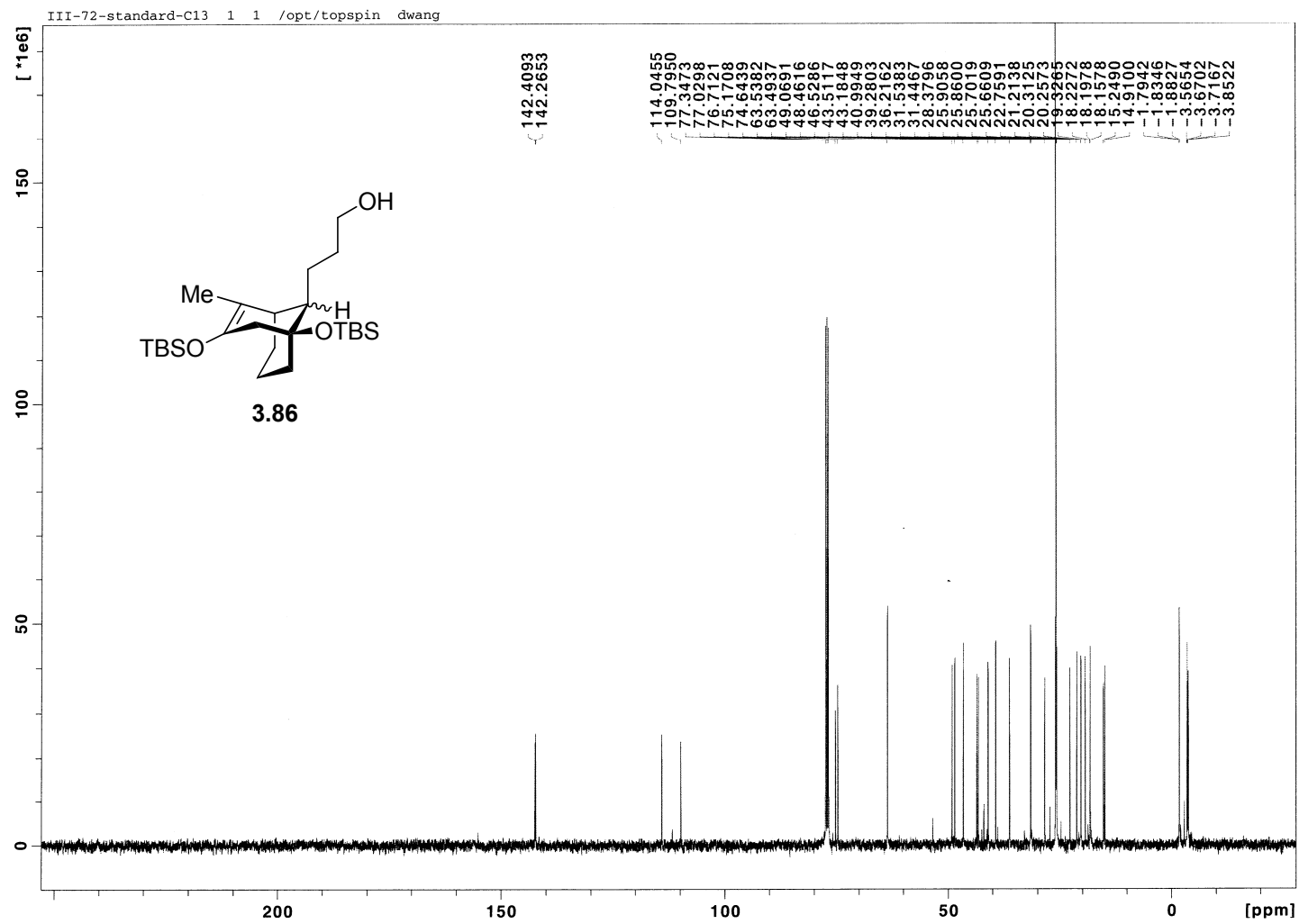


Figure 3.12 ^{13}C NMR (100 MHz, CDCl_3) of Compound 3.86

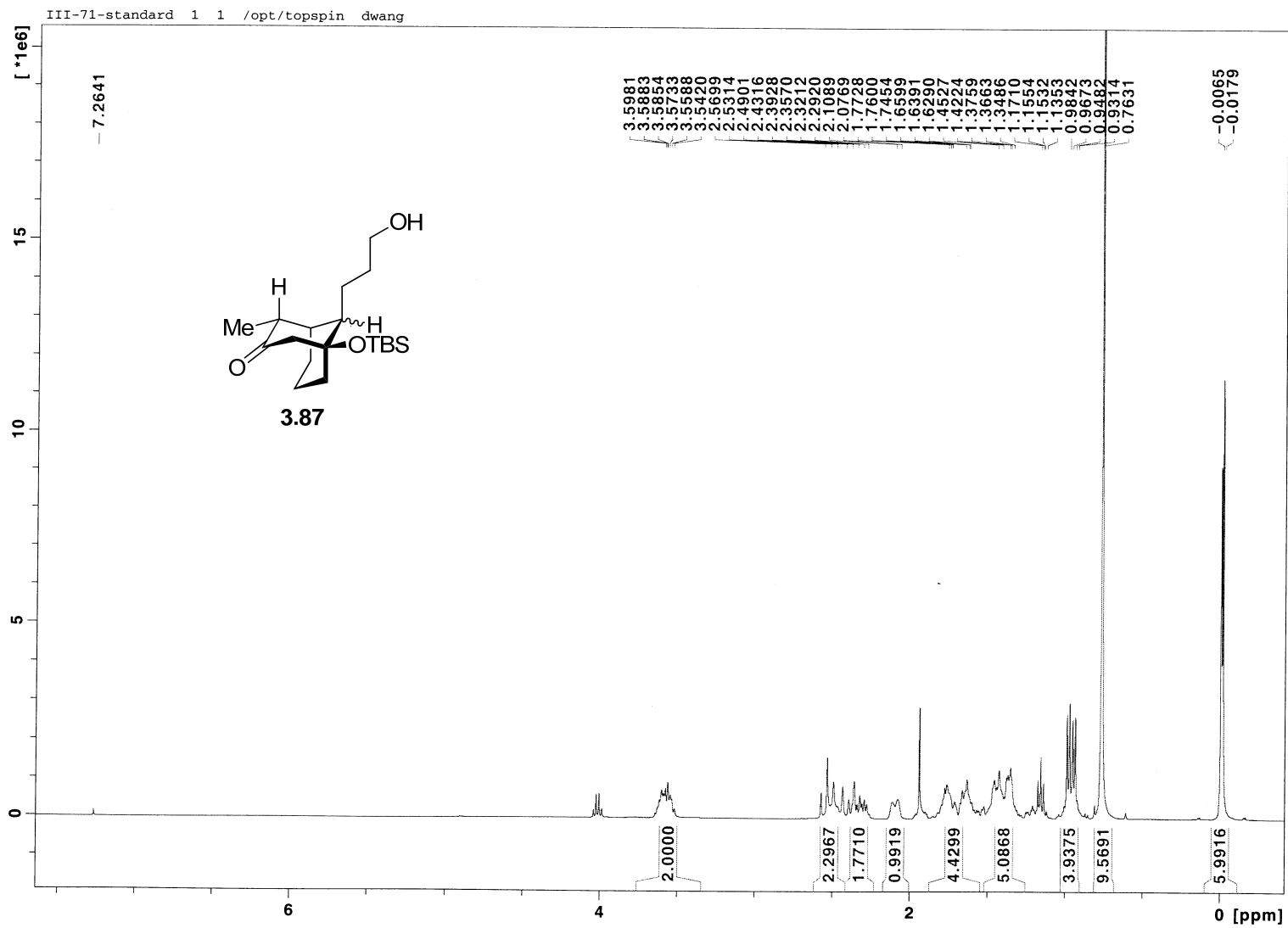


Figure 3.13 ^1H NMR (400 MHz, CDCl_3) of Compound 3.87

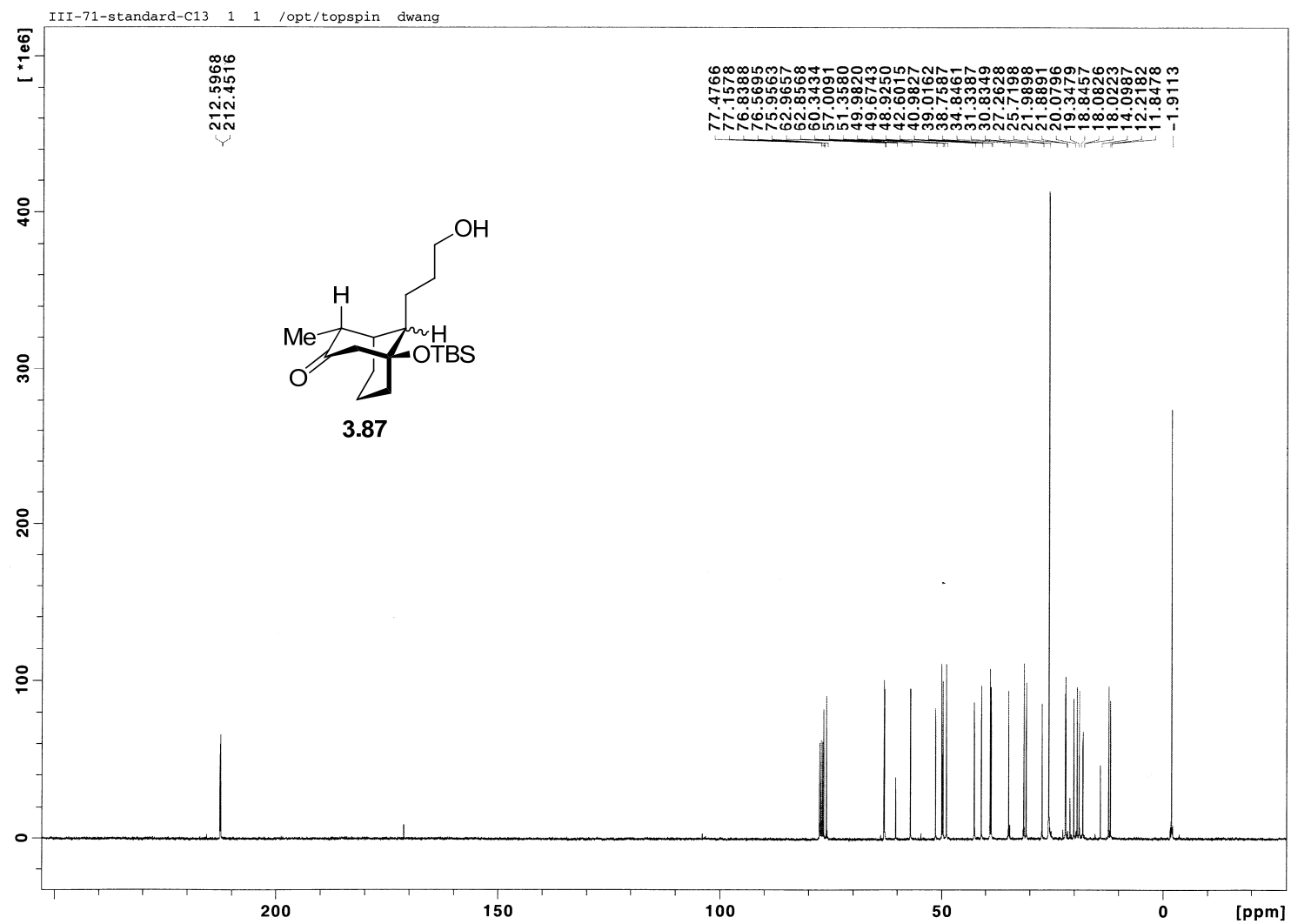


Figure 3.14 ^{13}C NMR (100 MHz, CDCl_3) of Compound 3.87

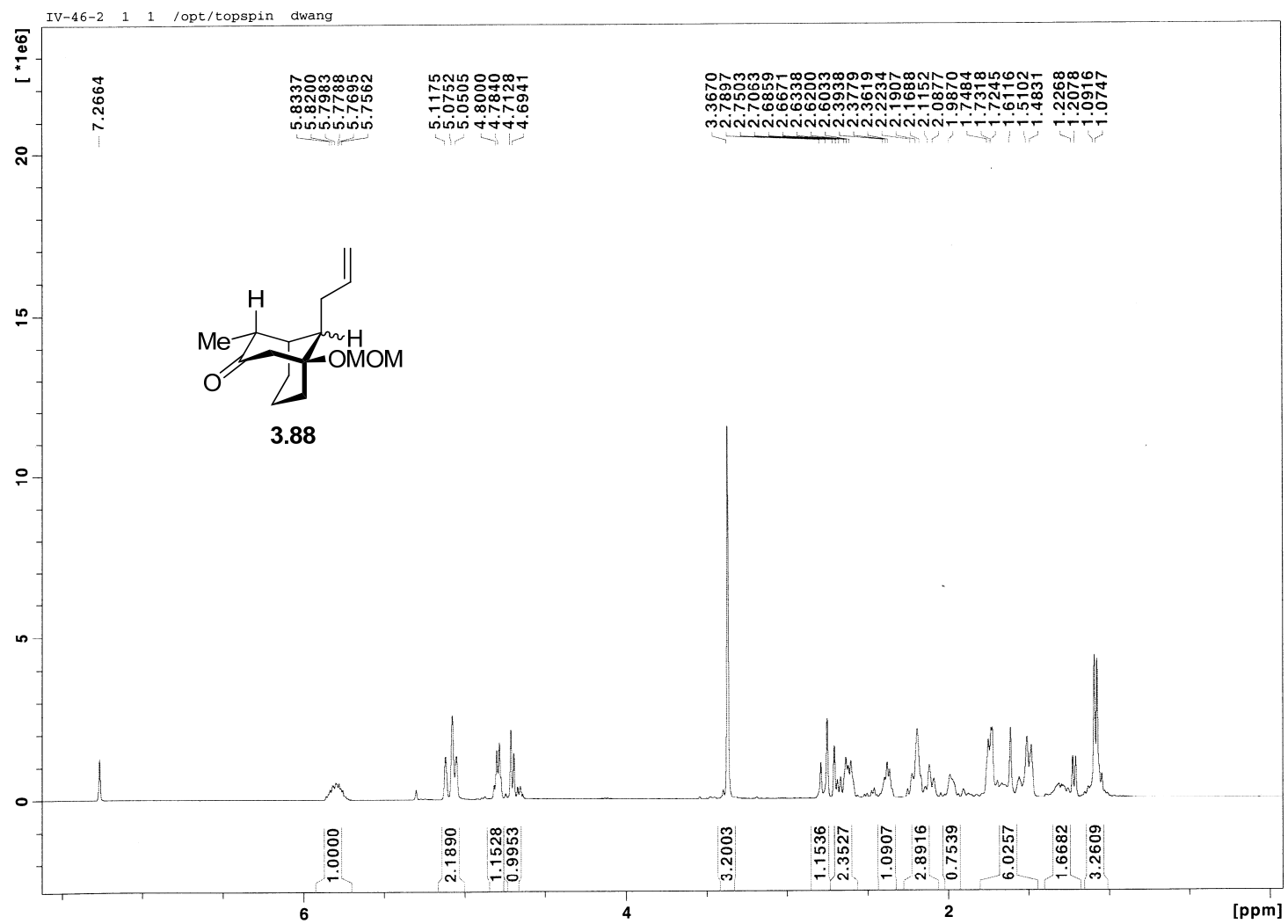


Figure 3.15 ^1H NMR (400 MHz, CDCl_3) of Compound 3.88

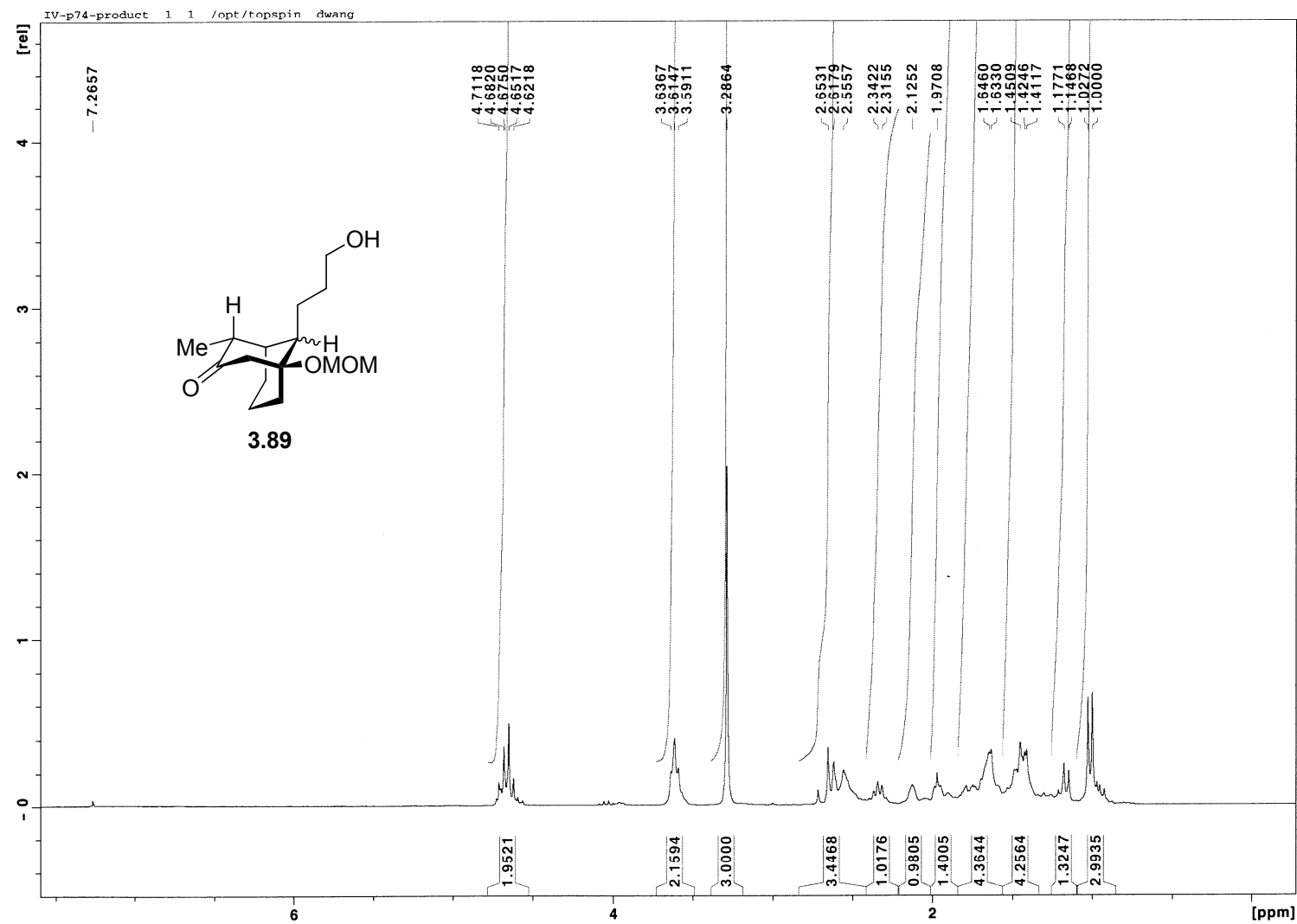


Figure 3.16 ^1H NMR (400 MHz, CDCl_3) of Compound 3.89

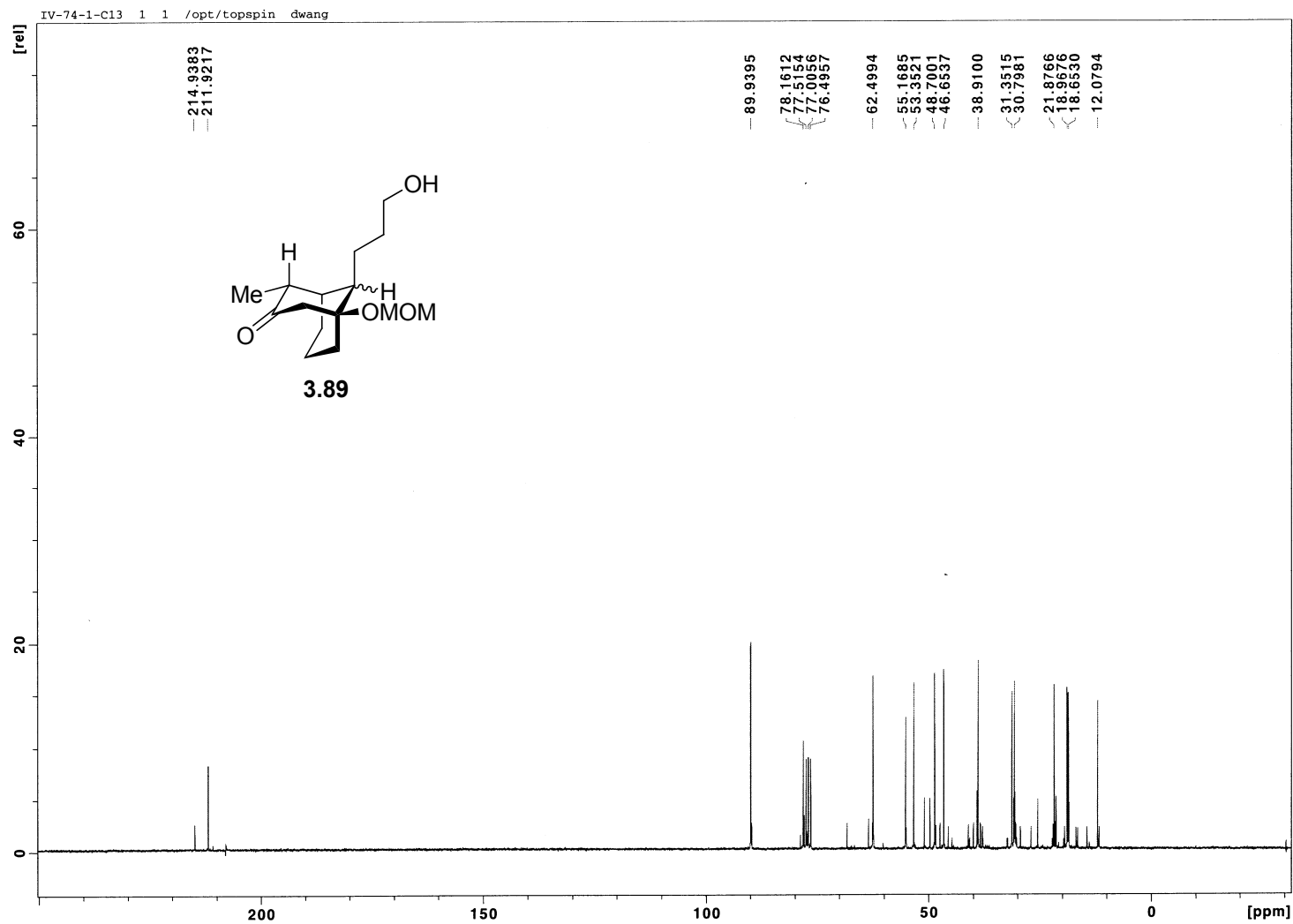


Figure 3.17 ^{13}C NMR (100 MHz, CDCl_3) of Compound 3.89

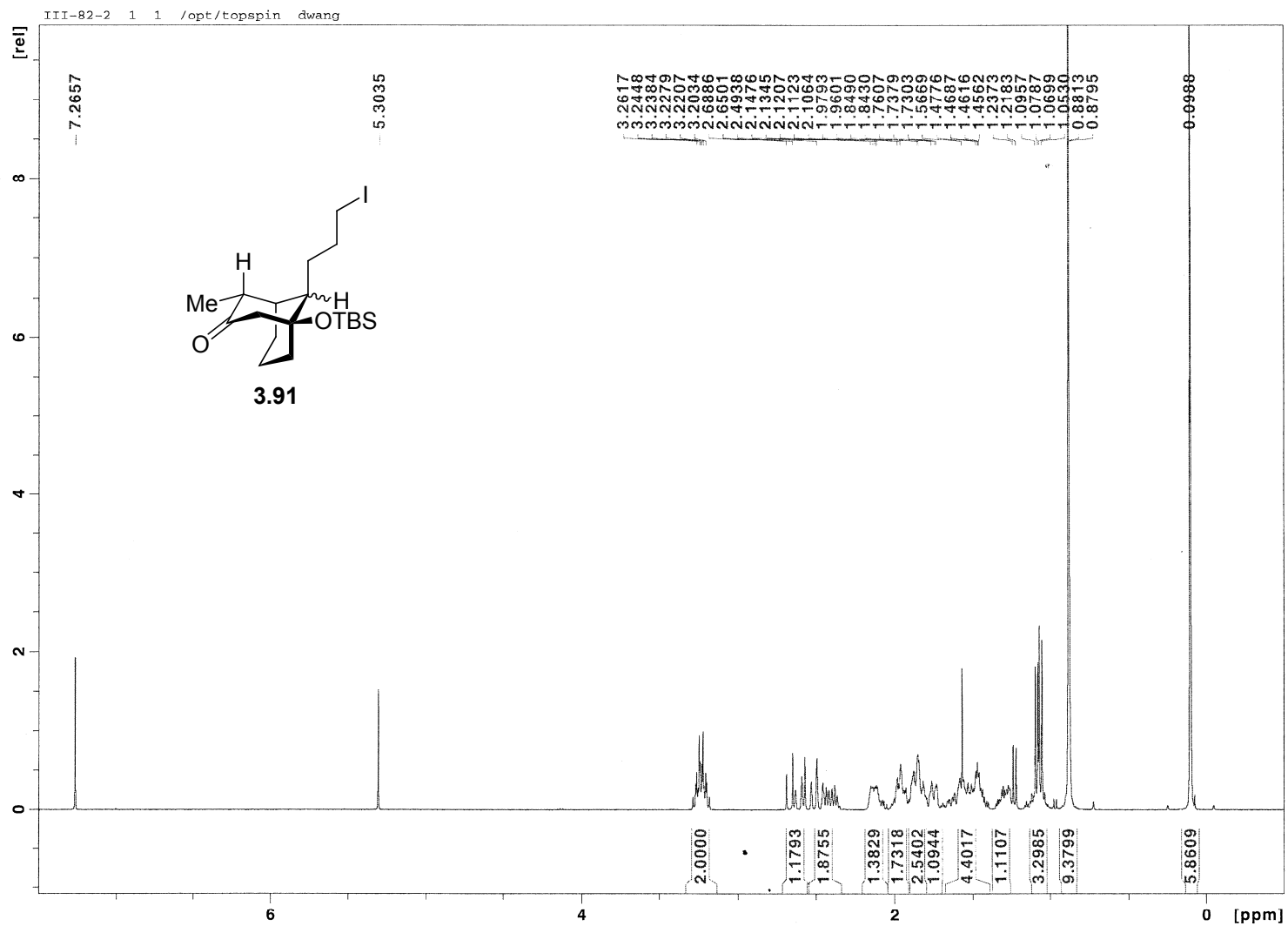


Figure 3.18 ^1H NMR (400 MHz, CDCl_3) of Compound 3.91

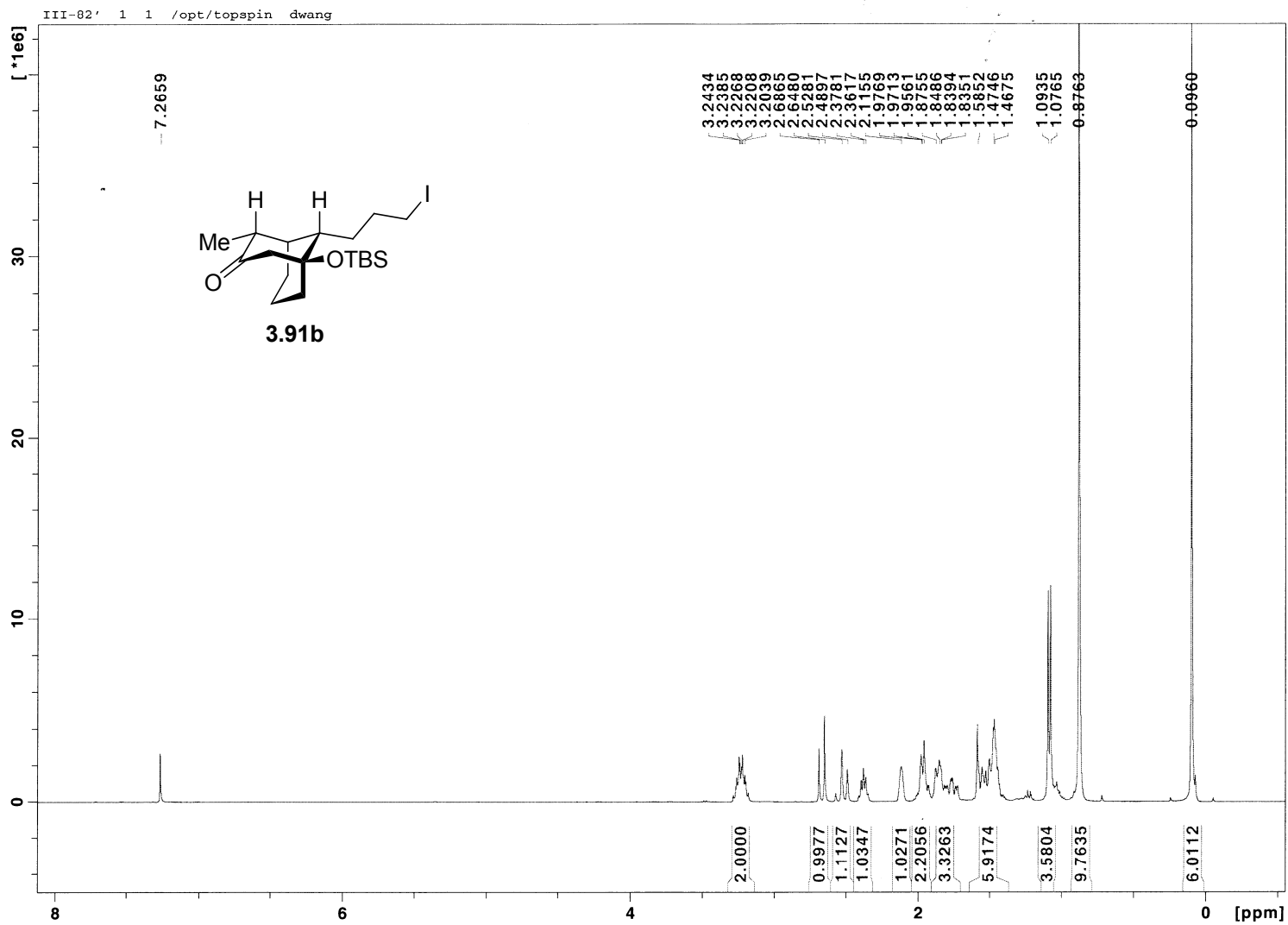


Figure 3.20 ^1H NMR (400 MHz, CDCl_3) of Compound 3.91b

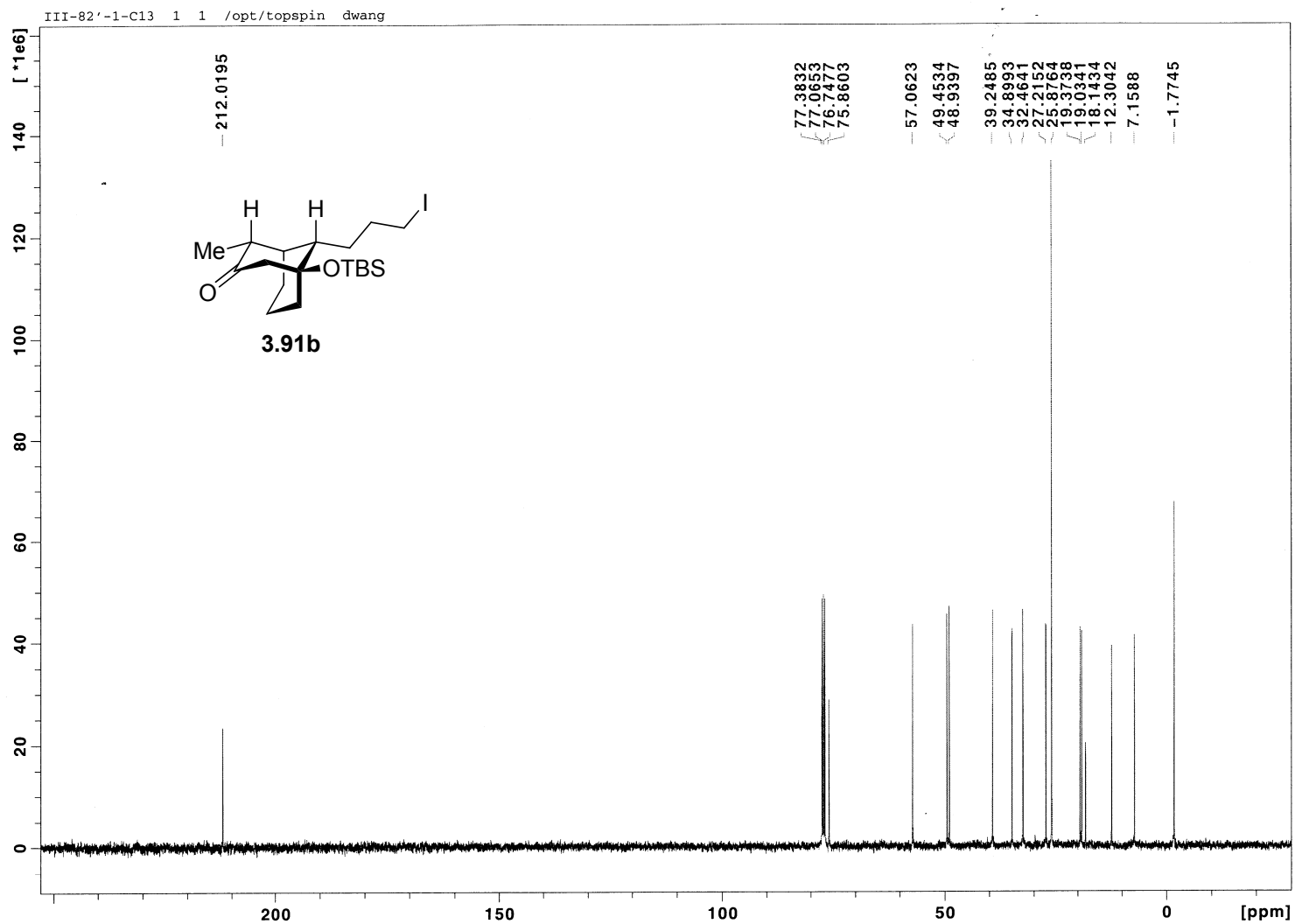


Figure 3.21 ^{13}C NMR (100 MHz, CDCl_3) of Compound 3.91b

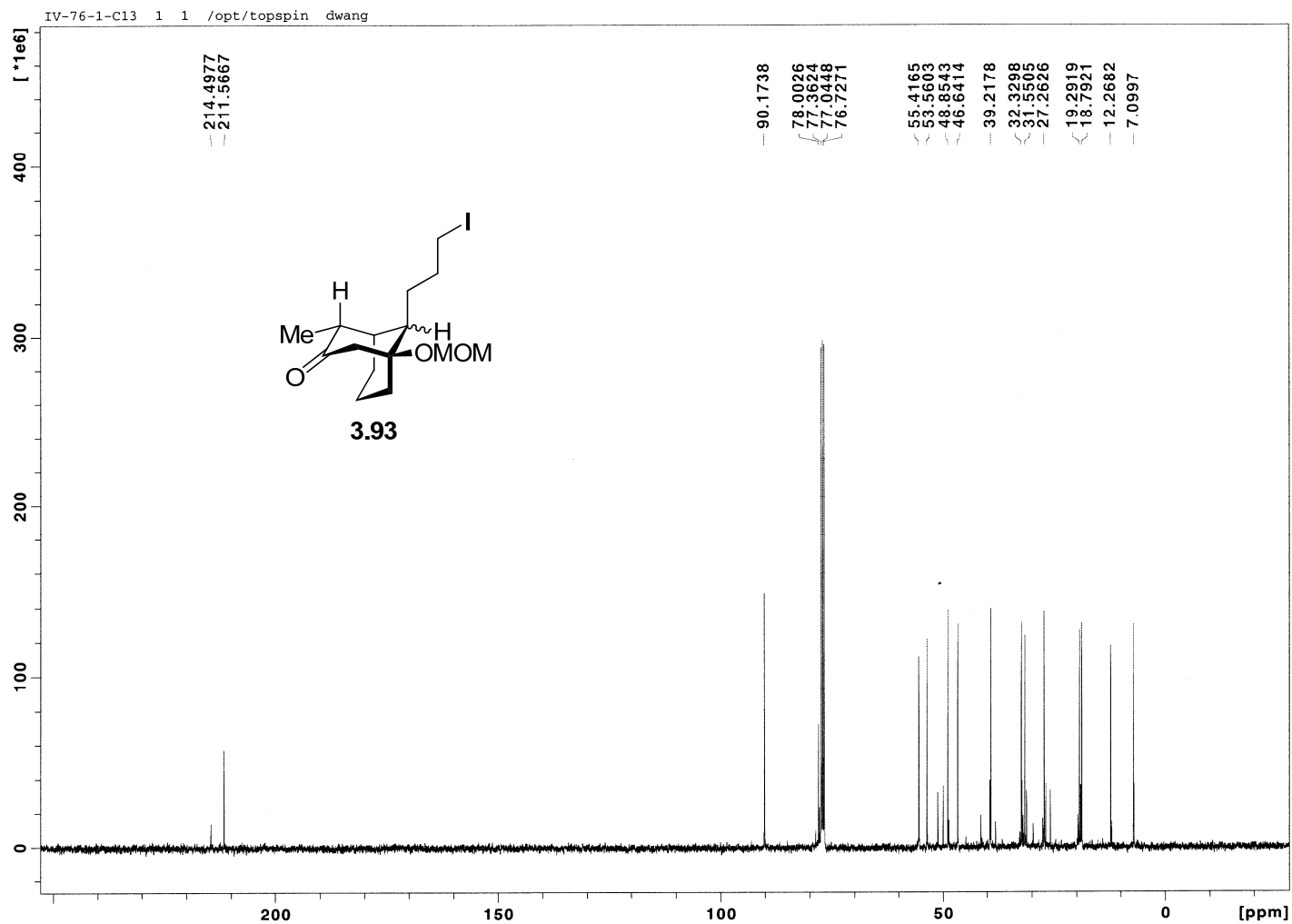


Figure 3.23 ^{13}C NMR (100 MHz, CDCl_3) of Compound 3.93

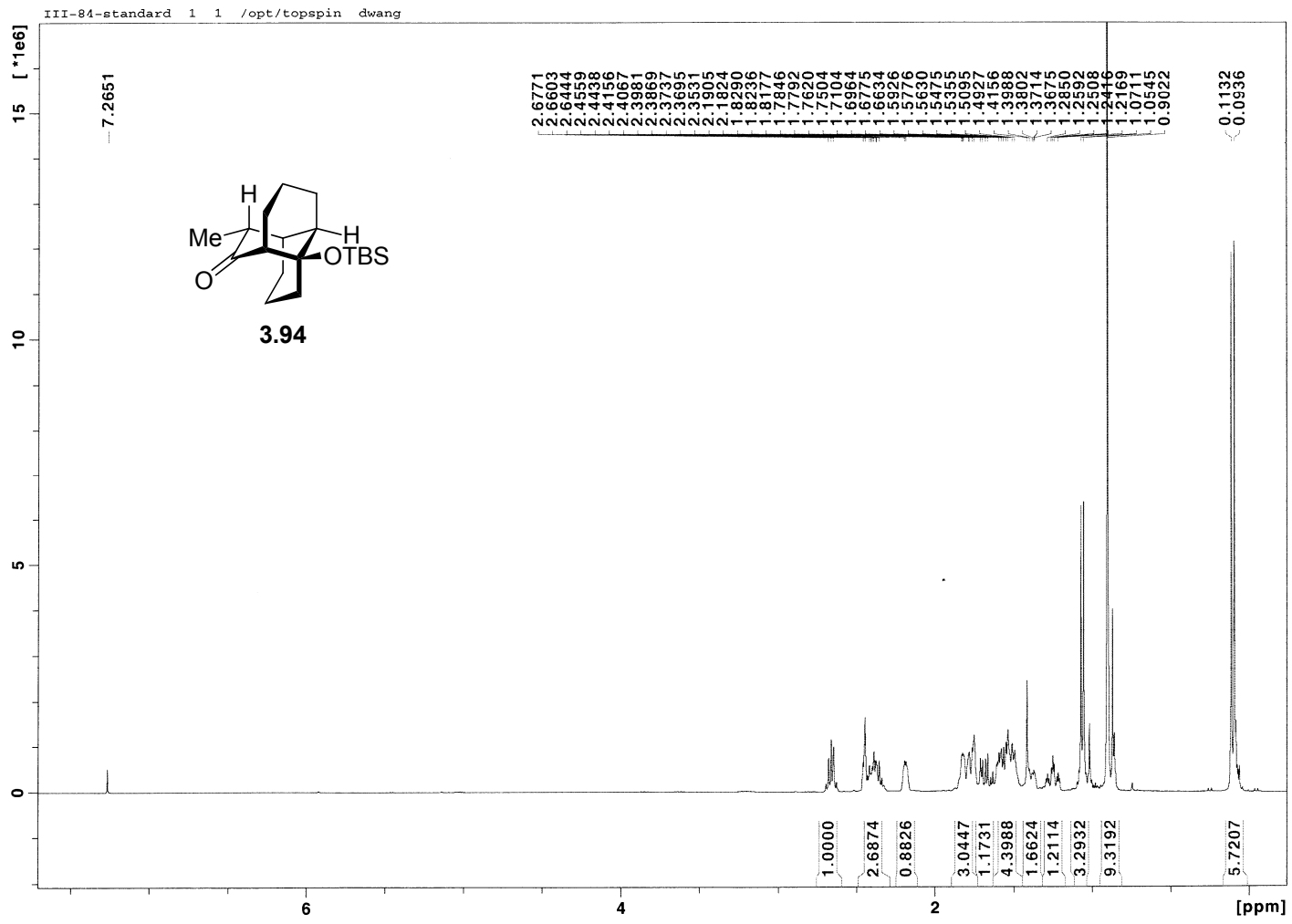


Figure 3.24 ¹H NMR (400 MHz, CDCl₃) of Compound 3.94

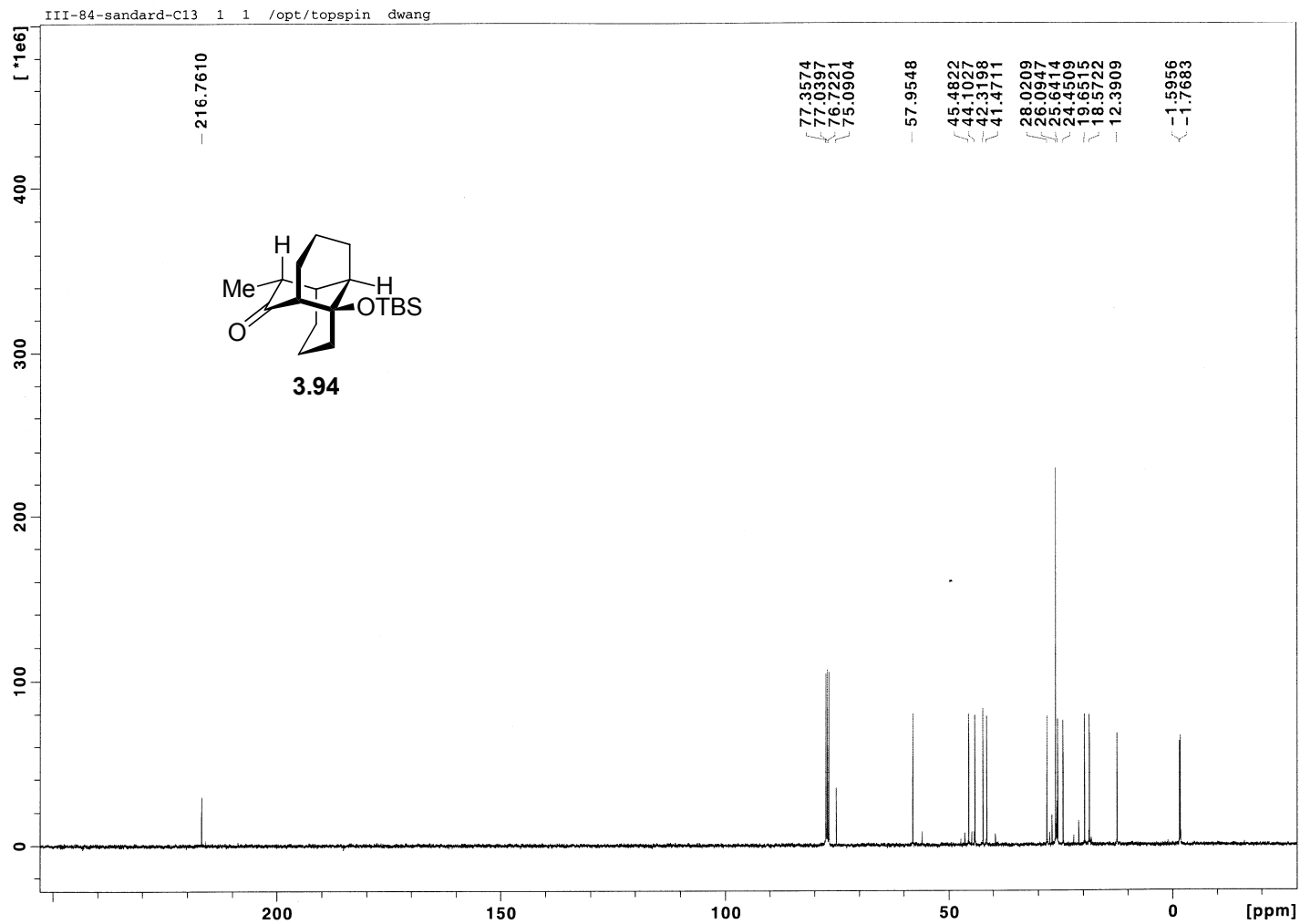


Figure 3.25 ^{13}C NMR (100 MHz, CDCl_3) of Compound 3.94

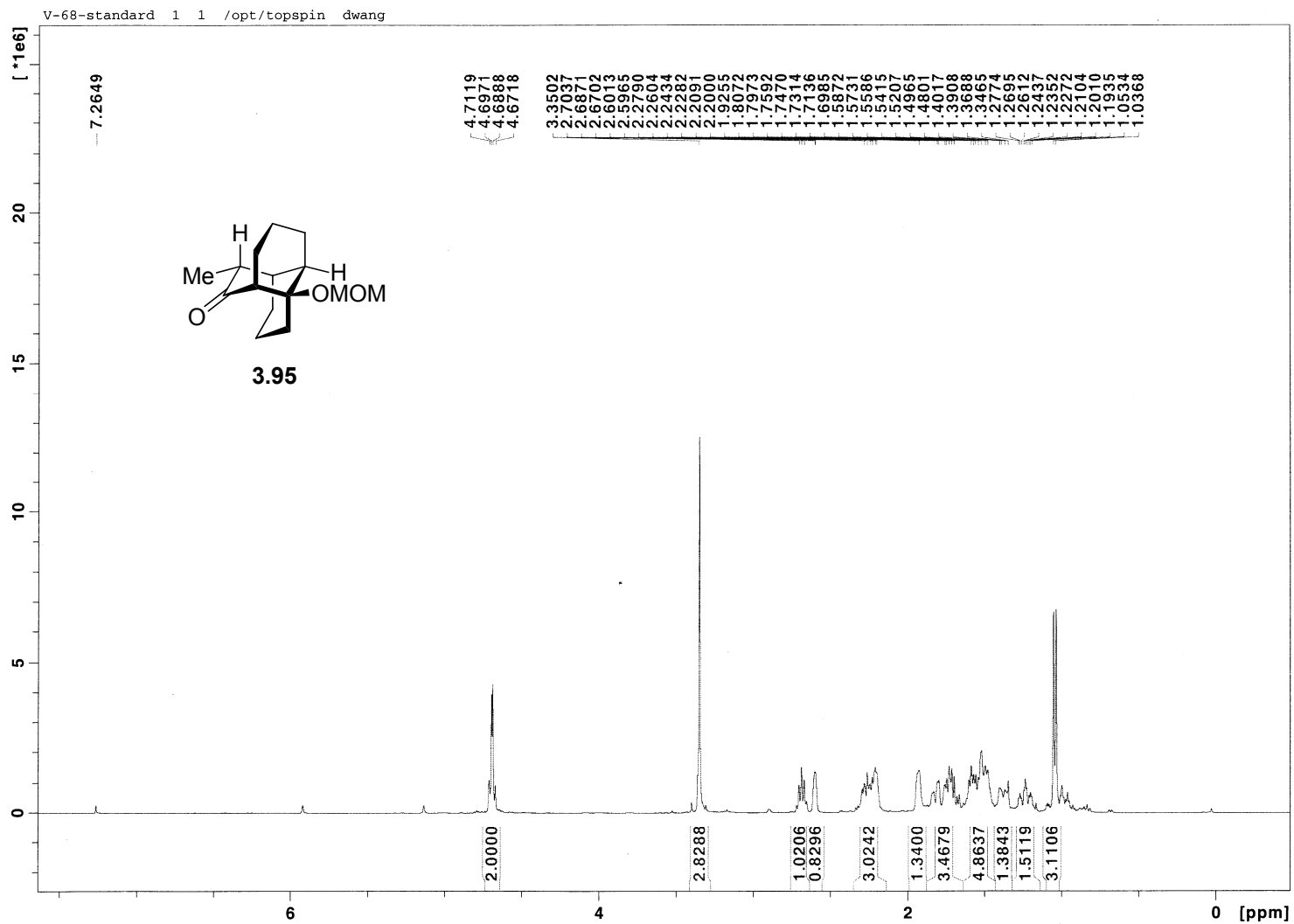


Figure 3.26 ^1H NMR (400 MHz, CDCl_3) of Compound 3.95

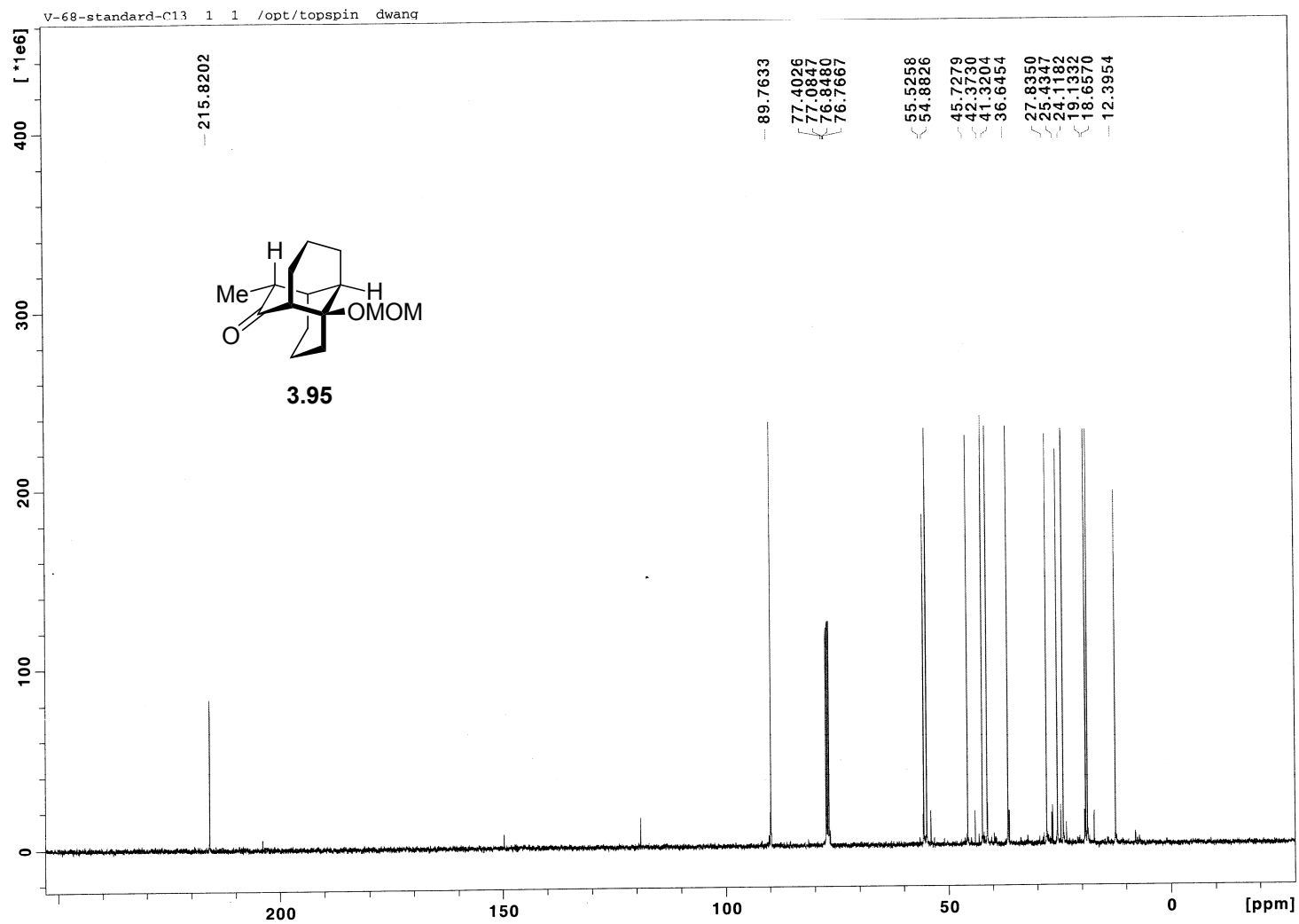


Figure 3.27 ^{13}C NMR (100 MHz, CDCl_3) of Compound 3.95

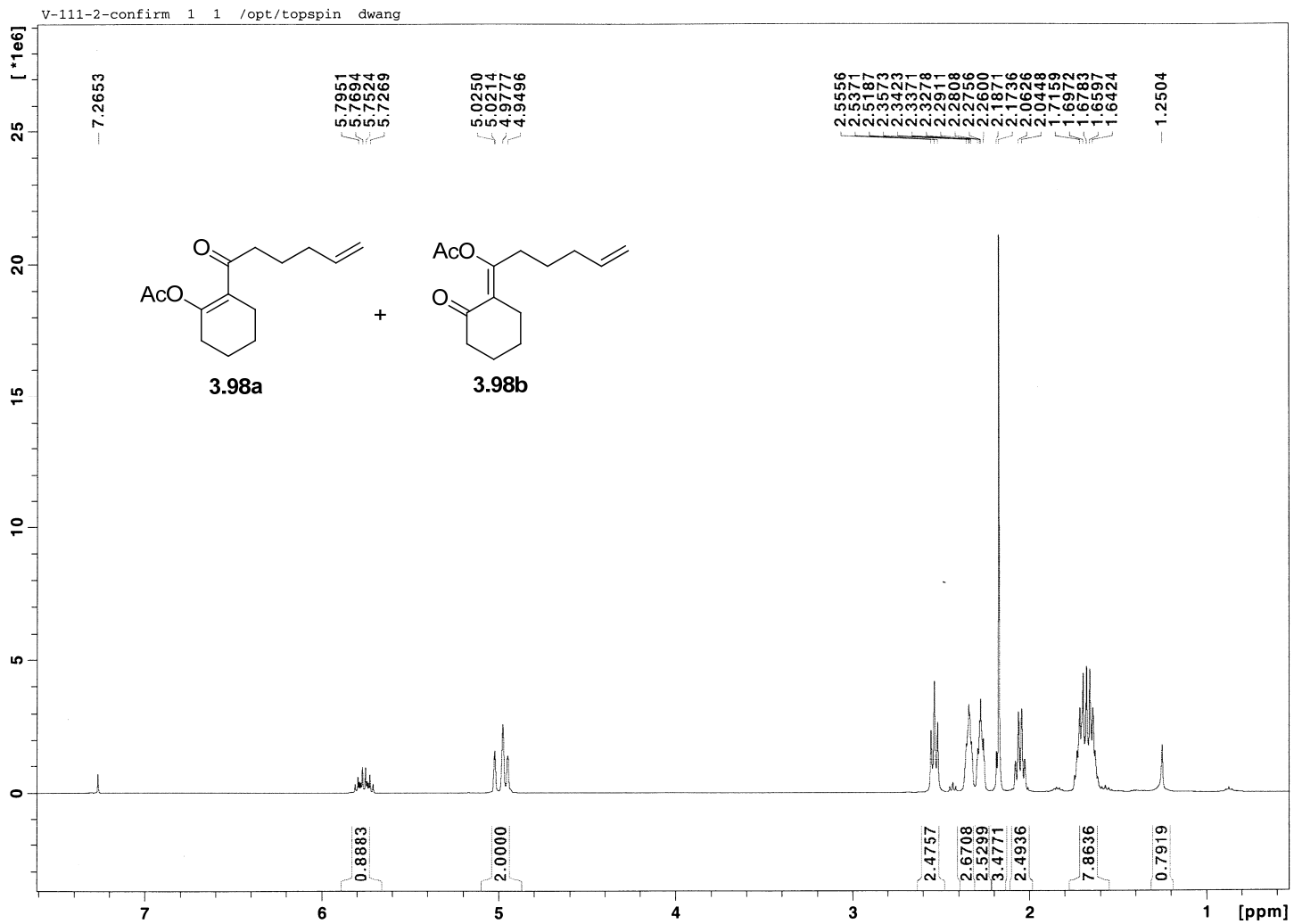


Figure 3.28 ^1H NMR (400 MHz, CDCl_3) of Compound 3.98

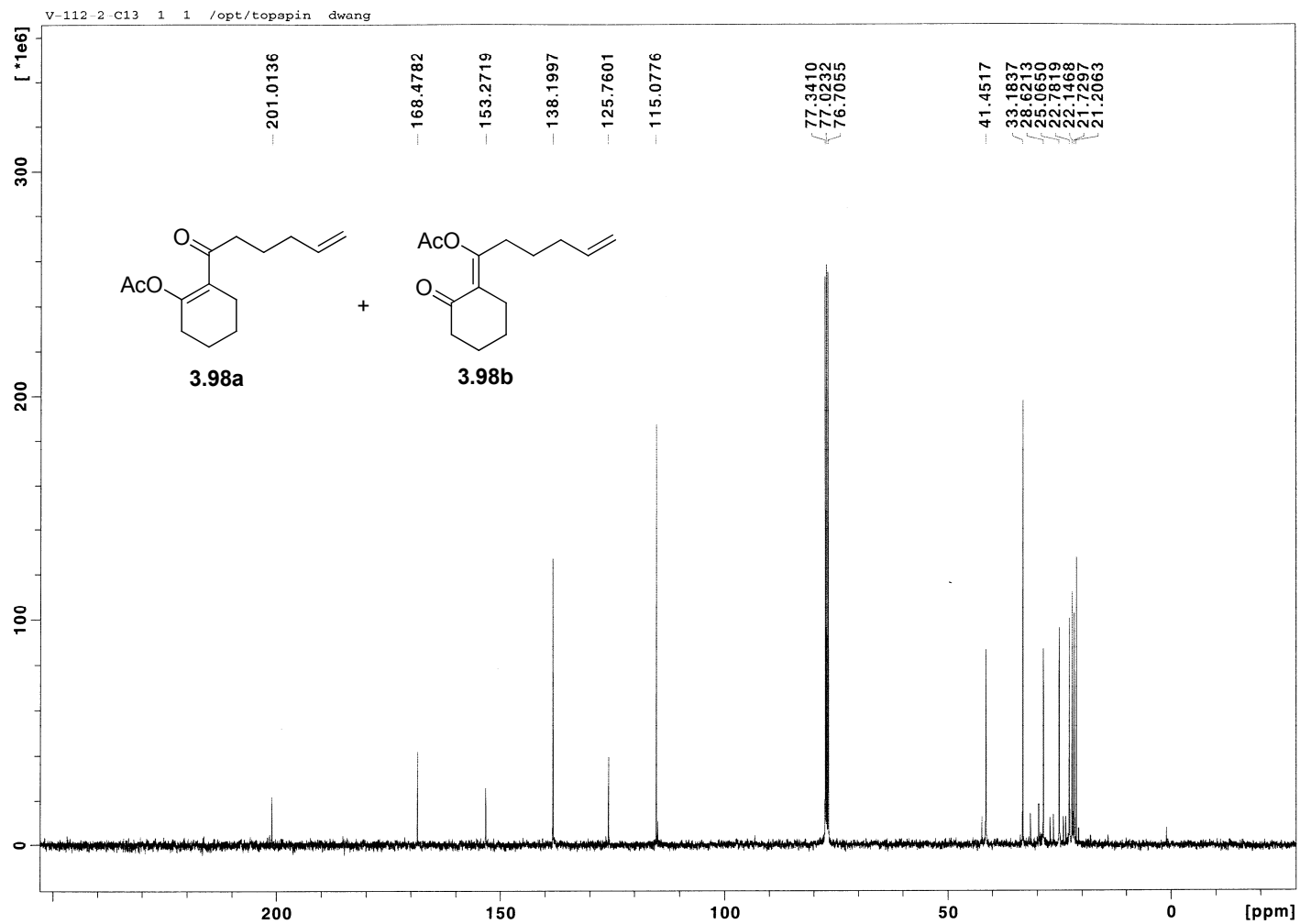


Figure 3.29 ^{13}C NMR (100 MHz, CDCl_3) of Compound 3.98

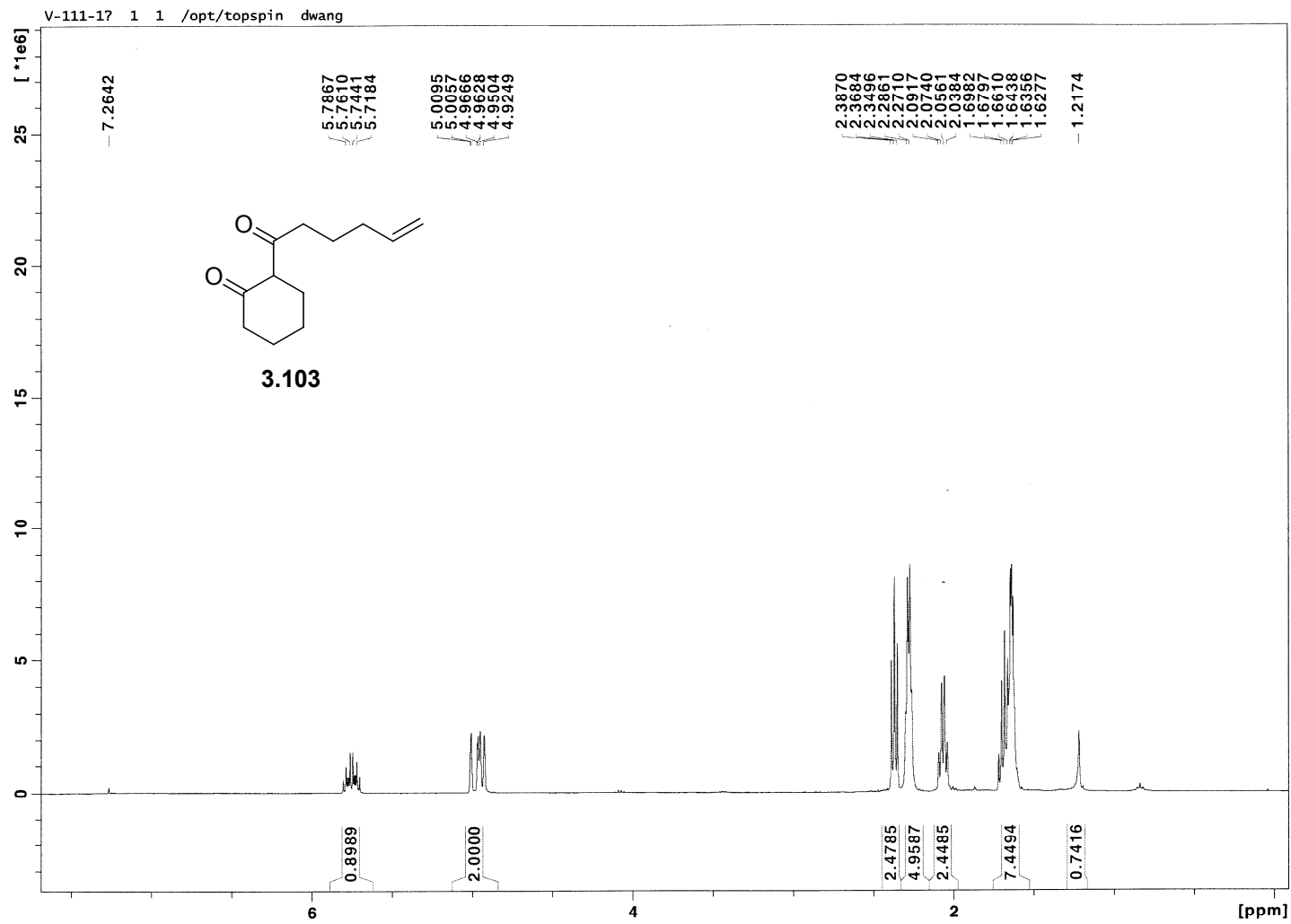


Figure 3.30 ¹H NMR (400 MHz, CDCl₃) of Compound 3.103

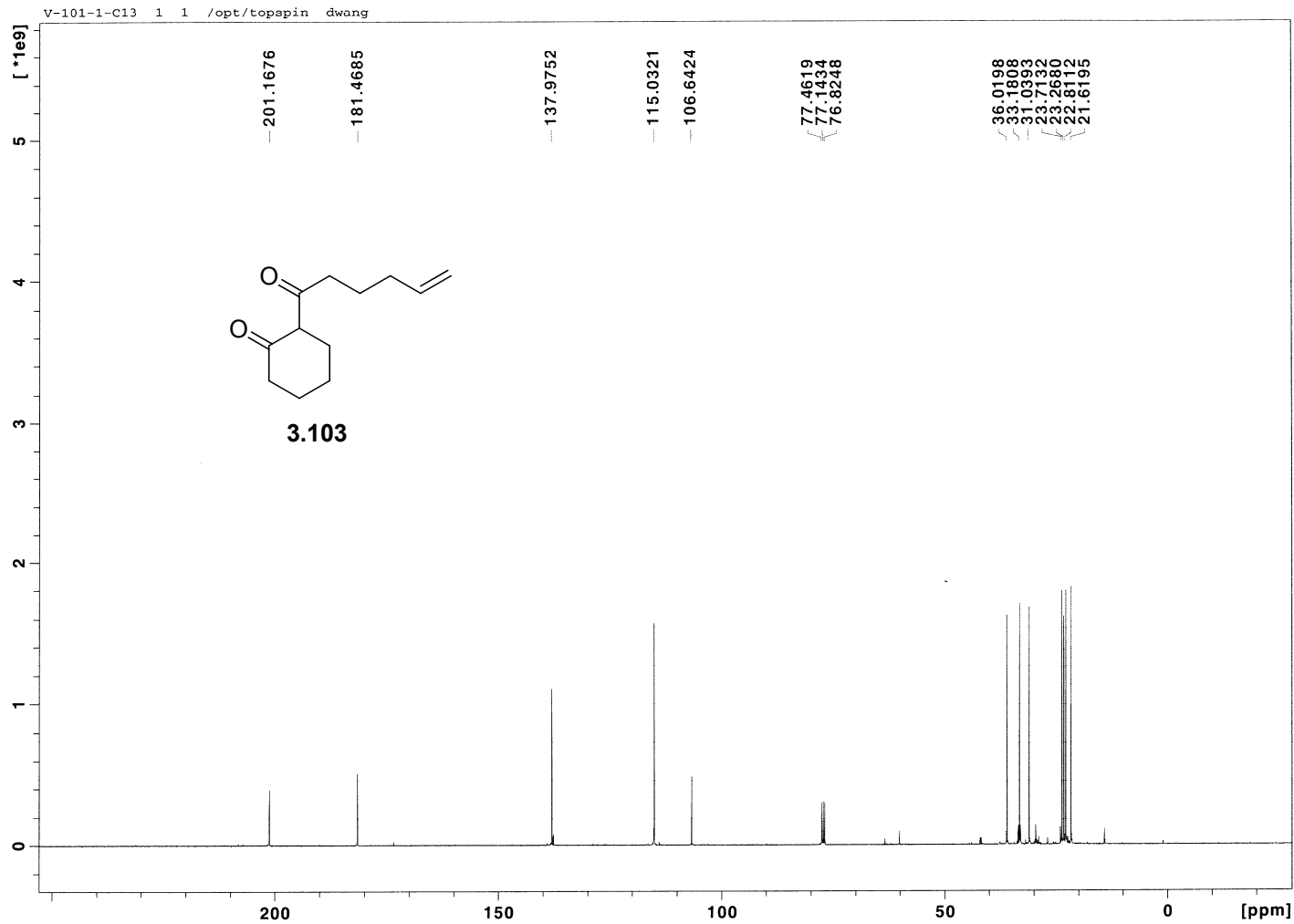


Figure 3.31 ^{13}C NMR (100 MHz, CDCl_3) of Compound 3.103

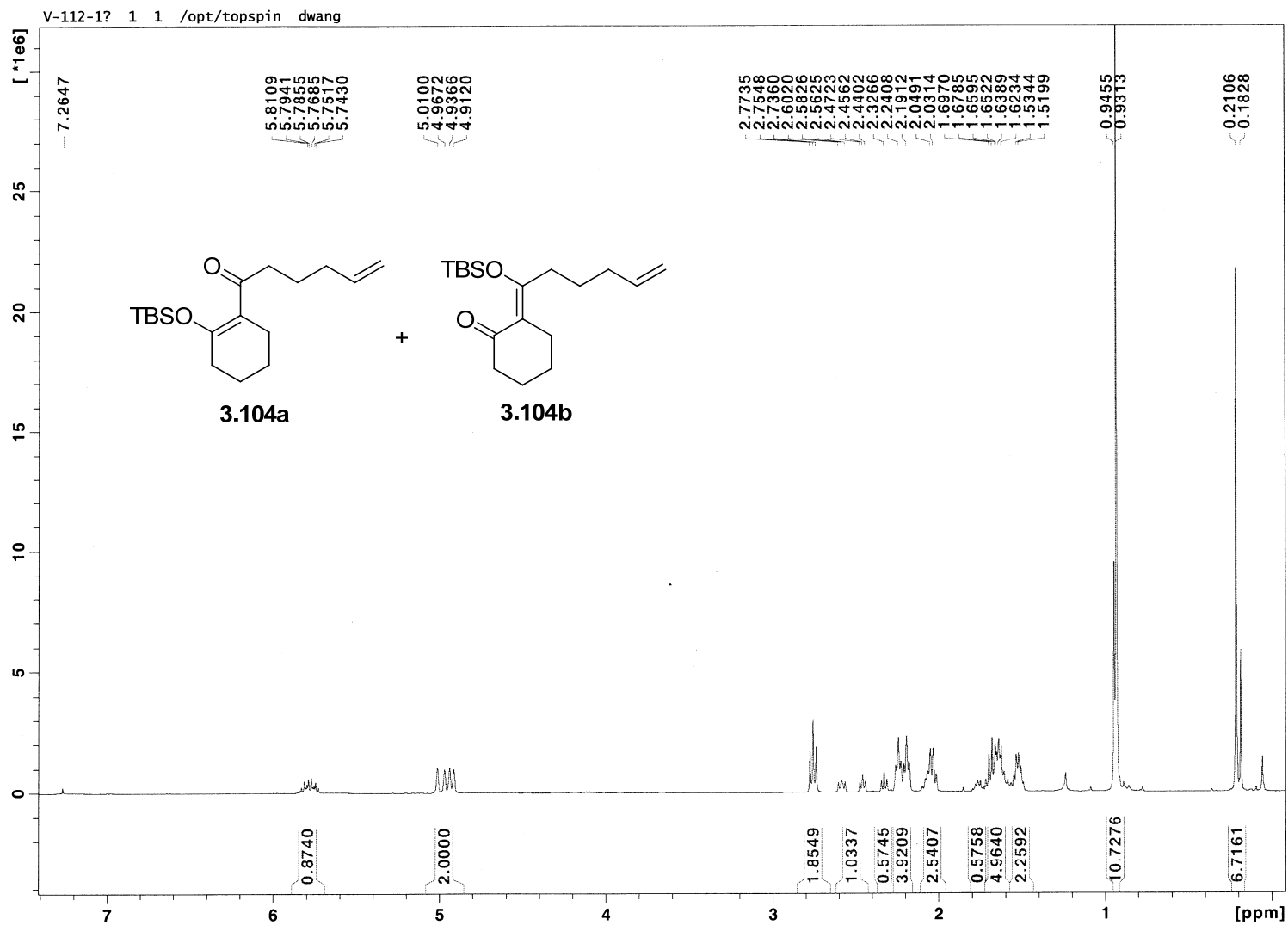


Figure 3.32 ^1H NMR (400 MHz, CDCl_3) of Compound 3.104

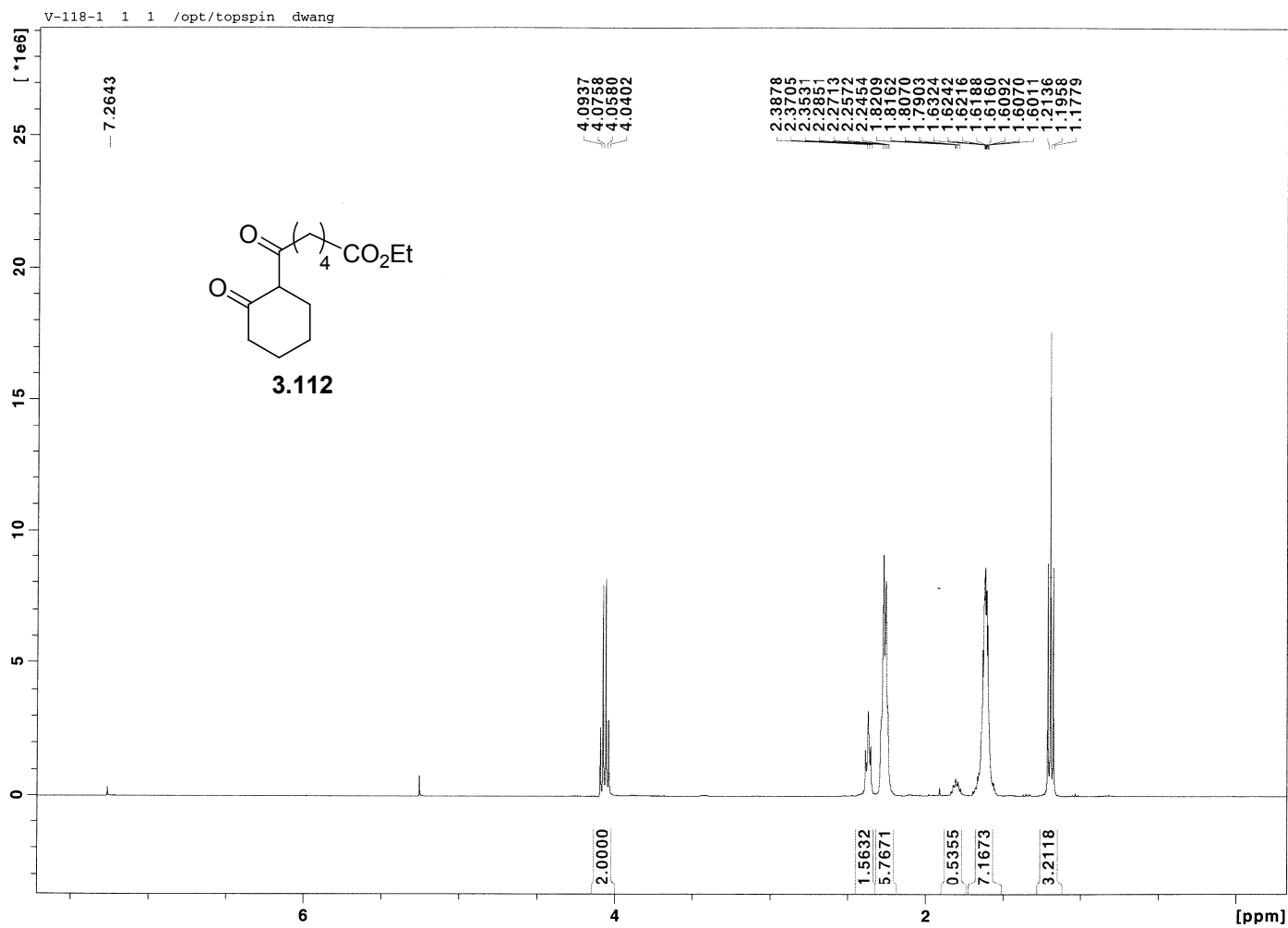


Figure 3.33 ^1H NMR (400 MHz, CDCl_3) of Compound 3.112

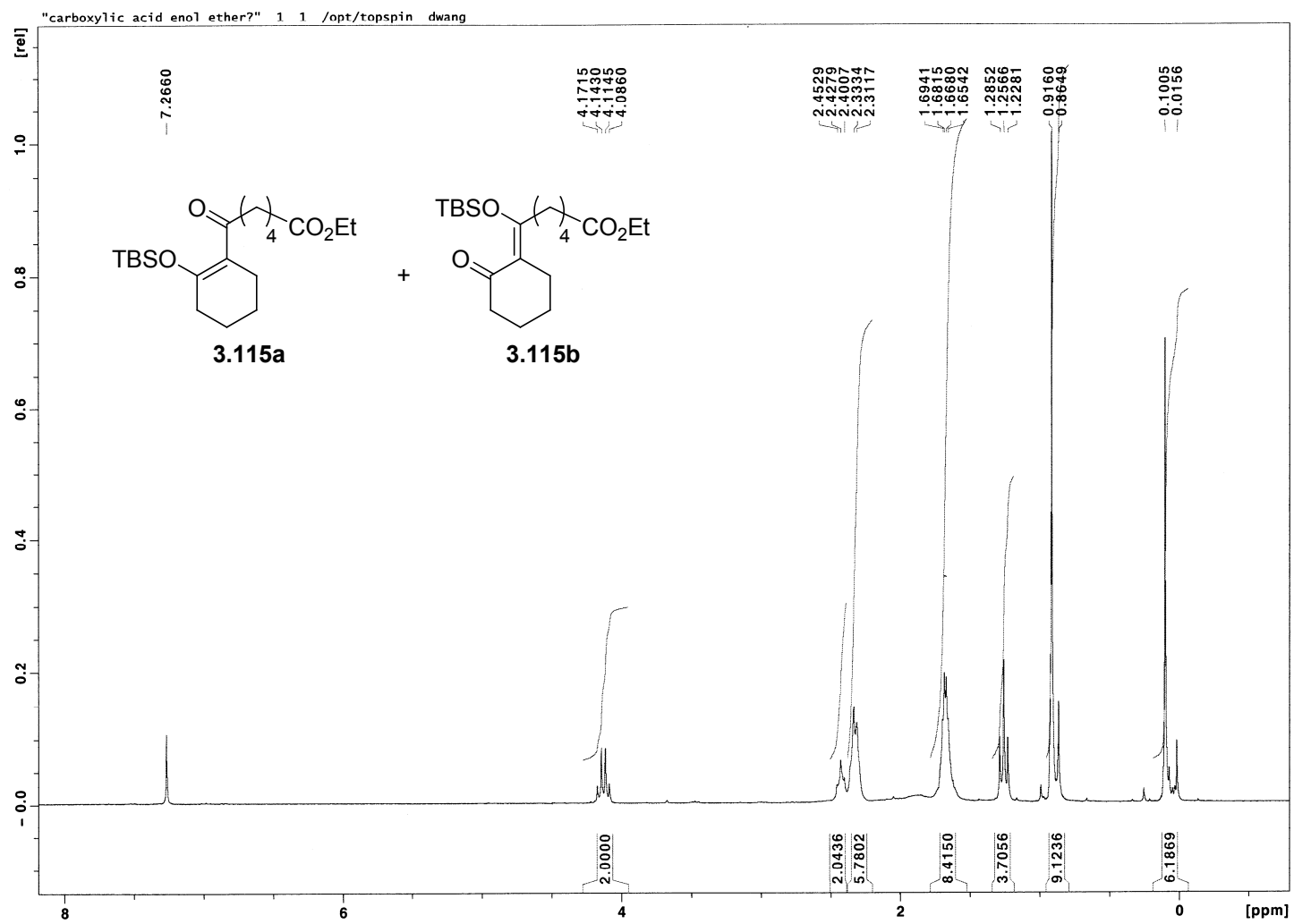


Figure 3.34 ^1H NMR (400 MHz, CDCl_3) of Compound 3.115

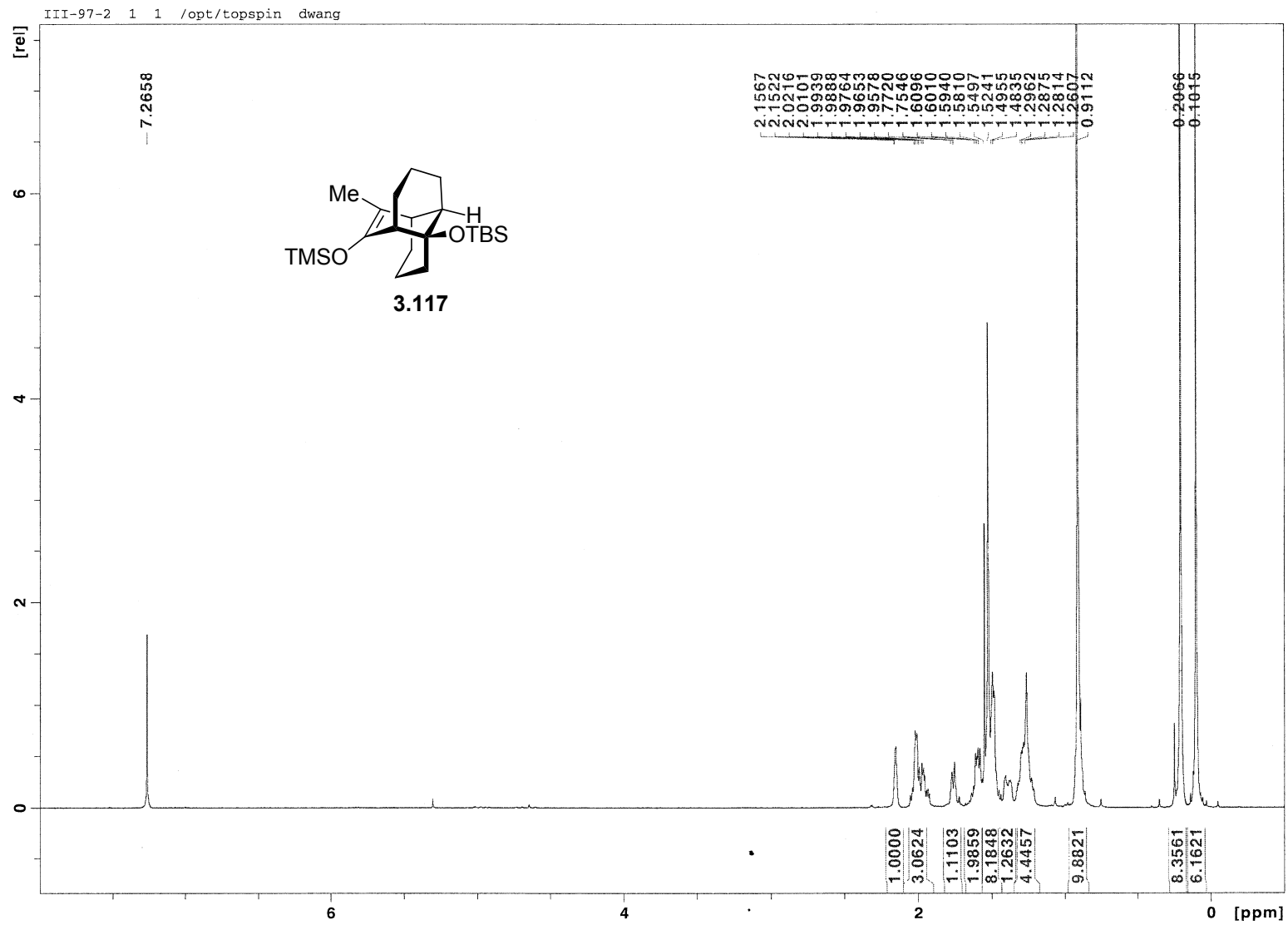


Figure 3.35 ^1H NMR (400 MHz, CDCl_3) of Compound 3.117

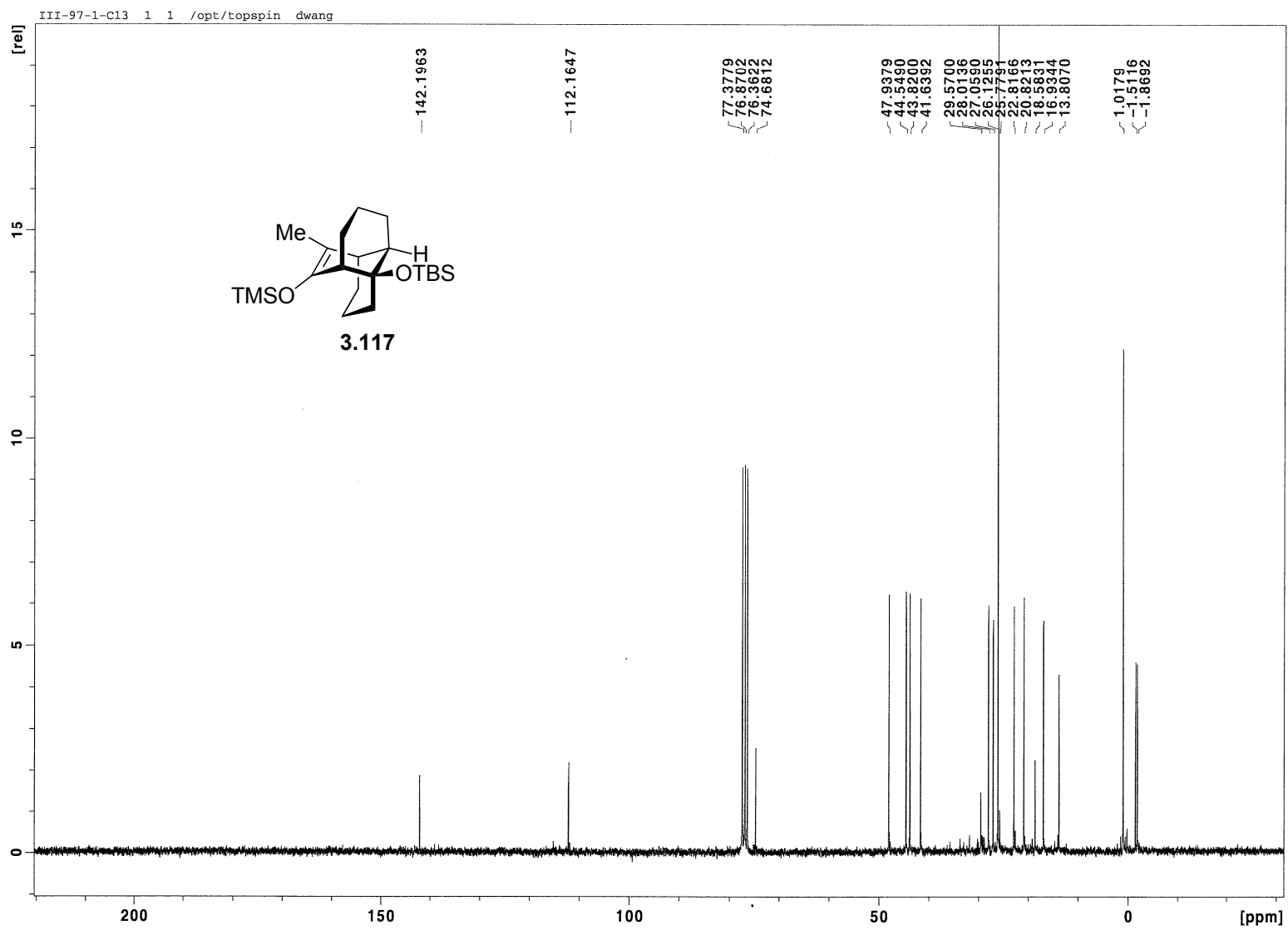


Figure 3.36 ^{13}C NMR (100 MHz, CDCl_3) of Compound 3.117

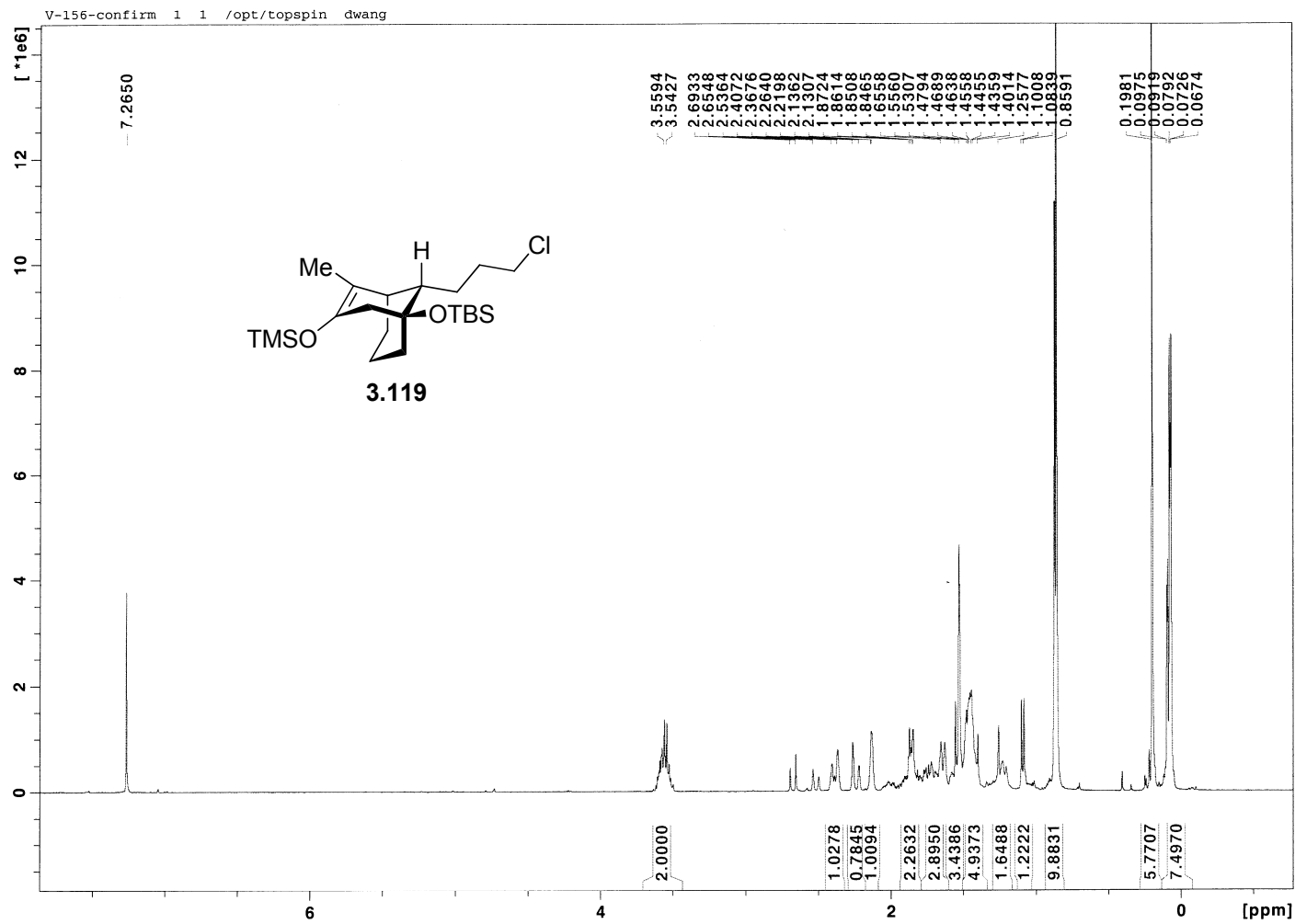


Figure 3.37 ^1H NMR (400 MHz, CDCl_3) of Compound 3.119

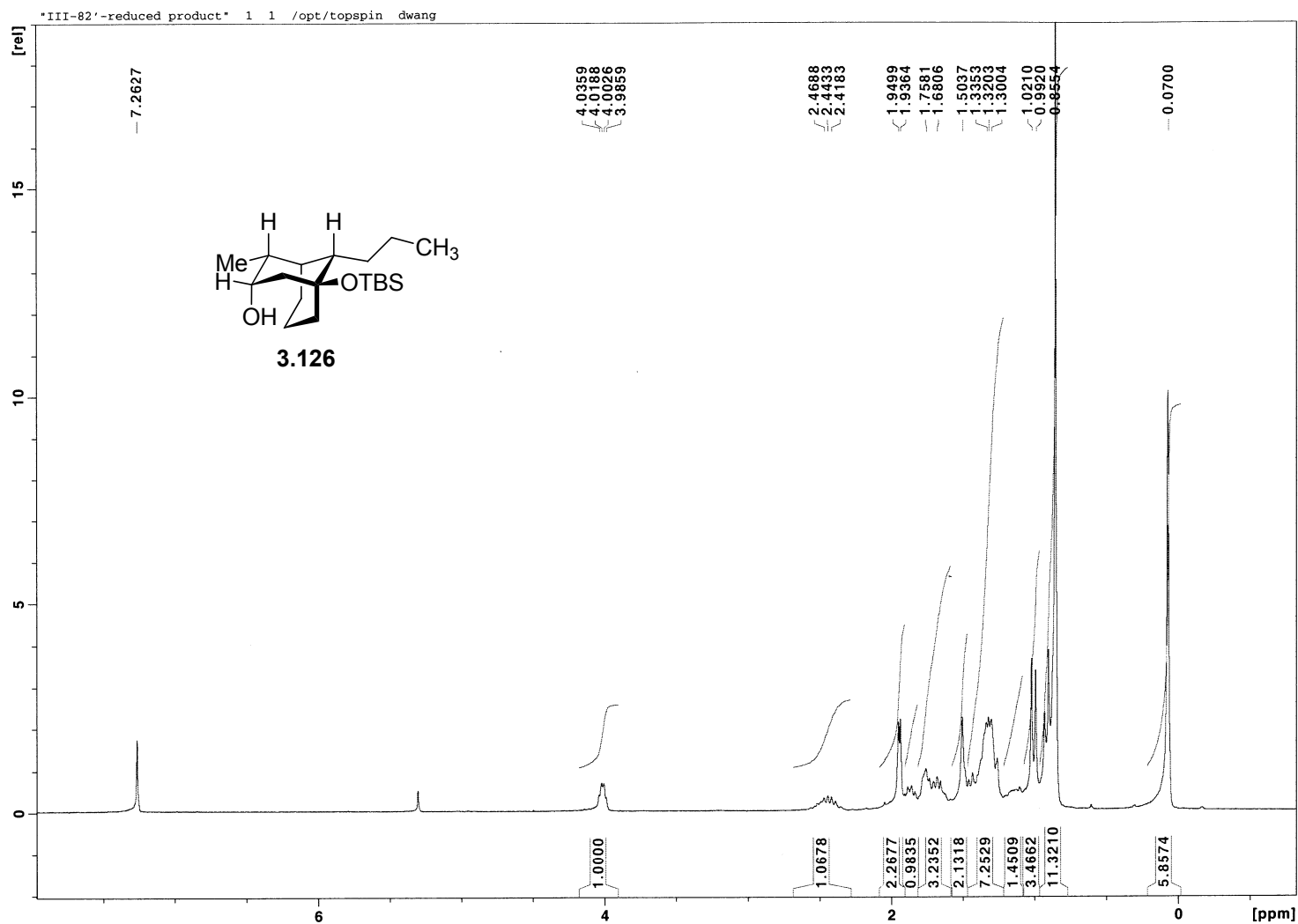


Figure 3.38 ¹H NMR (400 MHz, CDCl₃) of Compound 3.126

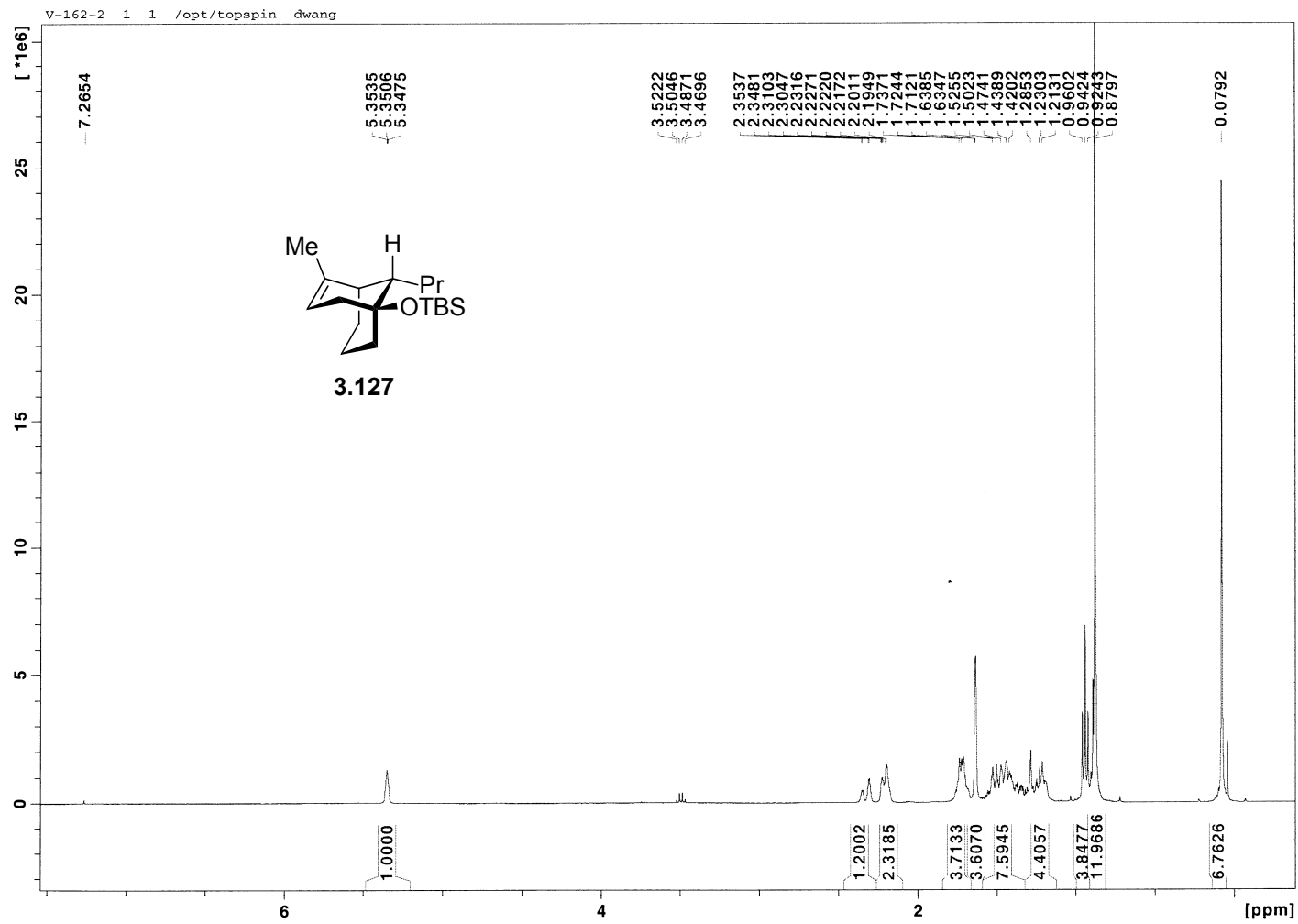


Figure 3.39 ^1H NMR (400 MHz, CDCl_3) of Compound 3.127

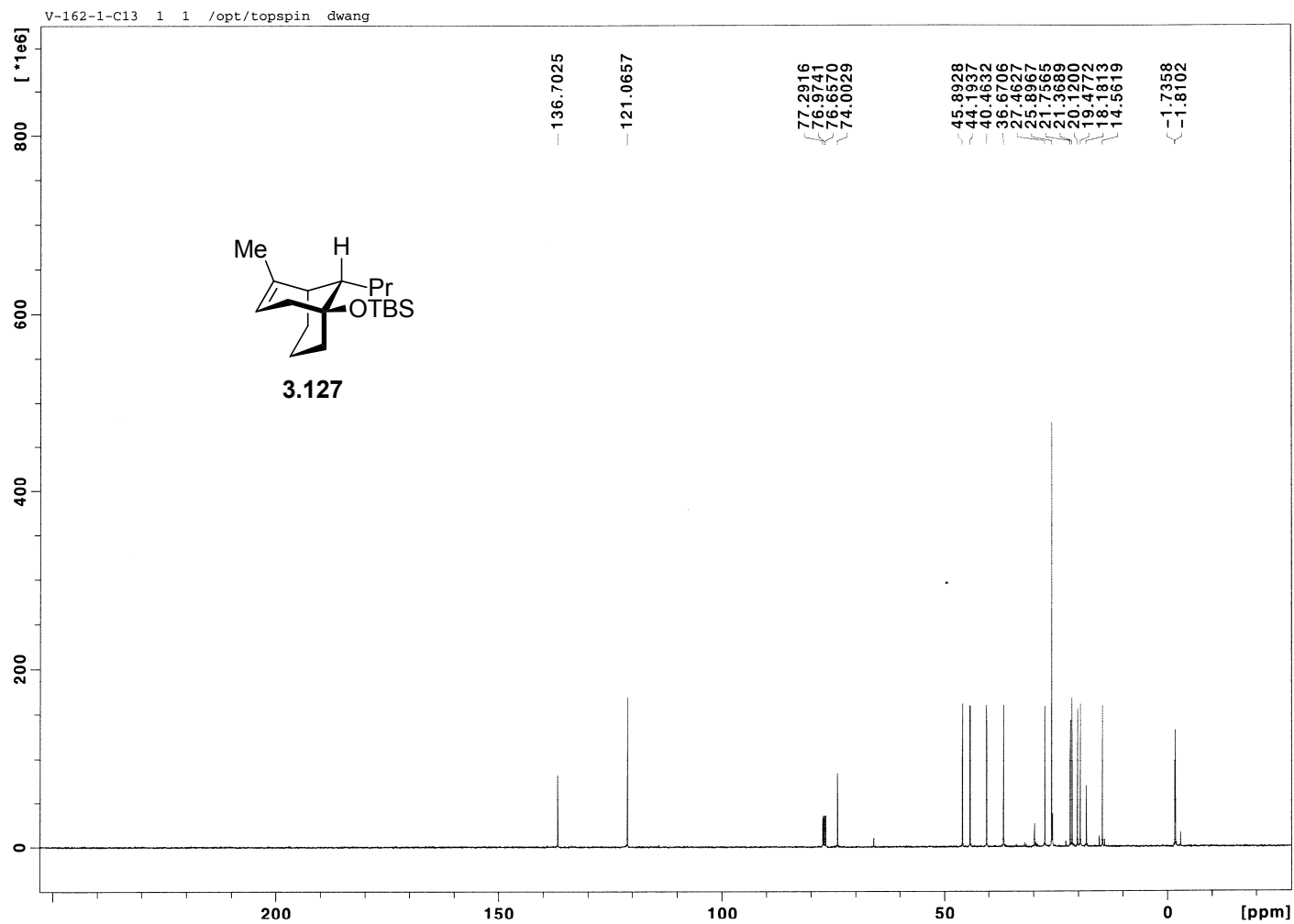


Figure 3.40 ^{13}C NMR (100 MHz, CDCl_3) of Compound 3.127

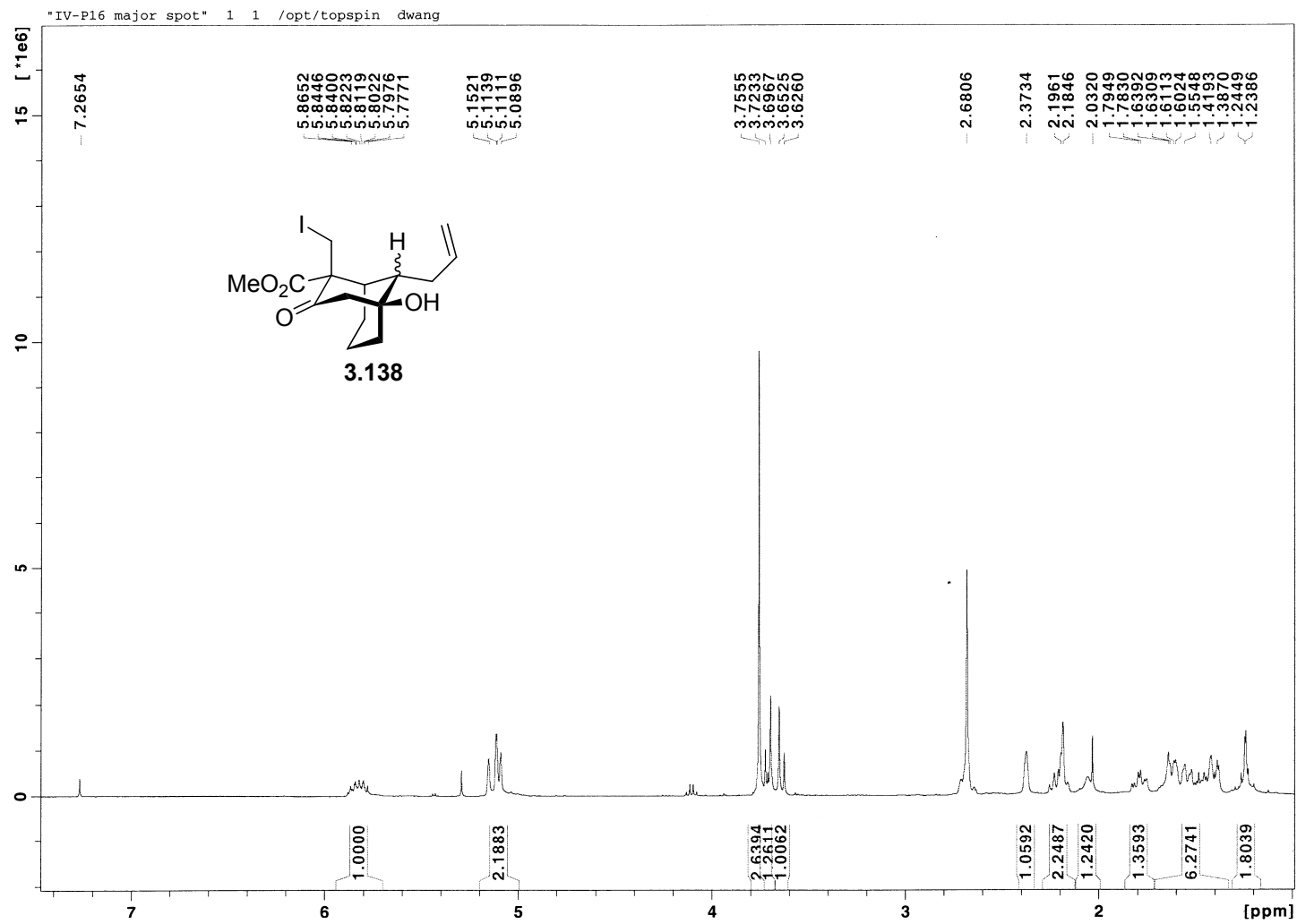


Figure 3.41 ¹H NMR (400 MHz, CDCl₃) of Compound 3.138

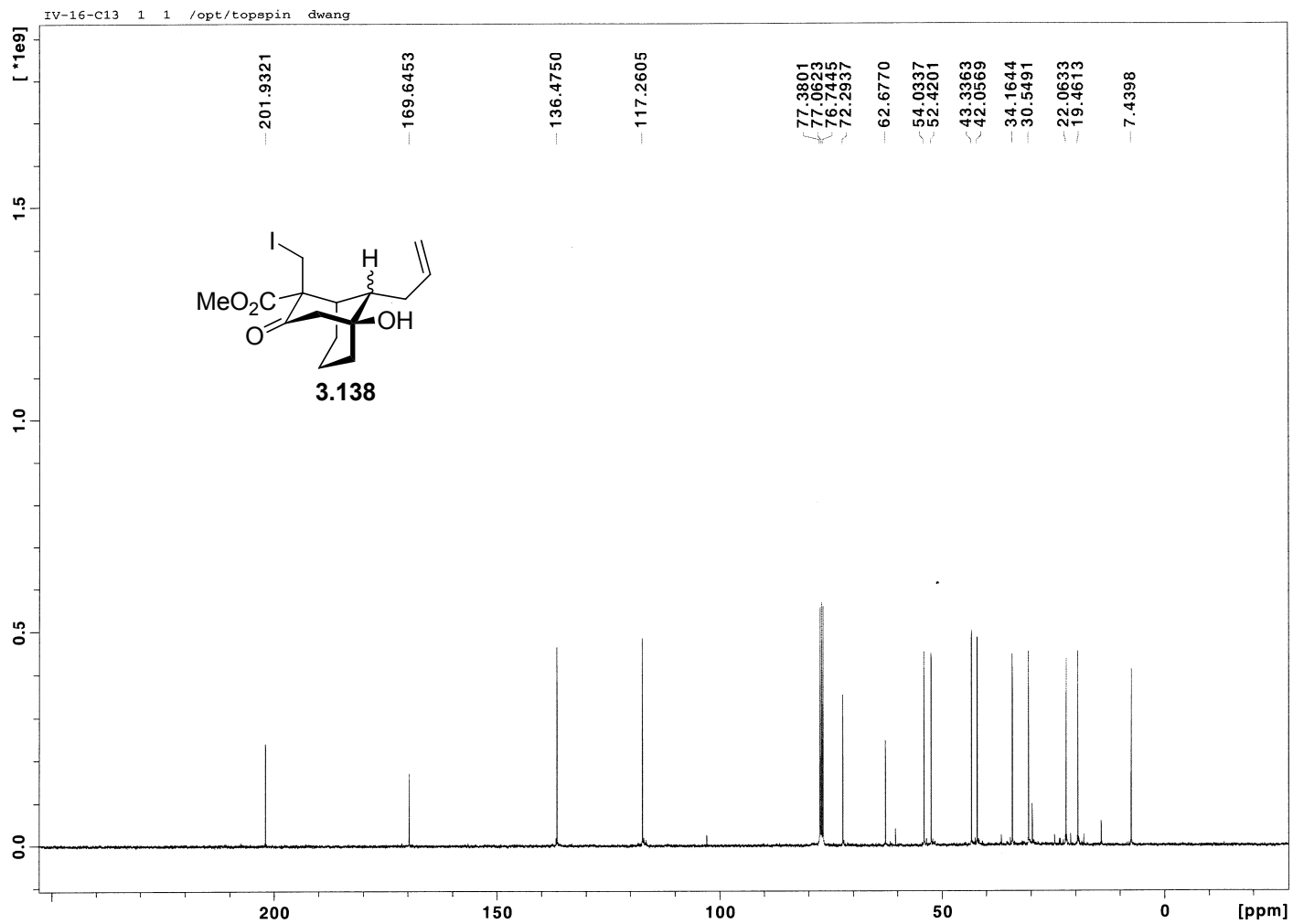


Figure 3.42 ^{13}C NMR (100 MHz, CDCl_3) of Compound 3.138

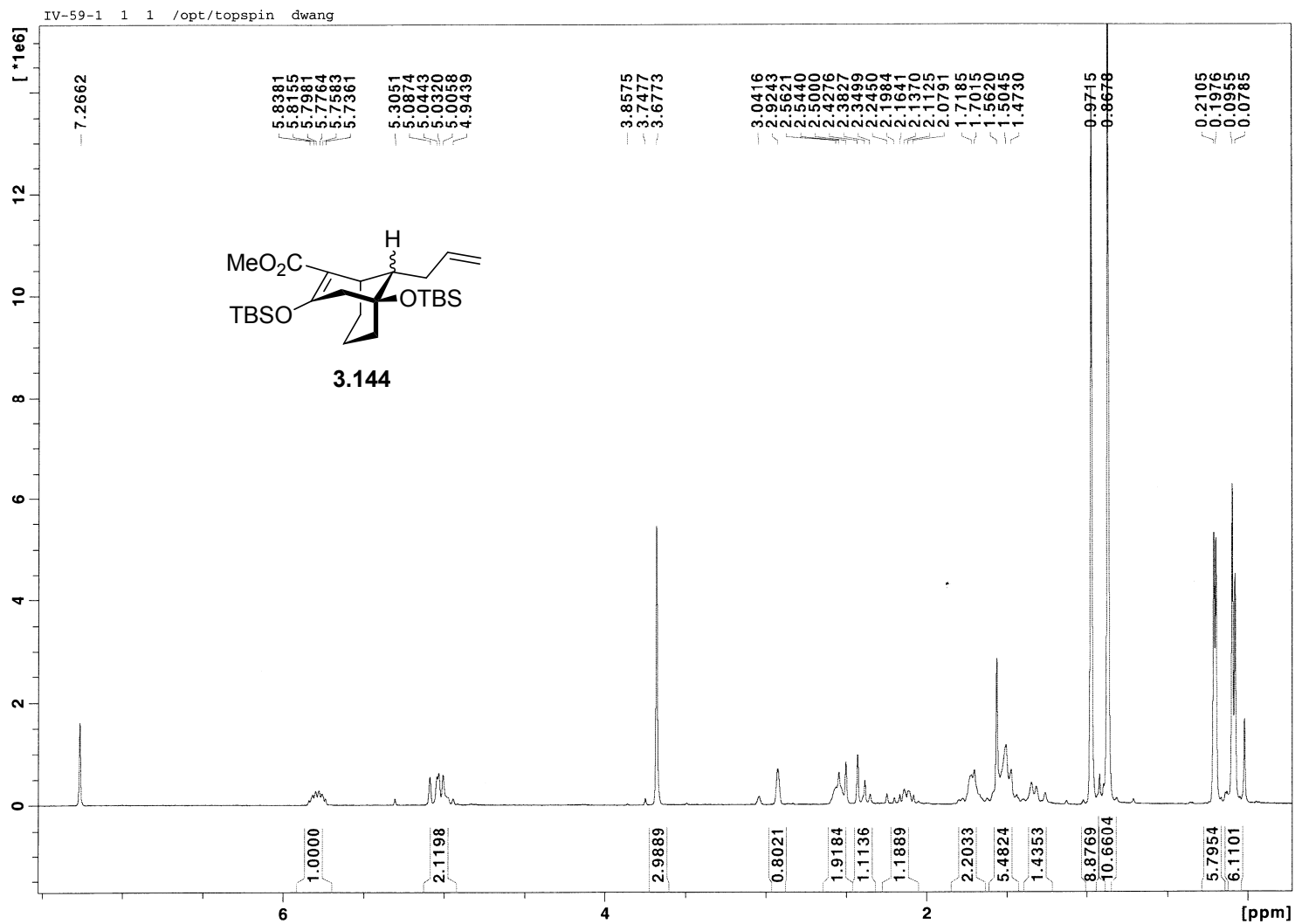


Figure 3.43 ¹H NMR (400 MHz, CDCl₃) of Compound 3.144

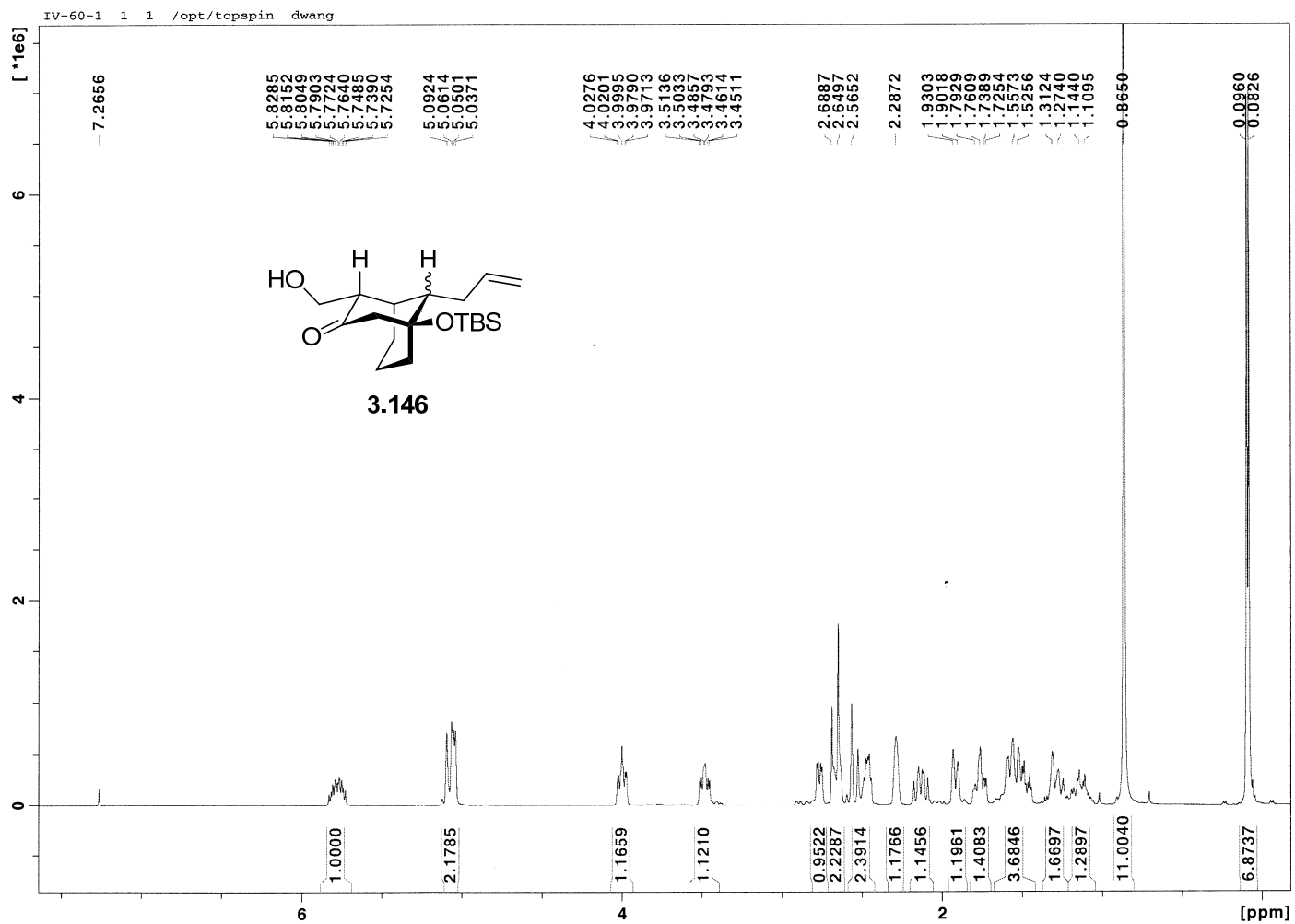


Figure 3.44 ^1H NMR (400 MHz, CDCl_3) of Compound 3.146

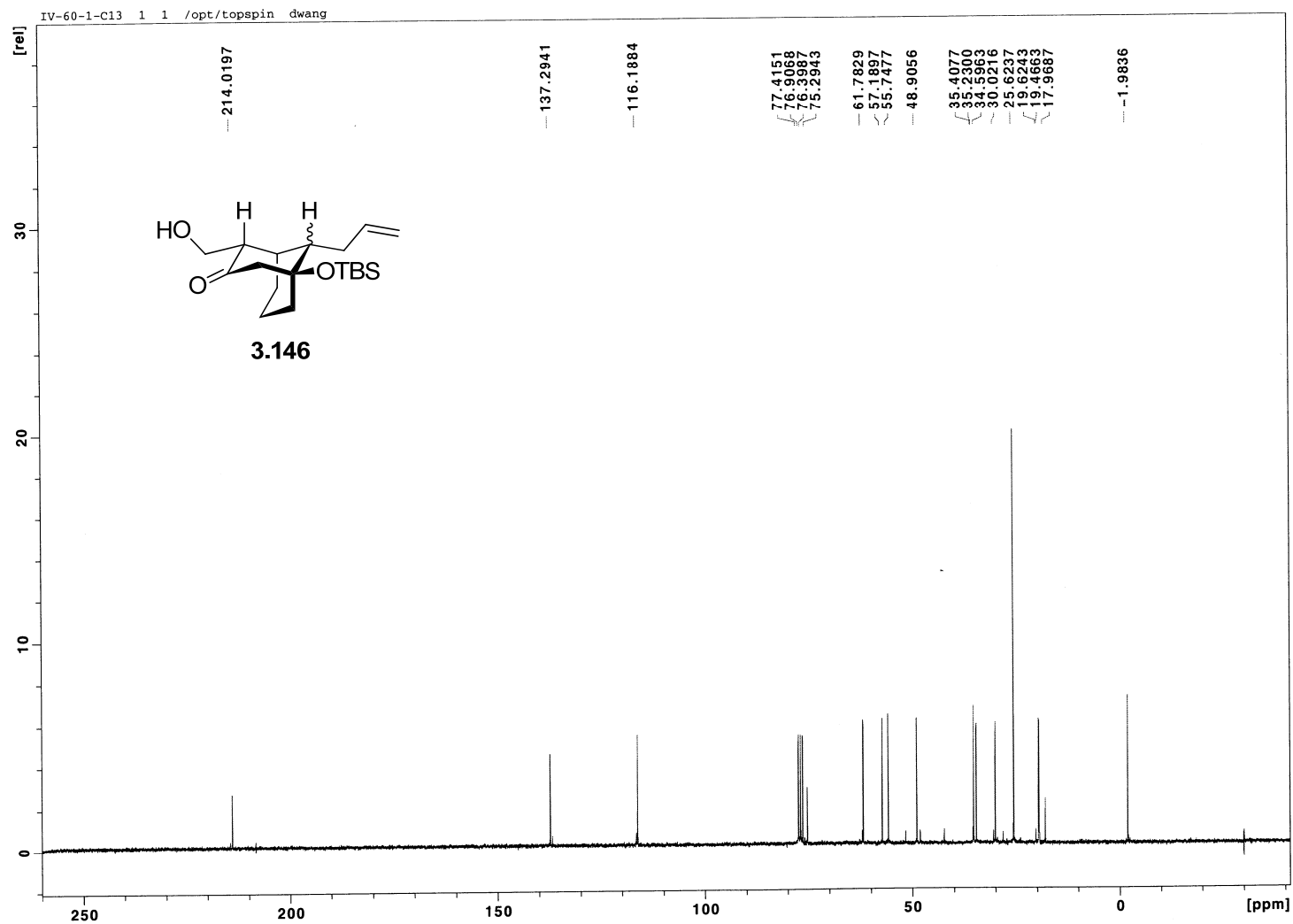


Figure 3.45 ^{13}C NMR (100 MHz, CDCl_3) of Compound 3.146

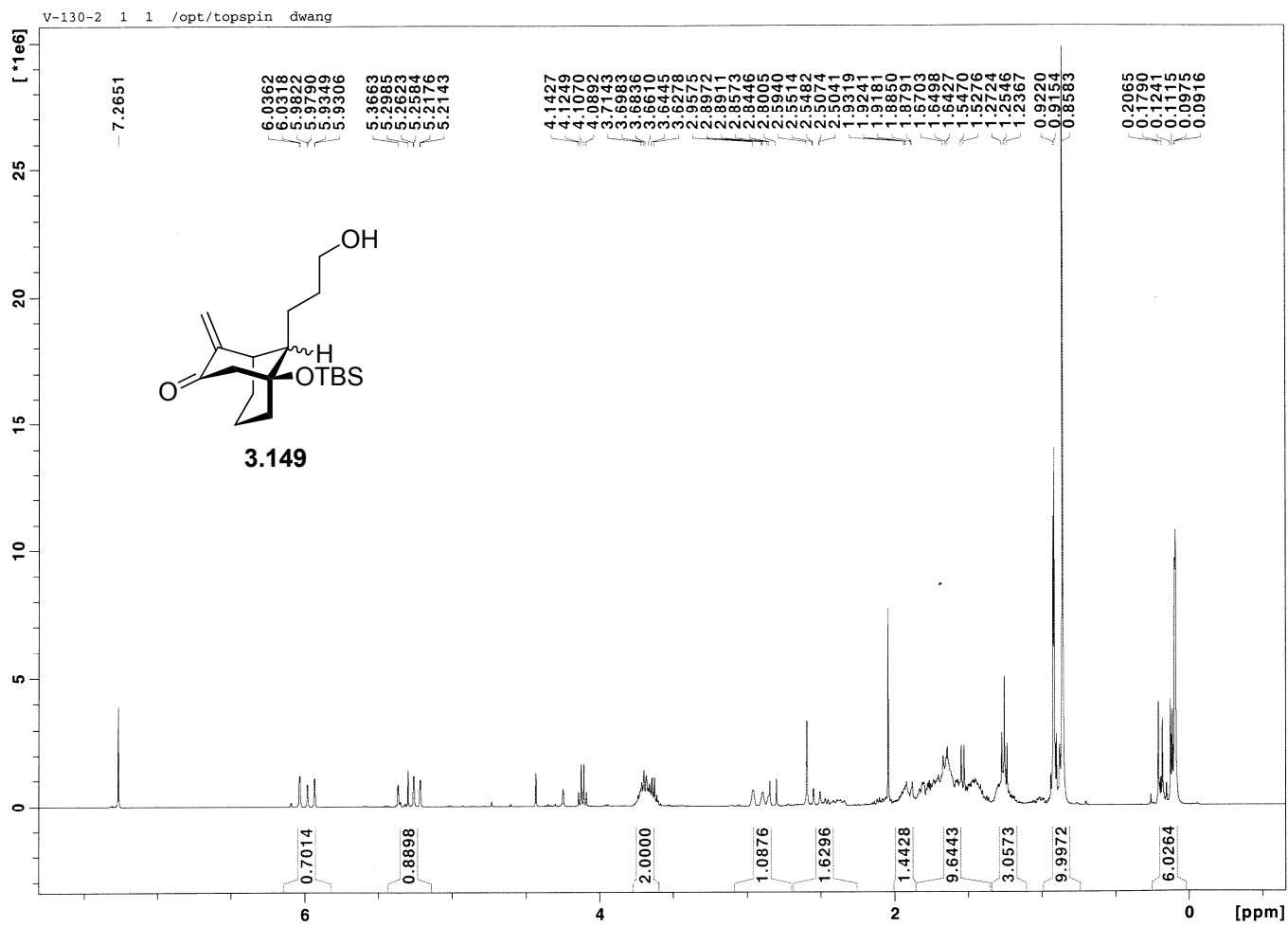


Figure 3.46 ^1H NMR (400 MHz, CDCl_3) of Compound 3.149

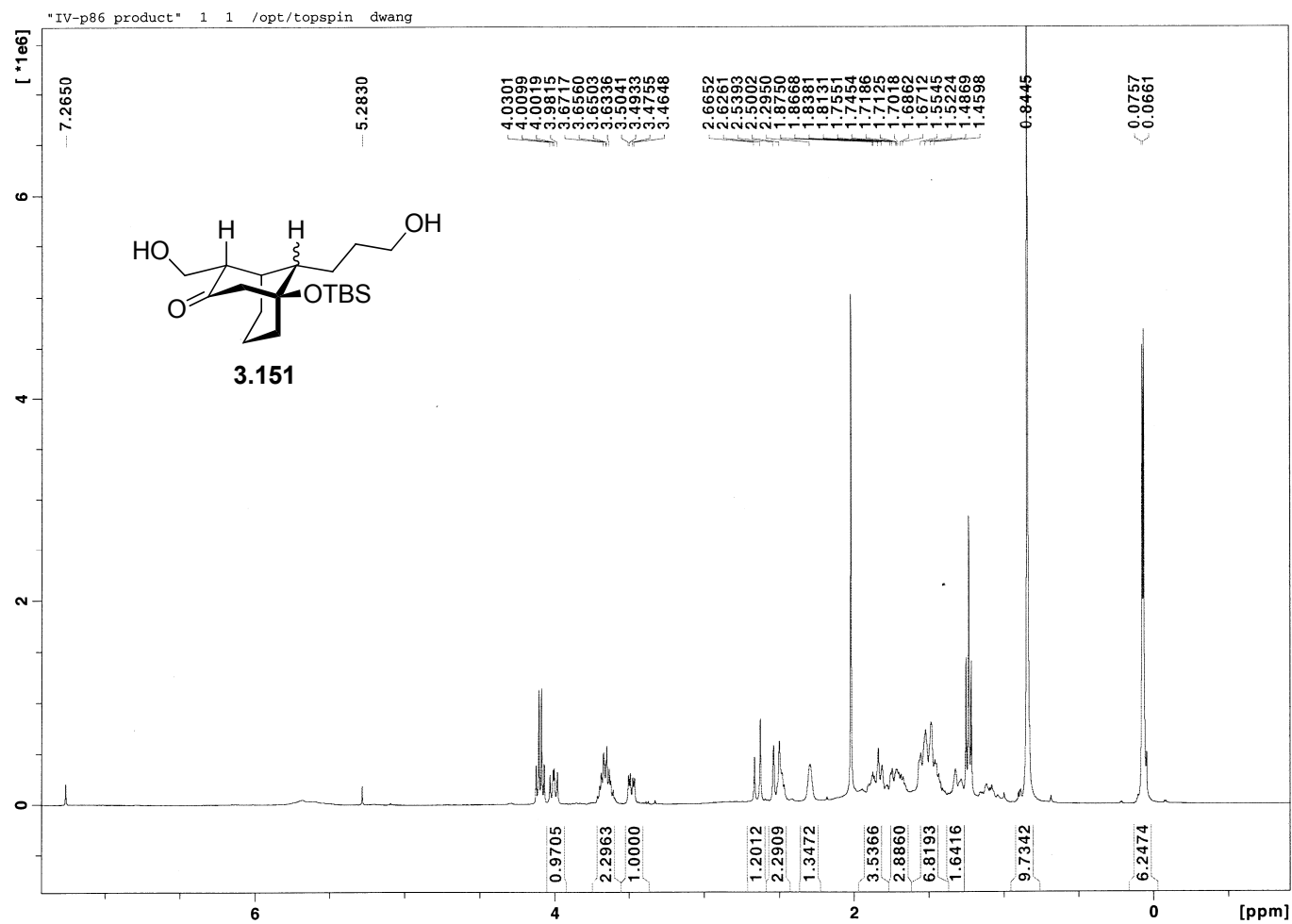


Figure 3.47 ^1H NMR (400 MHz, CDCl_3) of Compound 3.151

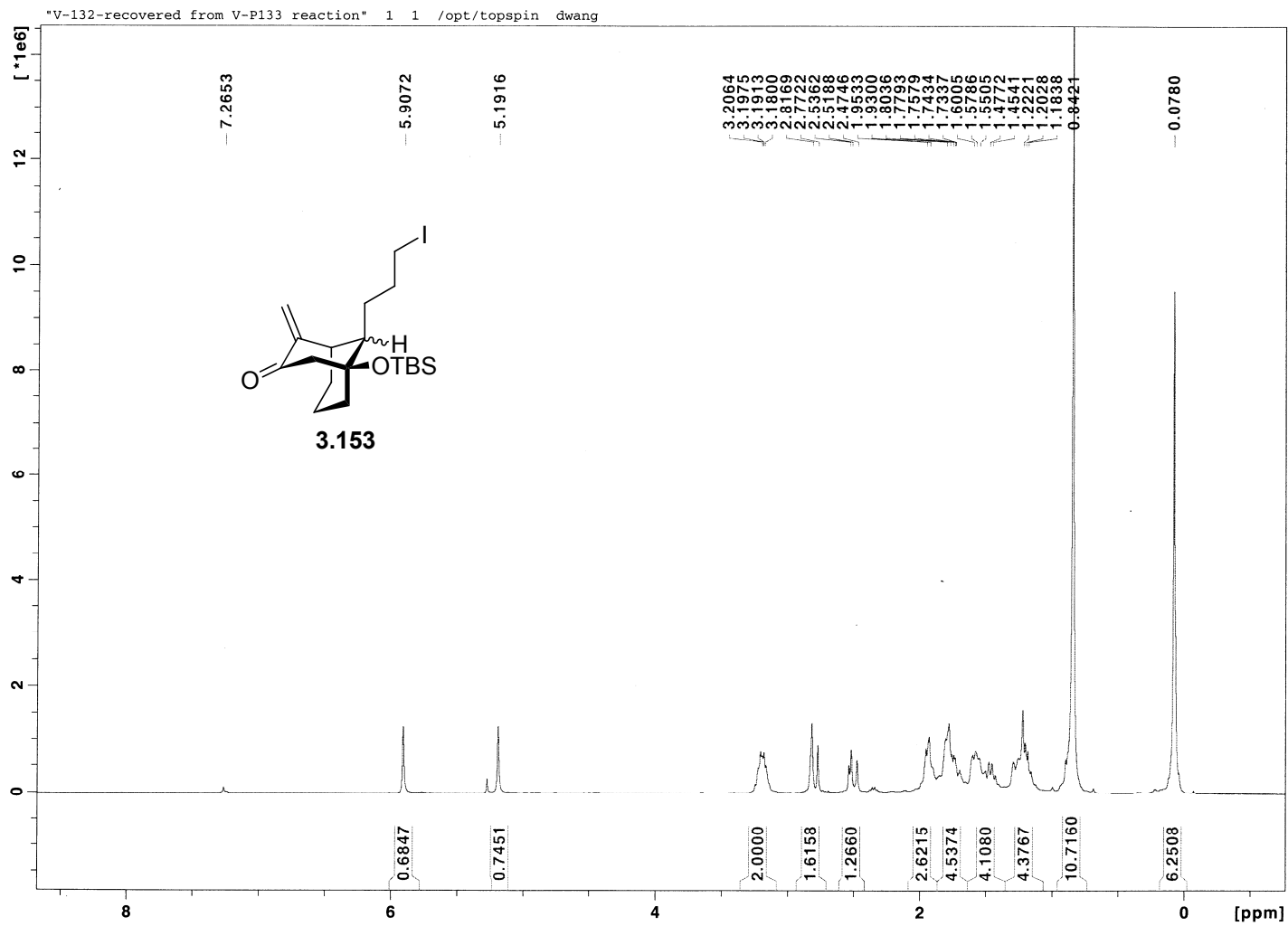


Figure 3.48 ^1H NMR (400 MHz, CDCl_3) of Compound 3.153

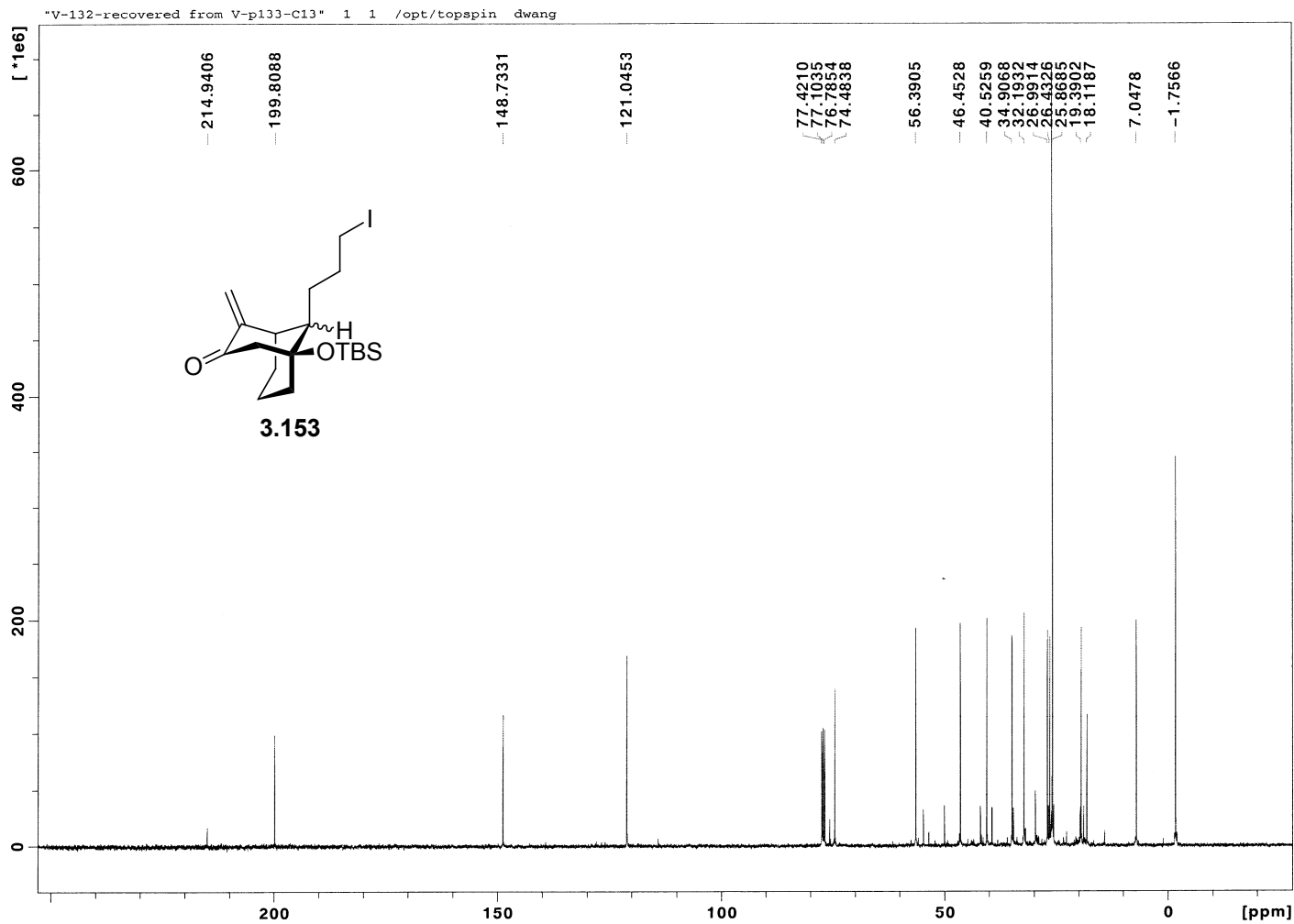


Figure 3.49 ^{13}C NMR (100 MHz, CDCl_3) of Compound 3.153

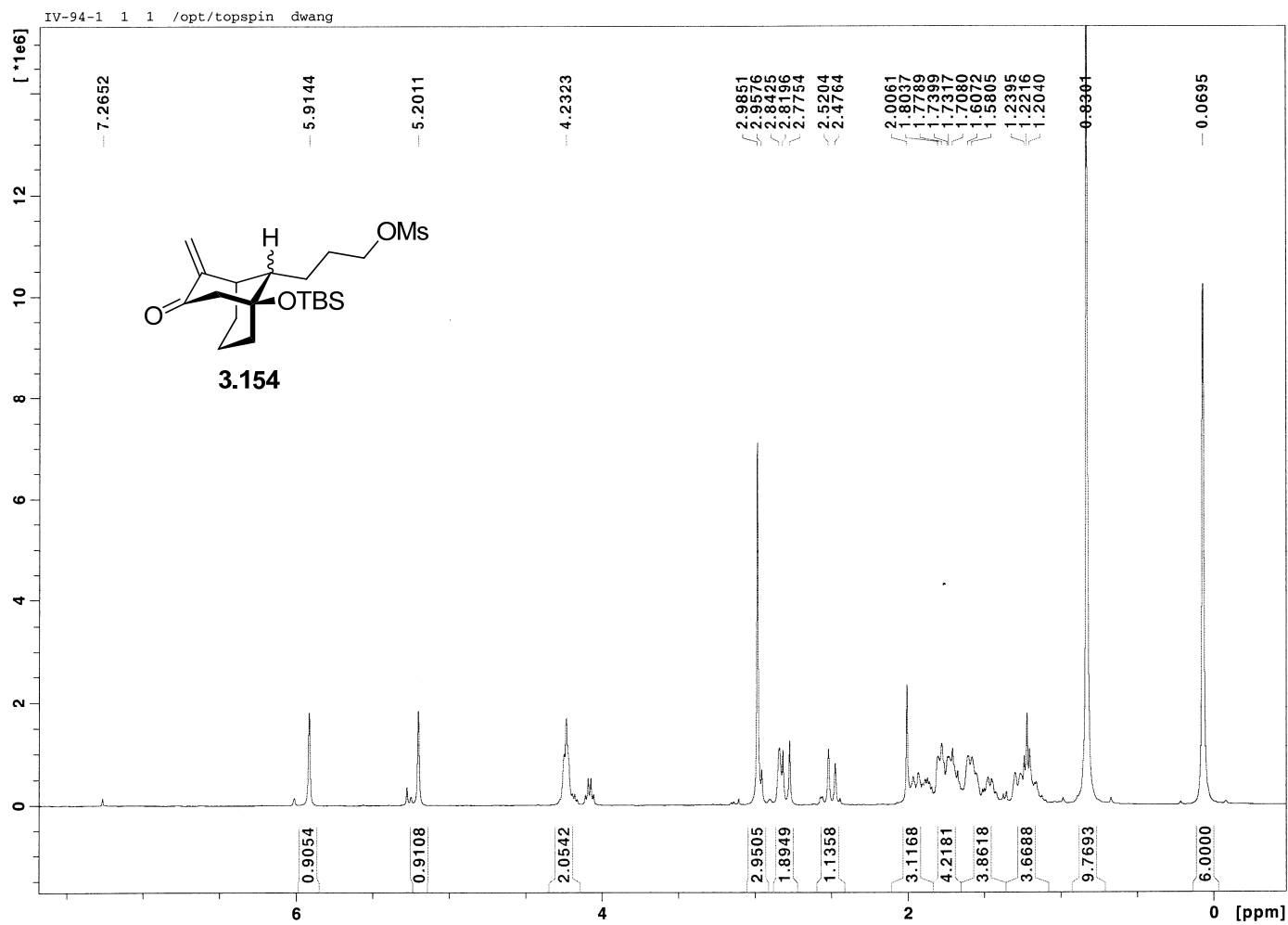


Figure 3.50 ^1H NMR (400 MHz, CDCl_3) of Compound 3.154

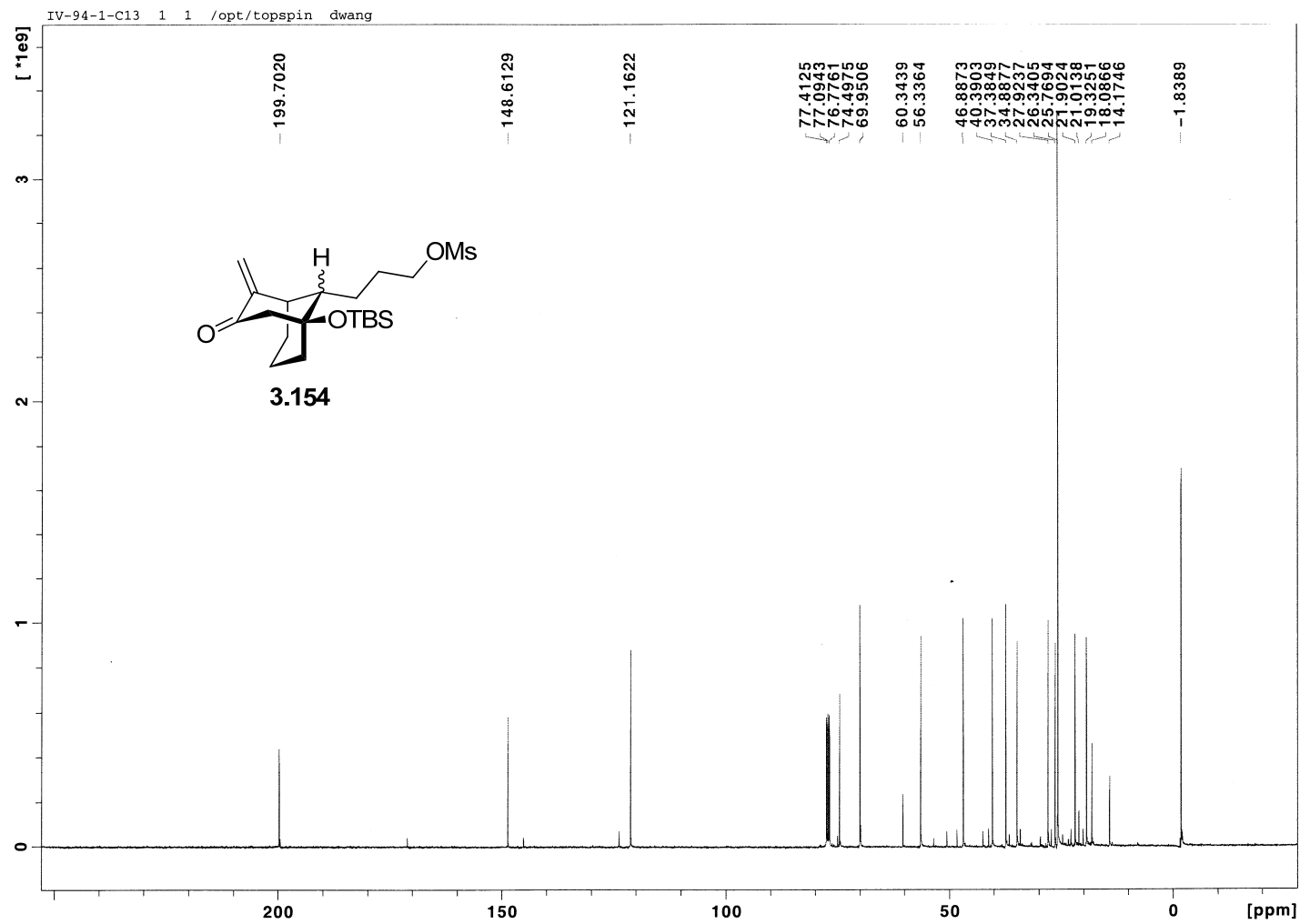


Figure 3.51 ^{13}C NMR (100 MHz, CDCl_3) of Compound 3.154

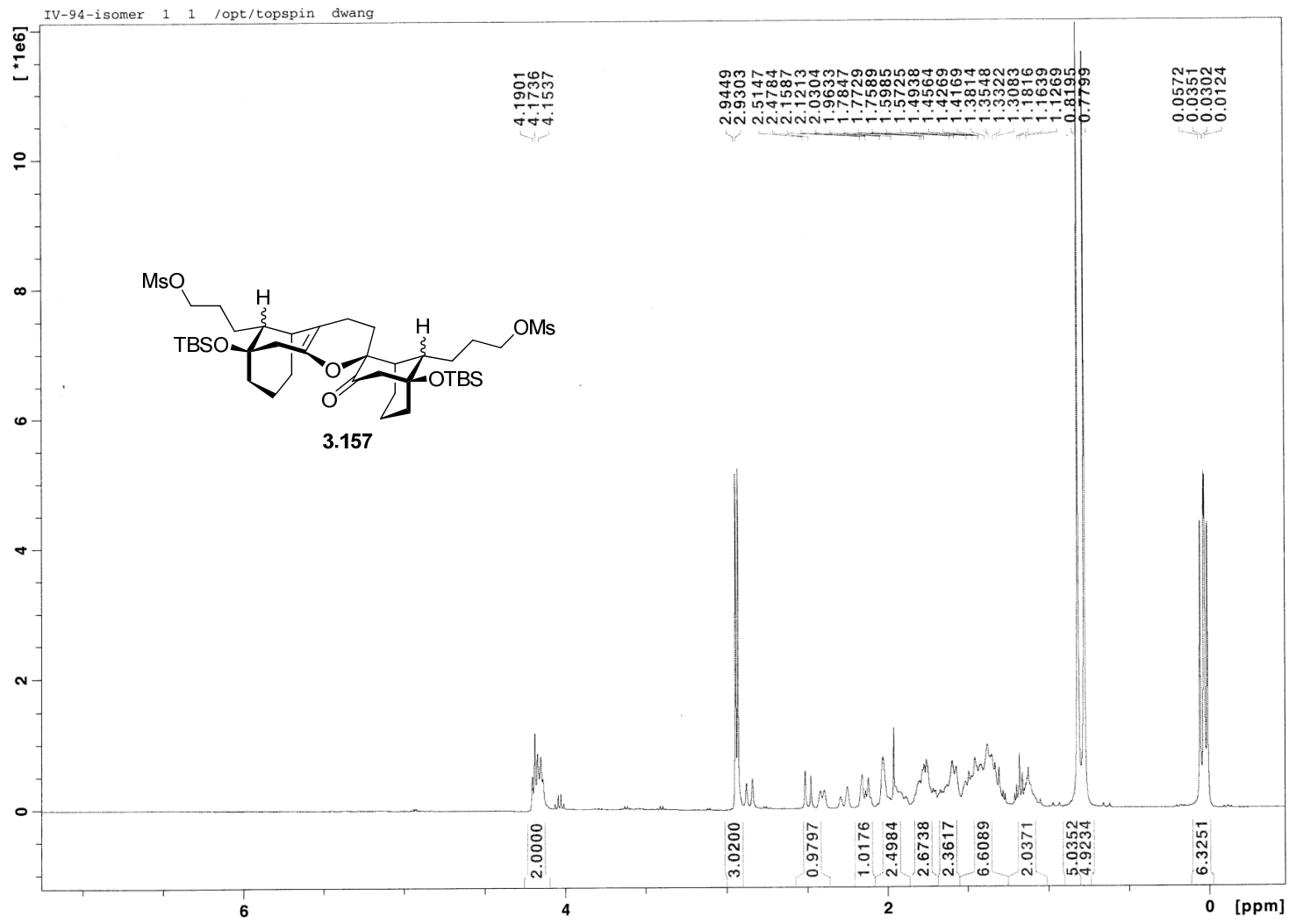


Figure 3.52 ¹H NMR (400 MHz, CDCl₃) of Compound 3.157

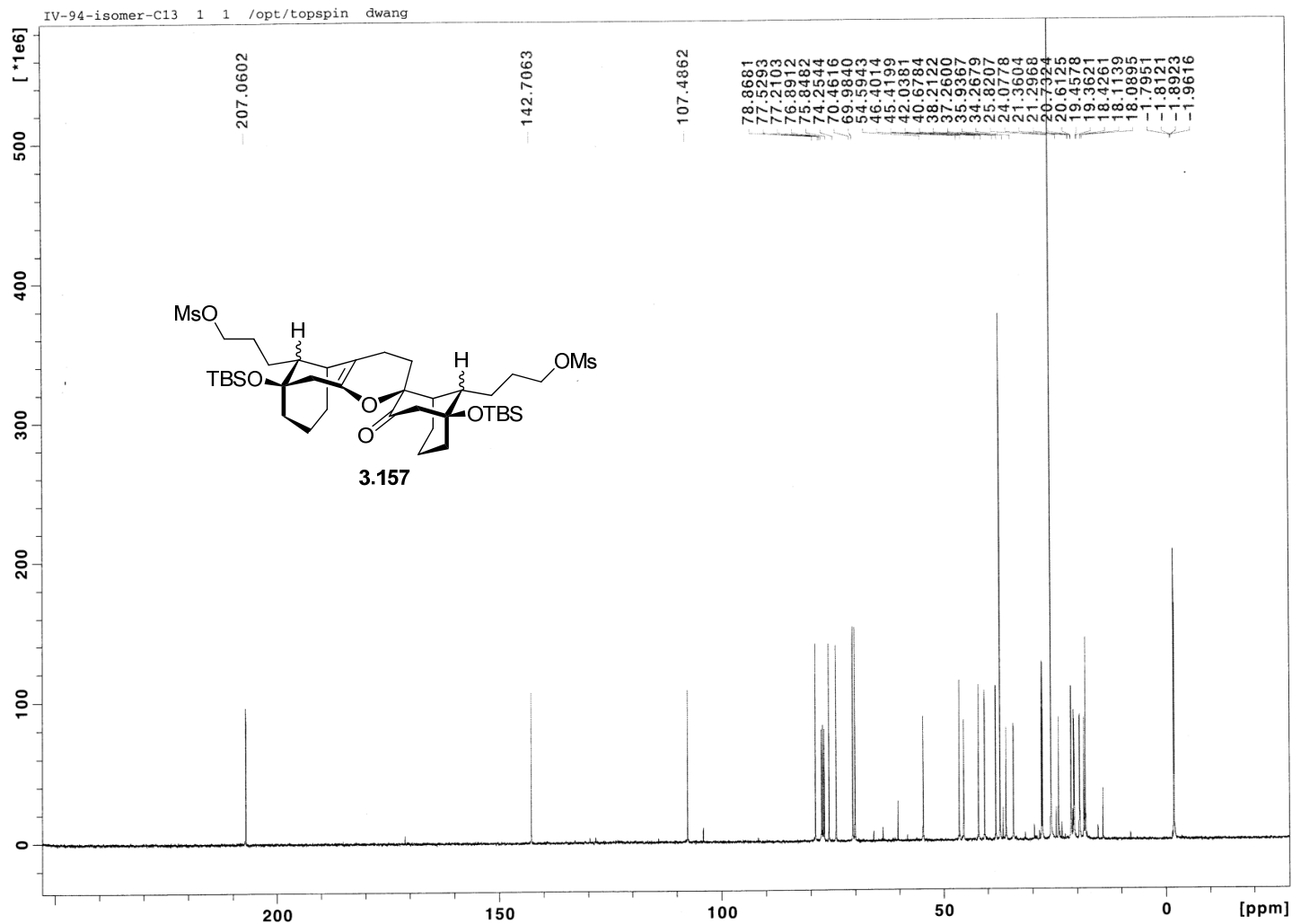


Figure 3.53 ^{13}C NMR (100 MHz, CDCl_3) of Compound 3.157

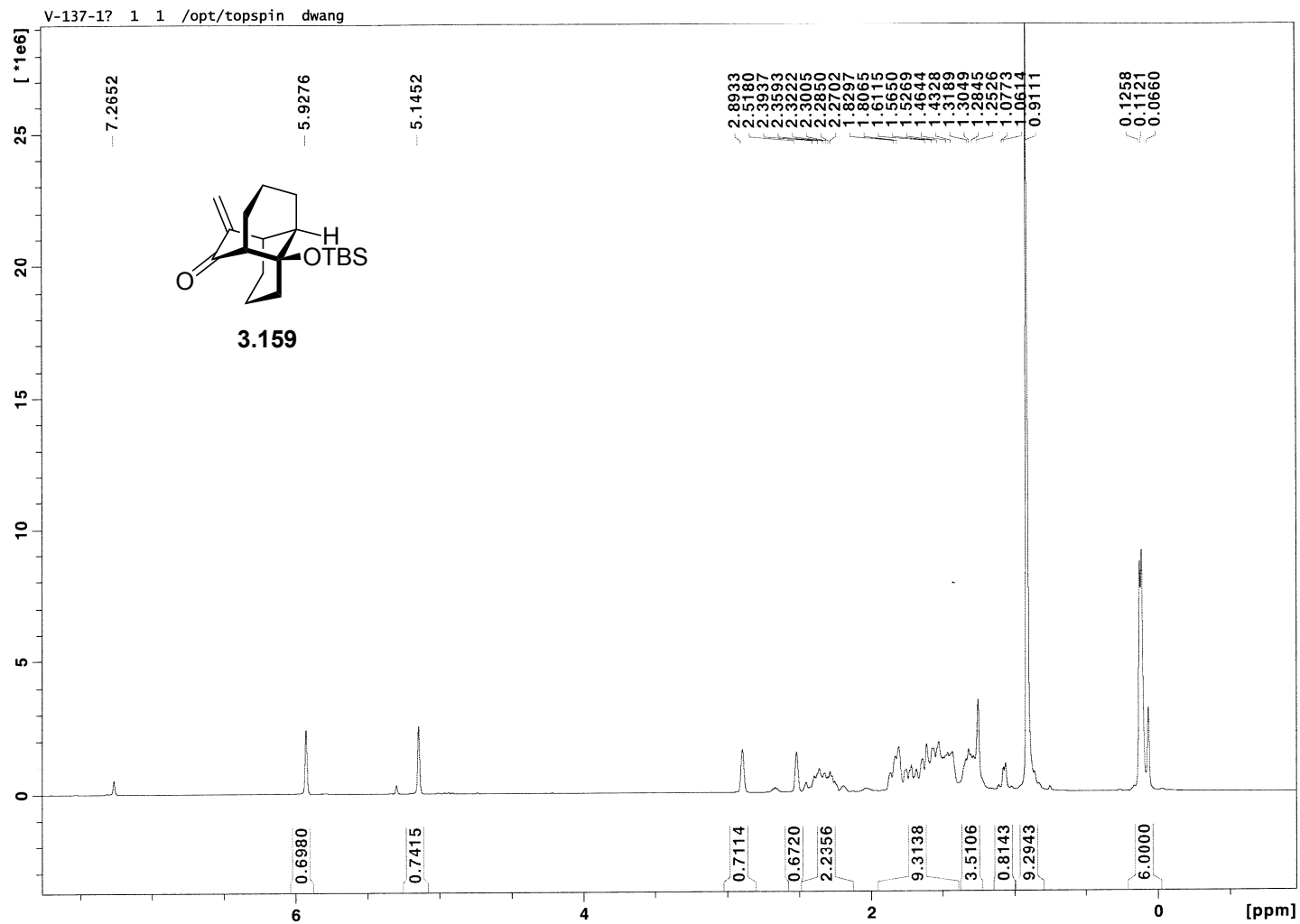


Figure 3.54 ^1H NMR (400 MHz, CDCl_3) of Compound 3.159

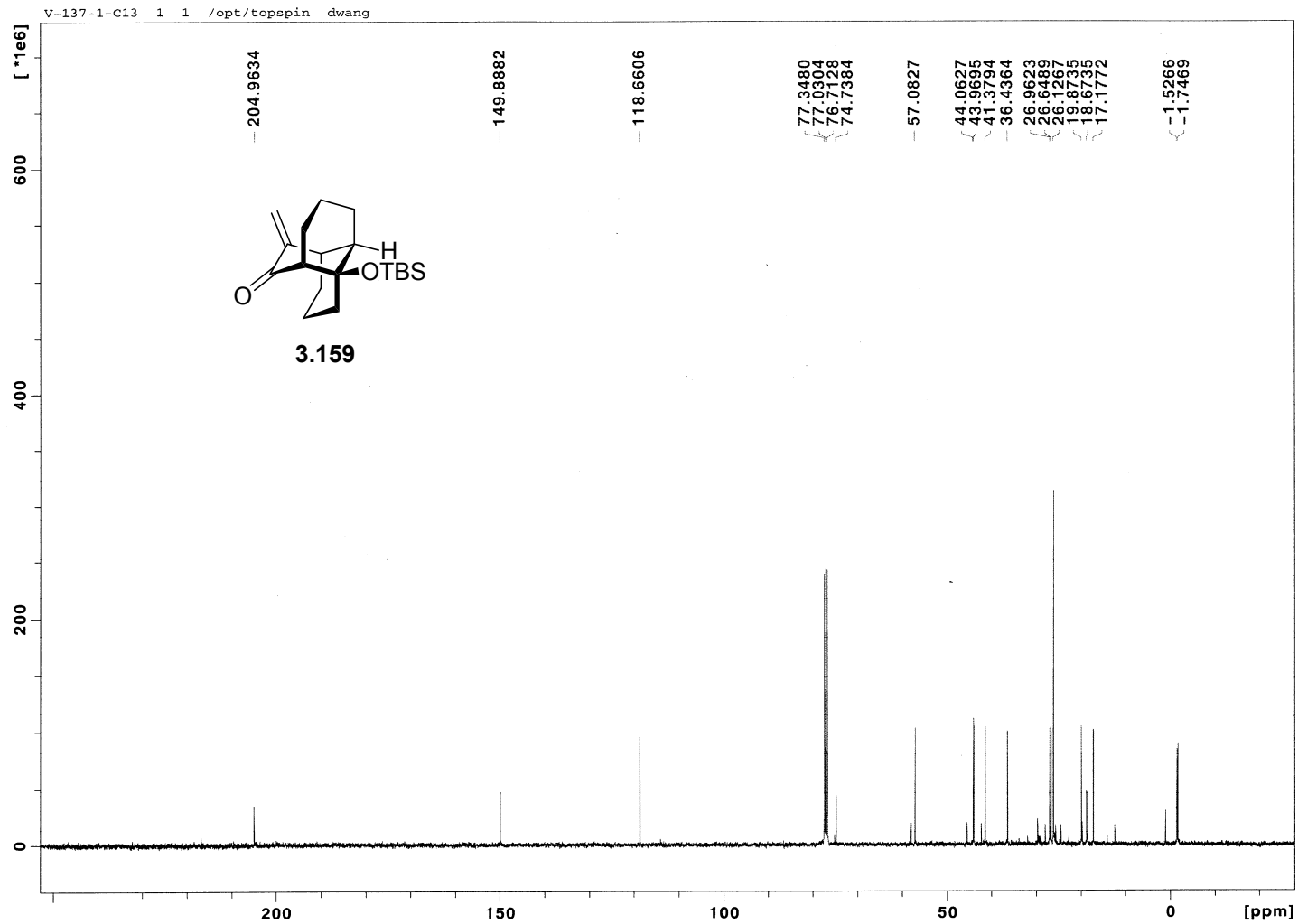


Figure 3.55 ^{13}C NMR (100 MHz, CDCl_3) of Compound 3.159

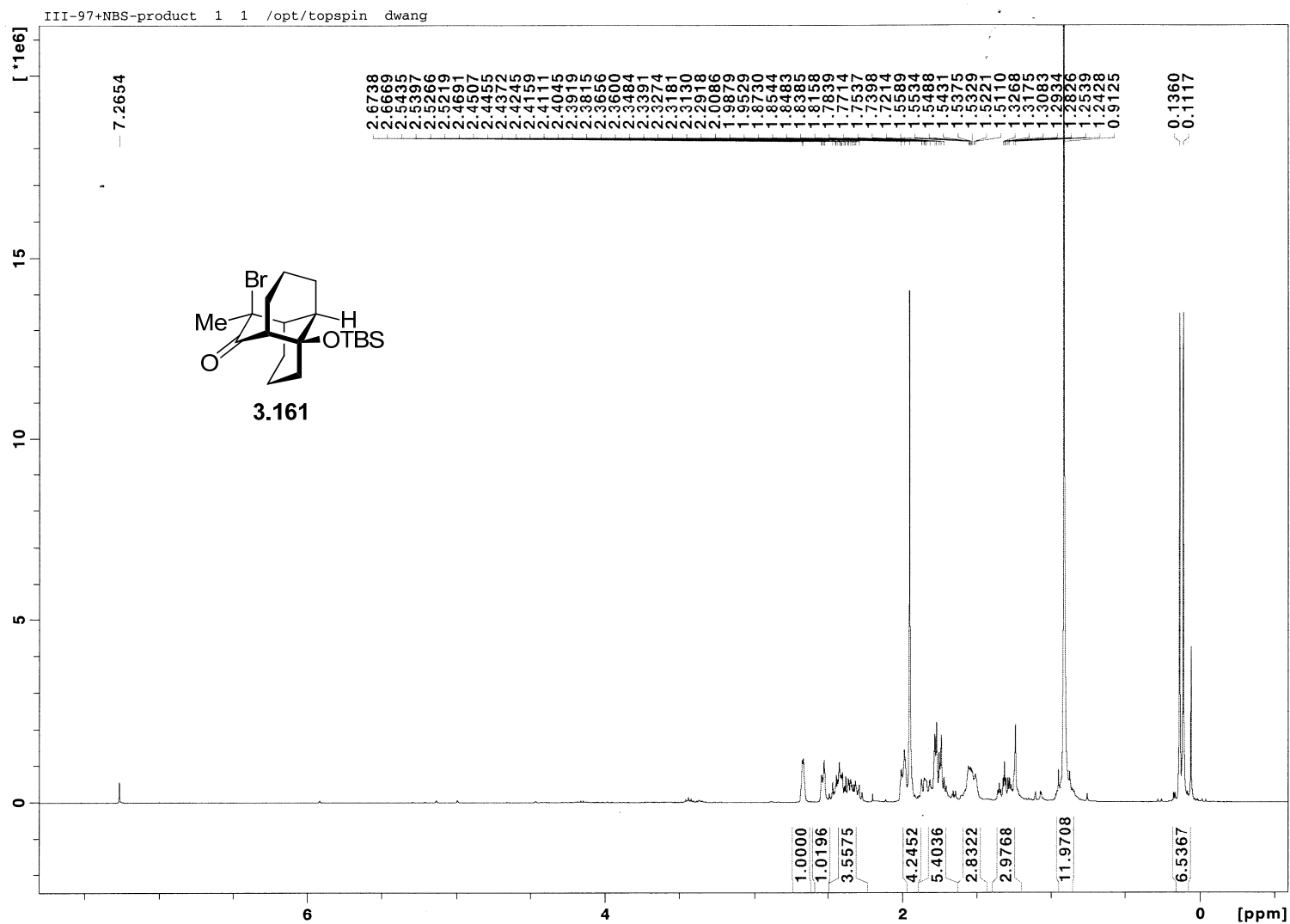


Figure 3.56 ¹H NMR (400 MHz, CDCl₃) of Compound 3.161

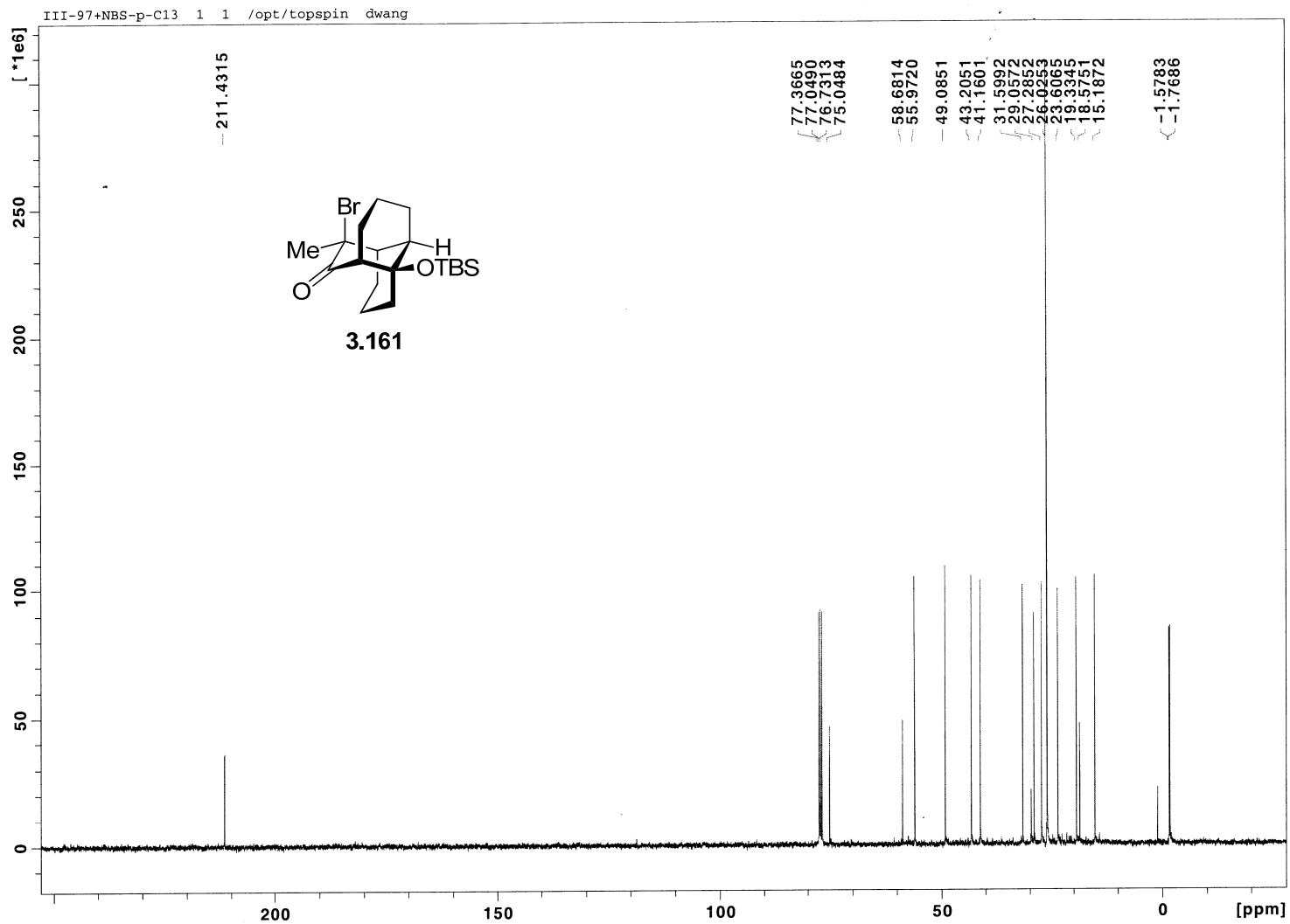


Figure 3.57 ^{13}C NMR (100 MHz, CDCl_3) of Compound 3.161

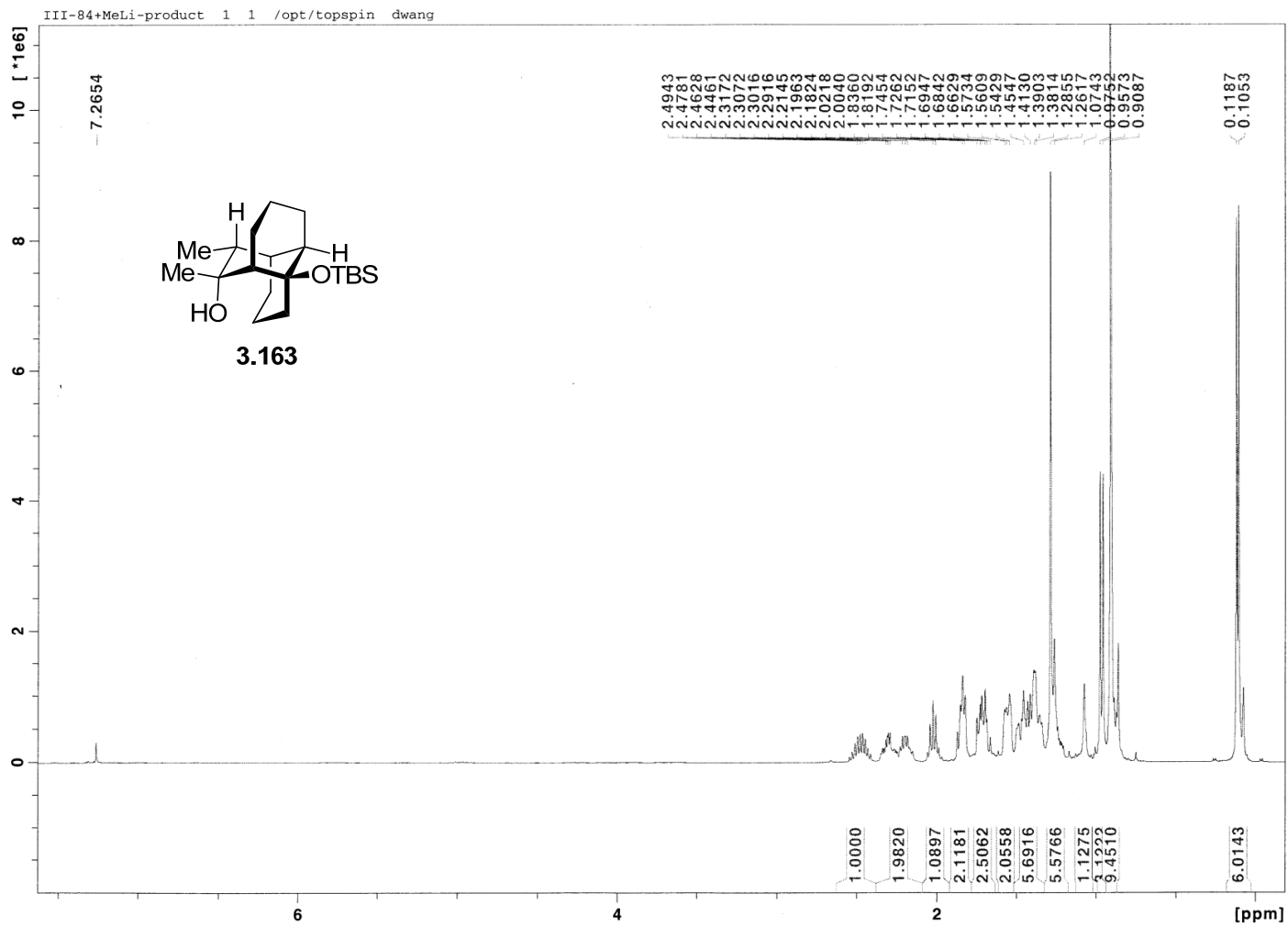


Figure 3.58 ^1H NMR (400 MHz, CDCl_3) of Compound 3.163

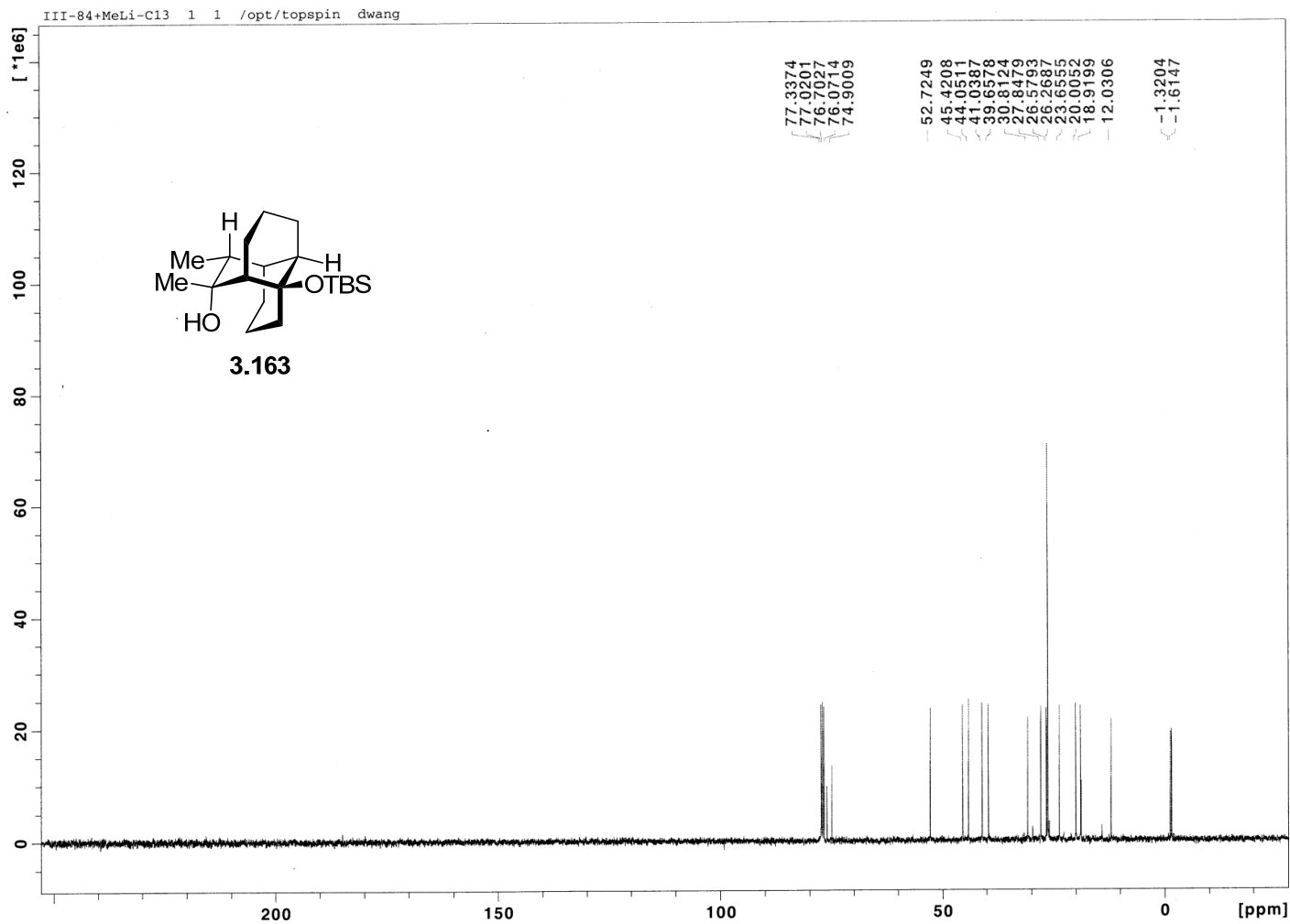


Figure 3.59 ^{13}C NMR (100 MHz, CDCl_3) of Compound 3.163

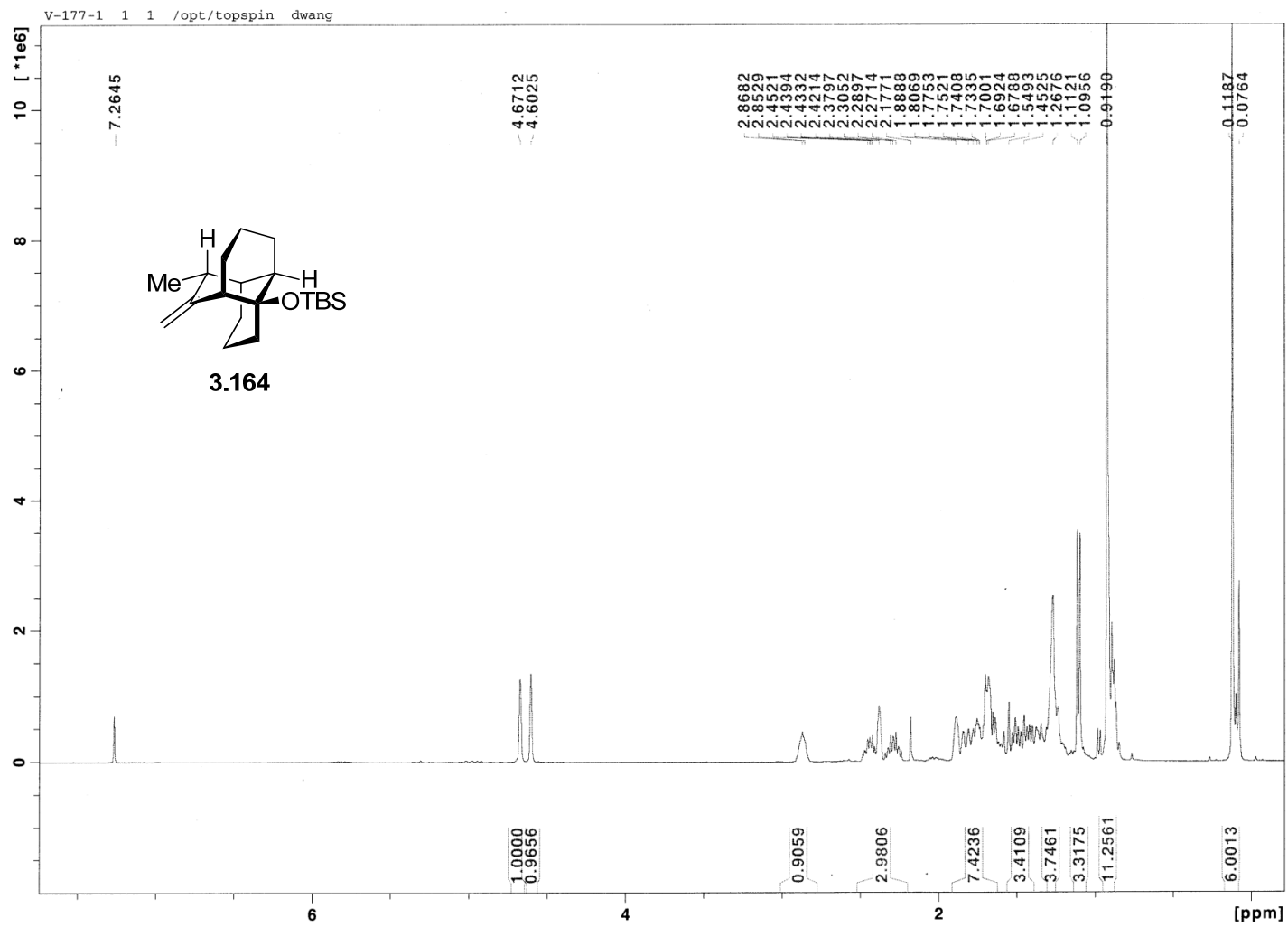


Figure 3.60 ^1H NMR (400 MHz, CDCl_3) of Compound 3.164

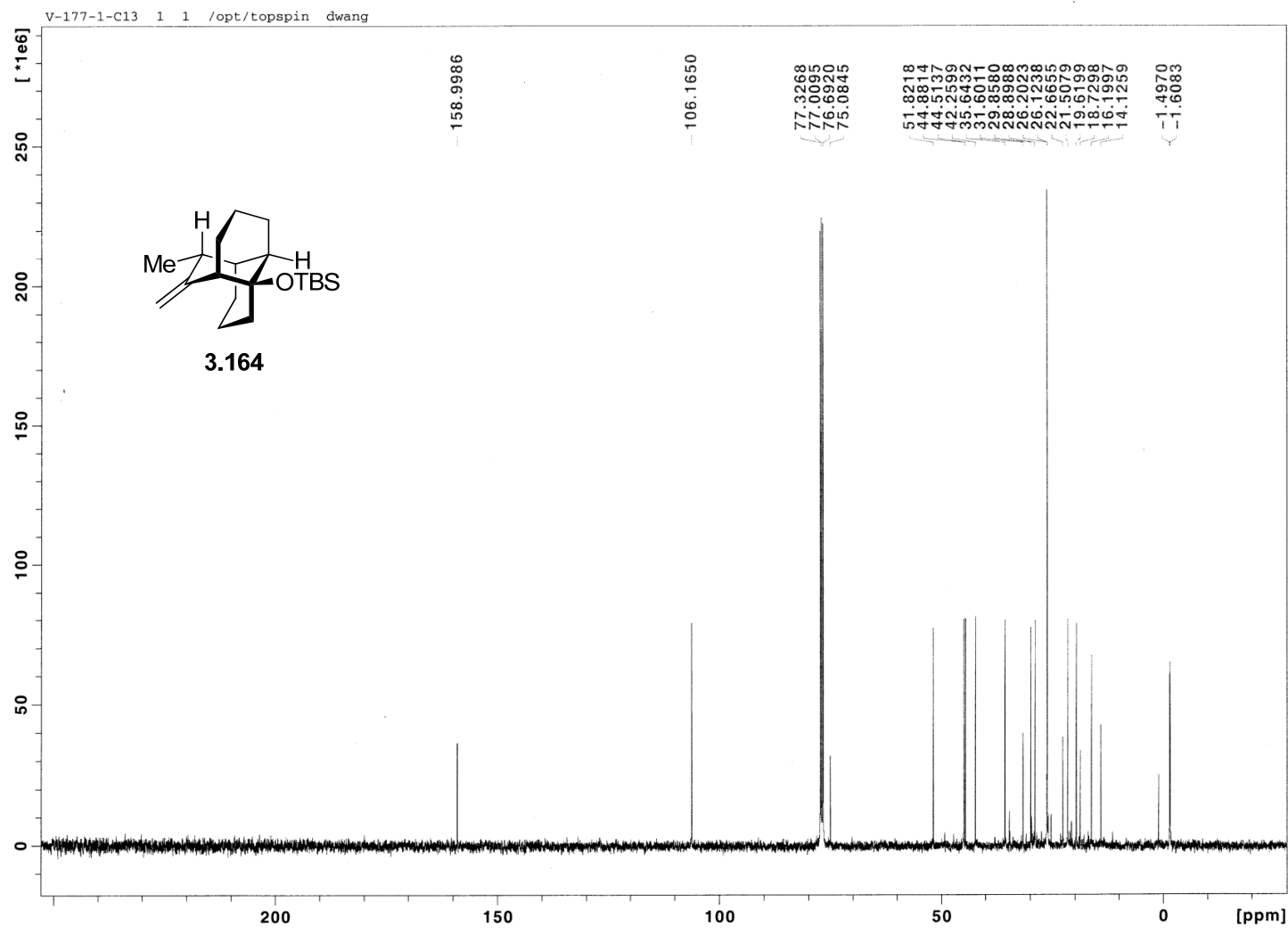


Figure 3.61 ^{13}C NMR (100 MHz, CDCl_3) of Compound 3.164

- [6] T. J. Maimone and P. S. Baran, *Nat. Chem. Biol.* **2007**, *3*, 396-407.
- [7] a) J. F. Devaux, I. Hanna and J. Y. Lallemand, *J. Org. Chem.* **1993**, *58*, 2349-2350; b) R. Guevel. Ph.D Thesis, The Ohio State University, **1994**; c) J. F. Devaux, I. Hanna, J. Y. Lallemand and T. Prange, *J. Chem. Res. Synth.* **1996**, 32-33; d) G. Mehta and K. S. Reddy, *Synlett* **1996**, 625-627; e) M. Kito, T. Sakai, N. Haruta, H. Shirahama and F. Matsuda, *Synlett* **1996**, 1057-1060; f) J. F. Devaux, I. Hanna and J. Y. Lallemand, *J. Org. Chem.* **1997**, *62*, 5062-5068; g) M. Kito, T. Sakai, H. Shirahama, M. Miyashita and F. Matsuda, *Synlett* **1997**, 219-220; h) F. Matsuda, T. Sakai, N. Okada and M. Miyashita, *Tetrahedron Lett.* **1998**, *39*, 863-864; i) F. Matsuda, M. Kito, T. Sakai, N. Okada, M. Miyashita and H. Shirahama, *Tetrahedron* **1999**, *55*, 14369-14380; j) I. V. Efremov. Ph.D. Thesis, The Ohio State University, **2001**; k) L. Gentric, I. Hanna and L. Ricard, *Org. Lett.* **2003**, *5*, 1139-1142; l) L. A. Paquette, R. Guevel, S. Sakamoto, I. H. Kim and J. Crawford, *J. Org. Chem.* **2003**, *68*, 6096-6107; m) L. Morency and L. Barriault, *Tetrahedron Lett.* **2004**, *45*, 6105-6107; n) L. Morency and L. Barriault, *J. Org. Chem.* **2005**, *70*, 8841-8853; o) L. A. Paquette, I. Efremov and Z. S. Liu, *J. Org. Chem.* **2005**, *70*, 505-509; p) L. A. Paquette and I. Efremov, *J. Org. Chem.* **2005**, *70*, 510-513; q) L. A. Paquette, Z. S. Liu and I. Efremov, *J. Org. Chem.* **2005**, *70*, 514-518; r) L. Morency. Ph.D. Thesis, University of Ottawa, **2006**; s) C. M. Grise, G. Tessier and L. Barriault, *Org. Lett.* **2007**, *9*, 1545-1548; t) M. S. Souweha, G. D. Enright and A. G. Fallis, *Org. Lett.* **2007**, *9*, 5163-5166; u) T. J. Maimone, A. F. Voica and P. S. Baran, *Angew. Chem., Int. Ed.* **2008**, *47*, 3054-3056; v) J. A. Brekan. Ph.D. Thesis, State University of New York, **2008**; w) J. G. M. Morton, L. D. Kwon, J. D. Freeman and J. T. Njardarson, *Tetrahedron Lett.* **2009**, *50*, 1684-1686; x) J. G. M. Morton, L. D. Kwon, J. D. Freeman and J. T. Njardarson, *Synlett* **2009**, 23-27; y) J. G. M. Morton, C. Draghici, L. D. Kwon and J. T. Njardarson, *Org. Lett.* **2009**, *11*, 4492-4495; z) T. J. Maimone, J. Shi, S. Ashida and P. S. Baran, *J. Am. Chem. Soc.* **2009**, *131*, 17066-17067; aa) T. J. Maimone. Ph.D. Thesis, The Scripps Research Institute, **2009**; ab) L. Gentric, X. Le Goff, L. Ricard and I. Hanna, *J. Org. Chem.* **2009**, *74*, 9337-9344.
- [8] a) G. Tessier and L. Barriault, *Org. Prep. Proc. Int.* **2007**, *39*, 311-353; b) J. Y. Lu and D. G. Hall, *Angew. Chem., Int. Ed.* **2010**, *49*, 2286-2288; c) A. D. Hutters and N. K. Garg, *Chem.—Eur. J.* **2010**, *16*, 8586-8595.
- [9] a) J. E. Baldwin, *J. Chem. Soc., Chem. Commun.* **1976**, 734-736; b) J. E. Baldwin and M. J. Lusch, *Tetrahedron* **1982**, *38*, 2939-2947.
- [10] P. G. Baraldi, A. Barco, S. Benetti, G. P. Pollini and V. Zanirato, *Tetrahedron Lett.* **1984**, *25*, 4291-4294.
- [11] G. W. Kabalka, S. Yu and N. S. Li, *Tetrahedron Lett.* **1997**, *38*, 5455-5458.
- [12] a) H. Seto, Y. Fujimoto, T. Tatsuno and H. Yoshioka, *Synth. Commun.* **1985**, *15*, 1217-1224; b) H. Seto, M. Sakaguchi, Y. Fujimoto, T. Tatsuno and H. Yoshioka, *Chem. Pharm. Bull.* **1985**, *33*, 412-415; c) H. Seto, S. Tsunoda, H. Ikeda, Y. Fujimoto, T. Tatsuno and H. Yoshioka, *Chem. Pharm. Bull.* **1985**, *33*, 2594-2597.
- [13] a) P. Demayo, H. Takeshita and A. Sattar, *Proc. Chem. Soc. (London)* **1962**, 119-119; b) E.

- J. Corey, R. Lemahieu, R. B. Mitra and J. D. Bass, *J. Am. Chem. Soc.* **1964**, *86*, 5570-5583.
- [14] G. Cardinale, J. A. M. Laan and J. P. Ward, *Tetrahedron* **1985**, *41*, 2899-2902.
- [15] D. Bellus and P. Hrdlovic, *Chem. Rev.* **1967**, *67*, 599-609.
- [16] J. Regourd, A. A. S. Ali and A. Thompson, *J. Med. Chem.* **2007**, *50*, 1528-1536.
- [17] W. Kirmse, *Eur. J. Org. Chem.* **2002**, 2193-2256.
- [18] L. R. Krepski and A. Hassner, *J. Org. Chem.* **1978**, *43*, 3173-3179.
- [19] G. Mehta and H. S. P. Rao, *Synth. Commun.* **1985**, *15*, 991-1000.
- [20] J. A. Ragan, T. W. Makowski, D. J. A. Ende, P. J. Clifford, G. R. Young, A. K. Conrad and S. A. Eisenbeis, *Org. Process Res. Dev.* **1998**, *2*, 379-381.
- [21] L. R. Krepski and A. Hassner, *J. Org. Chem.* **1978**, *43*, 2879-2882.
- [22] P. W. Jeffs, G. Molina, M. W. Cass and N. A. Cortese, *J. Org. Chem.* **1982**, *47*, 3871-3875.
- [23] R. D. Miller and D. R. McKean, *Tetrahedron Lett.* **1980**, *21*, 2639-2642.
- [24] D. A. Bak and W. T. Brady, *J. Org. Chem.* **1979**, *44*, 107-110.
- [25] K. C. Nicolaou, Y. L. Zhong and P. S. Baran, *J. Am. Chem. Soc.* **2000**, *122*, 7596-7597.
- [26] Y. Ito, T. Hirao and T. Saegusa, *J. Org. Chem.* **1978**, *43*, 1011-1013.
- [27] a) A. P. Krapcho, *Arkivoc* **2007**, 1-53; b) A. P. Krapcho, *Arkivoc* **2007**, 54-120.
- [28] K. Isobe, K. Mohri, H. Sano, J. Taga and Y. Tsuda, *Chem. Pharm. Bull.* **1986**, *34*, 3029-3032.
- [29] a) A. Chrobok, E. Gossinger, R. Kalb, E. Orglmeister and J. Schwaiger, *Tetrahedron* **2007**, *63*, 8326-8335; b) W. R. Esmieu, S. M. Worden, D. Catterick, C. Wilson and C. J. Hayes, *Org. Lett.* **2008**, *10*, 3045-3048; c) C. Li, X. L. Yu and X. G. Lei, *Org. Lett.* **2010**, *12*, 4284-4287. For reviews, see: d) G. Desimoni, G. Tacconi, *Chem. Rev.* **1975**, *75*, 651-692.

APPENDIX: LETTERS OF PERMISSION

A.1 Copyright Permission from RSC

From: dwang5@lsu.edu

Sent: 24 January 2011 06:04

To: CONTRACTS-COPYRIGHT (shared)

Subject: Permission Request Form: Dong Wang

Name: Dong Wang

Address: Department of Chemistry, Louisiana State University, Baton Rouge, LA 70803

Tel: +1-225-937-0813

Fax : +1-225-578-3458

Email: dwang5@lsu.edu

I am preparing the following work for publication:

Article/Chapter Title: Understanding the selective detection of homocysteine and studies
toward the synthesis of vinigrol (Ph.D. thesis)

Editor/Author(s): Dong Wang

Publisher: Louisiana State University's Intranet

I would very much appreciate your permission to use the following material:

Journal/Book Title: Chemical Communications

Editor/Author(s): Dong Wang, William E. Crowe, Robert M. Strongin and Martha Sibrian-Vazquez

Year of Publication : 2009

Description of Material: a communication

Page(s): 3

Any Additional Comments: Here is the page no. of the paper that I need your permission: 1876-
1878. Thanks!

Link to the paper: <http://pubs.rsc.org/en/Content/ArticleLanding/2009/CC/B819746F>

From: CONTRACTS-COPYRIGHT (shared) <Contracts-Copyright@rsc.org>

To: "dawang5@lsu.edu" dwang5@lsu.edu

Date: Tue, Jan 25, 2011 at 5:34 AM

Subject: RE: Permission Request Form: Dong Wang

Dear Dong Wang

The Royal Society of Chemistry (RSC) hereby grants permission for the use of your paper(s) specified below in the printed and microfilm version of your thesis. You may also make available the PDF version of your paper(s) that the RSC sent to the corresponding author(s) of your paper(s) upon publication of the paper(s) in the following ways: in your thesis via any website that your university may have for the deposition of theses, via your university's Intranet or via your own personal website. We are however unable to grant you permission to include the PDF version of the paper(s) on its own in your institutional repository. The Royal Society of Chemistry is a signatory to the STM Guidelines on Permissions (available on request).

Please note that if the material specified below or any part of it appears with credit or acknowledgement to a third party then you must also secure permission from that third party before reproducing that material.

Please ensure that the thesis states the following:

Reproduced by permission of The Royal Society of Chemistry and include a link to the paper on the Royal Society of Chemistry's website.

Please ensure that your co-authors are aware that you are including the paper in your thesis.

Regards

Gill Cockhead

Contracts & Copyright Executive

Gill Cockhead (Mrs), Contracts & Copyright Executive

Royal Society of Chemistry, Thomas Graham House

Science Park, Milton Road, Cambridge CB4 0WF, UK

Tel +44 (0) 1223 432134, Fax +44 (0) 1223 423623

<http://www.rsc.org>

A.2 Copyright Permission from ACS

Reproduced with permission from [Dong Wang and William E. Crowe. One-Carbon Bridge Stereocontrol in Robinson Annulations Leading to Bicyclo[3.3.1]nonanes. *Organic Letters*, 2010, 12(6), 1232-1235.] Copyright [2010] American Chemical Society.

Link for the detailed permission:

https://s100.copyright.com/CustomAdmin/PLF.jsp?IID=2011011_1295919704170

License Number	2595630848170
License Date	Jan 24, 2011
Licensed content publisher	American Chemical Society
Licensed content publication	Organic Letters
Licensed content title	One-Carbon Bridge Stereocontrol in Robinson Annulations Leading to Bicyclo[3.3.1]nonanes
Licensed content author	Dong Wang et al.
Licensed content date	Mar 1, 2010
Volume number	12
Issue number	6
Type of Use	Thesis/Dissertation
Requestor type	Not specified
Format	Electronic
Portion	50% or more of original article
Author of this ACS article	Yes
Order reference number	8888
Title of the thesis / dissertation	Understanding the selective detection of homocysteine and studies toward the synthesis of vinigrol
Expected completion date	Apr 2011
Estimated size(pages)	290

VITA

Dong Wang was born in August, 1981, in Pinglu County, Shanxi Province, China. He grew up in Pinglu and attended Pinglu High School from 1996-1999. After finishing high school, he enrolled in Beijing Institute of Technology, where he earned his Bachelor of Engineering degree in chemical engineering and technology in July of 2003.

He continued studying at Beijing Institute of Technology for master's degree, under the guidance of Professor Changjin Zhu. His master's research focused on the design and synthesis of aldose reductase inhibitors. He earned his Master of Engineering degree in applied chemistry in March of 2006. After earned his master's degree, he worked for WuXi AppTec, a pharmaceutical company in China.

In January of 2007, with the financial support from the Department of Chemistry of Louisiana State University (LSU), he came to LSU to begin his doctoral degree study in chemistry and soon joined Professor William E. Crowe's research group to begin doing his research in total synthesis.